PROBING THE INNATE IMMUNE RESPONSE TO INVASIVE FUNGAL INFECTIONS

Paula Ivana Seoane Denicola

A thesis submitted to the University of Birmingham for the degree of DOCTOR OF PHILOSOPHY

Institute of Microbiology and Infection
School of Biosciences
College of Life and Environmental Sciences
University of Birmingham

September 2019

"There are neither beginnings nor endings to the turning
of the Wheel of Time. But it was *a* beginning."

Robert Jordan, The Wheel of Time.

Acknowledgements

Four years of PhD have come and gone. During this time I have learnt a lot; about science, about people and about myself and I wouldn't change a thing (except maybe movie scoring times!). There are, of course, people without whom I would not have made it, and who deserve a special mention.

First, I would like to thank my supervisor Robin. You took a chance on me and helped me become a better scientist. Your unwavering optimism is an inspiration! I would also like to thank the wider HAPI lab, such a fantastic collection of people and an amazing place to work.

I would be remiss not to mention The Darwin Trust of Edinburgh. I am forever grateful to you for giving me this opportunity, and for making all of this possible.

A very heartfelt thank you to my family and friends, old and new. It is a hard task embarking on a PhD, and even more so doing it far away from your loved ones. Thank you for being there for me, for the constant encouragement and support. Gracias!!

Last, but definitely not least, thank you to my husband Dominik. I can honestly say that I would not have made it to this stage without you. Thank you for taking on this journey with me.

Abstract

Cryptococcus neoformans is an opportunistic fungal pathogen, which is widespread in the environment. Due to its global distribution and association with pigeon excreta, human exposure to this pathogen is frequent but initial infection is rapidly cleared or contained in immunocompetent hosts. In immunocompromised hosts, however, *C. neoformans* can cause severe disease often with dissemination to the central nervous system. Without rapid treatment disseminated infection is invariably lethal. With the rise of transplant and cancer therapy patients, the pool of vulnerable hosts is ever larger. Thus, studies of the interaction between *Cryptococcus neoformans* and the immune system are paramount for the development of novel treatment options.

In this study, different aspects of the interaction between *C. neoformans* and phagocytic cells, such as macrophages and dendritic cells, were explored.

One of the key features of Cryptococcal pathogenesis is its ability to persist and replicate within macrophages, as well as its ability to escape via a novel non-lytic mechanism known as vomocytosis. The impact of vomocytosis on disease progression is not yet fully appreciated, but it has been linked to dissemination of the fungal cell within the host. Vomocytosis is a highly regulated process, influenced by both fungal and host parameters. Macrophage polarisation is one such parameter, whereby alternatively activated macrophages show diminished occurrence of vomocytosis events. In this work, the interplay between two modulators of vomocytosis was explored. It was found that inhibition of the atypical MAP kinase ERK5, a known

regulator of vomocytosis, limits alternative activation of macrophages, thus, providing a link between both phenomena.

Cryptococcal meningitis occurs mainly in HIV^+ patients. The effect of chronic viral exposure on vomocytosis has not been studied before. My work revealed that viral exposure significantly enhances vomocytosis, acting through low levels of type-I interferons. Preliminary work expanded this finding to include bacterial co-infection settings, which can also elicit a type-I interferon response.

Lastly, the consequences of prolonged exposure to Cryptococcal cells or components on antigen presentation and antigen-induced T cell proliferation were explored. This setting emulates long-term latent infection within the lungs of immunocompetent hosts, which are frequently exposed to this fungus. The presence of Cryptococcal capsule components negatively impacts antigen-induced T cell proliferation by altering the antigen processing capabilities of antigen presenting cells.

Overall, this work highlights the complex interaction between *C. neoformans* and the innate immune system and underscores the importance of incorporating biological context cues into our experimental systems.

List of Contents

List of Figures and Tables

List of Abbreviations

AIDS	Acquired Immunodeficiency Syndrome
ANOVA	Analysis of variance
Arp2/3	Actin-related protein 2 and 3 complex
ATG-5	Autophagy-related gene 5
ATP	Adenosine triphosphate
BMDC	Bone marrow-derived dendritic cells
BSA	Bovine serum albumin
C3/C4	Complement component 3 / 4
CCR	C-C motif receptor
CD	Cluster of differentiation
cDMEM	Complete DMEM: DMEM 2 mM L-Glutamine, 100 units/mL Streptomycin, 0.1 mg/mL Penicillin and 10% FBS
cDMEM-HI	Complete heat-inactivated DMEM: DMEM 2 mM L-Glutamine, 100 units/mL Streptomycin, 0.1 mg/mL Penicillin and 10% heat-inactivated FBS
CFSE	Carboxyfluorescein succinimidyl ester
cGAS	Cyclic GMP-AMP synthase
CMC	Chronic mucocutaneous candidiasis
CNS	Central Nervous System
CR3	Complement receptor 3

cRPMI	Complete RPMI: RPMI 100 units/mL Streptomycin, 0.1 mg/mL Penicillin and 5% heat-inactivated AB human serum
CTLA-4	Cytotoxic T-lymphocyte-associated protein 4
CXCR	C-X-C motif receptor
DC	Dendritic cell
DMEM	Dulbecco's Modified Eagle Media
DMSO	Dimethyl-sulfoxide
DNA	Deoxyribonucleic acid
dNTP	Deoxyribonuclotide triphosphate
DOPA	3,4-dihydroxyphenyalanine
EDTA	Ethylenediamine tetraacetic acid
EGF	Epidermal growth factor
EGTA	Ethyleneglycol tetraacetic acid
ELISA	Enzyme-linked immunosorbent assay
ER	Endoplasmic reticulum
ERK5	Extracellular signal-regulated kinase 5
FBS	Foetal Bovine Serum
GalXM	Galactoxylonmannan
GAS	IFNγ-activated site
GFP	Green fluorescent protein
GM-CSF	Granulocyte-macrophage colony-stimulating factor
GTP	Guanosine Triphosphate
GXM	Glucuronoxylonmannan
HIV	Human Immunodeficiency Virus

IFNAR	IFNα/β receptor
IFNAR1	Subunit 1 of IFNAR
IFNAR2	Subunit 2 of IFNAR
IFN	Interferon
IFNLR	IFNλ receptor
IKK	Inhibitor of nuclear factor κB kinase
IL-	Interleukin
IPR	Intracellular proliferation rate
IRF	interferon-regulatory factor
ISG	Interferon-stimulated gene
ISRE	Interferon-sensitive response element
JAK1	Janus kinase 1
KO	Knock-out
LB	Lysogeny Broth (also known as Luria Bertani broth)
LCMV	Lymphocytic choriomeningitis virus
LIF	Leukaemia inhibitory factor
LPS	Lipopolysaccharide
M-CSF	Macrophage colony-stimulating factor
MAP	Mitogen-activated protein
MDA-5	Melanoma differentiation associated gene-5
MeV	Measles virus
MGL	Macrophage galactose-type calcium-type lectin
MHC-II	Major histocompatibility complex class II
MR	Mannose receptor

MMR	Measles, mumps and rubella
MOI	Multiplicity of infection
Mx	Myxovirus resistance protein
NADPH	Nicotinamide Adenine Dinucleotide Phosphate
NF-κB	Nuclear factor κB
NK	Natural killer cell
OA	Oleic acid
OAS	2′-5′ oligoadenylate synthase
OVA	Chicken ovalbumin
OVAp	Ovalbumin peptide 323-339
PAMP	Pathogen-associated molecular pattern
PBMC	Peripheral blood mononuclear cells
PBS	Phosphate-buffered saline
pDC	Plasmacytoid Dendritic cells
PDL2	Programmed-death ligand 2
PKR	Protein kinase R
PLB1	Phospholipase B 1
PMA	Phorbol myrstate acetate
polyIC	Polyinosinic-polycytidilic acid
polyICLC	Polyinosinic-polycytidylic acid stabilized with polylysine and carboxymethylcellulose
RIG-I	Retinoic acid inducible gene-I
RNA	Ribonucleic acid
ROS	Reactive Oxygen Species

RPMI	Roswell Park Memorial Institute
RT	Reverse transcriptase
SAMHD1	Sterile α motif and histidine-aspartate domain–containing protein 1
SCID	Severe combined immunodeficiency
SIV	Simian Immunodeficiency virus
SLAM	Signalling lymphocyte activation molecule
SN	Supernatant
STAT	Signal transducer and activator of transcription
STING	Stimulator of interferon genes
TAM	Tumour-associated macrophages
TBK1	TANK binding kinase 1
TCR	T cell receptor
Th1	T helper response type 1
Th2	T helper response type 2
Th17	T helper response type 17
TLR	Toll-like receptor
TNFα	Tumour necrosis factor alpha
Tyk2	Tyrosine kinase 2
UPEC	Uropathogenic Escherichia coli
URE1	Urease 1
UV	Ultraviolet
VLP	Virus-like particle
VVC	Vulvovaginal candidiasis
YPD	Yeast Peptone Dextrose

1 Introduction

1.1 *Cryptococcus neoformans*

1.1.1 Discovery and classification

Cryptococcus neoformans was first isolated in 1894 almost simultaneously from human bone infection [1] and from fermented peach juice [2]. At that time, it was described as a "*Saccharomyces*-like" organism, but was later renamed as *Cryptococcus neoformans* in 1901 by Jean-Paul Vuillemin [3]. Under the current classification, *C. neoformans* is one of the thirty-nine species of the genus *Cryptococcus* [4]. *C. neoformans* is further classified into two varieties according to genotypic differences; *C. neoformans var. neoformans* and *C. neoformans var. grubii* [5]. A third variety, *C. neoformans var. gattii*, is now considered a separate species: *C. gattii* [6].

The work presented in this report was performed using two strains from *C. neoformans var. grubii*; the reference strain for this variety, H99, and a strain derived from H99 to generate congenic strains in the different mating types, Kn99 [7].

1.1.2 General characteristics

C. neoformans is, in its most abundant form, a unicellular (yeast) organism which replicates by budding. It is typically 4 – 10 μm in diameter and presents a thick polysaccharide capsule linked to its cell wall [8]. When cultured it yields cream-coloured colonies, except in the presence of laccase substrate such as 3,4-

dihydroxyphenyalanine (DOPA), where the colonies are brown as a result of melanin production [3]. During its sexual cycle, *C. neoformans* undergoes a morphological change and grows as a hyphal fungus. As part of this cycle it produces spores of 1 – 2 μm in diameter which are released into the environment. Nonetheless, yeast cells are the most predominant form both in the environment and during infection. Contrary to other human pathogens like *Candida albicans* whose dimorphic switch is considered a virulence trait, hyphal *C. neoformans* is unable to persist during mammalian infection [9, 10].

Unlike its sister species *C. gattii*, which is predominantly present in sub-tropical regions, *C. neoformans* has a worldwide distribution [11]. It is associated with avian excreta, particularly that of pigeons, which makes it readily available in urban as well as rural settings [12]. In fact, the production of antibodies against *Cryptococcus* at an early age supports that exposure to *C. neoformans* is common in humans even in urban areas [13].

1.1.3 Pathogenicity and infection

C. neoformans is an opportunistic fungal pathogen. As such, it infects animals, including humans, but only results in disease in previously weakened individuals (Figure 1.1). Cryptococcosis is particularly relevant in human immunodeficiency virus $(HIV)^+$ patients, where it is considered an acquired immunodeficiency syndrome (AIDS)-defining illness. A study conducted in 2014 estimated over 200000 cases of Cryptococcal meningitis in HIV^+ patients per year, 73% of which were reported in

sub-Saharan Africa. These amounted to 180000 deaths in 2014, which represents 15% of AIDS-related deaths [14].

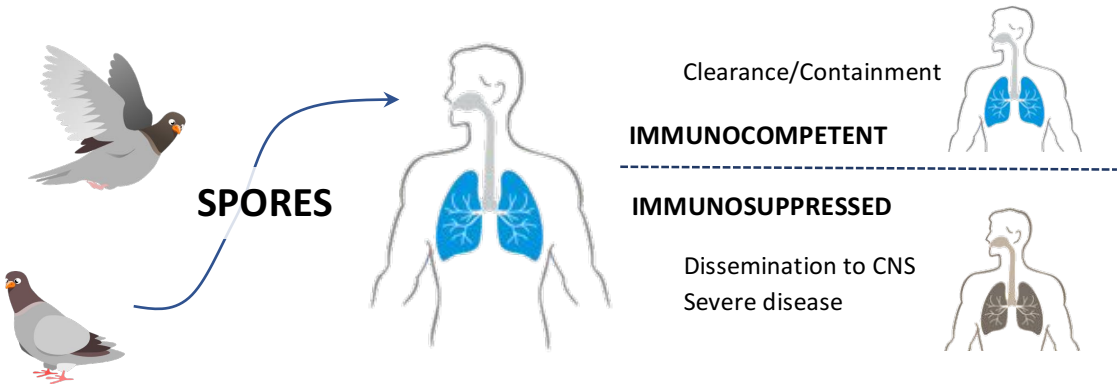

Figure 1.1 Schematic depiction of *C. neoformans* infectious cycle
See text below for description. CNS = Central Nervous System

The infection cycle begins with inhalation of the infectious propagule. This could be desiccated yeast cells (approx. 3 µm) or spores (1 – 2 µm), which are commonly found in the environment as mentioned before [12]. Once inside the host, the infection is rapidly cleared or contained in immunocompetent individuals. In immunocompromised hosts however, or upon immunosuppressive treatments combined with a latent infection, the infection can disseminate. *C. neoformans* has a tropism for the central nervous system and can bypass the brain-blood-barrier causing meningoencephalitis. In these cases, infection is invariably lethal without rapid treatment [12].

1.2 Immunology of *C. neoformans* infection

1.2.1 General remarks

As mentioned before, infection with *C. neoformans* is virtually unavoidable due to its availability in both rural and urban settings, and global distribution. Remarkably, infection is asymptomatic and rapidly cleared or contained in most cases. However, chronic or acute infections can be seen in immunocompromised hosts as is the case of cancer, transplanted or HIV^+/AIDS patients. In these cases, pulmonary infection can involve pneumonia and acute respiratory distress syndrome, whereas dissemination to the central nervous system (CNS) presents as meningoencephalitis [15]. Cryptococcal encephalitis is one of the leading causes of death in HIV^+/AIDS patients in sub-Saharan Africa [14]. Given the high prevalence of *Cryptococcus* infections in HIV^+ patients, further details regarding this particular immunological context will be given in section 1.5.

The impressive difference in terms of outcome of infection among immunocompetent and immunocompromised host reveals the importance of an intact immune response when dealing with this pathogen. A brief description of the adaptive and innate immune responses to *C. neoformans* infection is given below.

1.2.2 Adaptive immune response to *C. neoformans*

Immune responses can be broadly classified into T helper type 1 (Th1), Th2 and Th17. Each response is brought about by different cues or pathogen types, and is therefore tailored to deal with specific challenges. The immune system is constantly facing

diametrically different stimuli, and thus a balance is struck between the responses elicited by them. The position of such immunological balance, and the ability of skewing it towards one side or the other, will greatly influence the outcome of infection.

Protective responses to *C. neoformans* are predominantly orchestrated by Th1 $CD4^+$ T cell-mediated immune responses [16]. This kind of response is characterized by the release of Th1 cytokines, such as IFNγ and TNFα, which enhance uptake and killing of *C. neoformans* by neutrophils, macrophages and dendritic cells. Th1 cytokines also polarise macrophages to a "classical activation" phenotype, also termed M1, which possess enhanced phagocytic and antimicrobial activity.

Th2 cytokines, such as IL-4, IL-5, IL-9 and IL-13, induce eosinophil recruitment to the site of infection as well as polarisation of macrophages to an "alternative activation" phenotype, also termed M2. M2 macrophages have an important role in anti-parasitic responses and in tissue repair and remodelling [17]. Th2 responses are considered to be detrimental during *C. neoformans* infection, reducing the host's ability to eliminate the pathogen [15]. *C. neoformans* actively skews the Th1-Th2 balance towards a Th2 profile by expressing eicosanoids [18] and inducing production of IL-10 [19].

Th17 are also thought to be important for protection against *C. neoformans* [16]. There is some debate, however, as to the extent of the role of Th17 on cryptococcosis; Wozniak *et al* [20] propose that it is a secondary role, since inhibition of production and/or signalling of IL-17A showed no effect in the outcome of infection in an

experimental mouse model, whereas Murdock *et al* [21] suggest it is a primary role, since late fungal clearance was impaired in IL-17A-deficient mice.

B cells and antibody production also play a role in the immune response to *C. neoformans*, as highlighted by the presence of antibodies reactive to Cryptococcal antigens in the sera of immunocompetent children [13, 22]. This suggests that exposure to *C. neoformans* and subsequent mounting of an antibody response occurs early in life [13]. Moreover, low antibody titres and B cell deficiencies have been linked to higher risk of developing cryptococcal infections [23, 24]. This finding is also reflected in murine cryptococcosis models, where B cell deficiency and low IgM production correlates with increased susceptibility to *C. neoformans* infection and higher fungal burden in the lung [25-27].

Antibodies binding to *C. neoformans* can also act as opsonins and enhance uptake by host phagocytes [28-30].

1.2.3 Innate immune response to *C. neoformans*

The innate immune system constitutes the first line of defence against *C. neoformans* infection and serves a pivotal role for the mounting of long-lasting adaptive responses. Given that *C. neoformans* is responsible for severe disease almost exclusively in hosts with impaired adaptive immunity, such as AIDS, the importance of studying the innate immune response against this pathogen is heightened.

1.2.3.1 *Complement System*

The complement system is a cascade of serum proteins that *complements* the activity of antibodies and phagocytic cells in the clearance of pathogens and damaged cells. This system can be triggered by three different pathways, namely classical, alternative and lectin pathway, which differ in their recognition of non-self particles. The three pathways ultimately converge in the formation of the C3-convertase and the assembly of the membrane-attack complex [31].

It has long been known that the complement system is important for the clearance of *C. neoformans* [32]. Experiments restricting the activation by the classical and lectin pathways, either by using C4-deficient guinea pigs [32] or by studying the binding kinetics of C3 in the presence of Mg-EGTA [33], have showed that the alternative activation pathway has a predominant role in the clearance of *C. neoformans*. Deposition of complement molecules on *C. neoformans* act as opsonins and enhance phagocytosis mainly through engagement of the complement receptor 3 (CR3) [34].

1.2.3.2 *Phagocytes – Neutrophils, Dendritic Cells and Macrophages*

Cryptococcal cells are readily phagocytosed by a variety of leukocytes. This phenomenon is mediated by direct recognition of the yeast cells (Toll-like receptor (TLR)4 binds components of the capsule [35]) or by receptor-mediated recognition of complement [34] or antibody [36] opsonisation. In the lung environment, where the abundance of serum components is low, non-opsonic uptake predominates [37].

Neutrophils are the first to be recruited to the site of inflammation, and have the ability to kill *C. neoformans* cells by oxidative burst *in vitro*. Interestingly, neutropenia in mice has been shown to be beneficial for survival [38, 39]. In these reports, the beneficial effect was ascribed to altered cytokine release which enhanced protective responses, and was limited to pulmonary infection models [38, 39].

Dendritic cells (DC) act as a bridge between innate and adaptive immunity, having a predominant role in antigen presentation. In a murine model, cryptococcal cells were internalised by DC within 2 hours post inoculation. Activated DC were then retrieved 7 days post infection, and were capable of inducing T cell proliferation *ex vivo* [40].

Macrophages are at the heart of the interaction with *C. neoformans* cells. This pathogen is able to survive within the phagosome of macrophages. Unlike other intracellular pathogens, it does not escape to the cytosol and does not inhibit phagosome-lysosome fusion [41]. It does, however, interfere with the maturation/acidification process [42]. As mentioned before, macrophages can be polarised towards different activation phenotypes, M1 and M2 being the best studied ones. During *Cryptococcus* infection, M1 macrophages are considered to be beneficial for survival, whereas M2 macrophages to have the opposite effect [15, 16]. Regardless of their activation state, there is still debate as to whether macrophages play a role in the dissemination of *C. neoformans* to the CNS (see 1.3.3). Other than replicating within the phagosome, *Cryptococcus* can escape the macrophage via a lytic or non-lytic mechanism. The different outcomes of the interaction between macrophages and *Cryptococcus* will be described in section 1.3.2.

1.3 Immune evasion strategies of *C. neoformans*

1.3.1 Virulence factors

C. neoformans possesses a variety of virulence factors that aid in its pathogenicity. The three most important and well-studied virulence traits consist of its ability to grow at 37°C, the presence of a thick capsule and the ability to produce melanin [12].

C. neoformans is not only able to grow at 37°C, the mammalian host body temperature, but it thrives in it. Its optimal and maximum growing temperatures are 32°C and 40°C, respectively. It is considerably more thermotolerant than its non-pathogenic genus siblings, and is in fact the one of the two *Tremallelles* which can grow optimally at over 30°C (the second species being *C. gattii*) [43].

The presence of a thick polysaccharide capsule is arguably the most striking virulence factor in this organism, and the best studied one. The main components of the capsule are the polysaccharides glucuronoxylonmannan (GXM) and galactoxylomannan (GalXM) [44]. The size of the capsule is highly influenced by the environment encountered by the yeast, generally enlarging upon infection. *In vitro*, factors such as osmolarity, carbon source, pH, nutrient concentration and temperature influence capsule size [45]. While cell-bound, the polysaccharide capsule inhibits phagocytosis; the sugars can also be shed during infection to avert attachment [46]. Capsule components have been shown to dampen antigen presentation processes and produce a subdued lymphoproliferative response when compared to acapsular strains [19]. Shed components of the capsule have also been shown to have immunomodulatory

properties [8]. Remarkably, acapsular mutants are non-virulent [8], highlighting the importance of this structure for pathogenicity.

Finally, deposition of melanin in the cell wall is considered a virulence factor. This pigmented molecule confers protection from UV light and freeze-thaw cycles in the environment, and it also protects the yeast against reactive oxygen species (ROS) generated in the phagolysosome [4]. As stated before, melanin is produced by the enzyme laccase from the dopamine precursor.

In addition to the virulence factors mentioned above, the production of giant cells is yet another mechanism by which *C. neoformans* avoids clearance. Once inside the host and subjected to the lung environment, a proportion of the infecting yeast cells evades phagocytosis by expanding their cell size to form titan cells of up to 100 μm in diameter [47]. These cells are thought to arise from DNA replication without concomitant fission, since they are polyploid and uninucleate. The role of these giant cells during infection is poorly understood, but a hypothesis is that they act as seeding points for infection; their increased resistance to phagocytosis and oxidative stress enables them to persist in the lung while allowing their smaller counterparts to disseminate within the host [48].

1.3.2 Life in the phagosome

One of *C. neoformans* most remarkable properties is that it is able to not only survive but prosper within phagocytes. This characteristic is not exclusive to this pathogen,

being displayed by a myriad of pathogenic organisms, such as *Listeria monocytogenes*, *Legionella pneumophila*, *Mycobacterium tuberculosis* and *Salmonella enterica* [49].

Cryptococcus cells have developed numerous mechanisms to endure the harsh conditions present within the phagosomes of macrophages, and even to escape them. Phagosome maturation involves fusion with lysosomal vesicles, which results in the acidification of the phagosomal lumen, presence of multiple acidic proteases and the assembly of NADPH oxidase. This complex mediates the production of ROS aimed to damage the phagocytosed contents [31]. As previously mentioned, engulfed *Cryptococci* possess a melanin coat that absorbs ROS. They also present enzymes designed to fight the oxidative stress imposed by the phagolysosome environment (including superoxide dismutase, glutathione reductase and glutathione peroxidase, among others [8]). Yeast cells also secrete urease, which catalyses the hydrolysis of urea into ammonia thus neutralising the phagosome pH. Taken together these properties allow *Cryptococci* to establish a latent infection within macrophages [8, 50].

Cryptococci can also escape the macrophage via lytic or non-lytic pathways. No pore-forming proteins have been found in *Cryptococcus* cells, therefore lytic expulsion is thought to be driven by excessive yeast replication causing physical stress on the host cell. Non-lytic exocytosis, also known as vomocytosis, is a highly regulated process seen so far in *C. neoformans* [51, 52], *C. albicans* [53] and *C. krusei* [54] infection. As a result of vomocytosis, both the expelled *Cryptococci* and the macrophage are undamaged, with no obvious signs of diminished replication capacity for the former or dysfunction for the latter. Hence, this escape mechanism ensures minimal

proinflammatory signalling, and is therefore thought to pose an advantage over lytic escape [50, 55]. A comprehensive review of vomocytosis can be found in section 1.4.

1.3.3 Traversing to the brain

One of the key features behind the mortality of *C. neoformans* infection is its ability to trespass the blood-brain barrier. The mechanism by which this pathogen conquers this immunologically-privileged site is not yet understood. However, there are three proposed mechanisms that could allow *Cryptococcus* to accomplish this feat. The first is by paracytosis, which involves moving between tight junctions of endothelial cells. The presence of the metalloprotease Mpr1 is thought to be implicated in this process. Supporting this hypothesis, the introduction of the *MPR1* gene in *S. cerevisiae* resulted in the ability of this fungus to cross endothelial layers *in vitro* [56]. The second mechanism consists of transcytosis through endothelial cells. This process relies on the interaction between Cryptococcal hyaluronic acid and CD44, present on the luminal surface of endothelial cells. This binding leads to actin remodelling and engulfment of the fungus [57]. Finally, the third mechanism is termed "Trojan Horse", as it involves the fungus travelling within phagocytes to the CNS, analogous to the Greek myth. Supporting evidence for this mechanism includes reports of reduced fungal burden in the brain after depletion of alveolar macrophages [58] and enhanced dissemination to the CNS in infection via transfer of *Cryptococcus*-loaded monocytes compared to *Cryptococcus* alone [59].

1.4 Vomocytosis; what we know so far

The following section has been submitted for publication as an independent Review to the scientific journal Cellular Microbiology.

Vomocytosis, or non-lytic exocytosis, is the expulsion of live organisms that have previously been engulfed by a phagocyte, leaving both cells undamaged after the event (Figure 1.2). This process was first described in 2006 by two groups independently, while imaging macrophages infected with the yeast *Cryptococcus neoformans* [51, 52]. Various pathogens have evolved to survive within phagocytes or escape this harsh environment by destroying the phagocyte, but these were the first reports of a novel escape mechanism whereby a pathogen is released from a phagocyte without lysing of either cell.

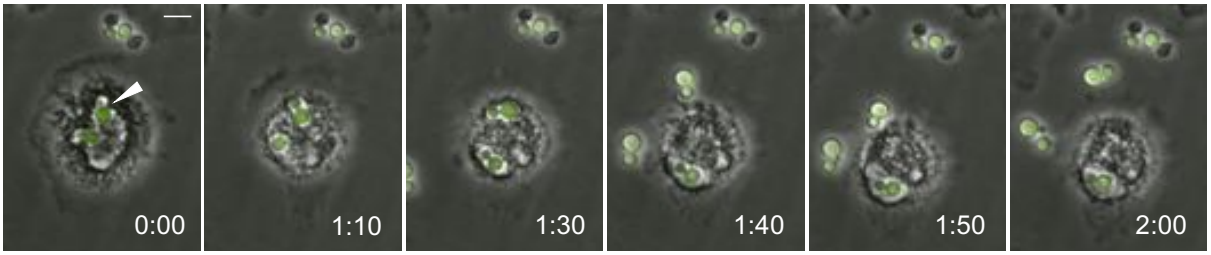

Figure 1.2 Vomocytosis event

Human monocyte-derived macrophages infected with GFP-tagged *C. neoformans*. Images from time-lapse microscopy showing a Cryptococcal cell (arrowed) undergoing vomocytosis. Number at the bottom of each frame indicates time post-infection (hours:minutes). Scale bar at the top corresponds to 5 μm.

1.4.1 Who is able to vomocytose?

Vomocytosis was first seen to occur with the fungal pathogen *Cryptococcus neoformans*, and its sister species *C. gattii* and *C. grubii* [51, 52]. Following its initial discovery, vomocytosis was soon reported with *Candida krusei* [54] and *Candida albicans* [53]. These represent a jump from the *Cryptococcus* genus and include fungal pathogens that form pseudohyphae or hyphae.

A related phenomenon termed "Lateral transfer" was soon described, whereby an internalised Cryptococcal cell is "transferred" from one infected macrophage to another [60, 61]. As with vomocytosis, both the transferred cell and macrophage remain undamaged after this event. Recently, Dragotakes *et al.* showed that lateral transfer is the combination of a non-lytic exocytosis event followed by phagocytosis by a nearby macrophage [62]. Events of lateral transfer have been observed for *Scedosporium apiospermum* and *Lomentospora prolificans* [63], although due to spore germination the accepting macrophage is lysed shortly after the event. Lateral transfer of *Aspergillus fumigatus* spores between macrophages has been reported. In this case, however, transfer is associated with necrosis of the donor macrophage [64].

Although first described in murine macrophage cell lines such as J774 and RAW246.7, vomocytosis has now been recorded in mouse, human, avian and fish primary macrophages [51, 52, 65, 66]. The interaction between *C. neoformans* and macrophages has been compared to that between the fungus and predatory amoebae in the environment. This has led to the proposal that the capacity *C. neoformans* has for mammalian infection evolved in response to selective pressure exerted during

interactions with such phagocytic predators. Amoebae are also able to vomocytose *C. neoformans* [67], although it should be noted that amoebae, unlike macrophages, also have a constitutive exocytosis pathway to release indigestible material [68].

Studying vomocytosis *in vivo* presents considerable technical challenges. However, in 2011 Nicola *et al.* reported that vomocytosis occurs *in vivo*, using a murine Cryptococcal infection model and quantifying the occurrence of non-lytic expulsion indirectly, through a novel flow cytometry approach [69]. This method involves sorting a highly pure pre-stained population of infected macrophages, and comparing numbers of infected macrophages after a 24-hour period either *in vitro* or recuperated from a live recipient. This approach allows for the analysis of large numbers of cells in a short time, although it suffers from a high "false positive background" as a result of Cryptococcal death and host cell proliferation. In 2016, Bojarczuk *et al.* were the first to directly show vomocytosis during whole organism infection using the transparent zebrafish larvae model [66]. To date, vomocytosis has not been directly evidenced in a mammalian host. Although intravital imaging could theoretically achieve this, in practice the rarity of the event and the extended periods of imaging required represent formidable technical challenges.

1.4.2 What is the mechanism of vomocytosis?

A key question for the field is the underlying mechanism that drives vomocytosis. How does this work? Why would phagocytes expel undamaged cargo? Is it triggered by the pathogen or the host cell? To date, most of these questions remain unanswered.

However, recent data has begun to open the door to a mechanistic description of this process (Figure 1.3, page 20).

One of the first observations was that vomocytosis does not occur with heat-killed *Cryptococcus* or with inert latex beads [51, 52]. This suggests that the phenomenon might be triggered by the fungus rather than the host cell, or alternatively that the host cell has a mechanism by which it can determine whether a phagosomal cargo is alive.

Another fungal characteristic that affects vomocytosis is the presence of capsule; acapsular strains of *C. neoformans* showed diminished vomocytosis rates [51]. Other virulence factors which have been linked to vomocytosis are secretion of phospholipase B 1 (*plb1*) and presence of urease. Both defective strains (*plb1*Δ and *ure1*Δ) have been shown to be hypovirulent in animal models [70, 71], and both show a decrease in occurrence of vomocytosis [72, 73]. It should be noted, though, that these mutants all show attenuation leading to higher intracellular killing rates, which could confound observations of vomocytosis rate.

Several host factors influence vomocytosis occurrence. Perhaps not surprisingly, given the involvement of Cryptococcal-urease, phagosomal pH has been linked to vomocytosis since its first description in 2006, with the addition of weak bases such as chloroquine or ammonium chloride resulting in enhanced vomocytosis of *C. neoformans* [51, 52, 69]. In line with this, it has been noted that vomocytosis occurs exclusively on non-acidified phagosomes [42]. Interestingly, it has recently been demonstrated that glucuronic acid residues in capsular polysaccharide are able to

buffer phagolysosomal pH [74], which could explain why acapsular strains of *C. neoformans* exhibit lower rates of vomocytosis.

Host membrane integrity and composition have also been seen to affect vomocytosis. Infection with *C. neoformans* results in the disruption of the phagolysosomal membrane [75], and such permeabilisation was later shown to precede vomocytosis events [76]. Extensive phagolysosomal membrane permeabilisation, however, leads to a decrease in the occurrence of non-lytic exocytosis [77]. The lipid composition of the membrane is also thought to affect vomocytosis. Addition of exogenous oleic acid (OA) to macrophages infected with *C. neoformans*, which is a building block for phospholipids found in membranes, resulted in enhanced occurrence of vomocytosis events [78].

Another host process that has been shown to affect vomocytosis is autophagy. This process allows eukaryotic cells to recycle cytoplasmic material and organelles and also has a role in the host's defence against intracellular pathogens [79]. Host molecules known to be associated with autophagy were seen to be recruited to *Cryptococcus*-containing phagosomes. Of these, autophagy-related 5 (ATG5) in particular was then shown to have an effect on vomocytosis, since ATG5 knockdown reduces vomocytosis of *C. neoformans* [80].

The process of vomocytosis requires that internal vesicles release their cargo onto the extracellular milieu. For this to happen, the vesicle itself needs to be positioned near the edge of the cell and the vesicle and plasma membranes fuse together to allow the

cargo to be released. In 2016, Stukes *et al.* showed that annexin A2, a membrane binding protein involved in bringing membranes together and promoting fusion during several cellular processes including exocytosis of secretory vesicles, affects the occurrence of vomocytosis [81]. Using annexin A2 deficient cells (anxa2$^{-/-}$), they noticed a decrease in phagocytosis and in vomocytosis of *C. neoformans*. Interestingly, the group showed that the absence of annexin A2, both *in vitro* and *in vivo*, results in an enlarged Cryptococcal capsule; suggesting that there might be a "sweet spot" in capsule size whereby too small (acapsular strains) or too large a capsule both abrogate vomocytosis.

The host cytoskeleton is an obvious target to affect vomocytosis, given its clear role both in maintaining normal cellular structure and in driving the expulsion of several pathogenic bacteria [82]. Addition of cytochalasin D, which inhibits actin polymerisation within host macrophages, enhances vomocytosis of *C. neoformans* [51]. Johnston *et al.* showed that *Cryptococci*-containing phagosomes experience rapid, transient increases in actin polymerisation surrounding them, which they termed actin flashes. These flashes are assembled through the Arp2/3 complex, a nucleator of actin filaments, and are sensitive to pharmacological manipulation with actin stabilising/depolymerising agents. Utilising these tools, they found that stabilising or destabilising these actin flashes (with jasplakinolide or cytochalasin D, respectively) correspondingly reduced or increased vomocytosis rates. Thus, they revealed a new mechanism by which the host cell tries to retain internalised cargo, and inhibits vomocytosis, through assembly of transient actin cages surrounding the phagolysosome [76].

Macrophages are very plastic cells, sensitive to myriad cellular signals, which underlie a wide spectrum of activation states. Not surprisingly, differently activated macrophages deal with Cryptococcal infection in different ways, including through modification of vomocytosis rates. At one end of this spectrum are so-called 'alternatively activated' macrophages, also termed M2, which have been exposed to interleukins four or thirteen (IL-4 or IL-13, respectively). These cells have a normal phagocytic capacity but show an increased intracellular proliferation rate of fungal cells and reduced vomocytosis occurrence [83].

Lastly, to unravel the signalling pathways involved in vomocytosis, Gilbert *et al.* screened a panel of inhibitors directed at kinases known to be expressed in macrophages [84]. By doing so, they revealed that the host mitogen-activated (MAP) kinase ERK5 is a suppressor of vomocytosis, and as such, inhibition of ERK5 with the compound XMD17-109 leads to a significant enhancement of vomocytosis. Treatment of zebrafish larvae with this inhibitor recapitulated the increase of vomocytosis events seen *in vitro*, and moreover, showed that this resulted in decreased dissemination of the fungus [84], providing a molecular 'handle' for the future dissection of vomocytosis signalling. A more detailed comment on ERK5 signalling can be found in section 1.5.

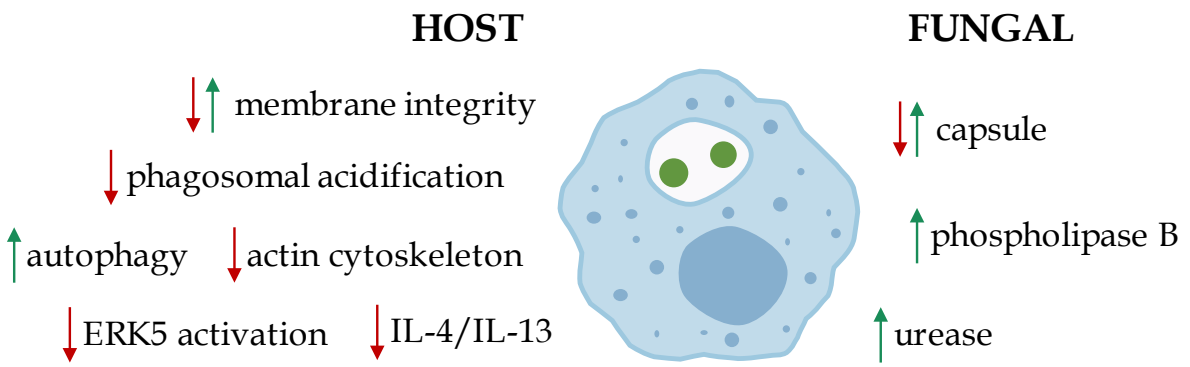

Figure 1.3 Molecular components affecting vomocytosis occurrence

Several host (left) and fungal (right) factors have been shown to affect vomocytosis. Phagosomal acidification, formation of actin cages, polarisation towards an alternative activation phenotype and ERK5 activation have all been shown to inhibit vomocytosis of *C. neoformans* (red downward arrows). On the other hand, autophagy has been reported to enhance it (green upward arrow). There have been reports arguing both a promoting and an inhibiting effect of host membrane integrity and composition on vomocytosis.

From the fungal side, absence of phospholipase B or urease leads to decreased vomocytosis occurrence. Capsule size also plays a role; acapsular and large capsule both inhibit vomocytosis.

1.4.3 What is the biological significance of vomocytosis?

Vomocytosis poses an attractive "stealth" escape mechanism from phagocytes, without damage to the host cell and thus no release of immune-flagging molecules. Therefore, it has long been thought to play a role in dissemination. The mechanism for crossing of the blood-brain barrier, needed for dissemination to the central nervous system (CNS), is still not fully understood. One hypothesis involves the hijacking of phagocytes to transport it to distal sites of infection followed by vomocytosis, much like a Trojan Horse. Supporting evidence for this mechanism includes reports of reduced fungal burden in the brain after depletion of alveolar macrophages [58] and enhanced dissemination to the CNS in infection via transfer of *Cryptococcus*-loaded

monocytes compared to free *Cryptococcus* [59]. Gilbert *et al*. provided the first direct evidence that vomocytosis plays a role in dissemination of *C. neoformans*, since pharmacological enhancement of vomocytosis lead to reduced fungal dissemination in the zebrafish model [84]. It should be noted though, that the net effect on dissemination is highly dependent on the timing of the vomocytosis event and could increase dissemination at later points after initial infection.

1.4.4 Bacterial "vomocytosis-like" events

Even though the term vomocytosis has been used exclusively to describe expulsion of fungal pathogens, several reports describe similar processes occurring with bacterial entities. In 2009, Hagedorn *et al.* described a new non-lytic exit mechanism for *Mycobacterium marinum* from the amoeba *Dictyostelium discoideum*, which they propose could aid in the spreading of this bacterial pathogen [85]. Other reports in 2009 and 2016 describe the non-lytic expulsion of uropathogenic *E. coli* (UPEC) from bladder epithelial cells [86, 87]. In this case, the expulsion serves to reduce intracellular bacterial burden and eliminate live bacteria from the host with the flow of bodily fluids. Also very reminiscent of vomocytosis, an article describes the non-lytic release of the opportunistic bacterial pathogen *Serratia maracescens* from an epithelial cell line, with both cells remaining viable and undamaged after the event [88]. Taken together, these suggest that vomocytosis might be a conserved mechanism employed by different pathogens with varying consequences for infection.

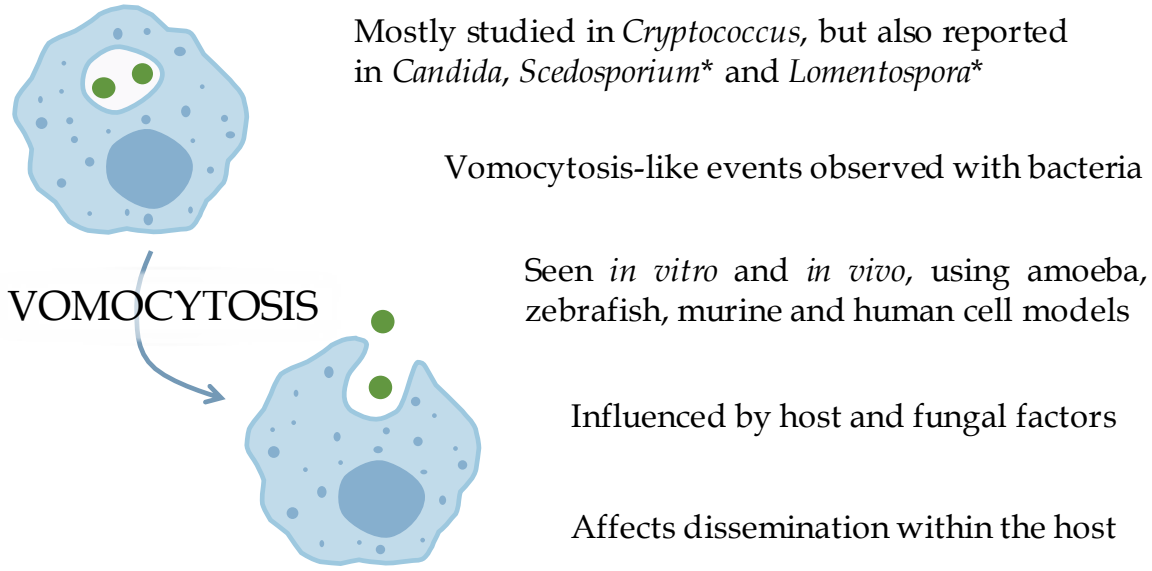

Figure 1.4 Key features of vomocytosis
* In these species lateral transfer, a form of vomocytosis, was reported.

1.4.5 Concluding Remarks

Since its discovery in 2006, vomocytosis has piqued the interest of the scientific community, revealing a novel process in the plethora of host and pathogen interactions. Slowly but steadily, the repertoire of pathogens and hosts seen to make use of this unusual escape mechanism has been expanding. This suggests that this process is not merely anecdotal for the infection of macrophages with *C. neoformans*, but rather a much more widely used escape/emptying mechanism (Figure 1.4).

How does this process come about? What are the consequences for the outcome of infection? These questions have puzzled scientists for over a decade. The exact mechanism that drives this event remains elusive to date. However, recent advances in understanding some of the regulatory steps that underpin expulsion may open the

door to a detailed mechanistic understanding in the near future. In addition, the use of whole animal transparent models, such as zebrafish larvae, and the automation of time-lapse scoring with machine learning algorithms will undoubtedly accelerate our gain of new insights into this fascinating process.

1.5 Extracellular-signal regulated kinase (ERK) 5

1.5.1 Mitogen-activated protein kinases

Mitogen-activated protein kinases (MAPKs) are highly conserved enzymes, expressed in all eukaryotic cells, which mediate multiple intracellular processes. Their signalling cascade (Figure 1.5) consists of the sequential activation of 3 modules; MAPK kinase kinase (MAPKKK), MAPK kinase (MAPKK) and MAPK, and is triggered after sensing of extracellular signals such as presence of growth factors, cytokines or environmental stresses [89]. Four members of the MAPK family have been identified: extracellular-signal-regulated kinase 1/2 (ERK1/2), c-Jun-amino-terminal kinase (JNK), p38 and ERK5 [90].

1.5.2 ERK5 discovery and structure

ERK5 was simultaneously reported by two independent groups in 1995 [91, 92], one of them naming it big MAPK (BMK)-1 due to its large size compared to ERK1/2 (ERK5 weighs 102 kDa while ERK1/2 are 44 kDa and 42 kDa, respectively).

Structurally, the kinase domain present in the N-terminus is similar to that of ERK1/2 [91], whereas the extended 410 amino acid long C-terminal tail is unique to ERK5 [91]. Within this C-terminal tail there is a nuclear localisation signal (NLS) domain [93], important for subcellular localisation of ERK5, two proline-rich (PR) domains and a myocyte enhancer factor 2 (MEF2)-interacting region [94]. Truncation of the C-terminal tail results in enhanced ERK5 activity [93], thus suggesting that it may have an autoinhibitory function.

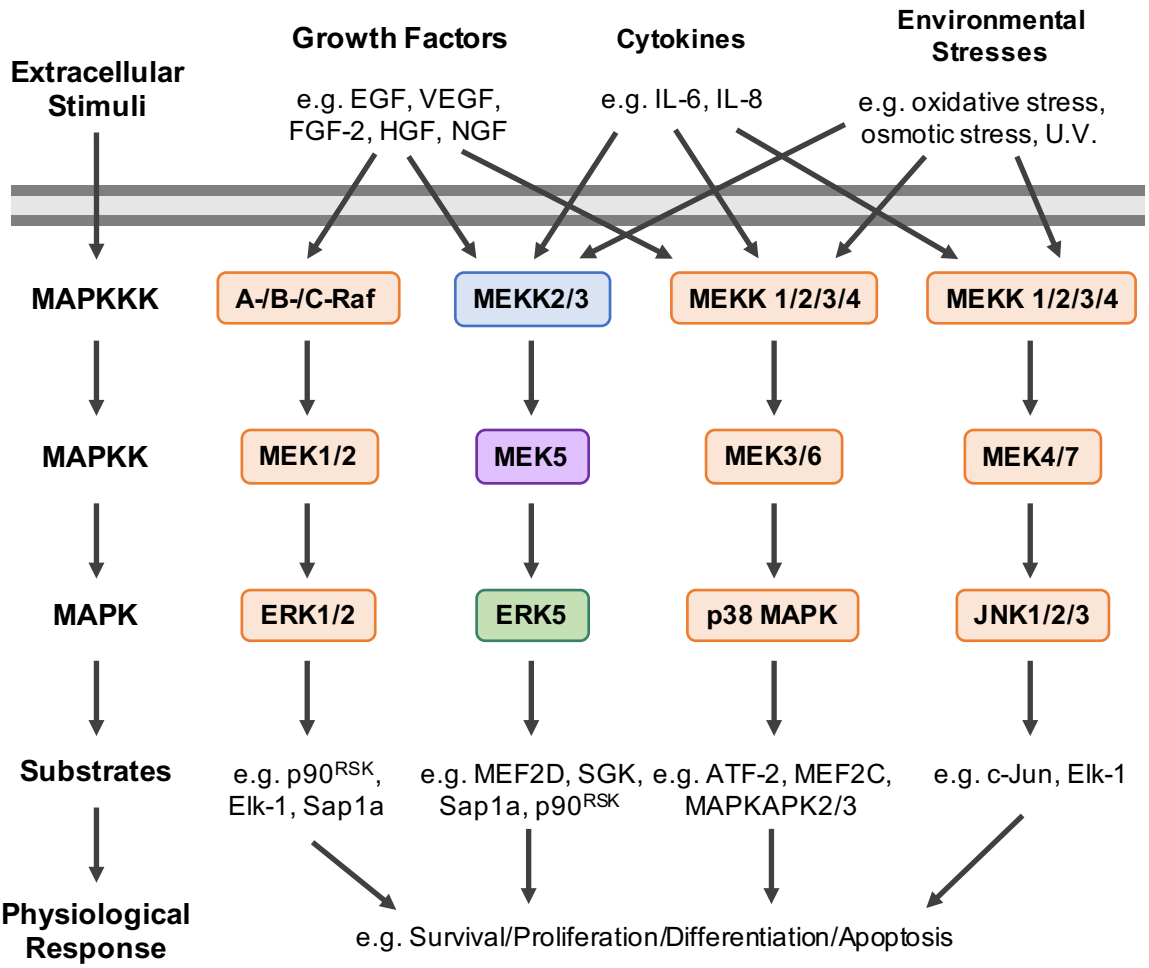

Figure 1.5 Mitogen-activated protein kinase (MAPK) signalling cascade

MAPK signalling cascade transduces extracellular signals, such as presence of growth factors, cytokines or environmental stresses, into cellular responses. There are four MAPK cascades; ERK1/2, ERK5, p38 MAPK and JNK 1/2/3. The response is brought about by the sequential phosphorylation and activation of three modules; MAPK kinase kinase (MAPKKK), MAPK kinase (MAPKK) and MAPK. Activated MAPK then phosphorylate their substrates, usually transcription factors but could also include structural proteins, cytoplasmic enzymes and phospholipids, to exert their cellular response. Image modified from Nithianandarah-Jones *et al*, Cellular Signalling, 2012 [89].

1.5.3 ERK5 signalling cascade

MEK5 is the upstream MAPKK capable of phosphorylating and activating ERK5 [89].

Once phosphorylated by MEK5, ERK5 undergoes autophosphorylation in several

sites of its C-terminal tail [95]. Downstream targets of ERK5 include members of the myocyte enhancer factor (MEF) family; MEF2A, C and D [96], as well as c-Myc, CREB and Sap1-a [97, 98]. Activation of these effector molecules results in changes in cellular proliferation, survival and differentiation [89].

Activation of ERK5 has been observed in the response to stress (H_2O_2 [99]), growth factors (G-CSF [100] and EGF [101]) and cytokines (LIF [102]). Most recently, it has been described as a negative regulator of vomocytosis of *C. neoformans* [84]. The exact mechanism by which ERK5 is able to influence vomocytosis remains to be elucidated, but its relationship with other known modulators of vomocytosis has been explored in this work (see Chapter 4).

1.6 *Cryptococcus* and HIV co-infection

For the first 100 years after the initial discovery of *C. neoformans*, this was a relatively "low profile" rare fungus, only known to mycologists and few clinicians. It was not until the onset of the HIV pandemic in 1980 that the deadly potential of this fungus was really discovered. Ever since, the HIV^+ population, together with an increase in immunosuppressed population due to organ transplant and cancer, has kept *Cryptococcus* in the limelight [103, 104].

A lot of work has focused on the HIV-*Cryptococcus* relationship, revealing the undoubted requirement for T cells to effectively clear or contain the infection. Aside from a diminished $CD4^+$ T cell count at the later stages of infection, HIV^+ patients experience a long-lasting viral infection with the concomitant mounting of an anti-viral immune response [105]. Therefore, the immunological context encountered by *Cryptococcus* in this population differs from that of an uninfected host and will be described in more detail below.

1.6.1 The anti-viral immune response

As it happens with the other pathogens, the response mounted towards viral infection can be classified into innate and adaptive. The first one being the fastest, charged with recognising the threat and instructing the adaptive response to produce and activate $CD8^+$ T cells [31]. This report will focus on the innate anti-viral response, where recognition and induction of type-I interferons are key.

Type-I interferons were originally termed viral interferons due to their role in anti-viral response [106]. This group is comprised of IFNα, IFNβ, IFNε, IFNκ and IFNω in humans. The two most studied type-I interferons are IFNα and IFNβ, of which there are 13 and 1 subtypes, respectively. The genes for type-I interferons share chromosomal location (clustered in chromosome 9 in humans) and the resulting cytokines have similarities in structure, regulation and function, a key feature being that they all signal through the IFNα/β receptor (IFNAR) [107]. More recently, a third family of interferons was described. Type-III interferons, IFNλ1, IFNλ2 and IFNλ3, are more closely related in structure and sequence to IL-10 than to IFNα/β. They do not signal through the shared IFNAR receptor but through their own IFNLR, which is expressed primarily on epithelial cells. Nonetheless, they are induced by viral infections and are capable of eliciting an anti-viral response, thereby justifying their classification as interferons [108].

Virtually every cell in our body has the ability to produce type-I interferons, although plasmacytoid dendritic cells produce the highest titres and are considered natural producers of these cytokines [109, 110]. Type-I interferons can be induced by a viral infection *per se* through the activation of intracellular sensors (such as the helicases RIG-I or MDA-5) or through signalling by the endosomal toll-like receptors TLR3, TLR7, TLR8 or TLR9. Alternatively, type-I interferons can be induced in a paracrine positive feed-back loop by type-I interferons produced by a neighbouring cell (see figure 1.6) [111].

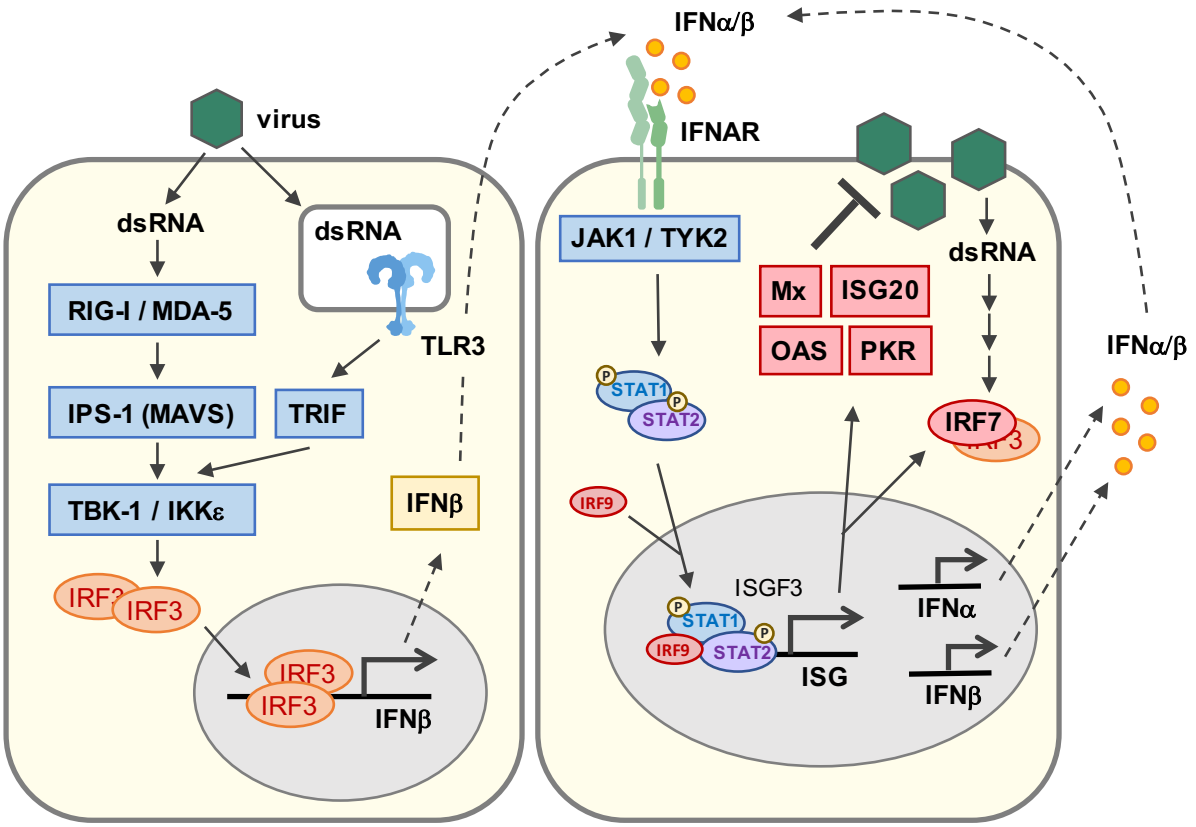

Figure 1.6 Induction of type-I interferons

Cytosolic sensors (RIG-I or MDA-5) or endosomal toll-like receptors (TLR3, TLR7-9 in plasmacytoid dendritic cells, not shown) recognize viral components and initiate a signalling cascade which ends with the production of IFNβ. IFNβ, and later IFNα, signal through the IFNα/β receptor (IFNAR) to induce the expression of interferon-stimulated genes. These include antiviral proteins and type-I interferons. See text for more detail. Image adapted from Haller *et al*, Virology, 2006 [111].

dsRNA = double-stranded Ribonucleic acid, IFN = interferon, IFNAR = IFNα/β receptor, IKK = inhibitor of nuclear factor κB kinase, IPS-1 = IFNβ promoter stimulator 1, IRF = IFN-regulatory factor, ISG = interferon-stimulated gene, ISGF = IFN-stimulated gene factor, JAK1 = Janus kinase 1, MAVS = mitochondrial antiviral signalling protein, MDA-5 = Melanoma Differentiation-Associated protein 5, Mx = Myxovirus resistance protein , OAS = 2′-5′ oligoadenylate synthase, PKR = protein kinase R, RIG-I = retinoic acid-inducible gene I, STAT = signal transducer and activator of transcription, TBK-1 = TANK binding kinase 1, , TLR3 = Toll-like receptor 3, TRIF = TIR-domain-containing adapter-inducing IFNβ, TYK2 = Tyrosine kinase 2.

Irrespective of how they came about, all type-I interferons signal through their shared receptor to induce the expression of "interferon-stimulated genes", ISG. Some of the ISG code for proteins which have known anti-viral properties, the best studied in this

respect are protein kinase R (PKR), 2′-5′ oligoadenylate synthase (OAS) and myxovirus resistance proteins (Mx). PKR is a dsRNA-dependent protein kinase which phosphorylates the alpha subunit of the protein synthesis initiation factor 2, eIF-2α. This phosphorylation inhibits translation of proteins dampening viral replication, as this depends on host machinery to produce its progeny. The second is an oligoadenylate synthase, which catalyses the synthesis of 2′-5′ oligoadenylates from ATP. These, in turn, activate RNAse L which degrades viral and cellular RNA. Finally, Mx proteins are GTPases which can interact with themselves and with viral ribonucleoproteins. Depending on whether this interaction takes place in the cytoplasm or in the nucleus, it inhibits viral assembly or transcription, respectively [31, 107].

The expression of ISG helps create an anti-viral state in infected and uninfected proximal cells, limiting viral spread and aiding NK cells, and $CD8^+$ T cells at a later stage, to clear or contain the infection.

1.6.2 Human immunodeficiency virus

Human immunodeficiency virus (HIV) is a single stranded positive lentivirus. It infects $CD4^+$ cells, mainly $CD4^+$ T cells, and causes their depletion leading to acquired immunodeficiency syndrome (AIDS). Upon infection, an anti-viral response is mounted which includes production of type-I interferons and activation of $CD8^+$ T cells. Over the first months of HIV infection, a race occurs between the $CD8^+$ cytolytic T cell response and the ability of the virus to mutate the epitopes targeted by this response. Reaching a balance defines the initial viral set point. Over time, the

depletion of $CD4^+$ T cells, coupled with exhaustion of both $CD4^+$ and $CD8^+$ T cells, causes the onset of AIDS. Type-I interferons are produced throughout the course of infection [105, 112, 113], with positive as well as negative effects in terms of prognosis. Apart from the anti-viral effects of type-I interferons mentioned in the previous section, prolonged production of these cytokines can lead to a state of "immune activation" which increases the risk of serious non-AIDS events such as atherosclerotic vascular disease.

The interplay between type-I interferons and cryptococcosis has been addressed before, with opposing findings in the literature [114, 115]. This disparity might be attributed to minute differences in the infection models or specific *Cryptococcus* strain used. Nonetheless, they clearly show a need for further study of this complex interaction. The next section describes the current knowledge on the impact of type-I interferons on fungal infections.

1.7 Type-I interferons and fungal infections

Type-I interferons are best known for their anti-viral effects on both virus-infected and uninfected bystander cells, where they induce the transcription of various interferon-stimulated genes, which interfere with multiple stages of viral replication and spread (see Figure 1.6). The best studied type-I interferons are IFNα and IFNβ, but this family also includes IFNε, IFNκ and IFNω. As mentioned before, all type-I interferons signal through a common receptor; interferon-α/β receptor (IFNAR), which is present in the surface membrane of virtually all human cells [116, 117]. These so-called "antiviral cytokines" also play a role in non-viral infectious settings, although these effects are still poorly understood and often need to be examined in a species-specific manner [118].

Among non-viral infectious settings, the vast majority of the work has focused on bacterial infections. Both protective as well as detrimental roles have been reported during infection with numerous bacteria [118].

The mechanisms of action responsible for their beneficial role, when elucidated, have been very diverse; regulating tryptophan availability through activation of 2,3-dioxygenase (*Chlamydia trachomatis* [119]), aiding in macrophage polarisation towards a classically activated phenotype with heightened bactericidal activity (*Legionella pneumophila* [120]), contributing to macrophage activation and production of pro-inflammatory cytokines (*Escherichia coli*, *Streptococcus pneumoniae* [121]).

Detrimental roles have also been attributed to type-I interferons during bacterial infections, with the most notable examples being *Listeria monocytogenes* and *Mycobacerium tuberculosis*. In the former, it has been shown that type-I interferons are responsible for sensitising lymphocytes to the pore-forming virulence factor listeriolysin O, leading to apoptosis [122-125], and blocking macrophage responsiveness to IFNγ through downregulation of its receptor IFNγR [126, 127]. For the latter, suppression of host-protective cytokines [128-131], blocking of macrophage responsiveness to IFNγ [130, 132, 133] and enhanced trafficking of *M. tuberculosis*-permissive cells [134, 135] have been reported to contribute to the negative role of IFNα/β in *M. tuberculosis* infection. Other bacterial infections where IFNα/β enhance susceptibility or contribute to the exacerbation of disease include *Brucella abortus* [136], *Yersinia pestis* [137] and *Staphylococcus aureus* [138].

The interplay between type-I interferons and fungal infections has not been extensively studied, although the reports available show that the effects also range from protective to detrimental for the host, depending on the fungal species (and sometimes on the protocol followed!). I will summarise the main findings pertaining to the most studied fungal species; *Histoplasma*, *Pneumocystis*, *Aspergillus*, *Candida* and *Cryptococcus* (Figure 1.7, page 40).

1.7.1 *Histoplasma*

Histoplasma capsulatum is a dimorphic primary fungal pathogen. Infection starts with inhalation of airborne conidia, where the higher body temperature of the host triggers differentiation into pathogenic yeasts. Within the host, yeasts are taken up primarily

by macrophages, and to a lesser extent by neutrophils and dendritic cells [139]. Early reports showed that macrophages co-infected with lymphocytic choriomeningitis virus (LCMV) and *H. capsulatum* exhibited decreased anti-histoplasma activity, which was reversed in the presence of an IFNAR neutralising antibody [140]. Thus suggesting a permissive role of type-I interferons in *H. capsulatum* infection. In line with these results, Inglis *et al.* showed that mice lacking IFNAR1, a subunit of IFNAR, better controlled infection with *H. capsulatum* in lungs and spleen than wildtype mice [141]. It was later described, however, that type-I interferons produced by dendritic cells are key to controlling the growth of *H. capsulatum* within the host. Their production is mediated by TLR7/9 recognition of yeast cells, and is required for the onset of a protective Th1 response [142], having an overall beneficial role for the host.

It is currently unclear what causes the difference between these studies and which factors determine whether type-I Interferons are protective or detrimental in *H. capsulatum* infection.

1.7.2 *Pneumocystis*

Pneumocystis jirovecii is an opportunistic human fungal pathogen. It causes severe pneumonia in immunocompromised patients, most often those suffering from AIDS [143]. Studies on the effect of type-I interferon during *Pneumocystis* infection have tried to mimic immunocompromised conditions such as low $CD4^+$ T cell count and bone marrow failure resulting in pancytopenia. Initial work in mice, using the murine strain *P. carinii*, showed that type-I interferon signalling has differential effects in CD4-depleted versus CD4-sufficient hosts. In CD4-depleted hosts, IFNAR signalling aids

the recruitment and activation of $CD8^+$ cells which ultimately leads to immune-mediated lung damage. In CD4-sufficient animals, however, IFNAR signalling helps down-regulate inflammation after pathogen clearance [144].

The same group then looked at *Pneumocystis* infection in mice lacking lymphocytes and IFNAR ($IFrag^{-/-}$). Using this model, they showed that type-I interferon signalling and B cells are important for the maintenance of haematopoiesis during *Pneumocystis* infection, which otherwise causes bone-marrow failure [145, 146].

1.7.3 *Aspergillus*

Aspergillus are saprotrophic fungi, often found on decaying matter in the environment. Upon starvation, they release airborne conidia which are routinely inhaled by humans [147]. These can reach the alveoli in the lung and, if unchallenged due to a weakened immune system, can germinate and cause disease known as invasive aspergillosis. *A. fumigatus* is the main species responsible for invasive aspergillosis and as such has been the principal focus of scientific research [148]. In fact, the first report of type-I interferons having an effect on fungal infection corresponds to Tandon *et al.*, where they show that treatment with IFNα or polyIC (a type-I interferon inducer) increases survival of mice infected with *A. fumigatus* [149]. Since then, several studies have confirmed the beneficial effect of type-I interferons on *A. fumigatus* infection. Gafa *et al.* showed that addition of exogenous IFNβ enhances activation of *A. fumigatus*-infected dendritic cells, which improves their ability to prime a Th1 response [150]. It was later reported that human bronchial epithelial cells

are able to internalise conidia, and this event induces the expression of IFNβ by these cells [151].

It is well known that plasmacytoid DC (pDC) are the main producers of type-I interferons [152]. Ramirez-Ortiz *et al.* demonstrated that depletion of these cells renders mice hypersusceptible to challenge with *A. fumigatus* [153], confirming their protective role. Later on, the same group showed that pDC detect *A. fumigatus* hyphae through the surface lectin Dectin-2, and respond with production of IFNα, TNFα and formation of extracellular traps [154].

Recently, monocytes have been described as an early source of type-I interferons in *A. fumigatus* infection [155]. They are reported to prime for production of type-III interferons in other pulmonary cells, and together activate neutrophils for clearance of *A. fumigatus* [155]. In line with these findings, treatment with polyICLC, a more stable version of polyIC, dramatically protected mice from invasive aspergillosis [156], through transient production of type-I interferons and early recruitment and activation of neutrophils.

1.7.4 *Candida*

Candida species are present on human mucosal surfaces as a commensal organism, mainly in the gastrointestinal tract. Upon immunosuppression or disturbance of the microbiome, *Candida* can cause disease ranging from superficial infection (oral and vaginal candidiasis) to life-threatening systemic infection (disseminated candidiasis) [157]. *C. albicans* is the leading cause of hospital-acquired infections [158], potentially

due to its ability to form biofilms on medically implanted devices [159], and has therefore been the focus of scientific studies.

Research on the effect of type-I interferons on infection with *C. albicans* have generated conflicting results, indicating that the effect of these pleiotropic cytokines is more complex than previously thought.

Initial reports showed that treatment with polyIC enhanced susceptibility to systemic candidiasis in mice with severe combined immunodeficiency (SCID) [160], suggesting that type-I interferons play a detrimental role on innate immunity to *Candida* infection. In line with these initial findings, Guarda *et al.* showed that type-I interferons inhibit IL-1 production and inflammasome activation, which then translates to a higher susceptibility to *C. albicans* challenge in wildtype mice [161].

Treatment with IFNβ specifically was shown to increase fungal burden and enhance mortality of mice infected with *C. albicans* through IFIT2-mediated inhibition of NADPH oxidase activity [162]. *In vitro*, it was shown to decrease expression of C-type lectins Dectin-1 and mannose receptor, and decrease uptake of unopsonised *C. albicans* in monocyte-derived macrophages [163].

Majer *et al.* also showed that type-I interferon signalling has a detrimental effect for the host in a mouse model of experimental candidiasis. Paradoxically, the mechanism observed in this case is enhanced activation and recruitment of neutrophils to the site of infection and exacerbated immunopathology [164]. Following a very similar

protocol, however, del Fresno *et al.* arrived at the opposite conclusion; IFNAR deficiency, through a decrease in neutrophil recruitment to the site of infection, results in a higher mortality rate [165]. This suggests a protective role of type-I interferon signalling during *Candida* infection. Supporting this notion, two further studies found protective type-I interferon responses, mediated by TLR7/9 in conventional DC [166, 167].

Earlier work had found that type-I interferons enhance the antifungal activity of neutrophils in oral candidiasis [168]. This effect was later seen in a systemic candidiasis model, acting through production of IL-15 [169].

Furthermore, a genome-wide transcription approach revealed a very strong type-I interferon signature profile during *C. albicans* infection in human peripheral blood mononuclear cells. Association analysis then confirmed that defects in this pathway enhance susceptibility to candidiasis [170].

A few studies investigated the therapeutic capability of IFNα in vulvovaginal candidiasis (VVC), having promising results using vaginal epithelium cell lines [171] and in a rat model [172]. *In vivo* data from VVC patients showed decreased levels of IFNβ and IL-23 compared to healthy controls, suggesting a protective role for these cytokines in VVC [173].

1.7.5 *Cryptococcus*

Research on the effects of type-I interferons on cryptococcal infection have yielded conflicting results. On the one hand, Sato *et al.* showed that IFNAR KO mice had increased mucus production in their lungs which allowed for an enhanced fungal clearance rate, suggesting a detrimental role for type-I interferons in *C. neoformans* infection [114].

On the other hand, using the same model, Biondo *et al.* found that IFNAR KO mice were incapable of controlling infection with *C. neoformans*, showing higher fungal burden and a Th2-skewed immune response [174]. Thus, this study implies that type-I interferon signalling is necessary to establish a protective Th1 response. Consistent with these findings, Sionov *et al.* showed that treatment with polyICLC greatly enhanced survival of mice infected with *C. neoformans*, and that this protective effect was mediated by type-I interferon production and polarisation to a Th1/Th17 response [115].

Beneficial effects of type-I IFN		Detrimental effects of type-I IFN
Key for induction of a protective Th1 response.	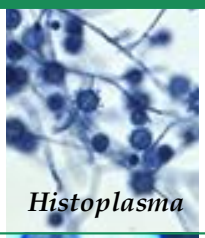 *Histoplasma*	IFNAR1 KO mice show lower fungal burden in lungs and spleen. Co-infection with LCMV in macrophages results in diminished anti-fungal activity.
IFNAR signalling dampens inflammation after pathogen clearance. IFN-I help maintain extra-medullar haematopoiesis in Ifrag$^{-/-}$ mice.	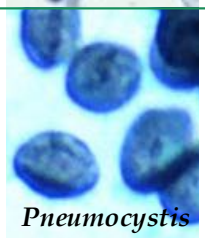 *Pneumocystis*	IFN-I mediate lung damage in CD4-depleted mice.
Increases survival of infected mice. Enhances activation of infected DC and induce protective Th1 response. Activation of neutrophils.	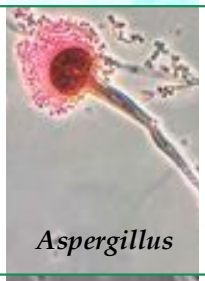 *Aspergillus*	
Enhances mortality in IFNAR KO mice, due to lower recruitment of neutrophils. Enhances antifungal activity of neutrophils in oral and systemic candidiasis. Treatment with IFNα improves symptoms in VVC model.	 *Candida*	polyIC treatment enhances susceptibility in SCID mice. Inhibition of IL-1 production, NADPH-oxidase and inflammasome activation. Inhibition of phagocytosis of unopsonised *C. albicans*. Exacerbated immunopathology, through recruitment and activation of neutrophils.
Higher fungal burden and Th2-skewed response in IFNAR KO mice. Enhanced survival with polyICLC treatment, due to induction of protective Th1/Th17 response.	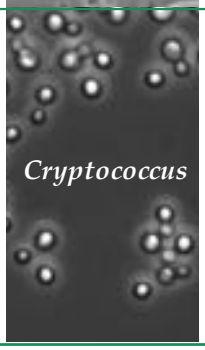 *Cryptococcus*	Enhanced fungal clearance in IFNAR KO mice.

Figure 1.7 Reported effects of type-I interferons on fungal infections

Main findings regarding the effects of type-I interferons on the host undergoing a fungal infection, as discussed in text. Credits for figures: Centers for Disease Control and Prevention website -*Histoplasma*, *Pneumocystis* and *Aspergillus*- and Microbiology Society -*Candida*-.

1.7.6 Genetic deficiencies in Type-I interferon signalling

Genetic deficiencies in the IFN-I signalling pathway have not yet been directly linked to increased incidence of fungal infections. There is, however, an association between gain-of-function mutations in the signal transducer and activator of transcription 1 (STAT1) and chronic mucocutaneous candidiasis (CMC) disease [175]. STAT1 is involved in the signalling of type-I and type-II interferons [116]. This mutation causes enhanced type-II interferon (IFNγ) signalling, which inhibits transcription of IL-17 and impairs protective Th17 responses [175].

Signalling of type-I interferons requires the formation of a heterodimer between STAT1 and STAT2 [116]. Deficiencies in STAT2 are not common, with thus far only a single family being described [176]. In this case, one sibling developed disseminated measles after routine immunisation with the vaccine strain and an infant sibling died of severe disseminated viral infection. Other surviving family members, however, have remained generally healthy despite documented history of viral infections [176].

A couple of cases of IFNAR deficiencies have been reported [177, 178]. One patient presented with a severe case of cytomegalovirus infection, and was later found to have a deficiency in IFNAR1 subunit. This patient received attenuated measles, mumps and rubella (MMR) vaccine without adverse reaction [178]. A second patient with an IFNAR2 subunit deficiency developed a severe encephalitis as a complication of MMR vaccination [177]. Cells from either patient were unresponsive to type-I interferons [177, 178]. Given the increasing body of work describing the impact of type-I

interferons on fungal infections, interesting questions remain about how such patients might respond to fungal challenge.

1.7.7 Concluding remarks

Type-I interferons were first discovered for their role in controlling viral infections. Over the years, several research groups looked into the interplay of type-I interferons and other, non-viral pathogens, focusing mainly on bacteria. Evidence summarised here shows that their effect extends beyond viral and bacterial settings to include fungal pathogens.

The net effect of these pleiotropic cytokines on the outcome of fungal infections is not straightforward, ranging from beneficial to detrimental to the host in different fungal infection settings. However, an increasing body of research is looking to harness the immunomodulatory ability of type-I interferons as therapeutic tools to fight fungal infections and reduce inflammation and pathology.

2 Aims and Objectives

The findings presented in this Thesis aim to broaden the understanding of Cryptococcal infection. The work was carried out with a particular emphasis on the understudied phenomenon of vomocytosis, and on the incorporation of biological context cues into the experimental design.

With this in mind, the following objectives were proposed; the first objective was to delve deeper into the regulation of vomocytosis and explore how different modulators interact between them (Chapter 4). A second objective was to evaluate the potential impact of the biologically relevant viral infection context on vomocytosis (Chapter 5). Finally, the third objective was to explore the effects of prolonged exposure to *C. neoformans* or its components, on antigen presentation and antigen-induced T cell proliferation (Chapter 6).

3 Materials and Methods

Parts of this chapter have been published in research articles of which I am a co-author [84, 179]. The complete articles can be found in the Appendix.

A brief description of the experimental protocols and techniques used is detailed below. All reagents were purchased from SIGMA unless otherwise stated.

3.1 Generation of stocks and Cell culture

3.1.1 Cryptococcal strains

The main body of work was done using *C. neoformans* strain Kn99α, either wildtype or fluorescently-labelled. Wildtype strain was a kind gift of Dr. Kirsten Nielsen and was GFP-tagged [180] by Dr. Ewa Bielska in house. mCherry-expressing Kn99α [181] was a kind gift from Dr. JK Lodge.

Mutant strain of *C. neoformans* Δ*ras1* [182, 183] was supplied by Dr. Elizabeth Ballou and the acapsular strain Δ*cap59*Δ*uge1* [184], designated ΔCap, was provided by Guilhem Janbon.

3.1.2 Cryptococcal culture

Cryptococcal glycerol stocks were kept at -80°C. Every 2 – 4 weeks, working stocks were made by streaking glycerol stocks onto 5% Yeast Peptone Dextrose (YPD) 2% Agar plates. These were incubated at 25°C for 24 – 72 hours and stored at 4°C thereafter. When streaking GFP- or mCherry-modified strains, 250 µg/mL Hygromycin was added to the plate to select for the mutant.

"Overnight" liquid cultures were made by inoculating 3 mL YPD broth with a loopful of the working stock of the desired strain and incubating for 18 – 24 hours at 25°C on an orbital rotator set at 20 rpm.

3.1.3 Bacterial culture

Wildtype strain of *Pseudomonas aeruginosa*, strain PA14, was maintained on Lysogeny broth (LB) 2% Agar plates. "Overnight" liquid cultures were made by inoculating 10 mL LB broth with a loopfull of PA14 and incubating for 18 – 24 hours at 37°C on a shaking incubator set at 200 rpm.

3.1.4 Virus stocks and titration

HIV-1 and SIV*vpx* virus stocks were generated by Dr. Leanne Taylor-Smith while at Dr. Mahdad Noursadeghi's laboratory. A brief description of the strains and titration methods used is below.

HIV-1 virus stocks were generated by transfection of human embryonic kidney 293T cells (European Collection of Authenticated Cell Cultures) as previously described [185, 186]. The R9HIVΔ*env* virus was derived from clade B HIV-1 strain (NL43) with 500bp deletion in *env*, pseudotyped with vesiculostomatitis virus G envelope. SIV3mac single round virus-like particles (VLPs) containing vpx (SIV3*vpx*) were generated by transfection into 293T cells with pSIV3+ and pMDG plasmids [187, 188]. At 48, 72h and 96h viral containing supernatant was harvested, centrifuged at 800 x g for 10 min and filtered through 0.45 μm filter then centrifuged on a 20% sucrose cushion at 20,000 x g for 2h at 4°C. Purified virus was then re-suspended in RPMI media and frozen at -80°C.

To quantify single round HIV infection, a vial was thawed for each harvest and serial dilutions used to infect CCR5/CD4 and CXCR4/CD4 transfected NP-2 cells. At 72h post infection, wells were fixed in ice cold acetone-methanol and viral infection was assessed by p24 staining using a 1:1 mixture of the anti-p24 monoclonal antibodies EVA365 and EVA366 (NIBSC, Center for AIDS Reagents, UK). Infected cells were detected by light microscopy to provide a virus titre (focus-forming U/mL). The SIV3*vpx* particles were quantified after thawing using a reverse transcriptase (RT) assay colorimetric kit (Roche) following the manufacturer's instructions to provide a RT ng/mL titre.

Recombinant measles virus (MeV) strain IC323 expressing GFP (MeV-GFP) was a generous gift from Dr. Dalan Bailey. It was generated as previously reported in

Hashimoto *et al*. [189] and represents a virulent field isolate from Japan (Ichinose-B (IC-B) strain) isolated from a patient with acute measles in 1984 [190].

Virus stocks were generated using Vero cells (ATCC CCL-81) over-expressing human SLAM receptor (Vero-hSLAM cells), grown in DMEM supplemented with 0.4 mg/mL G418. Once at 80% confluency, Vero-hSLAM cells were infected with MeV-GFP at MOI of 0.01:1 in 5 mL media for 1 hour at 37°C. After 1h, a further 10 mL of DMEM supplemented with 10% foetal bovine serum (FBS) was added and infection allowed to continue for 48 h, when flasks were frozen at -80°C. After thawing, the collected supernatants were centrifuged at 2500 rpm for 10 min at 4°C to pellet cell debris, and virus-containing supernatant was aliquoted and kept at -80°C.

For titration of MeV-GFP virus, the TCID-50 method was followed. Vero-hSLAM cells were seeded into flat-bottomed 96 well plates and infected with serial dilutions of thawed MeV-GFP in triplicate. After 72 h, wells were scored for positive or negative infection under UV illumination on a Nikon TE- 2000 microscope.

3.1.5 Macrophage cell line J774A.1

The murine monocyte/macrophage cell line J774A.1 was cultured at 37°C with 5% CO_2 as described below. Dulbecco's Modified Eagle Media (DMEM) supplemented with 2 mM L- Glutamine, 100 units/mL Streptomycin, 0.1 mg/mL Penicillin and 10% FBS was used during culturing. This media will henceforth be referred to as Complete DMEM (cDMEM).

Stocks of J774A.1 were stored in a liquid nitrogen tank. When needed, cryovials were carefully retrieved from the stocks and quickly thawed in a 37°C water bath. Once completely thawed, the contents were added to 10 mL warmed cDMEM and spun at 1000 x g for 5 minutes at room temperature. The resulting pellet was re-suspended in 15 mL warmed cDMEM and transferred to a T75 tissue culture flask. Flasks were kept in a 37°C, 5% CO_2, humidified incubator.

Once confluent, as checked by observation under an inverted light microscope, cells were passaged. Old media was poured off and replaced with 10 mL fresh warmed cDMEM, and cells brought to suspension using a cell scraper. An appropriate dilution of the cell suspension was transferred to a new T75 flask and returned to the humidified incubator. Cells from passages 5 – 12 only were used for experiments.

3.1.6 Generation of stocks of J774A.1

Cells no older than passage 2 were used for generating stocks. Freezing media consisted of 50% FBS, 40% serum-free cDMEM and 10% dimethyl-sulfoxide (DMSO). Eight flasks of J774A.1 at confluent growth were brought to suspension in a total of 10 mL warmed cDMEM using a cell scraper. Cells were then spun at 1000 x g for 5 minutes at room temperature. The resulting pellet was re-suspended in 10 mL freezing media, yielding 4 – 6 million cells per mL. The suspension was aliquoted into 1 mL cryovials and frozen to -80°C at a 1°C/minute cooling rate using an isopropanol-containing chamber. Cryovials were kept at -80°C for 24 hours before being transferred to a liquid nitrogen tank.

3.1.7 Human macrophage isolation and culture

All work with human tissue was approved by the University of Birmingham Ethics Committee under reference ERN_10-0660. All donors provided written consent prior to donation. 20-40 mL of blood were drawn from healthy donors by venepuncture. 6 mL of whole blood were carefully layered on top of a double layer of Percoll (densities of 1.079 and 1.098 g/mL). Samples were centrifuged in a swing bucket rotor at 150 x g for 8 minutes, followed by 10 minutes at 1200 x g, with acceleration and brake set to zero. The resulting white disc of peripheral blood mononuclear cells (PBMC) was transferred to a clean vial and incubated with red blood cell lysis buffer at a ratio of 1:3 for 3 minutes, with gentle mixing throughout to prevent clot formation. Cells were then washed with ice cold phosphate-buffered saline (PBS) twice, with centrifugation at 400 x g for 6 minutes in between each wash, and counted with a haemocytometer. 1 x 10^6 PBMC were seeded onto 48-well plates in RPMI media containing 1% penicillin/streptomycin, 5% heat-inactivated AB human serum (which I will refer to as cRPMI) supplemented with 20 ng/mL M-CSF and kept at 37°C and 5% CO_2 in a humidified incubator. Cells were washed with PBS and re-suspended in fresh media on days 3 and 6 of differentiation. Macrophages were ready to use on day 7. A yield of 1 x 10^5 macrophages per well was estimated.

3.1.8 Generation of bone marrow-derived dendritic cells

Murine bone marrow-derived dendritic cells (BMDC) were produced following the method described in Lutz *et al* [191]. Briefly, bones from hind legs of wildtype BoyJ mice were exposed and cleaned with 70% ethanol. Within a cell culture hood, the epiphyses were excised with sterilized scissors, exposing the bone marrow. The bones

were then perfused with RPMI containing 2% heat-inactivated FBS using a syringe fitted with a 24G needle, washing down the bone marrow onto a petri dish. Clumps of cells were disaggregated by repeated passages through the needle. The cells were counted and made up to a concentration of 3 x 10^6 cells per 200 µL in PBS, spinning at 350 x g for 5 minutes if necessary. 200 µL of cell suspension were carefully dispensed onto a petri dish containing 10 mL DC-media supplemented with 20 ng/mL GM-CSF (hereto referred as differentiation media). DC-media consists of RPMI containing 1% penicillin/streptomycin and 10% heat-inactivated FBS. Cells were kept at 37°C and 5% CO_2 in a humidified incubator. On day 3, 10 mL differentiation media were added to the dish. On days 6 and 8, 9 mL of media were carefully aspirated from the dish and replaced with 10 mL fresh differentiation media. On day 10, 8 mL of media were discarded before collecting the cells in the remaining media. The resulting dendritic cells were counted and seeded onto culture plates for future assays.

3.1.9 $CD4^+$ T cell isolation

OT-II mice were generously provided by Dr. David Withers (University of Birmingham) and Prof Gordon Brown (University of Aberdeen). Splenocytes were isolated by Dr. Guillaume Desanti and the population was enriched in $CD4^+$ T cells following the manufacturer's instructions in a mouse $CD4^+$ T Cell isolation kit (Miltenyi Biotec, #130-104-454). The kit works by labelling the splenocytes with a negative selection cocktail coupled to biotin. Then adding anti-biotin microbeads, followed by magnetic cell separation using a MACS column separator. Unlabelled $CD4^+$ T cells were collected in the flow through of the column.

3.2 Experimental procedures

3.2.1 Cryptococcal growth curve protocol

To assess the effect of different compounds on the viability and growth rate of *Cryptococcus*, a growth curve assay was performed. This assay was carried out on a 48-well plate as follows: 495 µL of YPD broth containing the different compounds to be tested were dispensed into individual wells. Each well was subsequently inoculated with 5 µL of a ten-fold diluted cryptococcal overnight culture (final dilution in well: 1000-fold). Immediately after, the plate was sealed with a breathable membrane and taken to a fully automated plate reader (BMG Omega Fluostar). The plate was incubated at 37°C without CO_2 for 24 hours, with orbital shaking during the non-reading part of the cycle. Optical density measures at 600 nm were taken every 30 minutes during the incubation period.

3.2.2 Cryptococcal infection assay

Cryptococcal infection assays using human monocyte-derived macrophages were carried out in the same plate as the differentiation process described in section 3.1.7, to avoid unnecessary detaching and re-seeding steps. For the majority of the infection assays performed, macrophages were not previously activated. In initial experiments (Figures 5.5 and 5.7 – IFNα data only), human monocyte-derived macrophages were activated with 1 µg/mL LPS and 1000 IU/mL IFNγ in cRPMI overnight.

Immediately before infection, cryptococcal cells from an overnight liquid culture were opsonised by incubation with PBS containing 10% human serum (AB serum) for 1 hour at room temperature on an orbital rotator set at 20 rpm. Alternatively, opsonisation was done by incubation with 10 μg/mL anti-capsule antibody (18B7, a kind gift from Dr. Arturo Casadeval) in PBS for 1 hour (same conditions as with serum opsonisation).

Macrophage media was replaced with serum-free cRPMI, and opsonised-*Cryptococcus* were added to each well respecting an MOI = 10. If the effect of any compound was being tested, these would be added to the well at the desired concentration at this time.

Two hours later, the media was removed and each well washed 3 times with PBS. Fresh serum-free media, containing the appropriate drug concentration if applicable, was added to every well. This time point was noted as T_0.
This standard infection assay was followed by different techniques (see below) to allow for different read-outs.

3.2.3 *Cryptococcus*:virus co-infection assay

Human monocyte-derived macrophages were infected with either attenuated HIV or MeV-GFP, and subsequently infected with *C. neoformans* as follows:

For attenuated HIV co-infections, 24 h before Cryptococcal infection, human monocyte-derived macrophages were infected either with R9HIVΔ*env* at a MOI of

10:1, SIV3*vpx* at 3 ng/mL or both, in serum free-RPMI. At 24 h post infection, duplicate wells were fixed in ice cold acetone-methanol and infected cells were identified by staining for p24 protein as described above (see section 3.1.4). Experimental wells were infected with antibody opsonised-*Cryptococcus* Kn99α-GFP for 2 hours, washed to remove extracellular fungal cells, and replenished with fresh serum free-media.

Alternatively, macrophages were infected with MeV-GFP at an MOI of 5:1 in serum free-media and kept at 37°C with 5% CO_2. After 24 hours, cells were washed with PBS and fresh cRPMI was added. After 3 days, cells were co-infected with serum opsonised-*Cryptococcus* Kn99α-mCherry for 2 hours, washed to remove extracellular fungal cells, and replenished with fresh serum free-media.

3.2.4 *Cryptococcus*:bacteria co-infection assay

J774A.1 cells were seeded in a 48 well plate, at 0.5 x 10^5 cells per well, in cDMEM and kept at 37°C with 5% CO_2 overnight. As of this point, the culture media used was not supplemented with antibiotics.

Cells were activated using 150 ng/mL phorbol myrstate acetate (PMA) in serum free-DMEM for 1 hour, and subsequently infected with AB serum opsonised-*Cryptococcus* Kn99α-GFP at an MOI = 10.

P. aeruginosa PA14 from an overnight liquid culture was washed three times with PBS before bacterial concentration was inferred by optical density at 600 nm reading.

After 2 hours, *Cryptococcus*-infected wells were washed three times with PBS to remove extracellular fungal cells, and replenished with fresh serum free-media containing PA14 at an MOI = 0.25.

3.2.5 Macrophage polarisation assay

To study the impact of different compounds on the activation state of macrophages, a polarization assay was performed. This assay was performed on J774A.1 murine macrophages using cDMEM containing heat-inactivated FBS, which will be referred to as cDMEM-HI. Macrophages were seeded on a 96-well plate the day prior to the experiment at 0.2 x 10^6 cells/mL in cDMEM-HI and kept in the humidified incubator overnight. The following day macrophages were activated with PMA (as indicated in section 3.2.4) or incubated with fresh cDMEM-HI for 1 hour. After activation, cells were incubated with cDMEM-HI containing the polarising stimuli, in the presence or absence of the compound of interest, for 24 hours. Once the incubation was over, the plate was put on ice. Supernatants were transferred to a new plate and stored for further cytokine measurements and cells were stained for flow cytometry (see sections 3.3.1 and 3.3.3).

The polarising stimuli used were as follows: 20 ng/mL IL-4 (Immunotools), 20 ng/mL lipopolysaccharide (LPS) and 1000 IU/mL IFNγ (Immunotools). Compounds tested include ERK5 inhibitor XMD17-109 1 μM and DMSO control.

3.2.6 Dendritic cell activation assay

Cells were generated as described in section 3.1.8 and seeded onto a 48-well plate at 1 x 10^6 cells per well. One hour after seeding, the activating stimuli was added to the cells in RPMI containing 1% penicillin/streptomycin and 10% heat-inactivated FBS. Cells were incubated for 24 hours at 37°C with 5% CO_2. Once the incubation was done, the plate was placed over ice and the supernatant carefully removed. Cells were then stained for flow cytometry and the supernatant used in ELISA assays (see sections 3.3.3 and 3.3.1).

The activating stimuli used were 1 mg/mL chicken ovalbumin (OVA, Invitrogen #vac-pova-100) or 100 ng/mL ovalbumin peptide 323-339 (OVAp, #O1641), added in combination with AB serum-opsonised Δ*ras1* (see section 3.2.2) at an MOI = 1 or PBS 10% AB as control.

3.2.7 Dendritic cell:T cell co-culture assay

To explore the effect of Cryptococcal exposure on antigen presentation and T cell proliferation, an *in vitro* dendritic cell:T cell co-culture was set up. A schematic representation of this experimental system can be found in Chapter 6, Figure 6.1.

BMDC were generated as described in section 3.1.8 and seeded in a round-bottomed 96 well plate at 40 x 10^3 cells per well. Cells were kept in 50 μL of RPMI containing penicillin/streptomycin, supplemented with 10% heat-inactivated FBS, and activating stimuli was added in 50 μL increments to make up 200 μL final total volume.

BMDC were stimulated with OVA or OVAp (final concentration in well: 1 mg/mL and 100 ng/mL, respectively), and AB serum-opsonised *C. neoformans* (see section 3.2.2) at an MOI = 1 or PBS 10%AB serum as control. The majority of the work was done using the mutant strain Δ*ras1*, but wildtype Kn99α and Δ*cap59*Δ*uge1* were also tested.

If the effect of drugs or the presence of inert beads were being investigated in the system, they were also added at this point. Drugs tested include IFNα (R&D, #12100-1) at a final concentration of 10 pg/mL, ERK5 inhibitor XMD17-109 at a final concentration of 1 μM or DMSO control. 7 μm inert beads (Micro particles based on polystyrene, #78462) were treated in the same way as *C. neoformans* before being added to BMDC; they were washed with PBS three times and opsonised in PBS 10% AB serum for 1 hour (see section 3.2.2). Stimulated BMDC were incubated at 37°C with 5% CO_2 overnight.

$CD4^+$ T cells from spleen of OT-II mice were isolated as described in section 3.1.9. The population enriched in $CD4^+$ T cells was then labelled with carboxyfluorescein succinimidyl ester (CFSE) using CellTrace™ CFSE Cell Proliferation kit (Invitrogen, #C34554) and following manufacturer's instructions. CFSE-labelled CD4+ T cells were added to stimulated BMDC at 5:1 ratio (200 x 10^3 cells per well).

After 4 days-incubation, supernatants were carefully removed and stored at -80°C for further cytokine profiling, and cells were stained for flow cytometry (see sections 3.3.2 and 3.3.3).

3.3 Molecular Techniques

3.3.1 Enzyme-linked Immunosorbent assay (ELISA)

Supernatants from infection or polarisation assays were stored at -80°C until analysis. IL-10, IL-12p40, TNFα and Ym1 levels were measured by sandwich ELISA using various kits and antibody pairs, see table below. In all cases the ELISA protocol provided by R&D was followed, using an 8-point standard curve with recombinant protein.

Cytokine	Species	Brand	Capture Antibody # Catalogue	Detection Antibody # Catalogue	[Highest Std]
IL-10	mouse	R&D	DY417	DY417	2000 pg/mL
	human		DY217B	DY217B	
IL-12p40	mouse	R&D	DY499	DY499	2000 pg/mL
	human		DY1240	DY1240	4000 pg/mL
TNFα	mouse	R&D	DY410	DY410	2000 pg/mL
	human	BD	551220	554511	
Ym1	mouse	R&D	MAB2446	BAF2446	5000 pg/mL

Table 3.1 Antibody pairs used for ELISA measurements

3.3.2 Multianalyte profiling (Luminex)

Supernatants from DC:T cell co-cultures were stored at -80°C until analysis. IL-2, IFNγ, TNFα, IL-4, IL-13 and IL-17A levels were measured using a custom multiplex panel (ProcartaPlex Immunoassay, Invitrogen), following manufacturer's instructions and

acquired in a Luminex 200 system. Multianalyte profiling follows a similar protocol to conventional sandwich ELISA, but allows for the concentration of multiple proteins within one sample to be read simultaneously.

3.3.3 Flow Cytometry

The staining protocol was carried out on the same plate as the experiment was done previously, to avoid damaging potentially important epitopes during detachment of the cells. Throughout the staining protocol the cells were kept on ice, exposed to EDTA for a prolonged period of time and finally fixed with the fixative included in Foxp3 / Transcription Factor Staining Buffer Set (eBioscience #00-5523-00), ensuring the lifting of the majority of the cells within the samples.

Cells were placed on ice and washed twice with PBS, spinning at 350 x g for 5 minutes each time. Afterwards, the samples were incubated with 10 µL of a fixable live-dead dye (Thermo Fisher) at room temperature, protected from the light. After 10 minutes, 10 µL of a blocking solution was added on top, to inhibit non-specific binding of the labelling antibodies to the samples on the following step. The samples were kept on ice and protected from the light form here onwards. After at least 15 minutes, 30 µL of the antibody mix was added to the samples and incubated for 30 minutes. The cells were then washed twice with PBS containing 2 mM EDTA and 0.1% BSA, spinning at 350 x g for 5 minutes each time. The samples were then fixed by incubation with 100 µL of the fixative present in Foxp3 / Transcription Factor Staining Buffer Set (eBioscience #00-5523-00) overnight at 4°C or 20 minutes at room temperature.

Finally, the samples were washed twice with PBS containing 2 mM EDTA and 0.1% BSA, spinning at 350 x g for 5 minutes each time.

Fixed samples were acquired on an Attune flow cytometer and data was analysed using FlowJo v10.

A table containing the specific antibodies and dilutions used is below. Isotype controls were included for every activation marker used.

Antigen	Conjugate	Company	# Catalogue	Clone	Isotype	Dilution
CD4	eFluor450	eBioscience	48-0041-82	GK1.5	Rat IgG2b, κ	200
CD11c	PECy7	eBioscience	25-0114-82	N418	Arm. Hamster IgG	1000
CD11b	BV605	BD	563015	M1/70	Rat IgG2b, κ	300
CD40	PEDazzle594	BioLegend	124629	3/23	Rat IgG2a, κ	50
CD45	PerCPCy5.5	eBioscience	45-0451-80	30 F11	Rat IgG2b, κ	200
CD86	FITC	BD	561962	GL1	Rat IgG2a, κ	200
CD115	PEeFluor610	eBioscience	61-1152-82	AFS98	Rat IgG2a, κ	1000
CD135	PECy5	eBioscience	15-1351-81	A2F10	Rat IgG2a, κ	50
CCR7 (CD197)	PerCPCy5.5	eBioscience	45-1971-80	4B12	Rat IgG2a, κ	50
MR (CD206)	PECy7	BioLegend	141720	C068C2	Rat IgG2a, κ	200

OX40L (CD252)	FITC	Invitrogen	MA5-17912	OX89	Rat IgG1	50
PDL2 (CD273)	BV711	BD	740818	TY25	Rat IgG2a, κ	100
MGL (CD301)	PE	BioLegend	145704	LOM-14	Rat IgG2b, κ	100
MHC-II	PB	BioLegend	107619	M5/11 4.15.2	Rat IgG2b, κ	1000
Live-Dead	Aqua	Thermo	L34957	-	-	500

Table 3.2 Antibodies and reagents used in flow cytometry

3.3.4 Live imaging

Time-lapse imaging was performed following a standard infection assay, typically to study vomocytosis rates. Time-lapse movies were created by compiling images taken every 5 minutes over 18 hours. Throughout the imaging period, samples were incubated at 37°C in a 5% CO_2 atmosphere within the imaging chamber of a Ti-E Nikon Epifluorescence Microscope. The resulting files were analysed using NIS viewer software.

For analysis, time-lapse movie files were blinded and scored manually. Information regarding number of infected macrophages, proliferation of phagocytosed cryptococci, macrophage lysis and vomocytosis events was recorded.

3.4 Statistical analysis

The statistical analysis was performed using GraphPad Prism software version 6. The particular test used in each case is specified in the figure legend. Generally, differences in categorical data (vomocytosis occurrence and infection efficiency) were analysed by Chi^2 test followed by Fisher's Exact test; differences in percentage data (such as proliferation of T cells) were analysed by TwoWay ANOVA followed by Tukey's post-test on Arcsine-transformed data; all other data (IPR, expression of activation markers and cytokine levels) were analysed using Mann-Whitney test, or TwoWay ANOVA followed by Tukey's post-test.

4 Studying the effect of ERK5 inhibition on macrophage polarisation

Some of the results shown in this chapter have been published in a research article of which I am a co-author [84]. The complete paper can be found in the Appendix.

Macrophages are very plastic cells which can adopt different activation states according to the external cues they sense. In turn, their activation state will influence the way they respond to their environment [192]. One aspect that has been shown to be affected by macrophage polarisation is vomocytosis of *Cryptococcus neoformans*; IL-4-polarised cells exhibit lower occurrence of vomocytosis than their LPS-polarised counterparts [83]. More recently, inhibition of the MAP kinase ERK5 has been linked to vomocytosis [84]. This prompted us to explore whether ERK5 could affect macrophage polarisation.

The first insight into the ability of macrophages to display different activation phenotypes came in the 1990s, when Stein *et al.* reported that IL-4 stimulation produced an "alternative activation" to that elicited by IFNγ [193]. Since then, different activating stimuli responsible for specific activation states have been reported and compiled into what is now known to be a fluid activation spectrum [194]. Adoption of a systematic nomenclature to designate each activation phenotype, with its defining markers and effector molecules, has been challenging [195]. In this work, I have used the widely-accepted IL-4 and LPS + IFNγ polarising agents. These are known to

induce opposite ends of the activation continuum, traditionally termed alternative and classical activation phenotypes, or more accurately M(IL-4) and M(LPS + IFNγ), respectively [195].

4.1. Setting up a macrophage polarisation assay

To assess the impact of ERK5 inhibition on macrophage activation, a polarisation assay was devised. This consists of stimulating J774 cells with the prototypical polarising agents; IL-4 or LPS + IFNγ, and assessing their activation state 24 hours post-stimulation through expression of surface markers by flow cytometry and evaluation of secreted molecules in the culture supernatant by ELISA. The panel of surface markers and secreted proteins studied can be seen in the following table.

Marker	Function	Polarisation
CD11b	Integrin (myeloid marker)	
CD86	Co-stimulatory molecule (binds to CD28)	Classical
IL-12p40	Pro-inflammatory cytokine	
CD206	Mannose receptor	Alternative
MGL	Lectin	
Ym1	Chitinase-like protein	
Live-Dead	Viability dye	

Table 4.1. Surface markers and cytokines examined in polarisation assays.

M(IL-4) macrophages were characterised by expression of CD206, CD301 and secretion of Ym1. CD206 (C-type Mannose Receptor 1, also known as MR) and CD301 (Macrophage galactose-type C-type lectin, also known as MGL) are transmembrane receptors for glycoproteins whose expression is enhanced by IL-4-stimulation. Ym1, also termed Chitinase-3-like protein 3 (Chi3l3), is a lectin with affinity for glycosaminoglycans. As its name suggests, it binds chitin, but has no chitinase activity. Its expression is also enhanced by IL-4-stimulation.

M(LPS + IFNγ) were characterised by expression of CD86 and secretion of IL-12p40. CD86 is a co-stimulatory molecule, necessary for priming of T cells, where it binds to CD28 and CTLA-4 [196, 197]. IL-12 is a cytokine produced by activated antigen-presenting cells, such as macrophages and dendritic cells, which polarises the T cell response to Th1 [198, 199]. It should be noted that IL-12 is a heterodimer composed of p35 and p40 subunits [200]. The reagents used in this work only bind to the p40 subunit, which is shared with the cytokine IL-23. This cytokine can also be produced by macrophages, and has been implicated in polarisation to a Th17 response [201, 202].

Activating J774 cells with PMA before infection assays is standard practice, since it has been shown to increase the phagocytic ability of these cells [203]. However, it is also thought to drive production of IFNγ and hence polarise the cells towards a classical activation phenotype [204, 205], hindering any potential effect of IL-4. Initial experiments while optimising the assay were performed both with PMA-activated and non-activated J774 macrophages (Figure 4.1).

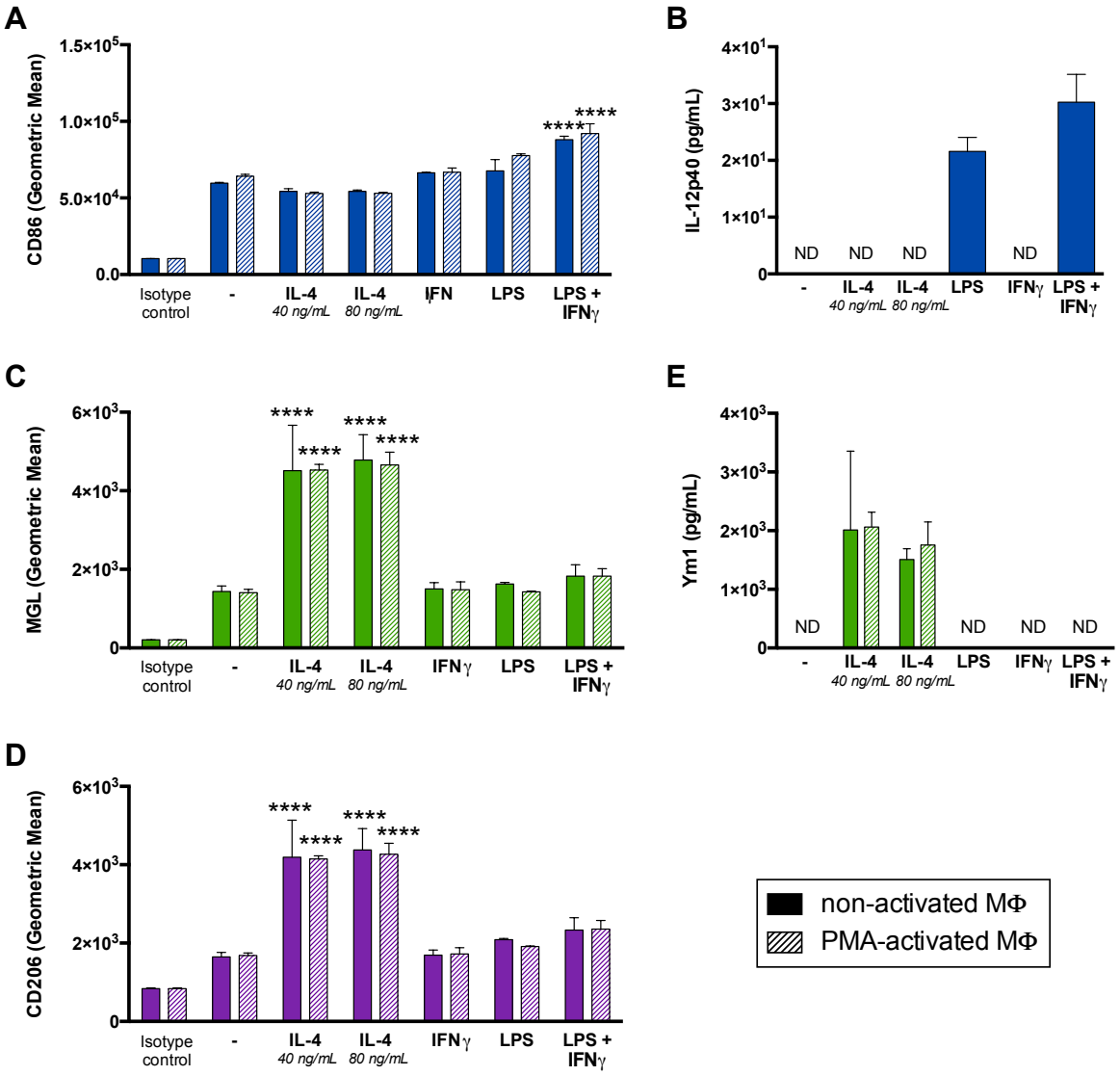

Figure 4.1 Optimisation of J774 polarisation assay

J774 macrophages were incubated with the indicated dose of IL-4, 1000 IU/mL IFNγ, 20 ng/mL LPS or LPS combined with IFNγ for 24 hours. After incubation, the cells were stained for different activation markers and analysed by flow cytometry, and the culture supernatant was probed for cytokine production by ELISA.

Bars correspond to Geometric Mean + SD of expression of CD86 (**A**), MGL (**C**) or CD206 (**D**). Flow cytometry data was analysed by Two-way ANOVA with Tukey's post-test. Asterisks over bars indicate a significant difference with the basal condition (indicated as "–"); * = $p<0.05$, ** = $p<0.01$, *** = $p<0.001$, **** = $p<0.0001$. Data shown is representative of two independent experiments.

Cell culture supernatants were analysed for different cytokines. Bars correspond to Mean + SD of levels of IL-12p40 (**B**) or Ym1 (**E**). Data corresponds to one pilot experiment.

Figure 4.1 shows that J774 cells were successfully polarised with LPS + IFNγ to express the surface marker CD86 (A) and secrete IL-12p40 (B). Conversely, stimulation with IL-4 leads to increased expression of the surface markers MGL (C) and CD206 (D), and secretion of Ym1 (E). Technically, it shows that the doses of IL-4 used during optimisation of the assay are already at saturating levels of the markers assayed, and that a combination of LPS + IFNγ achieves the more robust polarisation, compared to each stimulus on its own. Rather surprisingly, PMA-activation did not have an effect on the markers or secreted molecules studied. Nonetheless, the following experiments were carried out on non-activated J774 cells to dissect the effect of ERK5 inhibition exclusively and limit potential artefacts due to PMA-activation in conjunction with the treatment.

4.2 Inhibition of ERK5 during macrophage polarisation

Treatment with the ERK5 inhibitor XMD17-109 (XMD) at 1 μM, either on its own or in conjunction with LPS + IFNγ stimulation, did not affect the expression of the surface marker CD86, traditionally regarded as a "classical activation marker" (Figure 4.2A). On the other hand, treatment with this inhibitor significantly reduced the expression of MGL induced by IL-4, rendering it similar to basal level expression (Figure 4.2C). In terms of the secreted molecules evaluated, inhibition of ERK5 enhanced the secretion of IL-12p40 induced by LPS + IFNγ (Figure 4.2B) and reduced that of Ym1 in response to IL-4 (Figure 4.2D).

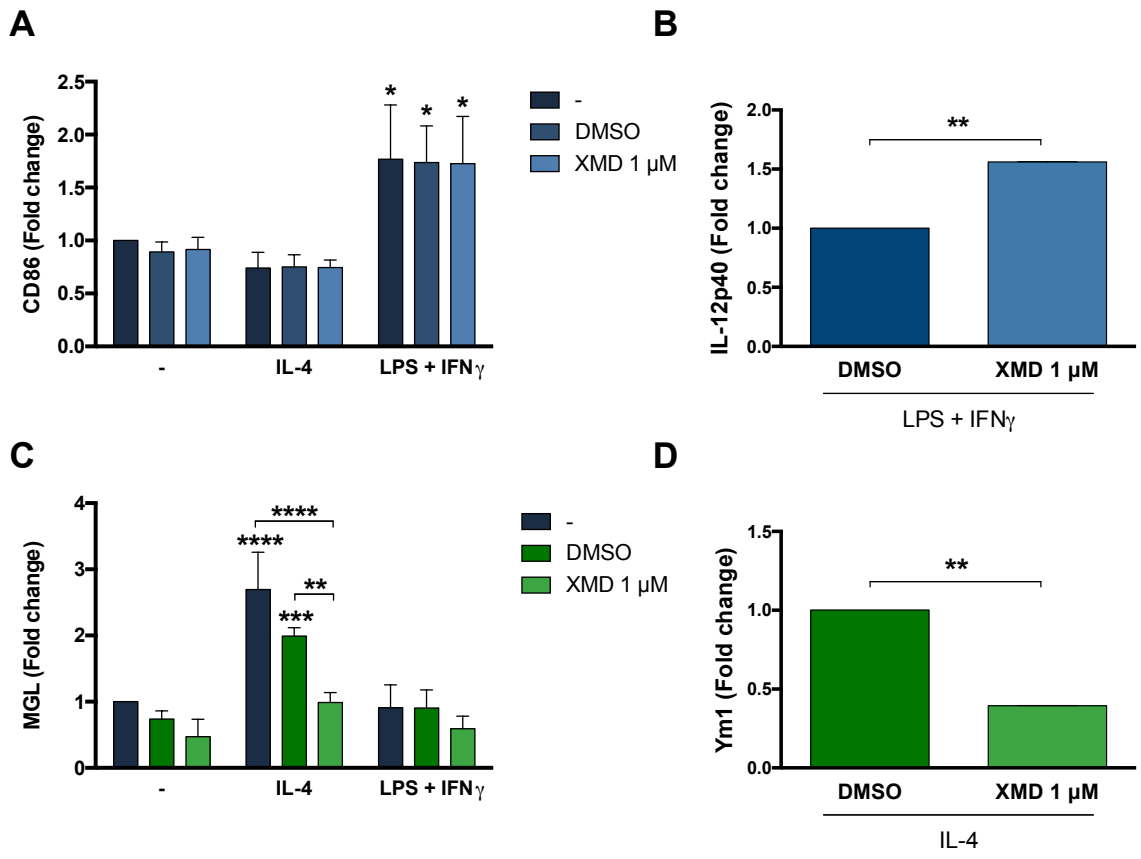

Figure 4.2 Inhibition of ERK5 enhances pro-inflammatory response in J774 cells

J774 macrophages were stimulated with 20 ng/mL IL-4 or 20 ng/mL LPS + 1000 IU/mL IFNγ for 24 hours, in the presence or absence of 1 μM ERK5 inhibitor XMD17-109 (XMD) or DMSO control. After incubation, cells were stained for activation markers by flow cytometry and supernatant was analysed for cytokine production by ELISA.

Bars correspond to Geometric Mean + SD of expression of CD86 (**A**) or MGL (**C**) with respect to the unpolarised condition. Data from three independent experiments, analysed by Two-way ANOVA with Tukey's post-test: * $p \leq 0.05$; ** $p \leq 0.01$; *** $p \leq 0.001$; **** $p \leq 0.0001$. Asterisks not associated with connecting brackets represent differences with respect to the basal expression on each group.

Cell culture supernatants were analysed for cytokine production. Bars correspond to levels of IL-12p40 (**B**) or Ym1 (**D**) with respect to the DMSO control. Data from three independent experiments, analysed by paired ratio t-test: ** $p \leq 0.01$.

Collectively this shows that inhibition of ERK5 in J774 cells leads to a shift in the population to a pro-inflammatory phenotype, with increased IL-12p40 secretion when stimulated with LPS + IFNγ and reduced response to IL-4 polarisation.

The effects of ERK5 inhibition on macrophage polarisation were also tested on human monocyte-derived macrophages. In this context, inhibition of ERK5 also lead to a pro-inflammatory phenotype, with enhanced TNFα secretion when stimulated with LPS + IFNγ and reduced secretion of IL-10 in response to IL-4 (Figure 4.3).

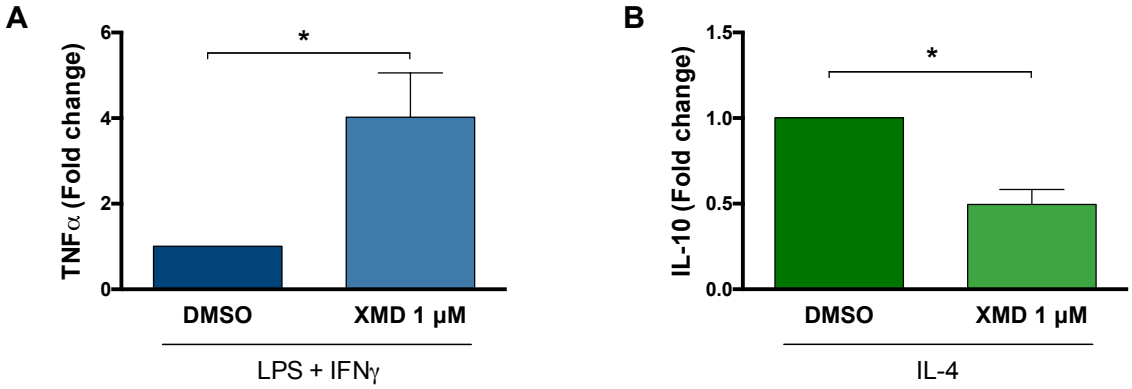

Figure 4.3 Inhibition of ERK5 enhances pro-inflammatory response in human macrophages

Human monocyte-derived macrophages were stimulated with LPS + IFNγ or IL-4, in the presence of the ERK5 inhibitor XMD17-109 (XMD) or DMSO control. After 24 hours, cell culture supernatants were analysed for pro-inflammatory cytokine TNFα (**A**) and regulatory cytokine IL-10 (**B**). Bars correspond to Mean + SD levels of cytokine with respect to that present in DMSO control condition. Data from at least three independent experiments, analysed by paired ratio t-test: * $p \leq 0.05$.

4.3 Closing remarks

Overall, the results shown in this chapter point to a clear link between macrophage polarisation and the atypical MAP kinase ERK5. Since earlier work has shown that both inhibition of ERK5 [84] and polarisation of macrophages [83] lead to changes in the occurrence of vomocytosis, it is plausible that the molecular mechanism for vomocytosis shares intermediary signalling molecules with either phenomenon. Previous work from this lab showed that inhibition of ERK5 was able to enhance vomocytosis beyond the effect of saturating doses of IFNγ [206]. This suggests that even though they may share signalling molecules, their mechanisms of action are not redundant. Further work is necessary to pinpoint the molecular mechanism by which ERK5 influences macrophage polarisation, and how it is able to modulate vomocytosis.

It has been discussed before that macrophage polarisation responds to the cells sensing different stimuli in their environment. *In vitro*, this has been recapitulated by stimulating with recombinant cytokines or sterile preparations. *In vivo*, however, macrophage polarisation is often seen during infection, with intracellular bacteria producing a "classical activation" phenotype [207, 208] and parasitic infections resulting in "alternatively activated" cells [17].

Cryptococcus neoformans is able to infect macrophages and persist within the host as a latent infection [12]. Thus, it is likely that *Cryptococcus*-infected macrophages will encounter different infectious scenarios, with different polarising abilities. The results presented here would relate to bacterial or parasite:cryptococcal co-infection. In

resource-poor settings like rural Africa, most cryptococcosis patients will also be endemically infected with parasites [209, 210]. The results here presented suggest that these co-infection settings could impact the fungus's vomocytosis rates. Nevertheless, cryptococcosis is most associated with HIV^+ patients [14], who suffer from a chronic viral infection. The effects of viral infection on vomocytosis will be addressed in the next chapter.

5 Exploring the impact of viral infection on vomocytosis

Some of the results presented in this chapter have been published in a research article of which I am a co-author [179]. The complete article can be found in the Appendix.

The relevance of cryptococcosis to HIV^+ patients is undeniable, and yet most studies on Cryptococcal infection have been performed on otherwise healthy cells. Co-infection settings can drastically alter the cellular response to any one pathogen, with important consequences for overall disease progression. In this chapter I describe our work looking at Cryptococcal infection on macrophages undergoing a viral infection, with a particular focus on vomocytosis.

As mentioned in the introduction to this work, viral infection triggers an anti-viral immune response. Sensing of viral PAMPS (Figure 5.1) and the ensuing of an appropriate immune response is a very complex process. It involves the recognition of viral PAMPS either from the extracellular media through Toll-like receptor (TLR)-binding or intracellularly via RNA or DNA sensors. Signalling cascades from these sensing steps converge in the activation of nuclear factor (NF)-kB for production of pro-inflammatory cytokines, and activation of the interferon regulatory factor (IRF) 3 or IRF7, which lead to the production of type-I interferons (IFN) [211, 212].

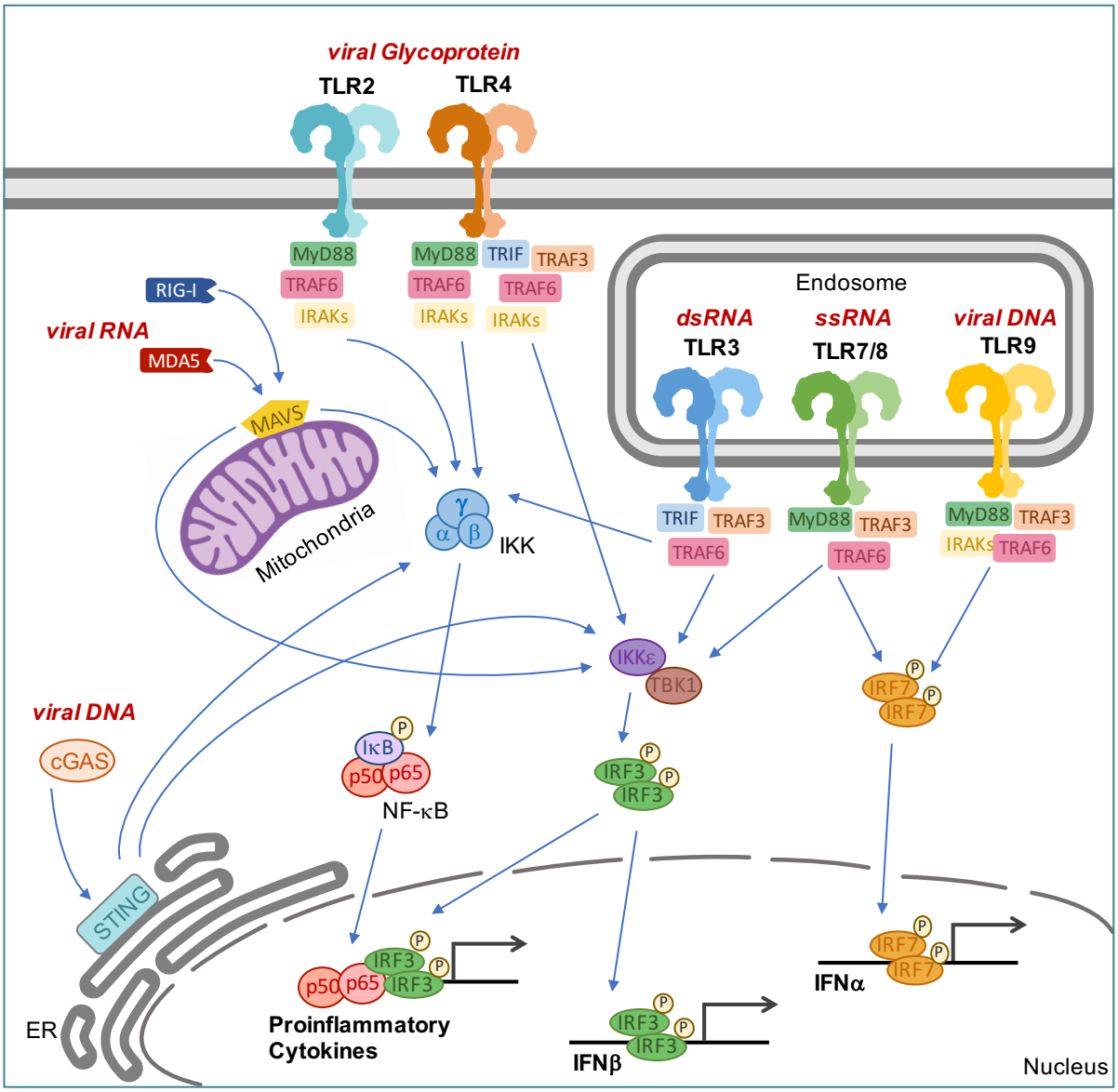

Figure 5.1 Viral sensing signalling cascade

Host cells have several innate receptors capable of sensing invading viruses. Toll-like receptors (TLR) present on the cell surface (TLR2 and TLR4) and endosomal membrane (TLR3, TLR7/8 and TLR9) recognise viral glycoproteins and nucleic acids, respectively. Within the cytoplasm, viral RNA is sensed by RIG-I and MDA-5, and viral DNA is sensed through cGAS-STING. Any virus may be sensed by multiple different receptors during its infection cycle. Once these pattern recognition receptors are engaged, they lead to the activation of NF-κB and expression of pro-inflammatory cytokines, and activation of IRF3 (via TBK1:IKKε) or IRF7, which lead to the production of type-I interferons. Figure adapted from Melchjorsen, J., *Viruses*, 2013 [211] and Takeuchi *et al.*, Cell, 2010 [212].

cGAS = cyclic GMP-AMP synthase, ER = Endoplasmic reticulum, IFN = interferon, IKK = inhibitor of nuclear factor κB kinase, IRF = interferon regulatory factor, MDA-5 = melanoma differentiation associated gene-5, NF-κB = nuclear factor κB, RIG-I = retinoic acid inducible gene-I, STING = stimulator of interferon genes, TBK1 = TANK binding kinase 1, TLR = toll-like receptor.

5.1 HIV infection enhances vomocytosis of *Cryptococcus neoformans*

As explained on the introduction, HIV targets $CD4^+$ cells such as T cells, macrophages and CD4-expressing dendritic cells. Over the course of infection, HIV will cause the decline of $CD4^+$ T cell numbers ultimately leading to the condition known as AIDS [31].

To gain entry into cells, two receptors, CD4 and a co-receptor, act sequentially to trigger fusion of viral and cellular membranes. Both receptors interact with the viral envelope glycoprotein [213]. Interaction with CD4 causes a conformational change within the viral protein subunit gp120, which exposes a binding site for a co-receptor [214]. Engagement of both CD4 and co-receptor with the viral envelope glycoprotein induces a further conformational change which exposes the membrane fusion peptide in the gp41 subunit, essential for membrane pore formation and cell entry of the viral particle [215].

The two co-receptors widely used *in vivo* are the chemokine receptors CCR5 and CXCR4 [216]. HIV strains can be broadly classified according to their co-receptor usage into R5, X4 or R5X4 strains, which use respectively CCR5, CXCR4 or either, as co-receptor [217]. An older system classified HIV strains as macrophage (M)-tropic or T cell (T)-tropic according to their ability to replicate in these cells *in vitro* [217].

Despite macrophages expressing both CD4 and CCR5 on their surface, HIV-1 does not replicate well in these cells [218-220]. This is due to the restriction factor SAMHD1, a dNTP hydrolase which limits reverse transcription and acts as a post-entry restriction step for HIV [221, 222]. The lentiviral accessory gene *vpx*, not present in HIV-1, encodes for a protein which targets SAMHD1 for proteasomal degradation [223].

In order to study the interaction of HIV and *Cryptococcus* within macrophages, we modified a system developed by the Noursadeghi lab which uses two virus-like particles (VLP) to achieve a fully infectious preparation. One of the VLP consists of the gene for *vpx* within the simian immunodeficiency virus envelope (SIV*vpx*), while the other is an envelope-deficient attenuated strain of HIV (R9HIVΔ*env*). When both VLPs are added to the culture well, this system ensures single-round replication of the attenuated virus within macrophages, yielding an infection rate similar to macrophage-tropic HIV strains [224].

The results shown below (Figures 5.2 and 5.3) were obtained by Dr. Leanne Taylor-Smith and are included in this thesis, with her consent, as they are integral to the development of my PhD research.

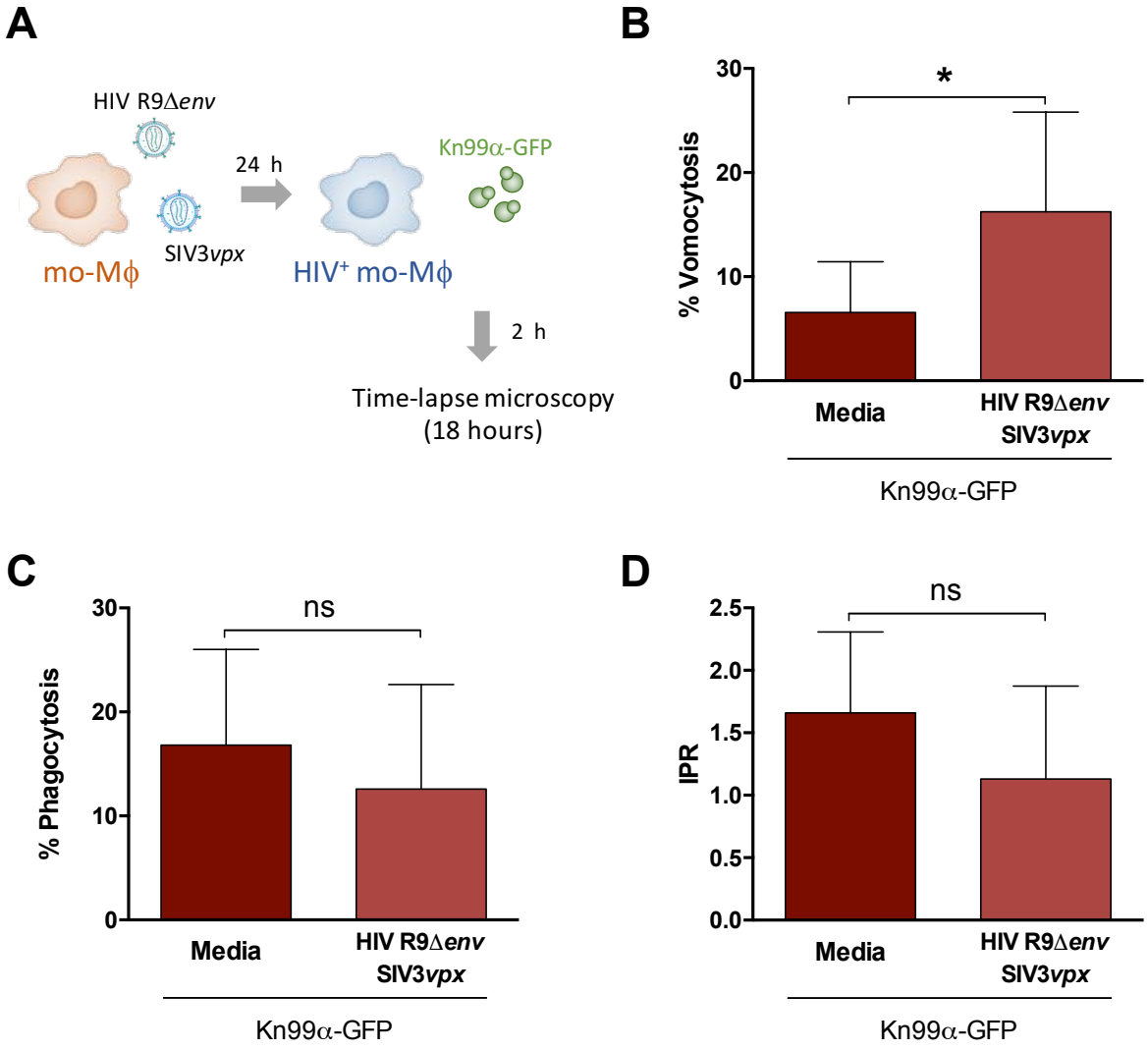

Figure 5.2 HIV infection enhances vomocytosis of *C. neoformans*

Human monocyte-derived macrophages were infected with attenuated HIV and subsequently infected with GFP-tagged *C. neoformans*. Infected cells were imaged every 5 minutes over a period of 18 hours (**A**). Time-lapse microscopy videos were manually scored for vomocytosis (**B**), uptake (**C**) and intracellular proliferation rate (IPR, **D**) of *C. neoformans*.

A. Schematic representation of the experimental plan.

B. Graph shows percentage of *Cryptococcus*-infected macrophages which have experienced at least one vomocytosis event during the 18 hour-experiment. Categorical vomocytosis data was analysed using Chi^2 followed by Fisher's exact test. * $p < 0.05$

C. Graph shows percentage of *Cryptococcus*-infected macrophages. Categorical phagocytosis data was analysed using Chi^2 followed by Fisher's exact test.

D. Graph shows intracellular proliferation rate (IPR) of *C. neoformans* over 18 hours. IPR data was analysed using Mann-Whitney test.

All data corresponds to 7 independent experiments. Approximately 580 macrophages were scored. Data obtained by Dr. Leanne Taylor-Smith.

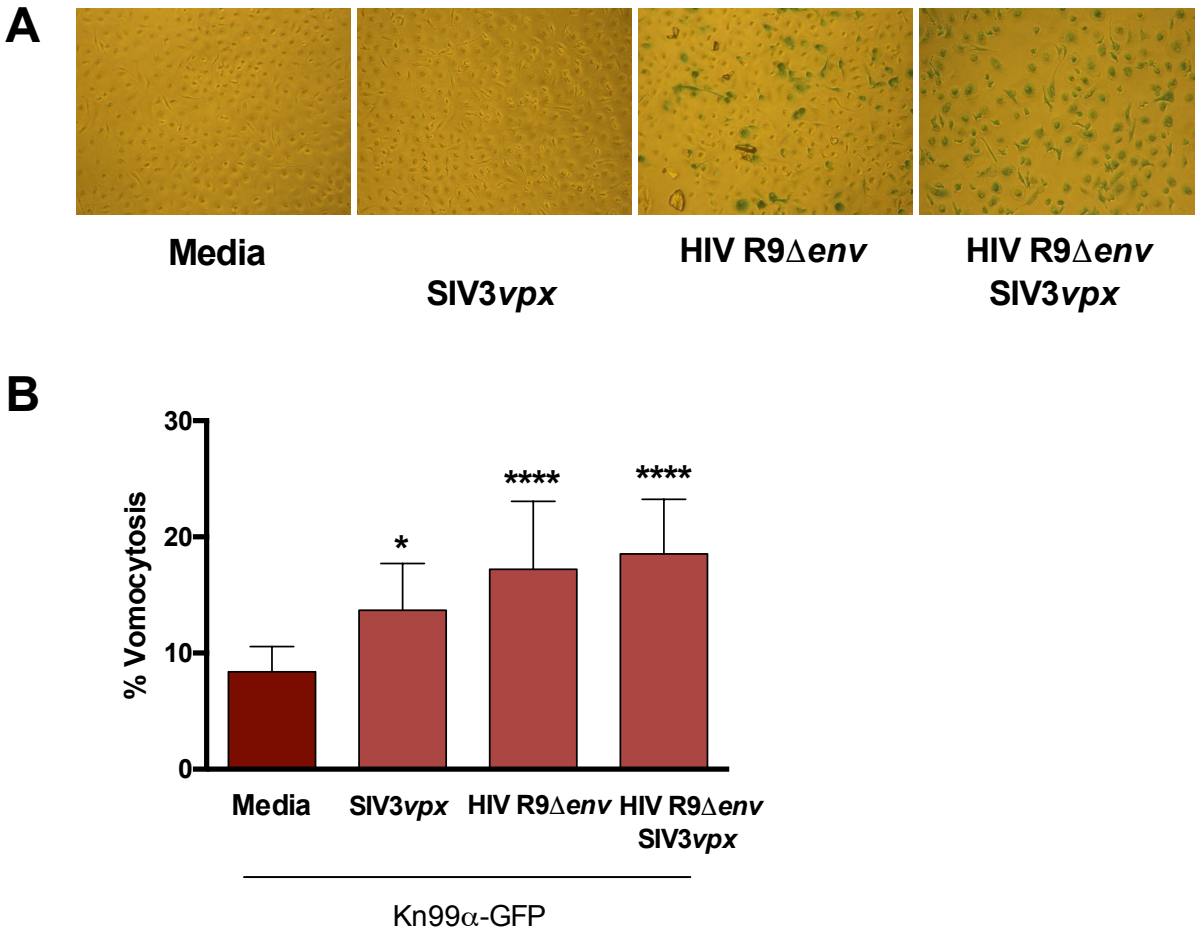

Figure 5.3 Viral exposure enhances vomocytosis of *C. neoformans*

A. Human monocyte-derived macrophages were infected with virus like particles (VLP) as indicated. After 24 hours, HIV viral infection was assessed by p24 staining (blue).

B. Human monocyte-derived macrophages were infected with VLPs as indicated, and subsequently infected with GFP-tagged *C. neoformans*. Time-lapse microscopy videos were manually scored for vomocytosis. Graph shows percentage of *Cryptococcus*-infected macrophages which have experienced at least one vomocytosis event during the experiment. Raw vomocytosis data was analysed by Chi^2 followed by Fisher's exact test. * $p < 0.05$; **** $p < 0.0001$. Data from 5 independent experiments. Approximately 810 macrophages were scored. Data from HIV + vpx condition also shown in Figure 5.2.

Data obtained by Dr. Leanne Taylor-Smith.

Human monocyte-derived macrophages were infected with attenuated HIV (in conjunction with SIV*vpx* to ensure macrophage infection) for 24 hours, and subsequently infected with GFP-labelled *C. neoformans*. The infected cells were then imaged over 18 hours and the resulting time-lapse movies were manually scored for vomocytosis, uptake and intracellular proliferation rate (IPR) of the fungus (Figure 5.2). The figure shows that infection with HIV induced an enhancement of vomocytosis of *C. neoformans*, without significantly altering phagocytosis or IPR.

Immunostaining of the capsid protein p24 was performed on infected wells to confirm HIV infection (Figure 5.3A). The images show that attenuated HIV alone was capable of replicating only in a minority of the cells present, whereas the fully infectious HIV + SIV*vpx* condition reached 100% infection. It is important to note that the Vpx complement was delivered to the cells within a viral envelope, but it does not contain p24. Interestingly, however, despite the varying infection rates in these different conditions, all three combinations enhanced vomocytosis (Figure 5.3B), albeit to different extents. Consequently, the effect on vomocytosis is not specific to HIV infection, but rather may be a broader effect of viral exposure.

5.2 Other viral infections affect vomocytosis

To test whether the effect seen is specific to HIV, we turned to a different virus; measles virus (MeV). MeV belongs to the family Paramyxoviridae within the genus Morbillivirus and, as the name suggests is the causative agent of measles. MeV infects cells primarily through interaction with the signalling lymphocyte activation

molecule (SLAM) [225], which is present on immature thymocytes, activated T lymphocytes, macrophages and dendritic cells. Thus, MeV is an excellent candidate to test whether the effects observed are exclusive to HIV infection, or can also be achieved with a distinct virus capable of infecting macrophages, whose prevalence has no correlation with that of cryptococcosis.

Human monocyte-derived macrophages were infected with GFP-tagged MeV, and subsequently infected with mCherry-labelled *C. neoformans*. Time-lapse microscopy movies were scored for vomocytosis, uptake and IPR of the fungus (Figure 5.4). The figure shows that infection with MeV also enhanced vomocytosis of *C. neoformans*, without altering phagocytosis rates or IPR.

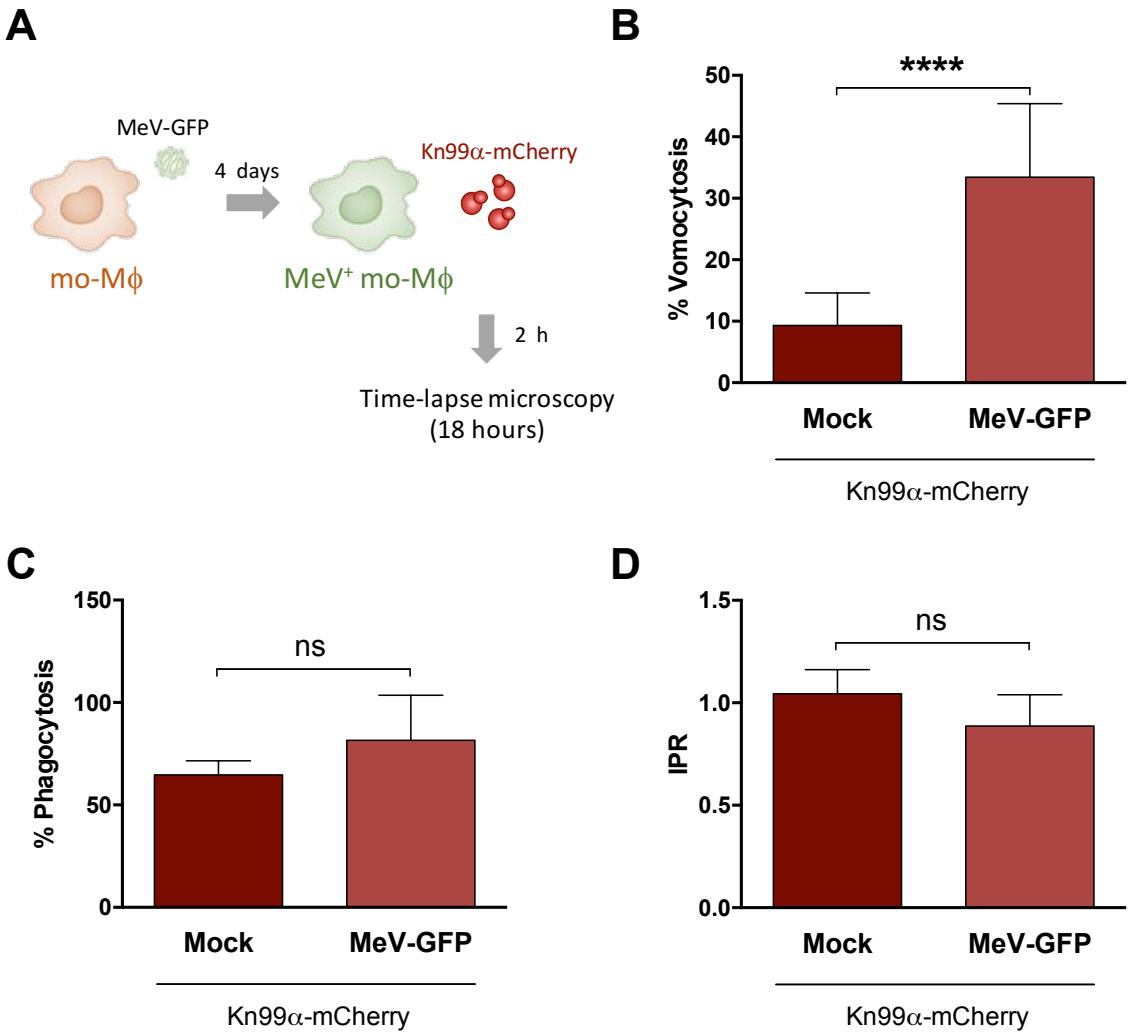

Figure 5.4 MeV infection enhances vomocytosis of *C. neoformans*

Human monocyte-derived macrophages were infected with GFP-tagged measles virus (MeV) and subsequently infected with mCherry-tagged *C. neoformans*. Infected cells were imaged every 5 minutes over a period of 18 hours (**A**). Time-lapse microscopy videos were manually scored for vomocytosis (**B**), uptake (**C**) and intracellular proliferation rate (IPR, **D**) of *C. neoformans*.

A. Schematic representation of the experimental plan.

B. Graph shows percentage of *Cryptococcus*-infected macrophages which have experienced at least one vomocytosis event during the 18 hour-experiment. Categorical vomocytosis data was analysed using Chi^2 followed by Fisher's exact test. * $p < 0.05$

C. Graph shows percentage of *Cryptococcus*-infected macrophages. Categorical phagocytosis data was analysed using Chi^2 followed by Fisher's exact test.

D. Graph shows intracellular proliferation rate (IPR) of *C. neoformans* over 18 hours. IPR data was analysed using Mann-Whitney test.

All data corresponds to 3 independent experiments. Approximately 300 macrophages were scored.

5.3 Active viral infection is not required to enhance vomocytosis

To further extend this finding and test whether an active viral infection is required, macrophages were stimulated with polyinosinic-polycytidilic acid (polyIC) before being infected with *C. neoformans* (Figure 5.5). polyIC is a double stranded RNA synthetic analogue, which binds to TLR3 and mimics a viral infection. Stimulation with this generic viral PAMP also induced an increase in vomocytosis (A), and did not affect uptake nor intracellular proliferation of the fungus (B and C).

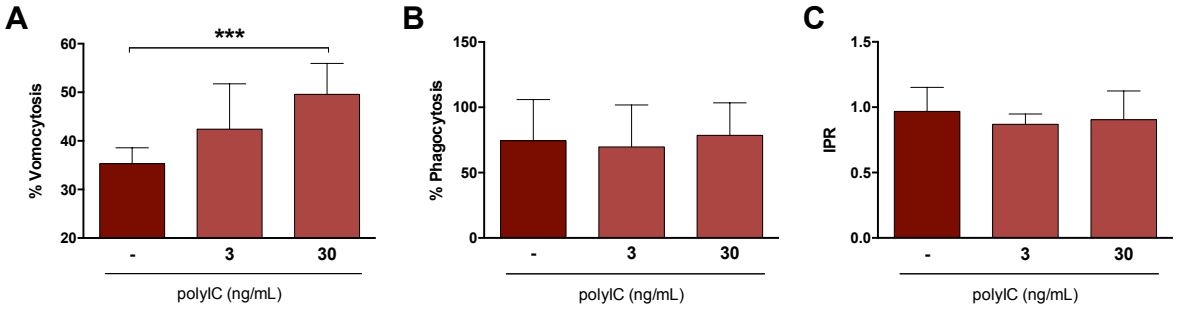

Figure 5.5 Active viral infection is not required for enhancement of vomocytosis

Human monocyte-derived macrophages were stimulated with different doses of a double-stranded RNA synthetic analogue, polyIC, and infected with *C. neoformans*. Time-lapse microscopy videos were manually scored for vomocytosis (**A**), uptake (**B**) and intracellular proliferation rate (IPR, **C**) of the fungus.

A. Graph shows percentage of infected macrophages which have experienced at least one vomocytosis event during the experiment. Chi^2 followed by Fisher's exact test were performed on vomocytosis raw counts. *** $p < 0.001$

B. Percentage of infected macrophages. Categorical phagocytosis data was analysed by Chi^2 followed by Fisher's exact test.

C. Intracellular proliferation rate (IPR) of *C. neoformans* over 18 hours. IPR data was analysed using Friedman followed by Dunn's post-test.

Data corresponds to 3 independent experiments. Approximately 830 macrophages were scored.

Taken together, the data above show that infection with two unrelated viruses leads to an enhancement in vomocytosis of *C. neoformans*. HIV and MeV belong to different

genera (Lentivirus and Morbillivirus, respectively) and achieve infection of macrophages through different receptors (CD4 and SLAM, respectively), but nevertheless cause an enhancement of vomocytosis of *C. neoformans* without affecting other parameters of fungal infection. Moreover, the same effect was seen when stimulating with the sterile viral PAMP polyIC, showing that an active viral infection is not required, something that is further supported by our observation that addition of Vpx complement in the form of a viral particle also causes an enhancement of vomocytosis.

5.4 Enhancement of vomocytosis is not dependent on TBK1:IKKε signalling nor TLR3 sensing

The different infection or stimulation settings studied in this chapter have all involved the sensing of viral antigens and concomitant triggering of an anti-viral response. Hence, we turned to the signalling cascade involved in these events in the search for a possible mechanism by which the enhancement of vomocytosis is accomplished (see Figure 5.1).

We initially tested pharmacological inhibition of the TBK1:IKKε complex, which is central to viral sensing. This complex is engaged in different viral sensing pathways, and leads to activation of IRF3 and type-I IFN production. The compound used, BX795, inhibits the catalytic activity of TBK1:IKKε by blocking its phosphorylation [226].

Similarly, we also tested the effect of inhibiting viral sensing through TLR3-binding. A dsRNA:TLR3 complex inhibitor was tested, which selectively inhibits TLR3-binding by direct and high affinity competition [227] (Figure 5.6A).

The figure shows that the compounds did not affect vomocytosis when used in a viral infection setting, despite them being able to abrogate the effect seen with polyIC stimulation. PolyIC is a defined PAMP, which triggers an anti-viral response through its engagement with TLR3 and signalling through TBK1:IKKε [228]. Both inhibitors revoked the effect of polyIC on vomocytosis, therefore serving as an indirect control for the compounds effectiveness (Figure 5.6B). Conversely, infection with HIV is a much more complex stimulus which is sensed through various mechanisms [229], and the effect of this infection on vomocytosis could not be abolished by inhibition of these two molecules alone. This suggests that the effect on vomocytosis is not due to a particular signalling molecule, but rather to the overall ensuing of an anti-viral state.

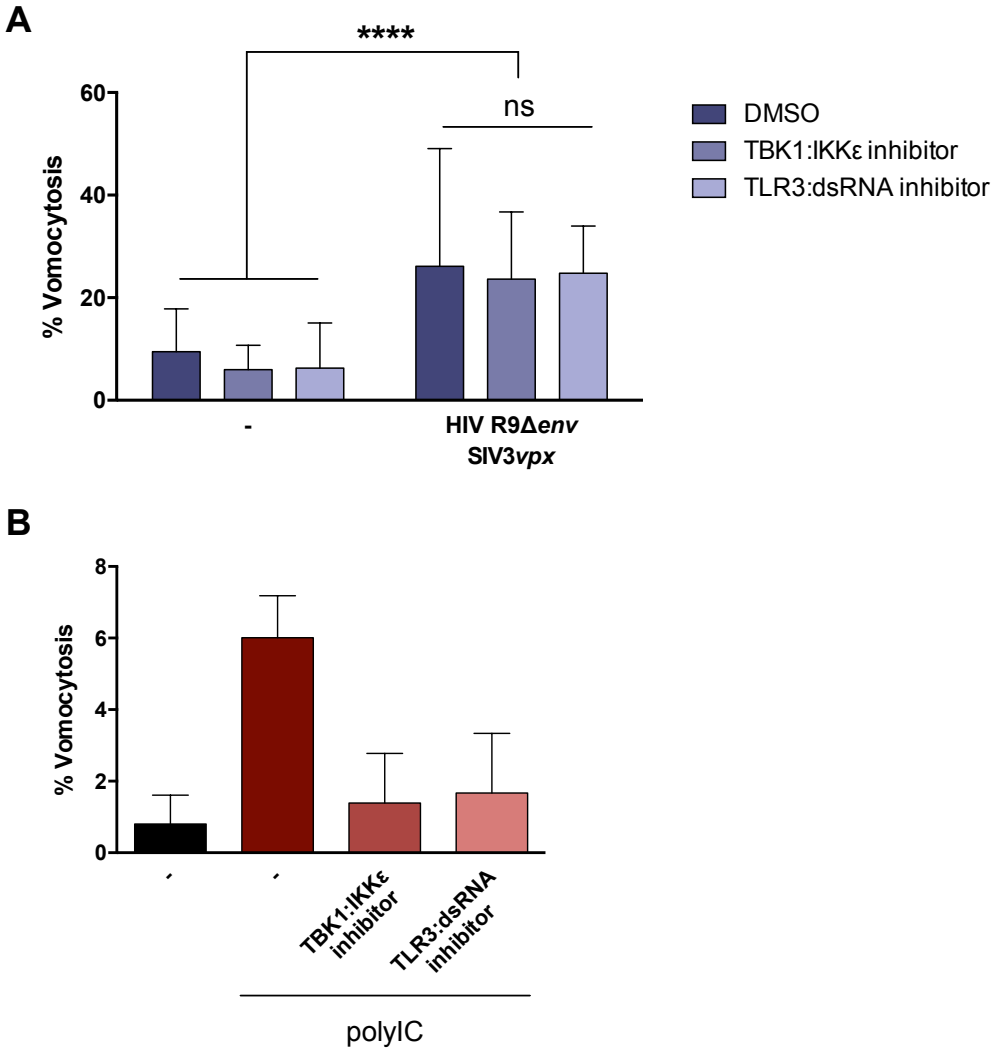

Figure 5.6 Vomocytosis effect is not dependent on TBK1:IKKε engagement nor TLR3 sensing

Human monocyte-derived macrophages were infected with attenuated HIV (**A**) or stimulated with polyIC (**B**) and subsequently infected with *C. neoformans*, in the presence or absence of a TBK1:IKKε or TLR3:dsRNA inhibitor.

Graphs show percentage of infected macrophages which have experienced at least one vomocytosis event during the experiment. Error bars correspond to SD. Raw vomocytosis data was analysed by Chi^2 followed by Fisher's exact test. **** $p < 0.0001$

Data corresponds to 2 (A) or a single (B) donors. Approximately 2000 and 350 macrophages were scored, respectively.

5.5 Type-I interferons enhance vomocytosis

The hallmark of an anti-viral response is the production of type-I interferons. This group is comprised of IFNα, IFNβ, IFNε, IFNκ and IFNω in humans [211]. The two most studied type-I interferons are IFNα and IFNβ, which are also the most abundant in plasma of HIV^+ patients [105]. We therefore tested whether stimulation with recombinant IFNα or IFNβ would be enough to enhance vomocytosis of *C. neoformans* (Figure 5.7).

Figure 5.7 Type-I interferons enhance vomocytosis of *C. neoformans*

Human monocyte-derived macrophages were stimulated with different doses of IFNα (left, yellow data) or IFNβ (right, green data), and infected with *C. neoformans*. Time-lapse microscopy videos were manually scored for vomocytosis (top row), phagocytosis (second row) and intracellular proliferation of the fungus (third row). Vomocytosis raw data was analysed by Chi^2 followed by Fisher's exact test. *** $p < 0.001$. Data corresponds to at least 3 independent experiments. Approximately 2300 macrophages were scored.

Extracellular growth of *C. neoformans* in the presence of type-I interferons was monitored (last row). Optical density readings at 600nm were taken every 30 minutes, in the presence of 10 pg/mL of IFNα (left, yellow), 50 pg/mL IFNβ (right, green), or un-supplemented YPD controls. Data representative of at least 2 independent experiments.

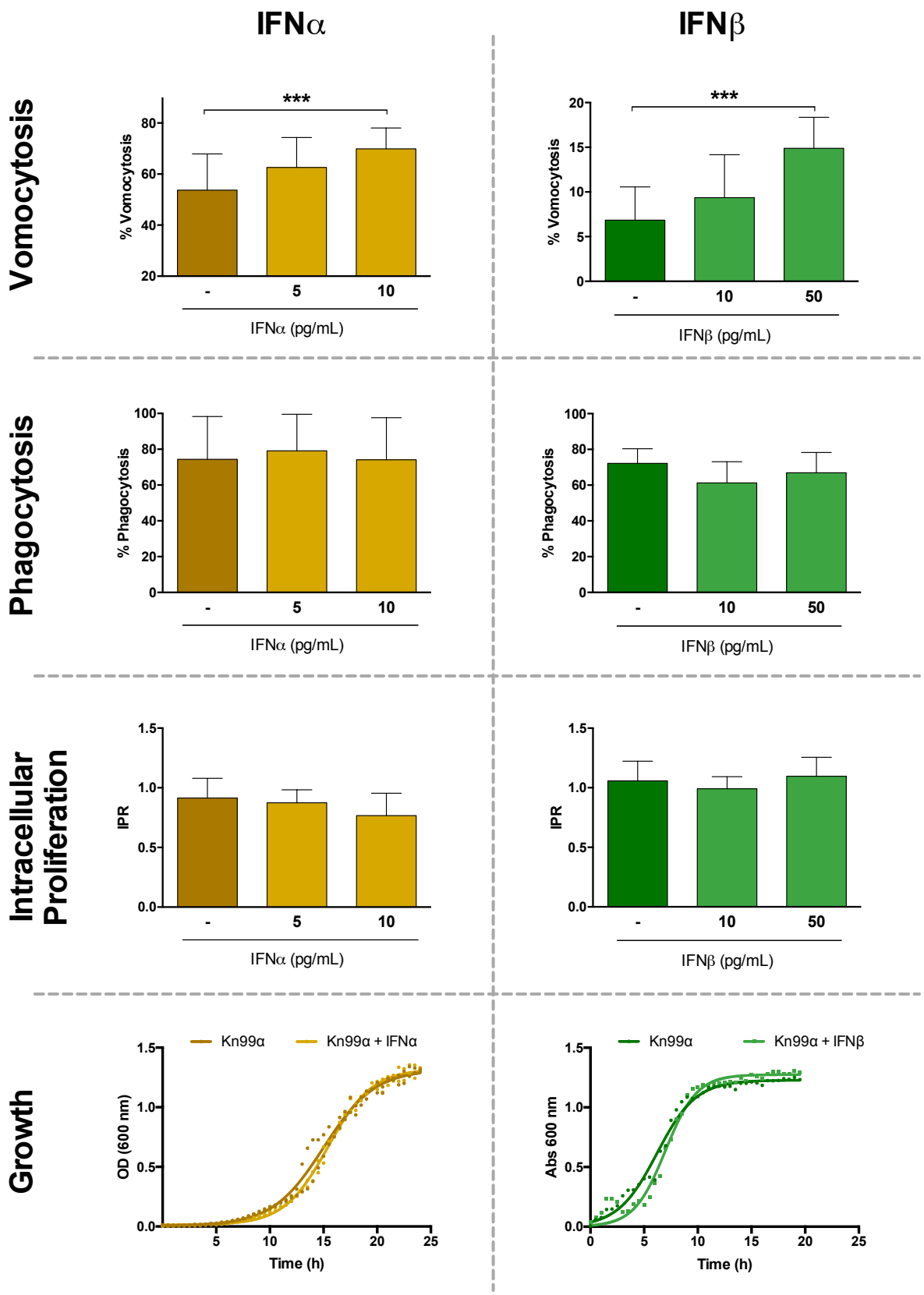
IFNα
IFNβ
Vomocytosis
Phagocytosis
Intracellular Proliferation
Growth
% Vomocytosis
% Phagocytosis
IPR
OD (600 nm)
Abs 600 nm
***
-
5
10
50
IFNα (pg/mL)
IFNβ (pg/mL)
Kn99α
Kn99α + IFNα
Kn99α + IFNβ
Time (h)

Stimulation with low doses of IFNα or IFNβ enhanced vomocytosis (first row), without affecting uptake or IPR (middle rows). The doses used are in line with those found in the plasma of HIV^+ patients [105], and translate to 7.3 and 14 IU/mL IFNα and IFNβ, respectively. At these doses, interferons did not affect cryptococcal growth (last row).

The genes for type-I interferons share chromosomal location (clustered in chromosome 9 in humans) and the resulting cytokines have similarities in structure, regulation and function, a key feature being that they all signal through the IFNα/β receptor (IFNAR) [107] to generate an anti-viral state.

To further confirm the role of type-I interferons in the enhancement of vomocytosis, *Cryptococcus*-viral co-infection experiments were repeated in the presence of an IFNAR blocking antibody (clone MMHAR-2, Figure 5.8). The reagent used is a monoclonal blocking antibody, which prevents interaction of the receptor with its ligand, without triggering intracellular signalling, and has been used extensively in the literature [230].

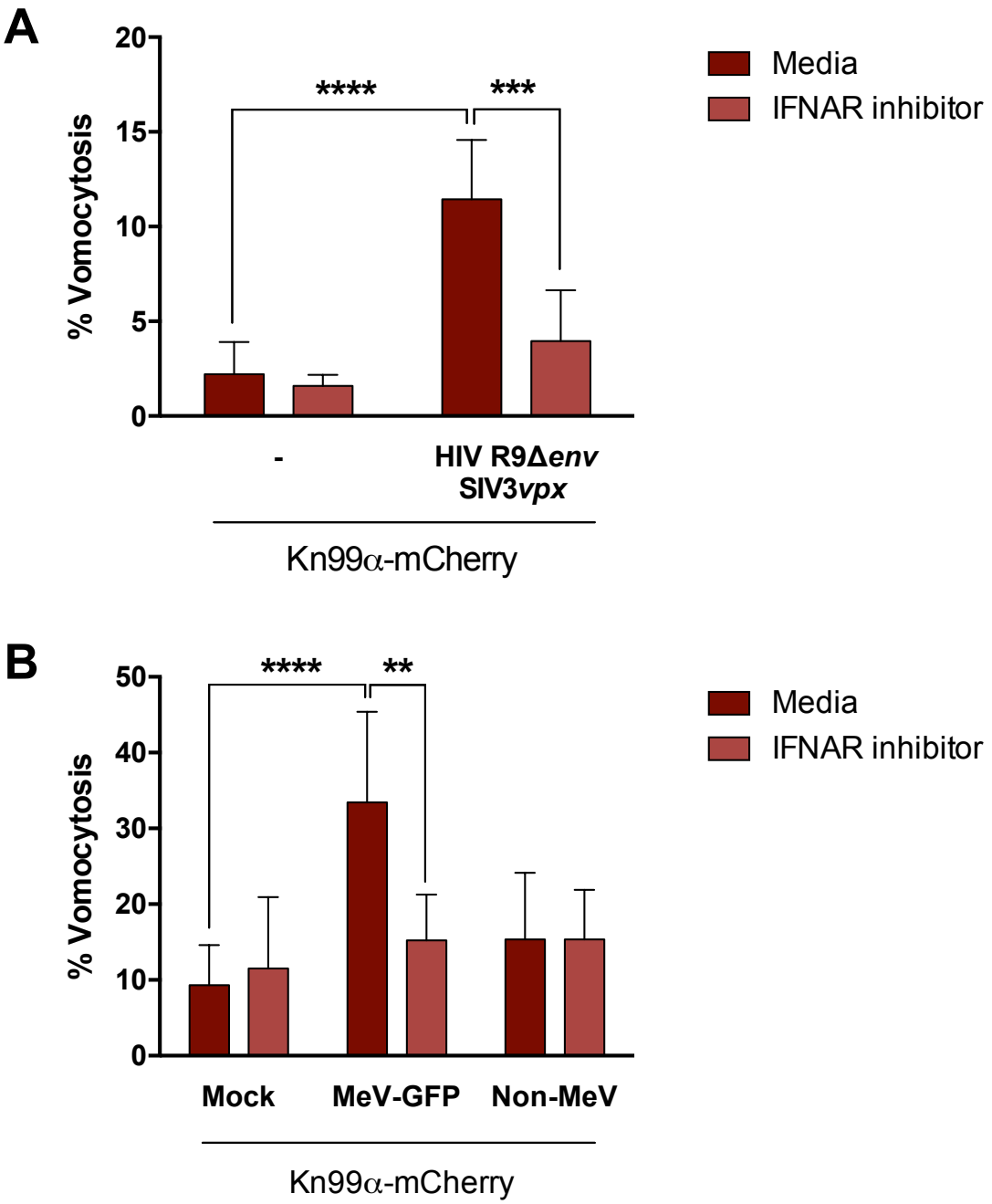

Figure 5.8 Type-I interferon signalling is necessary for effect on vomocytosis

Human monocyte-derived macrophages were infected with attenuated HIV (**A**) or GFP-tagged MeV (**B**) and subsequently infected with *C. neoformans*, in the presence or absence of a IFNα/β receptor (IFNAR) blocking antibody.

GFP-negative cells, which do not have a strongly active MeV infection, were termed "Non-MeV".

Graphs show percentage of *Cryptococcus*-infected macrophages which have experienced at least one vomocytosis event during the experiment. Raw vomocytosis data was analysed using Chi^2 followed by Fisher's exact test. ** $p < 0.01$: *** $p < 0.001$: **** $p < 0.0001$. Approximately 1500 macrophages were scored.

Data corresponds to 2 and 3 biological repeats, respectively.

Figure 5.8 shows that the enhancement of vomocytosis was completely abrogated when type-I interferon signalling is blocked, regardless of which virus is co-infecting. In the case of MeV, the GFP-tag allows for visual discrimination of cells with active viral infection from neighbouring GFP^- cells within the well, referred to as Non-MeV in Figure 5.8B. It is remarkable that the effect on vomocytosis is restricted to those cells where the infection with MeV is clearly distinguished as GFP^+. It should be noted that neighbouring "Non-MeV" cells might be infected with MeV but at a dose which falls below the detection limit of our instrument. Since type-I interferons have an autocrine and paracrine function, this data could be explained by two scenarios: the effect on vomocytosis requires both type-I interferon signalling and an active infection, or the levels elicited by MeV are too low to be active at greater distances. Figures 5.3 and 5.5 confirm that an active viral infection is not needed for enhancement of vomocytosis, therefore favouring the second option. Unfortunately, the levels of type-I interferons elicited by MeV in our *in vitro* settings could not be measured by conventional ELISA to confirm this hypothesis. However, it is well documented that MeV, and viruses in general, have developed multiple strategies to subvert detection and dampen anti-viral responses [231]. Thus, the possibility that the amount of type-I interferons elicited by the viral infections tested is too low to exert effects on distant cells is very likely.

5.6 Co-infection with *Pseudomonas aeruginosa* enhances vomocytosis of *C. neoformans*

Type-I interferons are traditionally regarded as "anti-viral" cytokines, which help create an antiviral state and thus help fight off the infection [31, 118]. More recently, their role in non-viral infections has been investigated [118]. Several bacterial infections have been found to elicit the production of type-I interferons (see signalling diagram in Figure 5.1), and in turn these "anti-viral" cytokines play a role in the outcome of bacterial infections [232]. Given the broad nature of the effect seen, preliminary work has been carried out to determine whether the effect on vomocytosis could be recapitulated in the context of bacterial co-infection.

Human monocyte-derived macrophages were co-infected with *C. neoformans* and *Pseudomonas aeruginosa*. *P. aeruginosa* is a Gram-negative bacterium commonly found in the environment. It is an opportunistic bacterial pathogen, mainly infecting hospital patients, and is able to colonise medical devices such as catheters [233]. *P. aeruginosa* can infect macrophages and rapidly leads to lysis of these phagocytes [234]. Different multiplicities of infection (MOI) were tested to accommodate for the rapid lysis of macrophages and an MOI = 0.25 was chosen (1 bacterium every 4 macrophages), which allows for 10 hours of imaging before most macrophages are lysed by the bacterial infection. Macrophages were also stimulated with LPS, to simulate a "sterile" bacterial infection. Time-lapse microscopy videos were manually scored for vomocytosis, IPR and macrophage lysis (Figure 5.9).

The following figure corresponds to data from a single donor, and should be repeated to attain the desired statistical stringency.

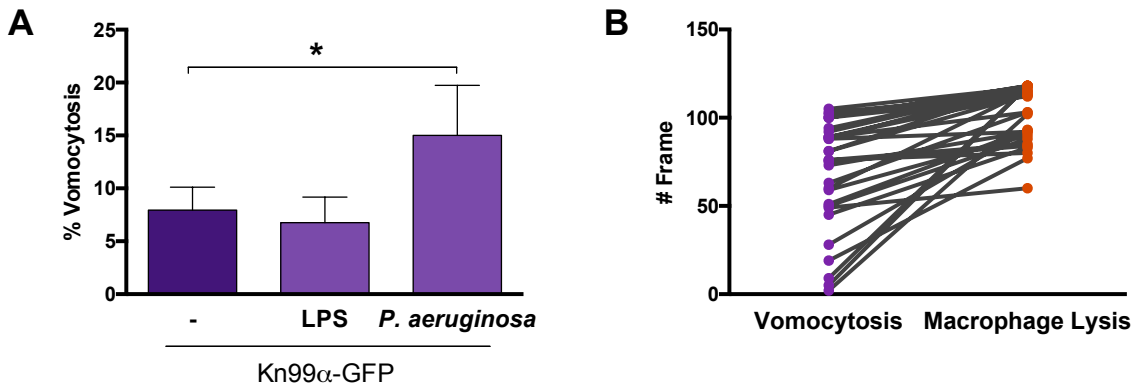

Figure 5.9 Co-infection with *P. aeruginosa* enhances vomocytosis of *C. neoformans*
Human monocyte-derived macrophages were stimulated with 20 ng/mL LPS or infected with *P. aeruginosa*, and subsequently infected with *C. neoformans*. Time-lapse microscopy videos were manually scored for vomocytosis (**A**). Vomocytosis raw counts were analysed by Chi^2 followed by Fisher's exact test. * $p < 0.05$
B. Paired times of vomocytosis and macrophage lysis events.
Data corresponds to a single pilot experiment. Approximately 500 macrophages were scored.

The figure shows that co-infection with *P. aeruginosa* enhanced vomocytosis of *C. neoformans* (Figure 5.9A). As mentioned before, even at this low MOI *P. aeruginosa* causes lysis of macrophages. Time-lapse videos were scored manually for vomocytosis, taking special care that the events recorded were not due to lysis but *bona fide* vomocytosis. Paired data of vomocytosis and lysis time (as frame number the events were recorded) is shown in Figure 5.9B. Vomocytosis events spread across the full time scored (120 frames in total), and when paired with macrophage lysis times it was clear that both events were separate in time.

Stimulation with LPS alone did not affect vomocytosis. This could mean that, unlike with viruses, an active bacterial infection is needed to enhance vomocytosis. Alternatively, it could mean that activation of the LPS sensing pathway alone is not sufficient to elicit the effect, or simply be due to the dose used. Further work is needed to dissect these options, and to solidify the findings pertaining bacterial infection and enhanced vomocytosis of *C. neoformans*.

5.7 Closing remarks

Throughout this chapter, I have explored the possibility that viral infection could have an effect on vomocytosis of *C. neoformans*. This stemmed from the prevalence of cryptococcosis on HIV^+ patients, but the research soon expanded beyond this particular co-infection pairing. Both viral co-infection settings explored, HIV and MeV, as well as sterile polyIC stimulation, lead to a significant enhancement of vomocytosis without altering fungal uptake nor IPR. This effect is not due to a particular sensing or signalling molecule, but rather a novel effect of type-I interferons.

Preliminary work suggests that co-infection with the bacterial opportunistic pathogen *P. aeruginosa* also results in an enhancement of vomocytosis. This would broaden the scope of effect reported beyond viral co-infection to include bacterial co-infection settings. Whether the effect observed with *P. aeruginosa* is also triggered by type-I interferons remains to be explored. Nonetheless, the role of type-I interferons in non-viral infections has been addressed in the past few years, and bacterial infections have

been found to elicit the production of these so-called "anti-viral" cytokines [232]. In fact, *P. aeruginosa* has been shown to elicit production of IFNβ [235], which would fit with the proposed novel effect of type-I interferons. Further work using different bacterial pathogens and blocking IFNAR would help assess whether type-I interferons are also playing a role in the enhancement of vomocytosis in bacterial co-infections.

6 *Cryptococcus* effect on antigen presentation

Research presented in the previous chapter stemmed from the prevalence of cryptococcosis in immunocompromised AIDS patients, although it soon grew beyond those settings. This chapter focuses on a different aspect of Cryptococcal infection; namely, how a latent infection in an immunocompetent host can affect T cell priming.

As mentioned in the introduction to this Thesis, infection with *C. neoformans* starts with the inhalation of desiccated yeast or spores from the environment (see Figure 1.1). Once within the host, Cryptococcal cells encounter alveolar macrophages and other phagocytes which, in immunocompetent hosts, are able to clear or contain the infection [12, 104, 236]. Dendritic cells (DC) in the lungs and surrounding tissues, sample their environment and present antigens to T cells in draining lymph nodes. In the lymph nodes, these antigen-presenting cells prime naïve T cells to induce a specific adaptive immune response [31, 237].

Studies show the presence of *Cryptococcus*-specific antibodies in children as young as 5-years old [13], confirming that exposure and development of an adaptive response occur at an early age. Disease is then caused by *de novo* infection under an immunocompromised state, or re-activation of a latent inoculum [238, 239]. Cryptococcal meningitis is particularly relevant in HIV^+ patients [14], thus underscoring the importance of a fully functional T cell response when dealing with this pathogen.

The work presented in this chapter set out to study the impact of the continued presence of *Cryptococcus* in the ability of DC to prime naïve T cells and mount an adaptive T cell response.

6.1 Bone marrow-derived DC:T cell co-culture system

To address this question, we developed the *in vitro* system described in Figure 6.1. The complete technical details can be found in Materials and Methods chapter.

This system uses T cells from transgenic mice, known as OT-II, which are specific for the chicken ovalbumin peptide 323-339 (OVAp) [240]. Using these T cells ensures a robust proliferation response when presented with the appropriate peptide:MHC-II complex, either exogenously processed ovabulmin peptide (hereafter referred to as OVAp) or the complete OVA protein (hereafter referred to as OVA), and thus provides a good system for testing modulating abilities of foreign entities on antigen presentation and processing.

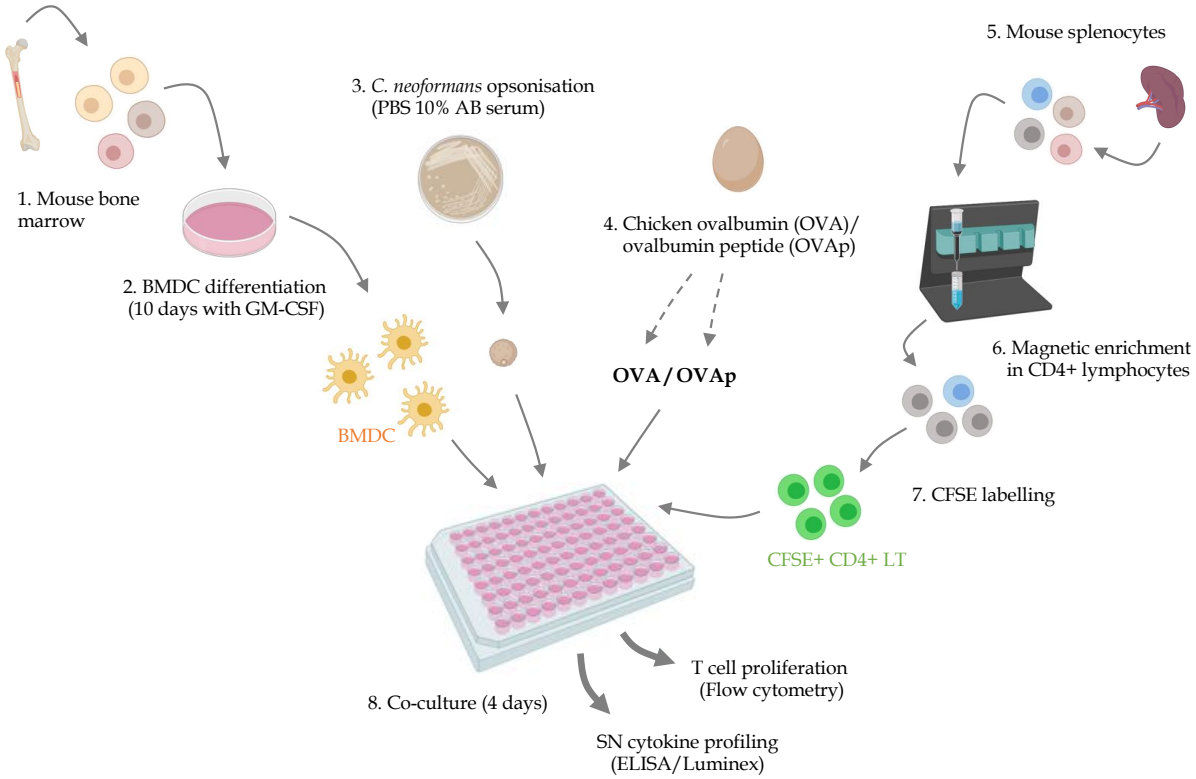

Figure 6.1 Experimental design for *in vitro* DC:T cell co-culture

1 – 2. Bone marrow-derived dendritic cells (BMDC) were generated from bone marrow precursors obtained from BoyJ mice (**1**), stimulated with GM-CSF for 10 days (**2**).

3 – 4. BMDC were seeded in a round-bottomed 96-well plate, and stimulated with opsonised *C. neoformans* or control (**3**), and with chicken ovalbumin (OVA) or ovalbumin peptide 323-339 (OVAp, **4**), overnight.

5. Splenocytes from an OT-II transgenic mouse were isolated (**5**) and enriched in $CD4^+$ lymphocytes using Miltenyi magnetic sorter (**6**).

7. Population enriched in $CD4^+$ lymphocytes was labelled with carboxyfluorescein succinimidyl ester (CFSE) following manufacturers guidelines, and added to the culture containing stimulated BMDC (**7**).

8. Culture plate was incubated for 4 days at 37°C and 5% CO_2 (**8**). Supernatant (SN) was then removed and stored for cytokine profiling, and cells were stained for T cell proliferation assessment.

For full details of each step please refer to Materials and Methods.

In brief, bone marrow-derived dendritic cells (BMDC) were stimulated with OVA or OVAp, in the presence of opsonised-*Cryptococcus* or control. After 18 hours, CFSE-labelled CD4+ T cells obtained from OT-II spleen were introduced to the culture. After 4 days-incubation, cells were stained for proliferation analysis and the supernatant stored for further cytokine profiling.

Carboxyfluorescein succinimidyl ester (CFSE) is a permeable, non-toxic fluorescent dye. When incubated with T cells, it permeates through the plasma membrane and covalently binds to all free amines [241]. Once the labelled T cells are added to the co-culture and start to proliferate, the CFSE-signal dilutes evenly across the progeny. As a result, multiple generations of T cells can be classified according to the brightness of their CFSE signal; the brightest signal corresponding to cells that have not divided.

The assay was optimised for use with the mutant strain of *C. neoformans* Δ*ras1*. Ras1 is a small-GTPase involved in filamentation, mating and thermotolerance of *C. neoformans*. Deletion of this factor results in cells with polarisation and growth defects, which arrest as large cells (7 – 8 μm compared to 5 μm for wildtype strain) when exposed to temperatures over 30°C [182, 183]. This means that in this system, which is incubated at 37°C over 4 days, the mutant will remain viable but not actively proliferating; thus mimicking a latent infection and preventing overgrowth of the DC:T cell co-culture by cryptococci.

Figure 6.2B shows that stimulation by OVAp (purple bars) or OVA (blue bars) triggered up to 7 rounds of T cell proliferation over the 4-day incubation period. The

latter means that the BMDC are able to process and present the complete protein antigen to present the constituent peptide in the correct MHC-II context. All proliferation seen was antigen-dependent, as shown by lack of substantial proliferation beyond 1 cycle when no OVAp or OVA was added (yellow and white bars).

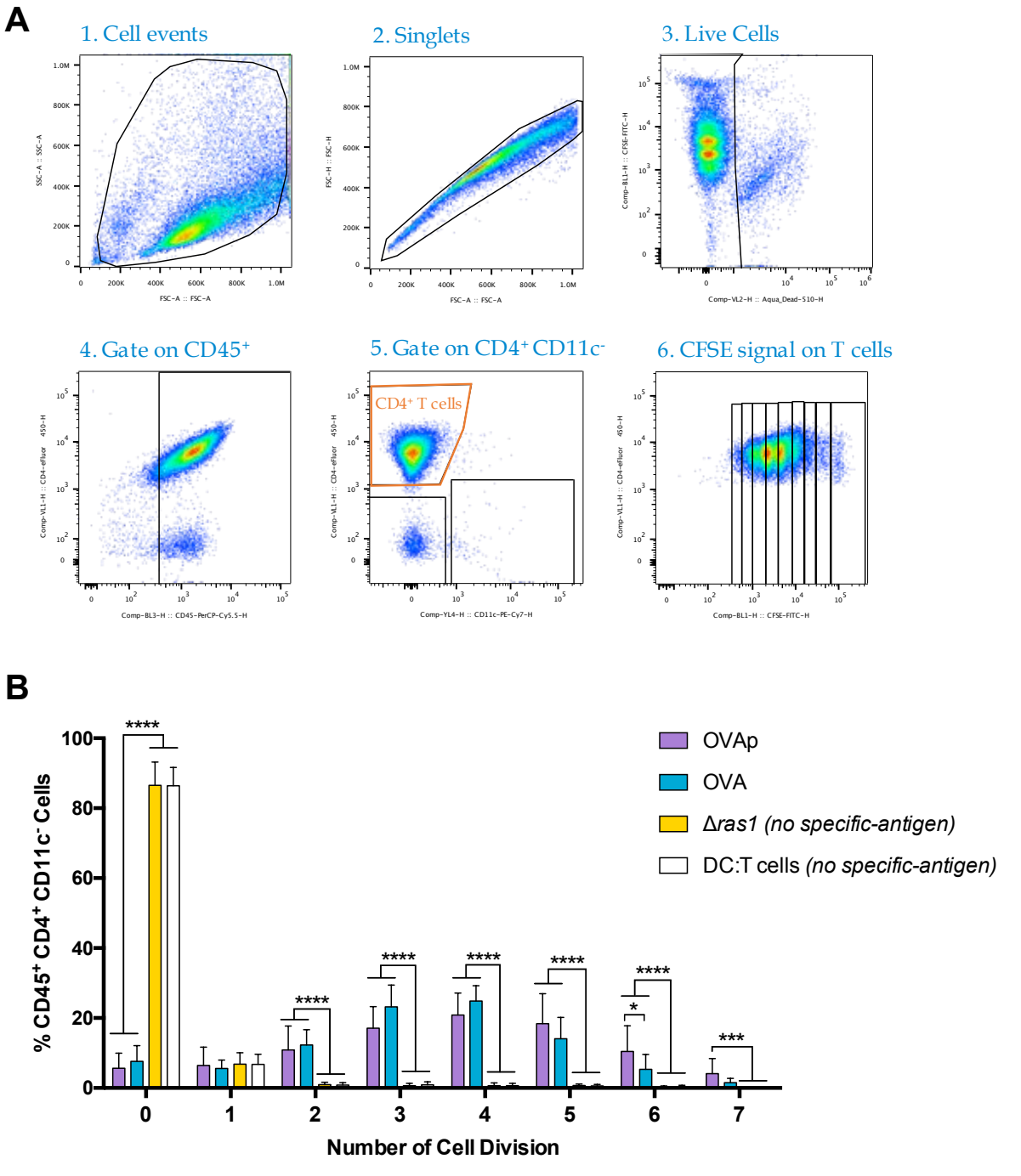

Figure 6.2 *In vitro* proliferation of T cells

A. Gating strategy applied to cells recovered from co-culture described in Figure 6.1 for T cell proliferation analysis.

B. The number of divisions experienced by a T cell during the experiment was determined by the intensity of its CFSE signal (see gating strategy in A). Graph shows percentage of T cells which experienced the designated number of divisions over the course of the co-culture experiment. Data corresponds to 9 independent repeats and error bars depict SD. Two-way ANOVA with Tukey's post-test was performed on Arcsine-transformed data. * $p < 0.05$; *** $p < 0.001$; **** $p < 0.0001$.

6.2 Effect of latent infection with *C. neoformans* on antigen presentation and T cell proliferation

The effect of the mutant strain of *C. neoformans* Δ*ras1* on T cell proliferation was tested with both OVAp and OVA-induced T cell proliferation (Figure 6.3). Even though both antigens result in similar proliferation patterns, addition of Δ*ras1* exclusively inhibited OVA-induced proliferation, typically by a mean 'delay' of 1-2 cell divisions (Figure 6.3A). Addition of exogenously processed OVAp does not require antigen processing and presentation by the BMDC, hence Δ*ras1* could be interfering with these processes.

An alternative possibility is that the physical size of the Cryptococci inhibits cell-cell interactions between DC and T cells. To test this, we applied beads of a similar size to Δ*ras1* cells (7 μm diameter) in the presence of OVA (Figure 6.4). However, T cells were not inhibited at all in these conditions, ruling out physical inhibition of MHC/T cell receptor (TCR) contact as a potential explanation. Interestingly, however, even though addition of beads did not affect OVA-induced proliferation on their own (blue-coloured bars), when tested in conjunction with Δ*ras1* cells, the presence of beads enhanced the inhibition of proliferation reported before (red-coloured bars). Thus, the presence of beads could have an additive effect on the inhibition of proliferation caused by Δ*ras1*.

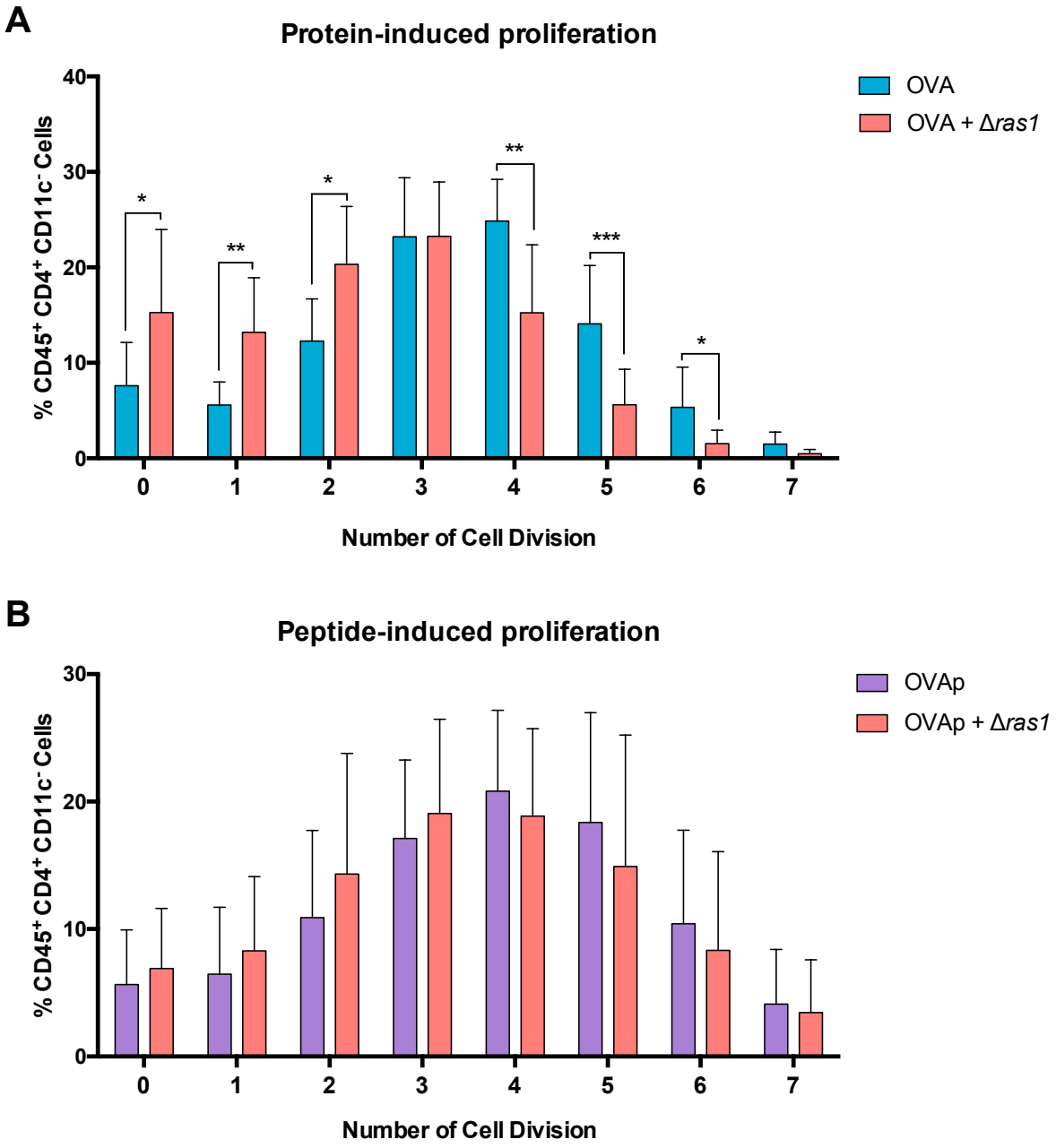

Figure 6.3 Δ*ras1* inhibits OVA-induced T cell proliferation

BMDC:T cells were cultured in the presence of Δ*ras1* or control, together with chicken ovalbumin (OVA, **A**) or ovalbumin peptide (OVAp, **B**). Graphs show percentage of T cells which experienced the designated number of cell divisions over the course of the co-culture experiment. OVA- and OVAp-induced proliferation (blue and purple bars, respectively) were shown in Figure 6.2. Data corresponds to 9 independent repeats and error bars depict SD. Two-way ANOVA and Tukey's post-test performed on Arcsine-transformed data. * $p < 0.05$; ** $p < 0.01$; *** $p < 0.001$.

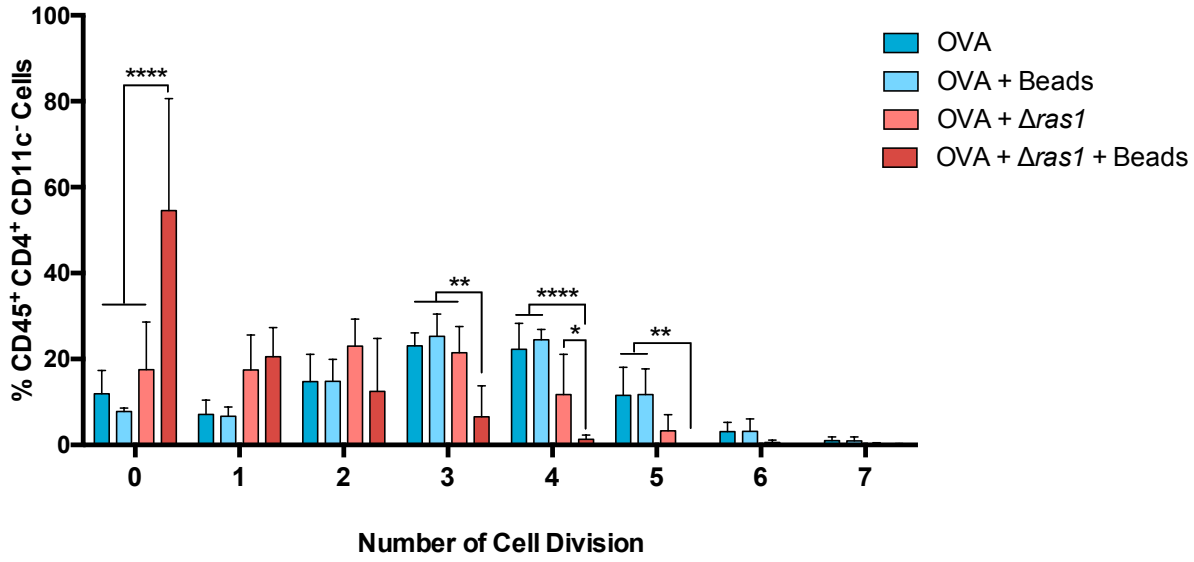

Figure 6.4 Beads do not inhibit OVA-induced T cell proliferation

OVA-stimulated BMDC:T cell co-culture was incubated in the presence of 7 μm inert beads (light blue bars), Δ*ras1* (red bars) or both (dark red bars). Graph shows percentage of T cell which experienced the designated number of cell divisions over the course of the experiment. Data corresponds to 3 independent repeats and error bars depict SD. Two-way ANOVA and Tukey's post-test was performed on Arcsine-transformed data. * $p < 0.05$: ** $p < 0.01$; **** $p < 0.0001$.

To test whether Δ*ras1* could be inhibiting T cell responses directly, rather than via antigen-presentation from DC, the OVA-induced proliferation experiment was repeated with addition of Δ*ras1* 24 hours after that of OVA, allowing the DC to process and present antigen prior to addition of the fungus (Figure 6.5). In this case, ("Delayed Δ*ras1*") T cell proliferation was not inhibited by the presence of Cryptococci, although it should be noted that this data corresponds to only 2 independent experiments, and should be repeated further.

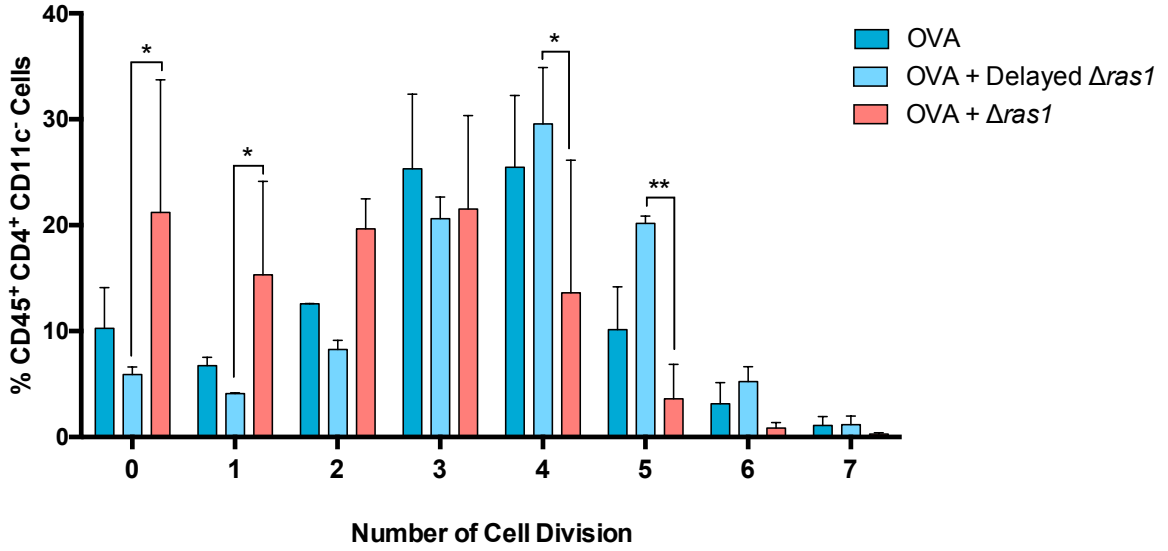

Figure 6.5 Delayed addition of Δ*ras1* lifts inhibition of proliferation

OVA-stimulated BMDC:T cell co-culture was incubated in the presence of Δ*ras1* or control. Δ*ras1* was added immediately after addition of OVA (normal conditions, red bars) or 24 hours after addition of OVA ("Delayed", light blue bars). Data corresponds to 2 independent repeats and error bars depict SD. Two-way ANOVA and Tukey's post-test was performed on Arcsine-transformed data. * $p < 0.05$: ** $p < 0.01$.

Taken together, these data indicate that the presence of Δ*ras1* inhibits T cell proliferation induced by OVA, but not by OVAp. The effect is not due to steric hindrance, since inert beads of the same size as Δ*ras1* do not result in the same effect and does not occur if Δ*ras1* is added at least 24 hours after addition of OVA. Thus, the most parsimonious explanation is that Δ*ras1* directly inhibits antigen processing and presentation abilities of BMDC.

6.3 Effect of *C. neoformans* on BMDC maturation

Priming of naïve T cells requires three signals; presentation of the specific antigen in the correct peptide:MHC context (signal 1), expression of co-stimulatory molecules to interact with their counterparts on T cells (signal 2) and production of cytokines to aid in the functional differentiation of T cells (signal 3) [31]. To confirm that a lack in signal 2 was not responsible for the decreased proliferation observed, the expression of a sample of co-stimulatory molecules [196, 242-245] on BMDC was studied (Table 6.1 and Figure 6.6).

Marker	Function
CCR7 (CD197)	Chemokine receptor expressed on activated APC. Provides a homing signal to secondary lymph nodes [242].
OX40L (CD252)	Co-stimulatory molecule expressed on activated APC. Binds to OX40 in T cells and promotes T cell expansion and survival [243].
CD86	Co-stimulatory molecule expressed on activated APC. Binds to CD28 or CTLA-4 on T cells, and regulates T cell activation and survival [196].
CD40	Co-stimulatory molecule expressed on activated APC. Binds to CD154 on T cells and induces expression of other co-stimulatory molecules [244].
PDL2 (CD273)	Negative regulator of T cell activation. It binds Programmed death-1 (PD-1) on T cells [245].

Table 6.1 Panel of co-stimulatory molecules measured on BMDC

It is generally accepted that culture of bone marrow-precursors with the growth factor GM-CSF results in a mixed population of CD11c+ MHC-II+ dendritic cells and macrophages [246]. Following the gating strategy devised in Helft *et al.* [246] to study *bona fide* dendritic cells, the expression of co-stimulatory molecules in this particular population was assessed (Figure 6.6).

The figure shows that addition of Δ*ras1* does not significantly impact on the expression of any of the molecules tested. Infection with *C. neoformans* is known to have a dampening immunomodulatory effect [247, 248], which agrees with the slight decrease seen, but it is not having a significant impact in these experimental conditions. This is not unexpected, since a change in DC activation would be reflected as a decrease in T cell proliferation for both OVA and OVAp.

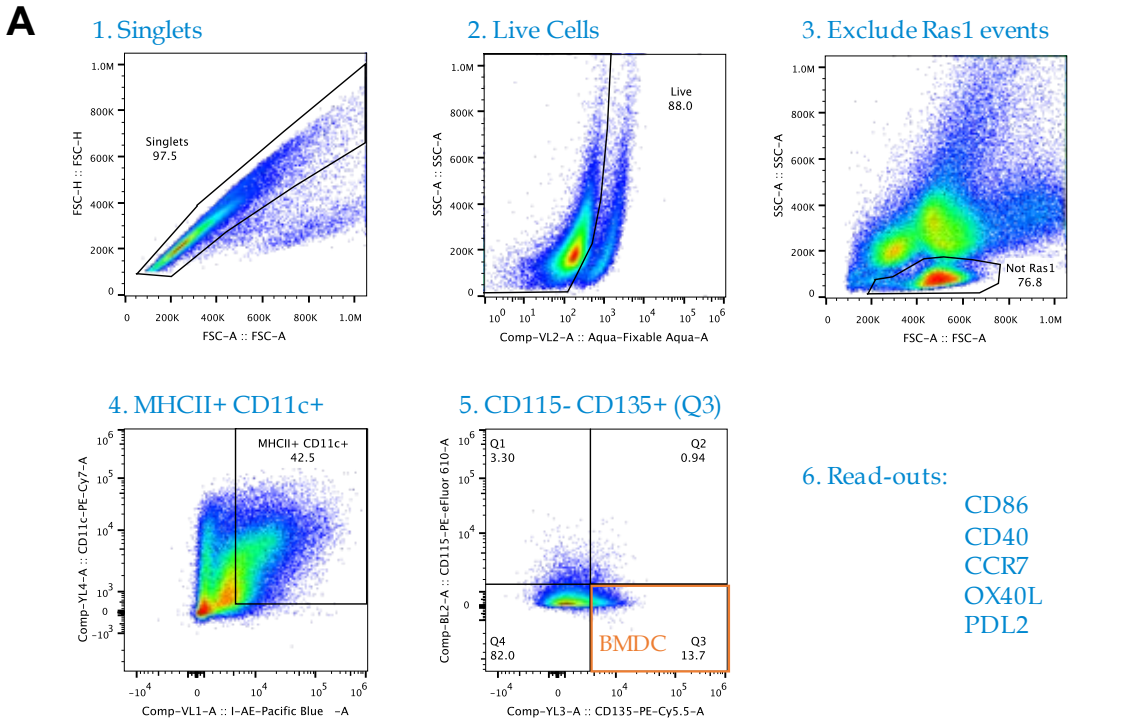

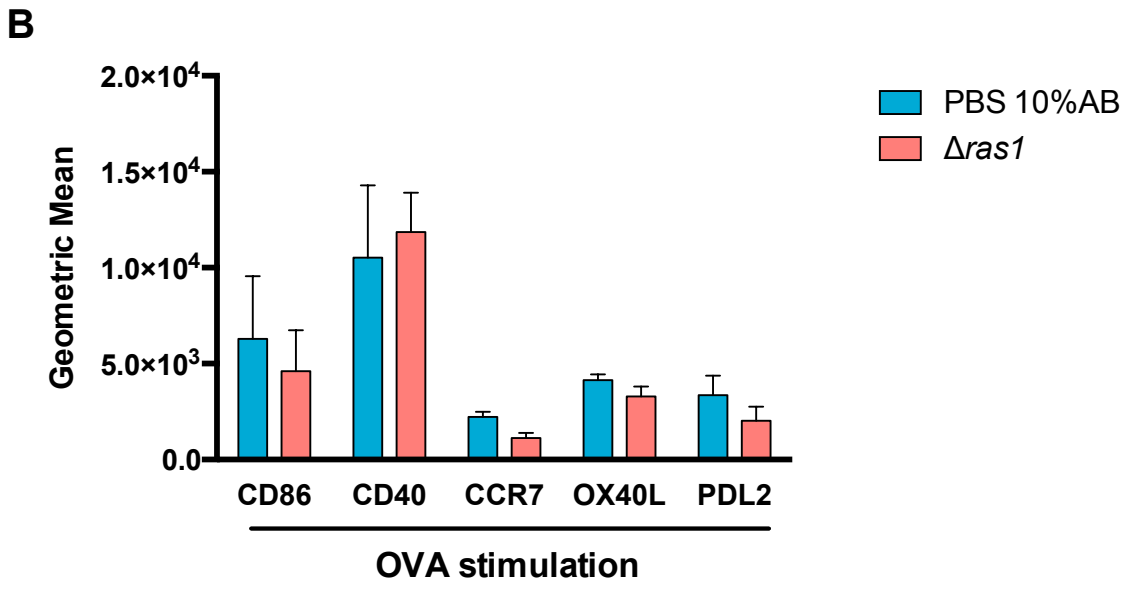

Figure 6.6 Δ*ras1* does not affect expression of co-stimulatory markers

A. Gating strategy applied to BMDC recovered from stimulation with OVA, in the presence of Δ*ras1* or control.

B. Geometric mean + SD of expression of different co-stimulatory molecules on gated BMDC. All cells were stimulated with OVA, in the presence of Δ*ras1* (red bars) or control (blue bars). Data corresponds to 2 independent experiments.

6.4 Effect of capsule on antigen presentation

The production of a thick polysaccharide capsule is one of the most evident virulence factors of *C. neoformans*. The main components of the capsule are the polysaccharides glucuronoxylonmannan (GXM) and galactoxylomannan (GalXM), which make up 90% and 7% of the capsule, respectively [249]. Capsule components can be shed during infection, serving anti-phagocytic and immune-modulating purposes. Shed GXM can be found in the lung of infected mice at a concentration of up to 250 μg/mL [250]. Therefore, the effect of purified capsule on the BMDC:T cell co-culture was tested (Figure 6.7).

The figure shows that addition of purified capsule at a concentration of 4.7 μg/mL (dark green bars) induces the same inhibition of T cell proliferation as addition of Δ*ras1* (A). Interestingly, addition of capsule does not inhibit proliferation of T cells induced by OVAp (B). This strongly suggests that the effect seen with Δ*ras1* is largely due to capsule components.

When added together with capsule, the effect of Δ*ras1* is dramatically enhanced, with most T cells not going beyond one cell division (Figure 6.8).

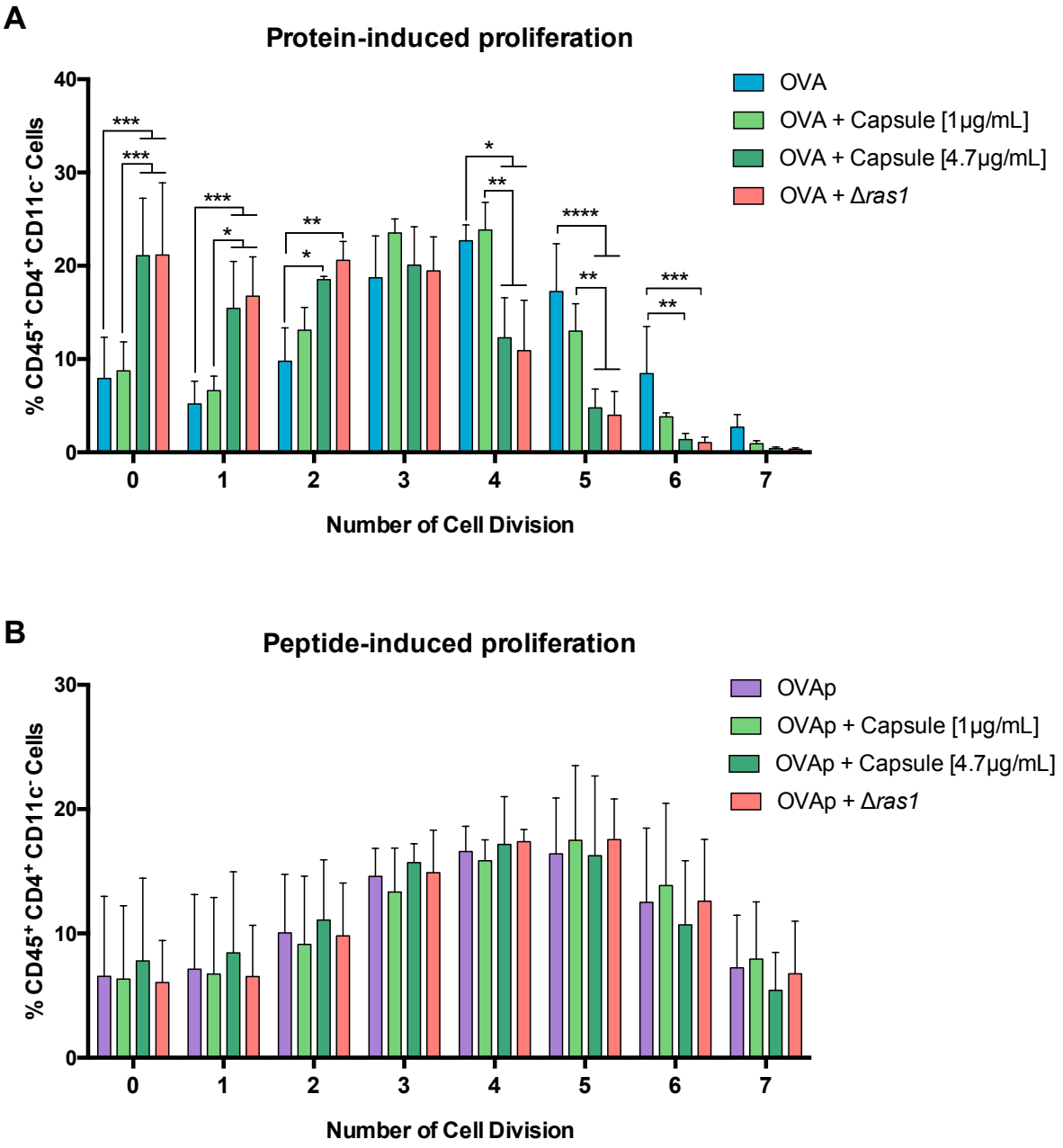

Figure 6.7 Addition of capsule inhibits OVA-induced T cell proliferation

BMDC:T cell co-cultures were stimulated with OVA (**A**, blue bars) or OVAp (**B**, purple bars), in the presence of different doses of capsule (green bars) or of Δ*ras1* (red bars).

Graphs show percentage of T cells which experienced the designated number of divisions over the course of the experiment. Data corresponds to 3 independent repeats and error bars depict SD. Two-way ANOVA followed by Tukey's post-test was performed on Arcsine-transformed data. * $p < 0.05$; ** $p < 0.01$; *** $p < 0.001$; **** $p < 0.0001$.

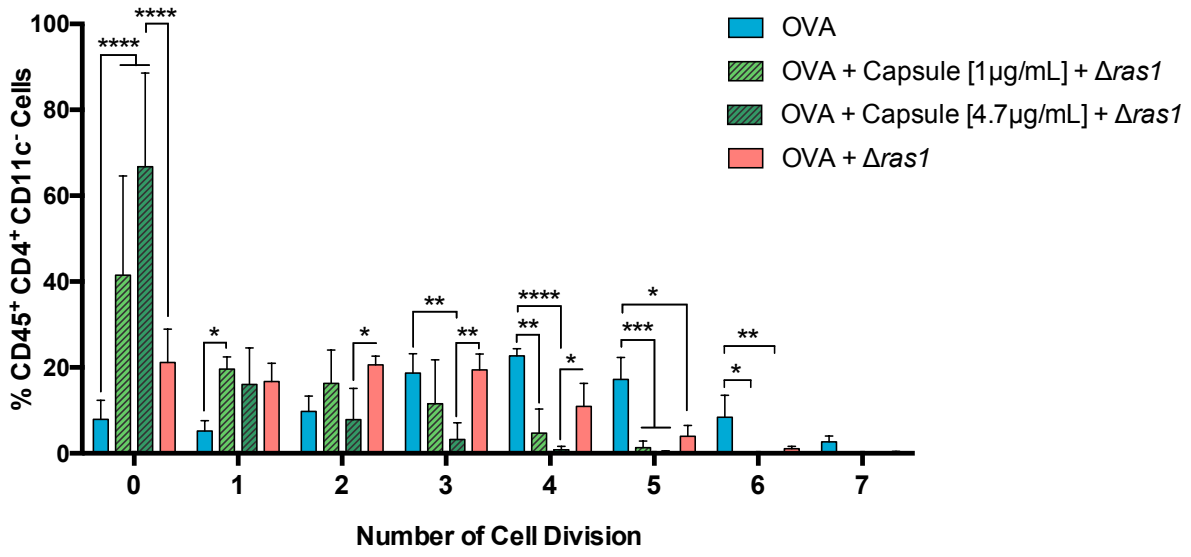

Figure 6.8 Capsule enhances Δ*ras1* inhibitory effect

OVA-stimulated BMDC:T cell was performed in the presence of different doses of capsule and Δ*ras1* (green shaded bars) or Δ*ras1* alone (red bars). Graph shows percentage of T cells which experienced the designated number of cell divisions during the course of the experiment.

OVA-induced proliferation (blue bars) and OVA + Δ*ras1* (red bars) were also shown in Figure 6.7. Data corresponds to 3 independent repeats and error bars depict SD. Two-way ANOVA followed by Tukey's post-test performed on Arcsine-transformed data. * $p < 0.05$; ** $p < 0.01$; *** $p < 0.001$; **** $p < 0.0001$.

To further explore this, the effect of wildtype and acapsular strains on OVA-induced T cell proliferation was tested (Figure 6.9). As with Δ*ras1*, the wildtype strain Kn99α inhibits OVA-induced T cell proliferation. Remarkably, the acapsular strain (Δ*cap59*Δ*uge1* mutant lacking both GXM and GalXM [184], designated ΔCap) does not inhibit but rather enhances OVA-induced T cell proliferation. This could be the result of heightened BMDC activation when infected with ΔCap compared to stimulation with OVA alone, leading to enhanced antigen presentation and T cell proliferation. It should be noted though, that this figure corresponds to a single repeat and the variation depicts SEM between technical replicates.

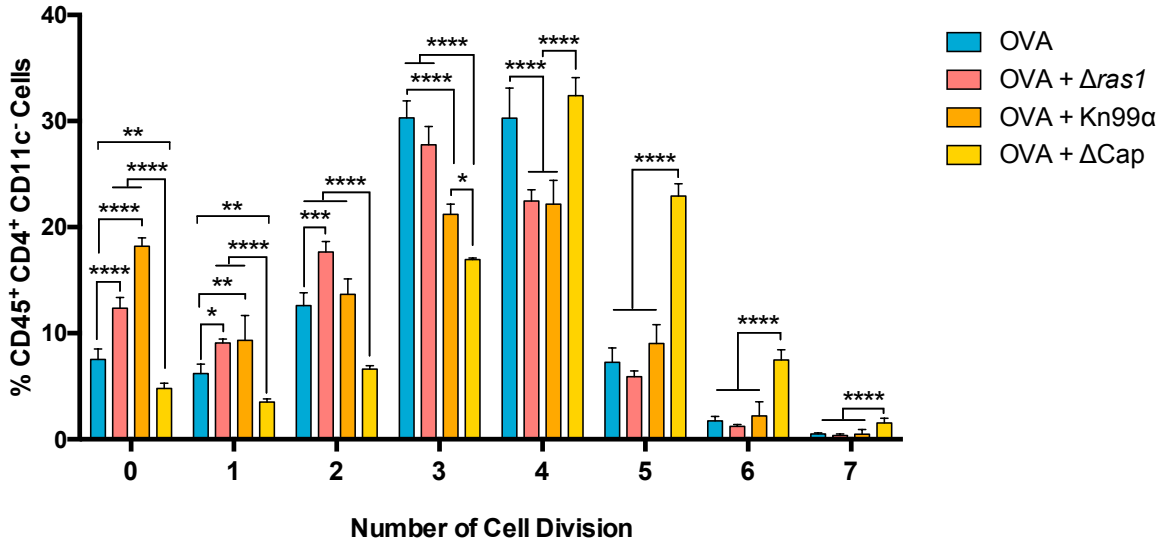

Figure 6.9 Acapsular strain of *C. neoformans* does not inhibit OVA-induced proliferation

OVA-stimulated BMDC:T cell co-culture was performed in the presence of Δ*ras1* (red bars), wildtype *C. neoformans* (Kn99α, orange bars) or the acapsular strain Δ*cap59*Δ*uge1* (ΔCap, yellow bars).

Graph shows percentage of T cells which experienced the designated number of divisions over the course of the experiment. Data corresponds to a single experiment and variation is SEM from technical replicates. Two-way ANOVA followed by Tukey's post-test performed on Arcsine-transformed data. * $p < 0.05$; ** $p < 0.01$; *** $p < 0.001$; **** $p < 0.0001$.

Taken together, these results clearly show that addition of capsule from *C. neoformans* recapitulates the effect seen with Δ*ras1*. Addition of capsule specifically inhibits OVA-induced T cell proliferation, in a dose-dependent manner. When added in conjunction with Δ*ras1*, the inhibitory effect is dramatically enhanced. Furthermore, an acapsular strain of *C. neoformans* had no inhibitory effect on this system. This argues for an effect of Δ*ras1*, through its shed capsule, on antigen processing and presentation by BMDC, which then leads to the reduction in T cell proliferation observed.

As mentioned before, antigen presentation is but one of the signals needed to induce a T cell response. Secretion of cytokines by the antigen presenting cell (Signal 3) aids

in the functional differentiation of the T cell response elicited [31]. Hence, supernatants from the co-cultures were analysed for their cytokine profile. The cytokines measured are listed in Table 6.2.

Cytokine		Response
IL-2	Necessary for T cell survival and replication	
IFNγ	Important macrophage activator	Th1
TNFα	Pro-inflammatory cytokine	
IL-4	Th2-inducing cytokines. Involved in allergic inflammation and IgE-switch	Th2
IL-13		
IL-17A	Pro-inflammatory cytokine	Th17

Table 6.2 Panel of cytokines measured in co-culture supernatant

Figure 6.10 shows the concentration of cytokines recovered from OVA-stimulated DC:T cell co-cultures, in the presence of increasing doses of capsule. Addition of the highest dose of capsule reduces the secretion of IL-2, IFNγ and TNFα (blue lines). The presence of Δ*ras1* (red lines) has an overall dampening effect on cytokine secretion, although this is not statistically significant.

Given the inhibitory effect of capsule and Δ*ras1* on T cell proliferation reported earlier, it is not surprising that these conditions also lead to a decrease in IL-2 secretion, which is necessary for T cell survival/replication [251]. The presence of capsule also decreases IFNγ and TNFα production; collectively skewing the co-culture away from

a Th1 response. The presence of Δ*ras1* results in a trend favouring a Th17 response. It should be noted that the panel used is very limited and any conclusions in terms of T helper response elicited are merely preliminary estimations. Further work, ultimately using a live animal model, should be carried out to allow for more comprehensive answers as to the quality of the T cell response elicited.

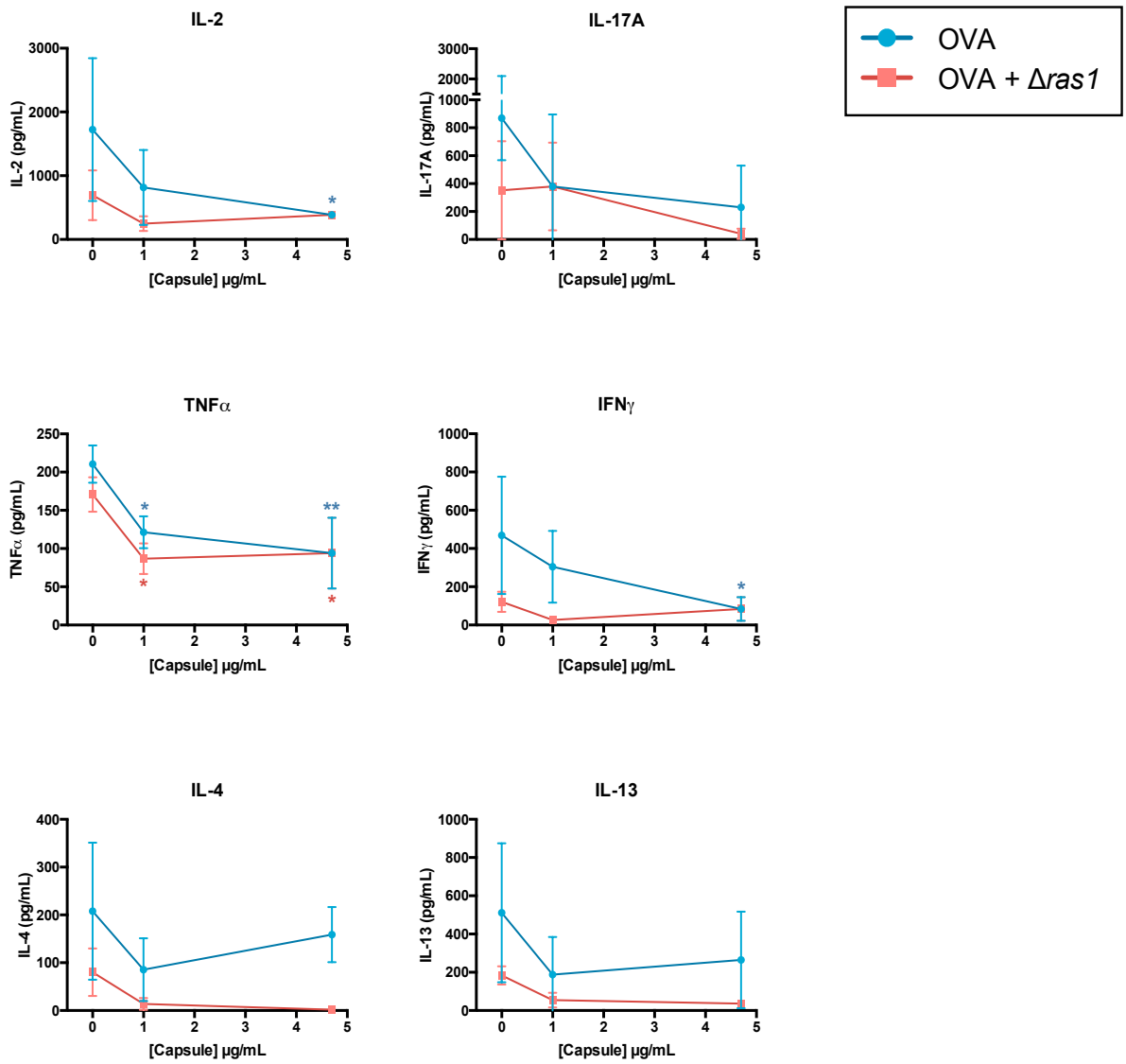

Figure 6.10 Capsule inhibits secretion of IL-2, IFNγ and TNFα

Cytokine profiling of supernatants from OVA-stimulated BMDC:T cell co-cultures in the presence of different doses of capsule, with or without Δ*ras1* (red and blue lines, respectively). Data corresponds to 3 independent experiments, whose proliferation data is shown in Figures 6.7 and 6.8. Error bars correspond to SD. Two-way ANOVA followed by Tukey's post-test. * $p < 0.05$; ** $p < 0.01$.

6.5 Effect of inhibition of ERK5 on antigen presentation

Given previous findings on the effects of ERK5 inhibition on macrophage polarisation and vomocytosis occurrence (discussed in chapter 4), the impact of ERK5 inhibition on this system was explored.

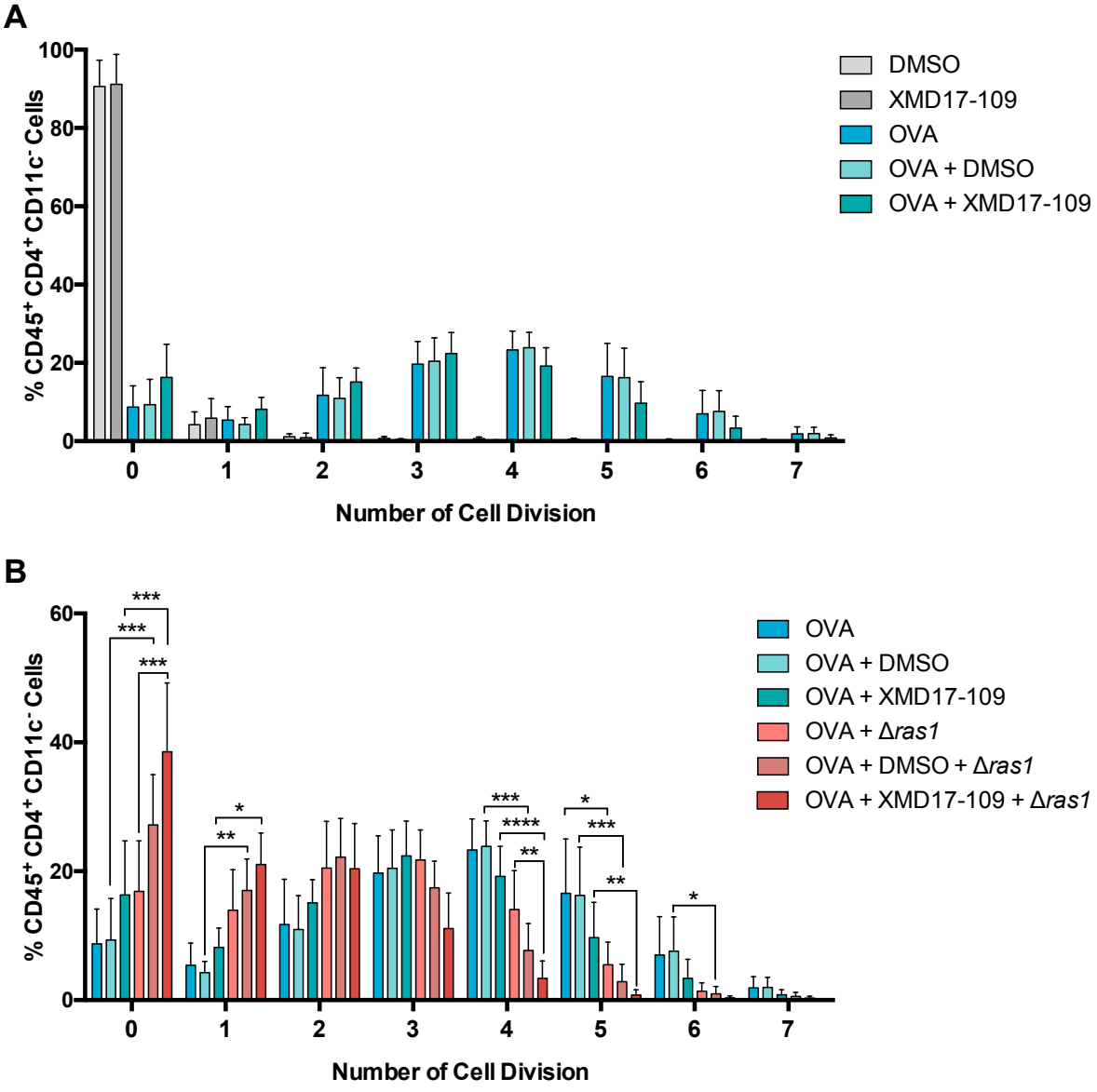

Figure 6.11 XMD17-109 does not affect OVA-induced T cell proliferation
OVA-stimulated BMDC:T cell co-cultures were performed in the presence of XMD17-109 (teal bars) or DMSO control (light teal bars), alone (**A**) or in conjunction with Δ*ras1* (red coloured bars, **B**). Data for proliferation in the absence of Δ*ras1* is the same in both graphs.
Graphs show T cell proliferation resulting over the course of the experiment. Data corresponds to 3 independent repeats and error bars depict SD. Two-way ANOVA followed by Tukey's post-test performed on Arcsine-transformed data. * $p< 0.05$; ** $p < 0.01$; *** $p < 0.001$; **** $p < 0.0001$.

The figure shows that neither the ERK5 inhibitor, XMD17-109, nor the DMSO control induce T cell proliferation in the absence of antigen, nor do they inhibit OVA-induced proliferation (Figure 6.11A). Moreover, in the presence of XMD17-109 Δ*ras1* has a slightly enhanced anti-proliferative effect (Figure 6.11B).

In the current system, addition of inhibitors and T cells was performed without prior washing. To eliminate possible effects of the inhibitors directly on T cells, a washing step immediately before addition of the T cells was carried out (Figure 6.12). In this case, the delay seen previously with the ERK5 inhibitor in the presence of Δ*ras1* is completely lifted. A direct effect of Δ*ras1* on T cells is tempting to suggest, however Δ*ras1* was not able to inhibit OVAp-induced proliferation even in "non-washed" settings (B), thus making this possibility less probable. The most likely explanation is that during the washing steps some of the Δ*ras1* inoculum was lost. This would argue that a threshold "dose" of Δ*ras1*, or a prolonged interaction of Δ*ras1* with BMDC beyond the first 18 hours, are necessary to impact T cell proliferation.

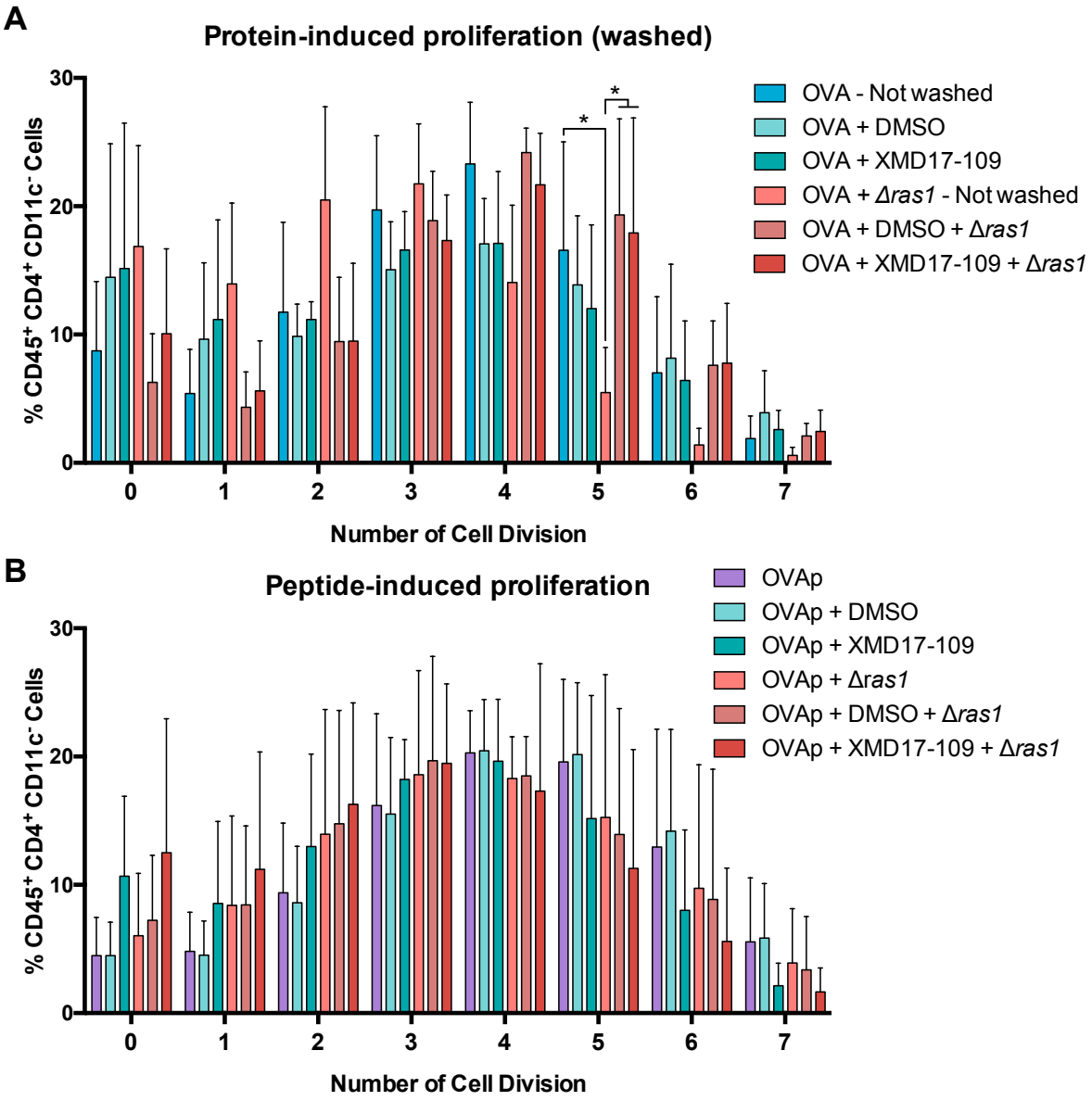

Figure 6.12 Washing step lifts inhibition on T cell proliferation

A. OVA-stimulated BMDC:T cell co-culture where ERK5 inhibitors were washed before addition of T cells. Data corresponding to controls without XMD17-109 or DMSO were not washed, and is the same as shown in Figure 6.11B.

B. OVAp-stimulated BMDC:T cell co-culture performed without washing step before addition of T cells.

Graphs show T cell proliferation resulting over the course of the experiment. Data corresponds to 3 independent repeats. Two-way ANOVA followed by Tukey's post-test performed on Arcsine-transformed data. * $p < 0.05$; ** $p < 0.01$; *** $p < 0.001$; **** $p < 0.0001$.

6.6 Effect of IFNα on T cell proliferation

The previous chapter discussed the impact of viral exposure, and of type-I interferons, on vomocytosis. Type-I interferons are antiviral cytokines, and as such can play a role in the induction of T cell effector responses. The impact of IFNα on this T cell proliferation system was tested (Figure 6.13).

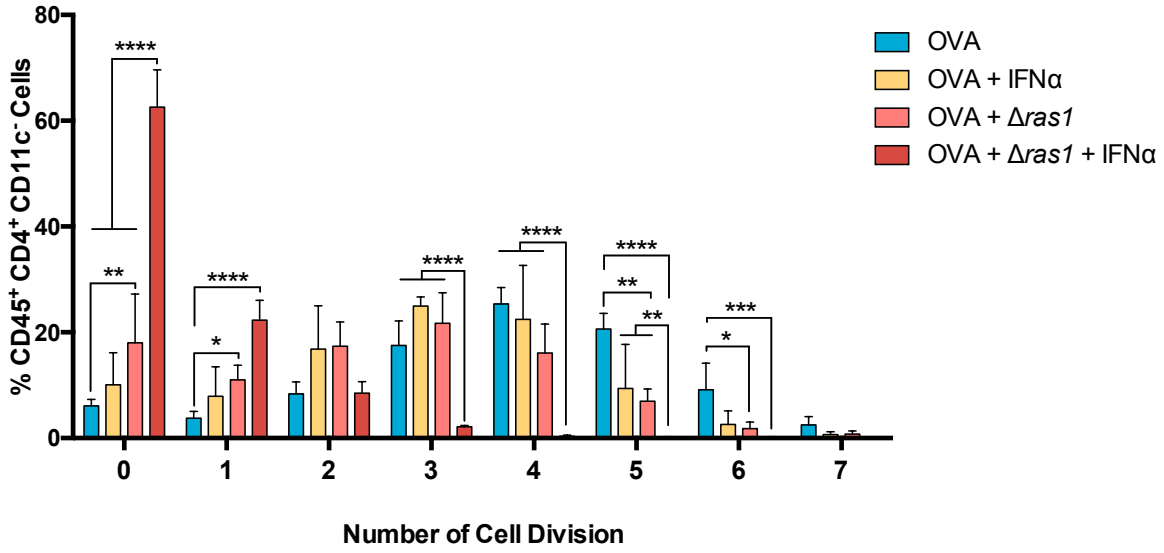

Figure 6.13 Stimulation with IFNα does not affect OVA-induced T cell proliferation
OVA-stimulated BMDC:T cell co-cultures were performed in the presence of 10 pg/mL IFNα (yellow bars), Δ*ras1* (red bars) or both (dark red bars).
Graph shows percentage of T cells which experienced the designated number of divisions over the course of the experiment. Data corresponds to 2 independent repeats and error bars to SD. Two-way ANOVA followed by Tukey's post-test performed on Arcsine-transformed data. * $p < 0.05$; ** $p < 0.01$; *** $p < 0.001$; **** $p < 0.0001$.

The figure shows that stimulation with IFNα alone did not affect OVA-induced T cell proliferation. In the presence of this cytokine, the impact of Δ*ras1* was greatly

enhanced, with over 60% of T cell not experiencing a single cell division over the course of the experiment and none going beyond 3 cycles.

The effect of IFNα on T cell proliferation has been subject of debate in the literature. Many early reports describe the anti-proliferative properties of IFNα on different systems. Holán *et al.* showed that stimulation with purified human IFNα inhibits proliferation of ConA-stimulated peripheral blood lymphocytes [252]. Furthermore, Erickson *et al.* proposed that this anti-proliferative effect could be achieved through changes in the cell cycle regulatory proteins, which then lead to a block of S-phase entry [253]. Mechanistically, Zella *et al.* showed that long-term stimulation with IFNα causes a decrease in CD3 and CD28 expression on T cells, which subsequently leads to lower levels of IL-2 and the anti-proliferative effect previously mentioned [254]. More recently, however, the reported effects of type-I IFN on T cells have expanded beyond anti-proliferative. It was described that IFNα-stimulation is important for the induction of Th1 responses to allergens [255] and to viral infections [256]. Moreover, Tough *et al.* showed that low doses of IFNβ induce T cell proliferation *in vivo* [257], and Le Bon *et al.* reported type-I IFN acting directly on T cells to increase $CD8^+$ expansion and cross-presentation [258]. In our system, addition of IFNα alone did not impact T cell proliferation, although it drastically enhanced the inhibitory effect of Δ*ras1*. Further work is needed to unravel the mechanism(s) at play.

7 Discussion

Cryptococcus neoformans is a ubiquitous environmental fungus [12]. Due to its global distribution and association with pigeon excreta, it is able to reach rural and urban populations, as it is evident from the presence of antibodies to Cryptococcal antigens in children [13]. It is an opportunistic fungal pathogen, meaning that the vast majority of cases are in patients suffering from other debilitating illness such as AIDS. Even though the AIDS pandemic is much more manageable than it was in the 1980s, when Cryptococcal meningitis started to make its way to headlines, the rise in immunosuppressed patients from transplant therapy and cancer keep cryptococcosis as a significant healthcare issue. It is therefore paramount that we, the scientific community, continue to study this opportunistic fungus so as to gain better understanding of the infection process and develop novel treatment options.

Throughout my PhD I have studied Cryptococcal infection using *in vitro* models. For the first part, I focused on the interaction of *Cryptococcus* with macrophages, and on the process of vomocytosis. For the last part, I looked at the effect of a latent Cryptococcal infection on antigen presentation.

7.1 Inhibition of ERK5 affects macrophage polarisation and enhances vomocytosis of *C. neoformans*

Vomocytosis is a non-lytic exocytosis event, which was first described for *Cryptococcus neoformans* in 2006 using J774A.1 cells [51, 52]. Since then, it has been described in many different models, including live infection of zebrafish [65-67]. What is more, vomocytosis-like events have been reported for bacterial species [85-88]. Despite these advances, the process of vomocytosis remains poorly understood. Recently, our lab uncovered the first molecular handle capable of modulating vomocytosis; inhibition of the atypical MAP kinase ERK5 enhances vomocytosis [84].

ERK5 has been implied in the response to stress (H_2O_2 [99]), growth factors (G-CSF [100] and EGF [101]) and cytokines (LIF [102]). The activation of this signalling cascade affects several cellular processes such as proliferation, cell survival, motility and angiogenesis [259]. Initially, research on ERK5 focused mainly on cardiovascular cells and neuronal development. Generation of an ERK5 null mice revealed that this mutation leads to defects in angiogenesis and cardiac development, resulting in embryonic lethality [260]. More recently, however, the effects of this signalling cascade on myeloid cells have been addressed. Using a myeloid-specific ERK5 deficient mouse model, it was shown that ERK5 activation impedes M1 polarisation under steady-state conditions [261].

My work expanded this finding using both murine and human macrophages, and the widely-accepted polarising stimuli LPS + IFNγ and IL-4. Using these models and the ERK5 inhibitor XMD17-109, I found that inhibition of ERK5 enhances (LPS + IFNγ)-induced M1 polarisation, and dampens IL-4-induced M2 phenotype. This was linked

to an effect on vomocytosis of *C. neoformans*, which is known to be affected by macrophage polarisation [83].

Our findings are in line with recent research from Dr. Tournier's group, where they report that ERK5 deficiency enhances pro-inflammatory (anti-tumour) polarisation in tumour-associated macrophages (TAM) [262]. In this model, pro-inflammatory polarisation was dependent on STAT3 activation. The involvement of this signalling molecule on the effect of ERK5 inhibition on vomocytosis remains to be explored.

7.2 Viral exposure enhances vomocytosis

Cryptococcosis is particularly relevant among AIDS patients [14]. A study conducted in 2014 estimated that cryptoccocal meningitis was responsible for 15% of AIDS-related deaths worldwide [14]. This highlights the importance of incorporating the context of a viral infection when studying *C. neoformans* infection. Thus, we set out to study vomocytosis of *C. neoformans* in macrophages co-infected with a viral agent.

The main finding pertaining this research is that viral exposure enhances vomocytosis of *C. neoformans*. This result was obtained using an attenuated strain of HIV (HIVR9Δ*env* + SIV*vpx*) as well as fully infectious GFP-tagged MeV. It was also recapitulated when macrophages were stimulated with polyIC, IFNα or IFNβ, and abrogated when type-I interferon signalling was blocked.

The effect of type-I interferons on cryptococcosis has been looked at in the past, and different groups have arrived at opposing conclusions [114, 115, 174]. Using a murine model of cryptococcosis, Sato *et al*. showed that IFNAR KO animals had enhanced survival than wildtype animals. The effect was attributed to increased mucus production in the lung and improved fungal clearance in IFNAR KO animals, suggesting a detrimental role of type-I interferons on cryptococcosis [114].

Almost in parallel and using a very similar murine cryptococcal infection model, Sionov *et al*. showed that treatment with polyICLC, a more stable version of polyIC, greatly enhanced survival of mice infected with *C. neoformans*. The protective effect was mediated by type-I interferon production and polarisation to a protective Th1/Th17 response [115]. In line with these findings, a beneficial role of type-I interferons on cryptococcosis had been reported earlier by Biondo *et al*. In this case, infection of IFNAR KO animals led to increased mortality, higher fungal burden and a non-protective Th2-skewed immune response [174].

Our findings fit in with the results presented by Sionov *et al*. In their system, stimulation with polyICLC induces production of type-I interferons, which leads to decreased dissemination to the CNS and reduced mortality [115]. We show that type-I interferons enhance vomocytosis of *C. neoformans*. Therefore, a possible mechanistic explanation for the effect of polyICLC observed is that elevated vomocytosis occurrence within the lungs (due to induction of type-I interferons) leads to fewer Cryptococcal cells within macrophages, reducing their ability to hijack these cells as a *Trojan horse* to disseminate to distal sites within the body such as the CNS. In agreement with this suggested mechanism, Sionov *et al*. mention that if the polyICLC

treatment is given 3 days post infection, when Cryptococcal cells have already reached the CNS, then they do not observe a protective effect [115].

Our research helps explain a previously observed phenomenon, and further highlights the importance of vomocytosis for disease progression. Given its covert escape nature, vomocytosis has always been thought to play a role in dissemination within the host. It was not until a decade after its first description, though, that the first evidence for this was put forward. Gilbert *et al*. showed that enhanced vomocytosis, through pharmacological inhibition of ERK5, leads to decreased dissemination in a zebrafish cryptococcosis model [84]. Nonetheless, it was noted that the location and timing of the vomocytosis event could render it beneficial or detrimental for the host. Sionov *et al*. remark that the protective effect of polyICLC is time-dependent further strengthens this notion.

As it was mentioned in the introduction, there have been reports of vomocytosis-like events for some bacterial pathogens [85-88]. In these cases, assessment of whether the vomocytosis-like event was beneficial or detrimental to the host was also context-dependent. In the case of UPEC, for example, release of intracellular bacteria was deemed beneficial for the host as it allowed for bacterial load to be eliminated with the flow of bodily fluids [87]. In the case of *Serratia maracescens* however, non-lytic exocytosis from epithelial cells was considered detrimental for the host as it aided bacterial dissemination [88].

7.3 Bacterial exposure enhances vomocytosis

Type-I interferons have historically been regarded as anti-viral cytokines [106, 263]. However, in more recent years, their effect into other non-viral infections has been explored [118]. Moreover, some non-viral pathogens have been seen to induce their production [129, 165, 264]. Thus, the possibility of other non-viral pathogens having an effect on vomocytosis of *C. neoformans* was explored.

Pseudomonas aeruginosa is an opportunistic bacterial pathogen, present in soil and water. It causes disease in previously weakened individuals, being very relevant in cystic fibrosis patients [233]. It was chosen for the preliminary study of bacteria:*Cryptococcus* co-infection since both pathogens cause chest infections, and could therefore interact in pathophysiological conditions. It has also been reported that *P. aeruginosa* induces production of type-I interferons [235], which were shown to affect vomocytosis. Preliminary results show that *P. aeruginosa* is able to enhance vomocytosis of *C. neoformans*. It would be interesting to explore whether other bacterial pathogens have the same effect on vomocytosis. Stimulation with bacterial LPS had no impact on vomocytosis occurrence, suggesting that activation of this signalling pathway (LPS-TLR4) alone is not sufficient to elicit the effect. Further work testing different doses of LPS, other bacterial pathogens and addition of heat-killed bacteria is needed.

With the results presented so far, the emerging working model is that vomocytosis is triggered in response to stress, such as viral or bacterial infection. *Cryptococcus*-containing macrophages, when exposed to a second infection, expel their phagosomal cargo potentially to devote resources and energy to dealing with the new threat. This would only apply to persisting live intracellular pathogens, since vomocytosis is not observed with heat-killed *Cryptococcus*. *Cryptococcus*-free macrophages would then be engaged in combating the ongoing second infection and secreting cytokines to recruit more immune cells to the site of infection. Recruited cells, such as neutrophils, could in turn phagocytose and kill the expelled *Cryptococci*.

We showed that vomocytosis is modulated by the MAP kinase ERK5, which is known to be involved in the response to osmotic stress. It is therefore an interesting possibility that ERK5 be the integrating signalling molecule to coordinate vomocytosis at times of stress.

7.4 Presence of *Cryptococcus* affects antigen presentation

As it has been mentioned before, humans are typically exposed to *C. neoformans* at an early age [13]. Initial contact can lead to clearance by a competent immune system, or containment as granulomas in the lung [236, 238, 239]. We therefore set out to explore the impact of prolonged presence of *C. neoformans* within the lung environment on antigen presentation and antigen-induced T cell proliferation.

To this end, together with Dr. Guillaume Desanti, an *in vitro* bone marrow-derived dendritic cell (BMDC):T cell co-culture system was optimised. This system uses T cells recovered from transgenic OT-II mice, which are specific for the chicken ovalbumin peptide 323-339 (OVAp). Addition of commercially available OVAp, or of the complete chicken ovalbumin protein (OVA), allows to test for effects on antigen presentation and processing, respectively.

This system was optimised for the use of *C. neoformans* mutant Δ*ras1* [182, 183]. As explained elsewhere, this mutant remains viable but not actively proliferating when incubated at 37 °C [182, 183]. As a result, Δ*ras1* is a good candidate to test the effects of prolonged exposure to *Cryptococcus* without overwhelming the culture system.

The main finding from this ongoing project is that the presence of *Cryptococcus* inhibits antigen-induced proliferation of T cells. The effect is seen as a delay in 1-2 divisions within the experimental timeframe. Importantly, this inhibition is exclusively seen with OVA-induced proliferation and can be recapitulated by addition of purified capsule.

Previous studies had commented on the inhibitory abilities of *C. neoformans'* capsule on T cell proliferation. Collins and Bancroft showed that encapsulated strain of *C. neoformans* B3501 inhibits proliferation of T cells, and attributed the effect to the anti-phagocytic effect of capsule on macrophages (macrophages were used as antigen presenting cells in this assay) [265]. Later on, Vecchiarelli *et al*. showed that the same strain did not induce maturation and activation of DC, which resulted in inhibited T cell proliferation when compared to an acapsular strain [266]. This effect was not due

to limited uptake, however, since the same result was shown after opsonising capsular *Cryptococcus* with anti-GXM antibody 18B7, which affords similar uptake to acapsular strain [266].

The results presented here expand these previous findings, adding that the capsule of *C. neoformans* interferes with processing of an unrelated antigen, OVA, which leads to diminished antigen presentation and T cell proliferation.

The mechanism behind this effect is currently unknown, although preliminary work shows that the presence of Δ*ras1* does not impede DC maturation. One tentative explanation could be that shed capsule components, either from extracellular *Cryptococci* or within *Cryptococcus*-containing phagosomes, interfere with antigen processing. Processing of exogenous proteins for presentation within an MHC-II complex involves degradation of the protein in acidified endosomes and incorporation of the resulting peptides to MHC-II molecules, the loaded complex is then trafficked to the cell surface [31]. Capsule components could be interfering with this process by protein adsorption to the sugar-rich capsule and masking of new potential antigens, or by buffering the phagosomal compartment to inhibit protein degradation. In support of this possible mechanism, it has been shown that the acid-base properties of glucuronic acid residues in capsular polysaccharides are able to buffer phagosomal pH [74]. It would be interesting to test for the presence of intracellular capsule material within BMDC in this system, and the phagosomal pH under these experimental conditions.

7.5 Final remarks

The work presented here was aimed to broaden our understanding of Cryptococcal infection making use of different techniques and *in vitro* systems. Throughout this Thesis I have tried to recreate physiologically relevant contexts in which to study this infection. Using time-lapse microscopy, I have looked at the interaction between *Cryptococcus* and human macrophages, focusing on the under-studied event of vomocytosis. I have explored the effects of including a second viral infection in this system, stemming from the high prevalence of cryptococcosis on HIV^+/AIDS patients [14]. I have set up an *in vitro* dendritic cell: T cell co-culture system, which permits the study of antigen presentation and antigen-induced T cell proliferation. Using a mutant strain of *C. neoformans* (Δ*ras1*), I have studied the effects of extended exposure to a dormant infection on these processes, relating to the prolonged presence of *C. neoformans* in human lungs *in vivo* [238, 239]. I found that incorporating these context-specific cues has important biological consequences; enhanced vomocytosis occurrence in viral co-infection and interference with antigen processing within antigen-presenting cells. Consequently, this work highlights the importance of incorporating environmental cues to previously established models and the effects these may have on cellular processes.

List of References

1. Busse, O., *Uber parasitare Zelleinschlusse und ihre Zuchtung.* Centralbl Bakt Parasit 1894. **16**.
2. Sanfelice, F., *Contributo alla morfologia e biologia dei blastomiceti che si sviluppano nei succhi de alcuni frutti.* Ann Ist Ig R Univ Roma, 1894(4): p. 463–469.
3. Srikanta, D., F.H. Santiago-Tirado, and T.L. Doering, *Cryptococcus neoformans: historical curiosity to modern pathogen.* Yeast, 2014. **31**(2): p. 47-60.
4. Ma, H. and R.C. May, *Virulence in Cryptococcus species.* Adv Appl Microbiol, 2009. **67**: p. 131-90.
5. Franzot, S.P., I.F. Salkin, and A. Casadevall, *Cryptococcus neoformans var. grubii: separate varietal status for Cryptococcus neoformans serotype A isolates.* J Clin Microbiol, 1999. **37**(3): p. 838-40.
6. Kwon-Chung, K.J. and A. Varma, *Do major species concepts support one, two or more species within Cryptococcus neoformans?* FEMS Yeast Res, 2006. **6**(4): p. 574-87.
7. Nielsen, K., et al., *Sexual cycle of Cryptococcus neoformans var. grubii and virulence of congenic a and alpha isolates.* Infect Immun, 2003. **71**(9): p. 4831-41.
8. Kronstad, J.W., et al., *Expanding fungal pathogenesis: Cryptococcus breaks out of the opportunistic box.* Nat Rev Microbiol, 2011. **9**(3): p. 193-203.
9. Kozubowski, L. and J. Heitman, *Profiling a killer, the development of Cryptococcus neoformans.* FEMS Microbiol Rev, 2012. **36**(1): p. 78-94.

10. Wang, L., B. Zhai, and X. Lin, *The link between morphotype transition and virulence in Cryptococcus neoformans.* PLoS Pathog, 2012. **8**(6): p. e1002765.

11. Harrison, T.S., *Cryptococcus neoformans and cryptococcosis.* J Infect, 2000. **41**(1): p. 12-7.

12. May, R.C., et al., *Cryptococcus: from environmental saprophyte to global pathogen.* Nat Rev Microbiol, 2016. **14**(2): p. 106-17.

13. Goldman, D.L., et al., *Serologic evidence for Cryptococcus neoformans infection in early childhood.* Pediatrics, 2001. **107**(5): p. E66.

14. Rajasingham, R., et al., *Global burden of disease of HIV-associated cryptococcal meningitis: an updated analysis.* Lancet Infect Dis, 2017. **17**(8): p. 873-881.

15. Voelz, K. and R.C. May, *Cryptococcal interactions with the host immune system.* Eukaryot Cell, 2010. **9**(6): p. 835-46.

16. Hole, C. and F.L. Wormley, Jr., *Innate host defenses against Cryptococcus neoformans.* J Microbiol, 2016. **54**(3): p. 202-11.

17. Ruckerl, D. and J.E. Allen, *Macrophage proliferation, provenance, and plasticity in macroparasite infection.* Immunol Rev, 2014. **262**(1): p. 113-33.

18. Noverr, M.C., et al., *Role of PLB1 in pulmonary inflammation and cryptococcal eicosanoid production.* Infect Immun, 2003. **71**(3): p. 1538-47.

19. Retini, C., et al., *Encapsulation of Cryptococcus neoformans with glucuronoxylomannan inhibits the antigen-presenting capacity of monocytes.* Infect Immun, 1998. **66**(2): p. 664-9.

20. Wozniak, K.L., et al., *Role of IL-17A on resolution of pulmonary C. neoformans infection.* PLoS One, 2011. **6**(2): p. e17204.

21. Murdock, B.J., et al., *Interleukin-17A enhances host defense against cryptococcal lung infection through effects mediated by leukocyte recruitment, activation, and gamma interferon production.* Infect Immun, 2014. **82**(3): p. 937-48.

22. Mukaremera, L. and K. Nielsen, *Adaptive Immunity to Cryptococcus neoformans Infections.* J Fungi (Basel), 2017. **3**(4).

23. Gupta, S., et al., *Disseminated cryptococcal infection in a patient with hypogammaglobulinemia and normal T cell functions.* Am J Med, 1987. **82**(1): p. 129-31.

24. Subramaniam, K., et al., *IgM(+) memory B cell expression predicts HIV-associated cryptococcosis status.* J Infect Dis, 2009. **200**(2): p. 244-51.

25. Rivera, J., O. Zaragoza, and A. Casadevall, *Antibody-mediated protection against Cryptococcus neoformans pulmonary infection is dependent on B cells.* Infect Immun, 2005. **73**(2): p. 1141-50.

26. Szymczak, W.A., et al., *X-linked immunodeficient mice exhibit enhanced susceptibility to Cryptococcus neoformans Infection.* MBio, 2013. **4**(4).

27. Zaragoza, O., et al., *The relative susceptibility of mouse strains to pulmonary Cryptococcus neoformans infection is associated with pleiotropic differences in the immune response.* Infect Immun, 2007. **75**(6): p. 2729-39.

28. Kelly, R.M., et al., *Opsonic requirements for dendritic cell-mediated responses to Cryptococcus neoformans.* Infect Immun, 2005. **73**(1): p. 592-8.

29. Kozel, T.R. and J.L. Follette, *Opsonization of encapsulated Cryptococcus neoformans by specific anticapsular antibody.* Infect Immun, 1981. **31**(3): p. 978-84.

30. Mukherjee, S., S.C. Lee, and A. Casadevall, *Antibodies to Cryptococcus neoformans glucuronoxylomannan enhance antifungal activity of murine macrophages.* Infect Immun, 1995. **63**(2): p. 573-9.

31. Murphy, K., Travers, P., Walport, M., *Immunobiology*. 7th edition ed. 2008: Garland Science.

32. Diamond, R.D., et al., *The role of late complement components and the alternate complement pathway in experimental cryptococcosis.* Proc Soc Exp Biol Med, 1973. **144**(1): p. 312-5.

33. Kozel, T.R., M.A. Wilson, and J.W. Murphy, *Early events in initiation of alternative complement pathway activation by the capsule of Cryptococcus neoformans.* Infect Immun, 1991. **59**(9): p. 3101-10.

34. Zaragoza, O., C.P. Taborda, and A. Casadevall, *The efficacy of complement-mediated phagocytosis of Cryptococcus neoformans is dependent on the location of C3 in the polysaccharide capsule and involves both direct and indirect C3-mediated interactions.* Eur J Immunol, 2003. **33**(7): p. 1957-67.

35. Shoham, S., et al., *Toll-like receptor 4 mediates intracellular signaling without TNF-alpha release in response to Cryptococcus neoformans polysaccharide capsule.* J Immunol, 2001. **166**(7): p. 4620-6.

36. Mitchell, T.G. and J.R. Perfect, *Cryptococcosis in the era of AIDS--100 years after the discovery of Cryptococcus neoformans.* Clin Microbiol Rev, 1995. **8**(4): p. 515-48.

37. Lim, J., et al., *Characterizing the Mechanisms of Nonopsonic Uptake of Cryptococci by Macrophages.* J Immunol, 2018. **200**(10): p. 3539-3546.

38. Mednick, A.J., et al., *Neutropenia alters lung cytokine production in mice and reduces their susceptibility to pulmonary cryptococcosis.* Eur J Immunol, 2003. **33**(6): p. 1744-53.

39. Wozniak, K.L., J.K. Kolls, and F.L. Wormley, Jr., *Depletion of neutrophils in a protective model of pulmonary cryptococcosis results in increased IL-17A production by gammadelta T cells.* BMC Immunol, 2012. **13**: p. 65.

40. Wozniak, K.L., J.M. Vyas, and S.M. Levitz, *In vivo role of dendritic cells in a murine model of pulmonary cryptococcosis.* Infect Immun, 2006. **74**(7): p. 3817-24.

41. Levitz, S.M., et al., *Cryptococcus neoformans resides in an acidic phagolysosome of human macrophages.* Infect Immun, 1999. **67**(2): p. 885-90.

42. Smith, L.M., E.F. Dixon, and R.C. May, *The fungal pathogen Cryptococcus neoformans manipulates macrophage phagosome maturation.* Cell Microbiol, 2015. **17**(5): p. 702-13.

43. Perfect, J.R., *Cryptococcus neoformans: the yeast that likes it hot.* FEMS Yeast Res, 2006. **6**(4): p. 463-8.

44. O'Meara, T.R. and J.A. Alspaugh, *The Cryptococcus neoformans capsule: a sword and a shield.* Clin Microbiol Rev, 2012. **25**(3): p. 387-408.

45. Zaragoza, O. and A. Casadevall, *Experimental modulation of capsule size in Cryptococcus neoformans.* Biol Proced Online, 2004. **6**: p. 10-15.

46. Gilbert, A.S., R.T. Wheeler, and R.C. May, *Fungal Pathogens: Survival and Replication within Macrophages.* Cold Spring Harbor perspectives in medicine, 2015. **5**(7): p. a019661.

47. Zaragoza, O. and K. Nielsen, *Titan cells in Cryptococcus neoformans: cells with a giant impact.* Curr Opin Microbiol, 2013. **16**(4): p. 409-13.

48. Okagaki, L.H., et al., *Cryptococcal cell morphology affects host cell interactions and pathogenicity.* PLoS Pathog, 2010. **6**(6): p. e1000953.

49. Price, J.V. and R.E. Vance, *The macrophage paradox.* Immunity, 2014. **41**(5): p. 685-93.

50. Gilbert, A.S., R.T. Wheeler, and R.C. May, *Fungal Pathogens: Survival and Replication within Macrophages.* Cold Spring Harb Perspect Med, 2015. **5**(7): p. a019661.

51. Alvarez, M. and A. Casadevall, *Phagosome extrusion and host-cell survival after Cryptococcus neoformans phagocytosis by macrophages.* Curr Biol, 2006. **16**(21): p. 2161-5.

52. Ma, H., et al., *Expulsion of live pathogenic yeast by macrophages.* Curr Biol, 2006. **16**(21): p. 2156-60.

53. Bain, J.M., et al., *Non-lytic expulsion/exocytosis of Candida albicans from macrophages.* Fungal Genet Biol, 2012. **49**(9): p. 677-8.

54. Garcia-Rodas, R., et al., *The interaction between Candida krusei and murine macrophages results in multiple outcomes, including intracellular survival and escape from killing.* Infect Immun, 2011. **79**(6): p. 2136-44.

55. Coelho, C., A.L. Bocca, and A. Casadevall, *The intracellular life of Cryptococcus neoformans.* Annu Rev Pathol, 2014. **9**: p. 219-38.

56. Vu, K., et al., *Invasion of the central nervous system by Cryptococcus neoformans requires a secreted fungal metalloprotease.* MBio, 2014. **5**(3): p. e01101-14.

57. Chang, Y.C., et al., *Cryptococcal yeast cells invade the central nervous system via transcellular penetration of the blood-brain barrier.* Infect Immun, 2004. **72**(9): p. 4985-95.

58. Kechichian, T.B., J. Shea, and M. Del Poeta, *Depletion of alveolar macrophages decreases the dissemination of a glucosylceramide-deficient mutant of Cryptococcus neoformans in immunodeficient mice.* Infect Immun, 2007. **75**(10): p. 4792-8.

59. Charlier, C., et al., *Evidence of a role for monocytes in dissemination and brain invasion by Cryptococcus neoformans.* Infect Immun, 2009. **77**(1): p. 120-7.

60. Ma, H., et al., *Direct cell-to-cell spread of a pathogenic yeast.* BMC Immunol, 2007. **8**: p. 15.

61. Alvarez, M. and A. Casadevall, *Cell-to-cell spread and massive vacuole formation after Cryptococcus neoformans infection of murine macrophages.* BMC Immunol, 2007. **8**: p. 16.

62. Dragotakes, Q., M.S. Fu, and A. Casadevall, *Dragotcytosis: Elucidation of the Mechanism for Cryptococcus neoformans Macrophage-to-Macrophage Transfer.* J Immunol, 2019. **202**(9): p. 2661-2670.

63. Trzaska, W.J., *Developing novel approaches to treat trauma-associated fungal infections*, in *Institute of Microbiology and Infection*. 2018, University of Birmingham.

64. Shah, A., et al., *Calcineurin Orchestrates Lateral Transfer of Aspergillus fumigatus during Macrophage Cell Death.* Am J Respir Crit Care Med, 2016. **194**(9): p. 1127-1139.

65. Johnston, S.A., K. Voelz, and R.C. May, *Cryptococcus neoformans Thermotolerance to Avian Body Temperature Is Sufficient For Extracellular Growth But Not Intracellular Survival In Macrophages.* Sci Rep, 2016. **6**: p. 20977.

66. Bojarczuk, A., et al., *Cryptococcus neoformans Intracellular Proliferation and Capsule Size Determines Early Macrophage Control of Infection.* Sci Rep, 2016. **6**: p. 21489.

67. Chrisman, C.J., M. Alvarez, and A. Casadevall, *Phagocytosis of Cryptococcus neoformans by, and nonlytic exocytosis from, Acanthamoeba castellanii.* Appl Environ Microbiol, 2010. **76**(18): p. 6056-62.

68. Watkins, R.A., et al., *Cryptococcus neoformans Escape From Dictyostelium Amoeba by Both WASH-Mediated Constitutive Exocytosis and Vomocytosis.* Front Cell Infect Microbiol, 2018. **8**: p. 108.

69. Nicola, A.M., et al., *Nonlytic exocytosis of Cryptococcus neoformans from macrophages occurs in vivo and is influenced by phagosomal pH.* MBio, 2011. **2**(4).

70. Cox, G.M., et al., *Extracellular phospholipase activity is a virulence factor for Cryptococcus neoformans.* Mol Microbiol, 2001. **39**(1): p. 166-75.

71. Cox, G.M., et al., *Urease as a virulence factor in experimental cryptococcosis.* Infect Immun, 2000. **68**(2): p. 443-8.

72. Chayakulkeeree, M., et al., *SEC14 is a specific requirement for secretion of phospholipase B1 and pathogenicity of Cryptococcus neoformans.* Mol Microbiol, 2011. **80**(4): p. 1088-101.

73. Fu, M.S., et al., *Cryptococcus neoformans urease affects the outcome of intracellular pathogenesis by modulating phagolysosomal pH.* PLoS Pathog, 2018. **14**(6): p. e1007144.

74. De Leon-Rodriguez, C.M., et al., *The Capsule of Cryptococcus neoformans Modulates Phagosomal pH through Its Acid-Base Properties.* mSphere, 2018. **3**(5).

75. Tucker, S.C. and A. Casadevall, *Replication of Cryptococcus neoformans in macrophages is accompanied by phagosomal permeabilization and accumulation of vesicles containing polysaccharide in the cytoplasm.* Proc Natl Acad Sci U S A, 2002. **99**(5): p. 3165-70.

76. Johnston, S.A. and R.C. May, *The human fungal pathogen Cryptococcus neoformans escapes macrophages by a phagosome emptying mechanism that is inhibited by Arp2/3 complex-mediated actin polymerisation.* PLoS Pathog, 2010. **6**(8): p. e1001041.

77. De Leon-Rodriguez, C.M., et al., *The Outcome of the Cryptococcus neoformans-Macrophage Interaction Depends on Phagolysosomal Membrane Integrity.* J Immunol, 2018. **201**(2): p. 583-603.

78. Nolan, S.J., et al., *Lipids Affect the Cryptococcus neoformans-Macrophage Interaction and Promote Nonlytic Exocytosis.* Infect Immun, 2017. **85**(12).

79. Deretic, V. and B. Levine, *Autophagy, Immunity, and Microbial Adaptations.* Cell Host Microbe, 2009. **5**(6): p. 527-549.

80. Nicola, A.M., et al., *Macrophage autophagy in immunity to Cryptococcus neoformans and Candida albicans.* Infect Immun, 2012. **80**(9): p. 3065-76.

81. Stukes, S., et al., *The Membrane Phospholipid Binding Protein Annexin A2 Promotes Phagocytosis and Nonlytic Exocytosis of Cryptococcus neoformans and Impacts Survival in Fungal Infection.* J Immunol, 2016. **197**(4): p. 1252-61.

82. Flieger, A., et al., *Pathways of host cell exit by intracellular pathogens.* Microb Cell, 2018. **5**(12): p. 525-544.

83. Voelz, K., D.A. Lammas, and R.C. May, *Cytokine signaling regulates the outcome of intracellular macrophage parasitism by Cryptococcus neoformans.* Infect Immun, 2009. **77**(8): p. 3450-7.

84. Gilbert, A.S., et al., *Vomocytosis of live pathogens from macrophages is regulated by the atypical MAP kinase ERK5.* Sci Adv, 2017. **3**(8): p. e1700898.

85. Hagedorn, M., et al., *Infection by tubercular mycobacteria is spread by nonlytic ejection from their amoeba hosts.* Science, 2009. **323**(5922): p. 1729-33.

86. Miao, Y., J. Wu, and S.N. Abraham, *Ubiquitination of Innate Immune Regulator TRAF3 Orchestrates Expulsion of Intracellular Bacteria by Exocyst Complex.* Immunity, 2016. **45**(1): p. 94-105.

87. Song, J., et al., *TLR4-mediated expulsion of bacteria from infected bladder epithelial cells.* Proc Natl Acad Sci U S A, 2009. **106**(35): p. 14966-71.

88. Di Venanzio, G., et al., *A pore-forming toxin enables Serratia a nonlytic egress from host cells.* Cell Microbiol, 2017. **19**(2).

89. Nithianandarajah-Jones, G.N., et al., *ERK5: structure, regulation and function.* Cell Signal, 2012. **24**(11): p. 2187-96.

90. Chang, L. and M. Karin, *Mammalian MAP kinase signalling cascades.* Nature, 2001. **410**(6824): p. 37-40.

91. Zhou, G., Z.Q. Bao, and J.E. Dixon, *Components of a new human protein kinase signal transduction pathway.* J Biol Chem, 1995. **270**(21): p. 12665-9.

92. Lee, J.D., R.J. Ulevitch, and J. Han, *Primary structure of BMK1: a new mammalian map kinase.* Biochem Biophys Res Commun, 1995. **213**(2): p. 715-24.

93. Buschbeck, M. and A. Ullrich, *The unique C-terminal tail of the mitogen-activated protein kinase ERK5 regulates its activation and nuclear shuttling.* J Biol Chem, 2005. **280**(4): p. 2659-67.

94. Yan, C., et al., *Molecular cloning of mouse ERK5/BMK1 splice variants and characterization of ERK5 functional domains.* J Biol Chem, 2001. **276**(14): p. 10870-8.

95. Morimoto, H., et al., *Activation of a C-terminal transcriptional activation domain of ERK5 by autophosphorylation.* J Biol Chem, 2007. **282**(49): p. 35449-56.

96. Kato, Y., et al., *Big mitogen-activated kinase regulates multiple members of the MEF2 protein family.* J Biol Chem, 2000. **275**(24): p. 18534-40.

97. English, J.M., et al., *Identification of substrates and regulators of the mitogen-activated protein kinase ERK5 using chimeric protein kinases.* J Biol Chem, 1998. **273**(7): p. 3854-60.

98. Kamakura, S., T. Moriguchi, and E. Nishida, *Activation of the protein kinase ERK5/BMK1 by receptor tyrosine kinases. Identification and characterization of a signaling pathway to the nucleus.* J Biol Chem, 1999. **274**(37): p. 26563-71.

99. Suzaki, Y., et al., *Hydrogen peroxide stimulates c-Src-mediated big mitogen-activated protein kinase 1 (BMK1) and the MEF2C signaling pathway in PC12 cells: potential role in cell survival following oxidative insults.* J Biol Chem, 2002. **277**(11): p. 9614-21.

100. Dong, F., J.S. Gutkind, and A.C. Larner, *Granulocyte colony-stimulating factor induces ERK5 activation, which is differentially regulated by protein-tyrosine kinases and protein kinase C. Regulation of cell proliferation and survival.* J Biol Chem, 2001. **276**(14): p. 10811-6.

101. Kato, Y., et al., *Bmk1/Erk5 is required for cell proliferation induced by epidermal growth factor.* Nature, 1998. **395**(6703): p. 713-6.

102. Nakaoka, Y., et al., *Activation of gp130 transduces hypertrophic signal through interaction of scaffolding/docking protein Gab1 with tyrosine phosphatase SHP2 in cardiomyocytes.* Circ Res, 2003. **93**(3): p. 221-9.

103. Hajjeh, R.A., M.E. Brandt, and R.W. Pinner, *Emergence of cryptococcal disease: epidemiologic perspectives 100 years after its discovery.* Epidemiol Rev, 1995. **17**(2): p. 303-20.

104. Idnurm, A., et al., *Deciphering the model pathogenic fungus Cryptococcus neoformans.* Nat Rev Microbiol, 2005. **3**(10): p. 753-64.

105. Hardy, G.A., et al., *Interferon-alpha is the primary plasma type-I IFN in HIV-1 infection and correlates with immune activation and disease markers.* PLoS One, 2013. **8**(2): p. e56527.

106. Isaacs, A. and J. Lindenmann, *Virus interference. I. The interferon.* Proc R Soc Lond B Biol Sci, 1957. **147**(927): p. 258-67.

107. Samuel, C.E., *Antiviral actions of interferons.* Clin Microbiol Rev, 2001. **14**(4): p. 778-809.

108. Levy, D.E., I.J. Marie, and J.E. Durbin, *Induction and function of type I and III interferon in response to viral infection.* Curr Opin Virol, 2011. **1**(6): p. 476-86.

109. Cella, M., et al., *Plasmacytoid monocytes migrate to inflamed lymph nodes and produce large amounts of type I interferon.* Nat Med, 1999. **5**(8): p. 919-23.

110. Siegal, F.P., et al., *The nature of the principal type 1 interferon-producing cells in human blood.* Science, 1999. **284**(5421): p. 1835-7.

111. Haller, O., G. Kochs, and F. Weber, *The interferon response circuit: induction and suppression by pathogenic viruses.* Virology, 2006. **344**(1): p. 119-30.

112. Herbeuval, J.P., et al., *Differential expression of IFN-alpha and TRAIL/DR5 in lymphoid tissue of progressor versus nonprogressor HIV-1-infected patients.* Proc Natl Acad Sci U S A, 2006. **103**(18): p. 7000-5.

113. Lehmann, C., et al., *Increased interferon alpha expression in circulating plasmacytoid dendritic cells of HIV-1-infected patients.* J Acquir Immune Defic Syndr, 2008. **48**(5): p. 522-30.

114. Sato, K., et al., *Cryptococcus neoformans Infection in Mice Lacking Type I Interferon Signaling Leads to Increased Fungal Clearance and IL-4-Dependent Mucin Production in the Lungs.* PLoS One, 2015. **10**(9): p. e0138291.

115. Sionov, E., et al., *Type I IFN Induction via Poly-ICLC Protects Mice against Cryptococcosis.* PLoS Pathog, 2015. **11**(8): p. e1005040.

116. Ivashkiv, L.B. and L.T. Donlin, *Regulation of type I interferon responses.* Nat Rev Immunol, 2014. **14**(1): p. 36-49.

117. Gibbert, K., et al., *IFN-alpha subtypes: distinct biological activities in anti-viral therapy.* Br J Pharmacol, 2013. **168**(5): p. 1048-58.

118. McNab, F., et al., *Type I interferons in infectious disease.* Nat Rev Immunol, 2015. **15**(2): p. 87-103.

119. Ishihara, T., et al., *Inhibition of chlamydia trachomatis growth by human interferon-alpha: mechanisms and synergistic effect with interferon-gamma and tumor necrosis factor-alpha.* Biomed Res, 2005. **26**(4): p. 179-85.

120. Plumlee, C.R., et al., *Interferons direct an effective innate response to Legionella pneumophila infection.* J Biol Chem, 2009. **284**(44): p. 30058-66.

121. Mancuso, G., et al., *Type I IFN signaling is crucial for host resistance against different species of pathogenic bacteria.* J Immunol, 2007. **178**(5): p. 3126-33.

122. Auerbuch, V., et al., *Mice lacking the type I interferon receptor are resistant to Listeria monocytogenes.* J Exp Med, 2004. **200**(4): p. 527-33.

123. Carrero, J.A., B. Calderon, and E.R. Unanue, *Type I interferon sensitizes lymphocytes to apoptosis and reduces resistance to Listeria infection.* J Exp Med, 2004. **200**(4): p. 535-40.

124. O'Connell, R.M., et al., *Type I interferon production enhances susceptibility to Listeria monocytogenes infection.* J Exp Med, 2004. **200**(4): p. 437-45.

125. Carrero, J.A., B. Calderon, and E.R. Unanue, *Lymphocytes are detrimental during the early innate immune response against Listeria monocytogenes.* J Exp Med, 2006. **203**(4): p. 933-40.

126. Rayamajhi, M., et al., *Induction of IFN-alphabeta enables Listeria monocytogenes to suppress macrophage activation by IFN-gamma.* J Exp Med, 2010. **207**(2): p. 327-37.

127. Kearney, S.J., et al., *Type I IFNs downregulate myeloid cell IFN-gamma receptor by inducing recruitment of an early growth response 3/NGFI-A binding protein 1 complex that silences ifngr1 transcription.* J Immunol, 2013. **191**(6): p. 3384-92.

128. Mayer-Barber, K.D., et al., *Innate and adaptive interferons suppress IL-1alpha and IL-1beta production by distinct pulmonary myeloid subsets during Mycobacterium tuberculosis infection.* Immunity, 2011. **35**(6): p. 1023-34.

129. Novikov, A., et al., *Mycobacterium tuberculosis triggers host type I IFN signaling to regulate IL-1beta production in human macrophages.* J Immunol, 2011. **187**(5): p. 2540-7.

130. McNab, F.W., et al., *Type I IFN induces IL-10 production in an IL-27-independent manner and blocks responsiveness to IFN-gamma for production of IL-12 and bacterial*

killing in Mycobacterium tuberculosis-infected macrophages. J Immunol, 2014. **193**(7): p. 3600-12.

131. Manca, C., et al., *Virulence of a Mycobacterium tuberculosis clinical isolate in mice is determined by failure to induce Th1 type immunity and is associated with induction of IFN-alpha /beta.* Proc Natl Acad Sci U S A, 2001. **98**(10): p. 5752-7.

132. de Paus, R.A., et al., *Inhibition of the type I immune responses of human monocytes by IFN-alpha and IFN-beta.* Cytokine, 2013. **61**(2): p. 645-55.

133. Teles, R.M., et al., *Type I interferon suppresses type II interferon-triggered human anti-mycobacterial responses.* Science, 2013. **339**(6126): p. 1448-53.

134. Antonelli, L.R., et al., *Intranasal Poly-IC treatment exacerbates tuberculosis in mice through the pulmonary recruitment of a pathogen-permissive monocyte/macrophage population.* J Clin Invest, 2010. **120**(5): p. 1674-82.

135. Mariotti, S., et al., *Mycobacterium tuberculosis diverts alpha interferon-induced monocyte differentiation from dendritic cells into immunoprivileged macrophage-like host cells.* Infect Immun, 2004. **72**(8): p. 4385-92.

136. de Almeida, L.A., et al., *MyD88 and STING signaling pathways are required for IRF3-mediated IFN-beta induction in response to Brucella abortus infection.* PLoS One, 2011. **6**(8): p. e23135.

137. Patel, A.A., et al., *Opposing roles for interferon regulatory factor-3 (IRF-3) and type I interferon signaling during plague.* PLoS Pathog, 2012. **8**(7): p. e1002817.

138. Martin, F.J., et al., *Staphylococcus aureus activates type I IFN signaling in mice and humans through the Xr repeated sequences of protein A.* J Clin Invest, 2009. **119**(7): p. 1931-9.

139. Ray, S.C. and C.A. Rappleye, *Flying under the radar: Histoplasma capsulatum avoidance of innate immune recognition.* Semin Cell Dev Biol, 2019. **89**: p. 91-98.

140. Villarete, L., et al., *Impaired responsiveness to gamma interferon of macrophages infected with lymphocytic choriomeningitis virus clone 13: susceptibility to histoplasmosis.* Infect Immun, 1995. **63**(4): p. 1468-72.

141. Inglis, D.O., et al., *Conidia but not yeast cells of the fungal pathogen Histoplasma capsulatum trigger a type I interferon innate immune response in murine macrophages.* Infect Immun, 2010. **78**(9): p. 3871-82.

142. Van Prooyen, N., et al., *CD103+ Conventional Dendritic Cells Are Critical for TLR7/9-Dependent Host Defense against Histoplasma capsulatum, an Endemic Fungal Pathogen of Humans.* PLoS Pathog, 2016. **12**(7): p. e1005749.

143. Siegel, M., H. Masur, and J. Kovacs, *Pneumocystis jirovecii Pneumonia in Human Immunodeficiency Virus Infection.* Semin Respir Crit Care Med, 2016. **37**(2): p. 243-56.

144. Meissner, N.N., et al., *Role of type I IFNs in pulmonary complications of Pneumocystis murina infection.* J Immunol, 2005. **174**(9): p. 5462-71.

145. Prigge, J.R., et al., *Type I IFNs Act upon Hematopoietic Progenitors To Protect and Maintain Hematopoiesis during Pneumocystis Lung Infection in Mice.* J Immunol, 2015. **195**(11): p. 5347-57.

146. Meissner, N., et al., *Type I interferon signaling and B cells maintain hemopoiesis during Pneumocystis infection of the lung.* J Immunol, 2007. **178**(10): p. 6604-15.

147. Latge, J.P., *Aspergillus fumigatus and aspergillosis.* Clin Microbiol Rev, 1999. **12**(2): p. 310-50.

148. van de Veerdonk, F.L., et al., *Aspergillus fumigatus morphology and dynamic host interactions.* Nat Rev Microbiol, 2017. **15**(11): p. 661-674.

149. Tandon, R.N., et al., *Interferon protects mice against an extracellular infection of Aspergillus fumigatus.* Ann N Y Acad Sci, 1988. **544**: p. 409-11.

150. Gafa, V., et al., *Enhancement of anti-Aspergillus T helper type 1 response by interferon-beta-conditioned dendritic cells.* Immunology, 2010. **131**(2): p. 282-8.

151. Beisswenger, C., C. Hess, and R. Bals, *Aspergillus fumigatus conidia induce interferon-beta signalling in respiratory epithelial cells.* Eur Respir J, 2012. **39**(2): p. 411-8.

152. Swiecki, M., et al., *Plasmacytoid dendritic cell ablation impacts early interferon responses and antiviral NK and CD8(+) T cell accrual.* Immunity, 2010. **33**(6): p. 955-66.

153. Ramirez-Ortiz, Z.G., et al., *A nonredundant role for plasmacytoid dendritic cells in host defense against the human fungal pathogen Aspergillus fumigatus.* Cell Host Microbe, 2011. **9**(5): p. 415-24.

154. Loures, F.V., et al., *Recognition of Aspergillus fumigatus hyphae by human plasmacytoid dendritic cells is mediated by dectin-2 and results in formation of extracellular traps.* PLoS Pathog, 2015. **11**(2): p. e1004643.

155. Espinosa, V., et al., *Type III interferon is a critical regulator of innate antifungal immunity.* Sci Immunol, 2017. **2**(16).

156. Seyedmousavi, S., et al., *Exogenous Stimulation of Type I Interferon Protects Mice with Chronic Granulomatous Disease from Aspergillosis through Early Recruitment of Host-Protective Neutrophils into the Lung.* MBio, 2018. **9**(2).

157. Mayer, F.L., D. Wilson, and B. Hube, *Candida albicans pathogenicity mechanisms.* Virulence, 2013. **4**(2): p. 119-28.

158. Nobile, C.J. and A.D. Johnson, *Candida albicans Biofilms and Human Disease.* Annu Rev Microbiol, 2015. **69**: p. 71-92.

159. Gulati, M. and C.J. Nobile, *Candida albicans biofilms: development, regulation, and molecular mechanisms.* Microbes Infect, 2016. **18**(5): p. 310-21.

160. Jensen, J., A. Vazquez-Torres, and E. Balish, *Poly(I.C)-induced interferons enhance susceptibility of SCID mice to systemic candidiasis.* Infect Immun, 1992. **60**(11): p. 4549-57.

161. Guarda, G., et al., *Type I interferon inhibits interleukin-1 production and inflammasome activation.* Immunity, 2011. **34**(2): p. 213-23.

162. Stawowczyk, M., et al., *Pathogenic Effects of IFIT2 and Interferon-beta during Fatal Systemic Candida albicans Infection.* MBio, 2018. **9**(2).

163. Cardone, M., et al., *Opposite regulatory effects of IFN-beta and IL-3 on C-type lectin receptors, antigen uptake, and phagocytosis in human macrophages.* J Leukoc Biol, 2014. **95**(1): p. 161-8.

164. Majer, O., et al., *Type I interferons promote fatal immunopathology by regulating inflammatory monocytes and neutrophils during Candida infections.* PLoS Pathog, 2012. **8**(7): p. e1002811.

165. del Fresno, C., et al., *Interferon-beta production via Dectin-1-Syk-IRF5 signaling in dendritic cells is crucial for immunity to C. albicans.* Immunity, 2013. **38**(6): p. 1176-86.

166. Biondo, C., et al., *Recognition of yeast nucleic acids triggers a host-protective type I interferon response.* Eur J Immunol, 2011. **41**(7): p. 1969-79.

167. Bourgeois, C., et al., *Conventional dendritic cells mount a type I IFN response against Candida spp. requiring novel phagosomal TLR7-mediated IFN-beta signaling.* J Immunol, 2011. **186**(5): p. 3104-12.

168. Fujioka, N., et al., *Potential application of human interferon-alpha in microbial infections of the oral cavity.* J Interferon Cytokine Res, 1995. **15**(12): p. 1047-51.

169. Dominguez-Andres, J., et al., *Inflammatory Ly6C(high) Monocytes Protect against Candidiasis through IL-15-Driven NK Cell/Neutrophil Activation.* Immunity, 2017. **46**(6): p. 1059-1072 e4.

170. Smeekens, S.P., et al., *Functional genomics identifies type I interferon pathway as central for host defense against Candida albicans.* Nat Commun, 2013. **4**: p. 1342.

171. Li, T., et al., *Recombinant Human IFNalpha-2b Response Promotes Vaginal Epithelial Cells Defense against Candida albicans.* Front Microbiol, 2017. **8**: p. 697.

172. Li, T., et al., *Therapeutic effectiveness of type I interferon in vulvovaginal candidiasis.* Microb Pathog, 2019. **134**: p. 103562.

173. Kolben, T., et al., *IL-23, IFN-alpha, and IFN-beta in the vaginal fluid of patients suffering from vulvovaginal candidosis.* Clin Exp Obstet Gynecol, 2017. **44**(1): p. 7-10.

174. Biondo, C., et al., *IFN-alpha/beta signaling is required for polarization of cytokine responses toward a protective type 1 pattern during experimental cryptococcosis.* J Immunol, 2008. **181**(1): p. 566-73.

175. Liu, L., et al., *Gain-of-function human STAT1 mutations impair IL-17 immunity and underlie chronic mucocutaneous candidiasis.* J Exp Med, 2011. **208**(8): p. 1635-48.

176. Hambleton, S., et al., *STAT2 deficiency and susceptibility to viral illness in humans.* Proc Natl Acad Sci U S A, 2013. **110**(8): p. 3053-8.

177. Duncan, C.J., et al., *Human IFNAR2 deficiency: Lessons for antiviral immunity.* Sci Transl Med, 2015. **7**(307): p. 307ra154.

178. Hoyos-Bachiloglu, R., et al., *A digenic human immunodeficiency characterized by IFNAR1 and IFNGR2 mutations.* J Clin Invest, 2017. **127**(12): p. 4415-4420.

179. Seoane, P.I., et al., *Viral infection enhances vomocytosis of intracellular fungi via Type I interferons.* BioRxiv, 2019.

180. Garelnabi, M., et al., *Quantifying donor-to-donor variation in macrophage responses to the human fungal pathogen Cryptococcus neoformans.* PLoS One, 2018. **13**(3): p. e0194615.

181. Upadhya, R., et al., *A fluorogenic C. neoformans reporter strain with a robust expression of m-cherry expressed from a safe haven site in the genome.* Fungal Genet Biol, 2017. **108**: p. 13-25.

182. Alspaugh, J.A., et al., *RAS1 regulates filamentation, mating and growth at high temperature of Cryptococcus neoformans.* Mol Microbiol, 2000. **36**(2): p. 352-65.

183. Ballou, E.R., et al., *Ras1 acts through duplicated Cdc42 and Rac proteins to regulate morphogenesis and pathogenesis in the human fungal pathogen Cryptococcus neoformans.* PLoS Genet, 2013. **9**(8): p. e1003687.

184. Moyrand, F., T. Fontaine, and G. Janbon, *Systematic capsule gene disruption reveals the central role of galactose metabolism on Cryptococcus neoformans virulence.* Mol Microbiol, 2007. **64**(3): p. 771-81.

185. Rasaiyaah, J., et al., *HIV-1 evades innate immune recognition through specific cofactor recruitment.* Nature, 2013. **503**(7476): p. 402-405.

186. Tsang, J., et al., *HIV-1 infection of macrophages is dependent on evasion of innate immune cellular activation.* AIDS, 2009. **23**(17): p. 2255-63.

187. Goujon, C., et al., *Characterization of simian immunodeficiency virus SIVSM/human immunodeficiency virus type 2 Vpx function in human myeloid cells.* J Virol, 2008. **82**(24): p. 12335-45.

188. Goujon, C., et al., *With a little help from a friend: increasing HIV transduction of monocyte-derived dendritic cells with virion-like particles of SIV(MAC).* Gene Ther, 2006. **13**(12): p. 991-4.

189. Hashimoto, K., et al., *SLAM (CD150)-independent measles virus entry as revealed by recombinant virus expressing green fluorescent protein.* J Virol, 2002. **76**(13): p. 6743-9.

190. Takeda, M., et al., *Recovery of pathogenic measles virus from cloned cDNA.* J Virol, 2000. **74**(14): p. 6643-7.

191. Lutz, M.B., et al., *An advanced culture method for generating large quantities of highly pure dendritic cells from mouse bone marrow.* J Immunol Methods, 1999. **223**(1): p. 77-92.

192. Martinez, F.O., et al., *Macrophage activation and polarization.* Front Biosci, 2008. **13**: p. 453-61.

193. Stein, M., et al., *Interleukin 4 potently enhances murine macrophage mannose receptor activity: a marker of alternative immunologic macrophage activation.* J Exp Med, 1992. **176**(1): p. 287-92.

194. Mosser, D.M. and J.P. Edwards, *Exploring the full spectrum of macrophage activation.* Nat Rev Immunol, 2008. **8**(12): p. 958-69.

195. Murray, P.J., et al., *Macrophage activation and polarization: nomenclature and experimental guidelines.* Immunity, 2014. **41**(1): p. 14-20.

196. Azuma, M., et al., *B70 antigen is a second ligand for CTLA-4 and CD28.* Nature, 1993. **366**(6450): p. 76-9.

197. Sansom, D.M., *CD28, CTLA-4 and their ligands: who does what and to whom?* Immunology, 2000. **101**(2): p. 169-77.

198. Hsieh, C.S., et al., *Development of TH1 CD4+ T cells through IL-12 produced by Listeria-induced macrophages.* Science, 1993. **260**(5107): p. 547-9.

199. Macatonia, S.E., et al., *Dendritic cells produce IL-12 and direct the development of Th1 cells from naive CD4+ T cells.* J Immunol, 1995. **154**(10): p. 5071-9.

200. Langrish, C.L., et al., *IL-12 and IL-23: master regulators of innate and adaptive immunity.* Immunol Rev, 2004. **202**: p. 96-105.

201. Oppmann, B., et al., *Novel p19 protein engages IL-12p40 to form a cytokine, IL-23, with biological activities similar as well as distinct from IL-12.* Immunity, 2000. **13**(5): p. 715-25.

202. Bettelli, E., et al., *Reciprocal developmental pathways for the generation of pathogenic effector TH17 and regulatory T cells.* Nature, 2006. **441**(7090): p. 235-8.

203. Kielian, M.C. and Z.A. Cohn, *Phorbol myristate acetate stimulates phagosome-lysosome fusion in mouse macrophages.* J Exp Med, 1981. **154**(1): p. 101-11.

204. Schwende, H., et al., *Differences in the state of differentiation of THP-1 cells induced by phorbol ester and 1,25-dihydroxyvitamin D3.* J Leukoc Biol, 1996. **59**(4): p. 555-61.

205. Maess, M.B., et al., *Reduced PMA enhances the responsiveness of transfected THP-1 macrophages to polarizing stimuli.* J Immunol Methods, 2014. **402**(1-2): p. 76-81.

206. Gilbert, A.S., *Investigating the molecular mechanisms of vomocytosis*. 2017, University of Birmingham.

207. Mackaness, G.B., *Cellular resistance to infection.* J Exp Med, 1962. **116**: p. 381-406.

208. Benoit, M., B. Desnues, and J.L. Mege, *Macrophage polarization in bacterial infections.* J Immunol, 2008. **181**(6): p. 3733-9.

209. Torgerson, P.R., et al., *World Health Organization Estimates of the Global and Regional Disease Burden of 11 Foodborne Parasitic Diseases, 2010: A Data Synthesis.* PLoS Med, 2015. **12**(12): p. e1001920.

210. Tyoalumun, K., S. Abubakar, and N. Christopher, *Prevalence of Intestinal Parasitic Infections and their Association with Nutritional Status of Rural and Urban Pre-School Children in Benue State, Nigeria.* Int J MCH AIDS, 2016. **5**(2): p. 146-152.

211. Melchjorsen, J., *Learning from the messengers: innate sensing of viruses and cytokine regulation of immunity - clues for treatments and vaccines.* Viruses, 2013. **5**(2): p. 470-527.

212. Takeuchi, O. and S. Akira, *Pattern recognition receptors and inflammation.* Cell, 2010. **140**(6): p. 805-20.

213. Wilen, C.B., J.C. Tilton, and R.W. Doms, *HIV: cell binding and entry.* Cold Spring Harb Perspect Med, 2012. **2**(8).

214. Kwong, P.D., et al., *Structure of an HIV gp120 envelope glycoprotein in complex with the CD4 receptor and a neutralizing human antibody.* Nature, 1998. **393**(6686): p. 648-59.

215. Chan, D.C., et al., *Core structure of gp41 from the HIV envelope glycoprotein.* Cell, 1997. **89**(2): p. 263-73.

216. Clapham, P.R. and A. McKnight, *HIV-1 receptors and cell tropism.* Br Med Bull, 2001. **58**: p. 43-59.

217. Berger, E.A., et al., *A new classification for HIV-1.* Nature, 1998. **391**(6664): p. 240.

218. Ochsenbauer, C., et al., *Generation of transmitted/founder HIV-1 infectious molecular clones and characterization of their replication capacity in CD4 T lymphocytes and monocyte-derived macrophages.* J Virol, 2012. **86**(5): p. 2715-28.

219. Parrish, N.F., et al., *Transmitted/founder and chronic subtype C HIV-1 use CD4 and CCR5 receptors with equal efficiency and are not inhibited by blocking the integrin alpha4beta7.* PLoS Pathog, 2012. **8**(5): p. e1002686.

220. Salazar-Gonzalez, J.F., et al., *Genetic identity, biological phenotype, and evolutionary pathways of transmitted/founder viruses in acute and early HIV-1 infection.* J Exp Med, 2009. **206**(6): p. 1273-89.

221. Laguette, N., et al., *SAMHD1 is the dendritic- and myeloid-cell-specific HIV-1 restriction factor counteracted by Vpx.* Nature, 2011. **474**(7353): p. 654-7.

222. Lahouassa, H., et al., *SAMHD1 restricts the replication of human immunodeficiency virus type 1 by depleting the intracellular pool of deoxynucleoside triphosphates.* Nat Immunol, 2012. **13**(3): p. 223-8.

223. Hrecka, K., et al., *Vpx relieves inhibition of HIV-1 infection of macrophages mediated by the SAMHD1 protein.* Nature, 2011. **474**(7353): p. 658-61.

224. Mlcochova, P., et al., *Vpx complementation of 'non-macrophage tropic' R5 viruses reveals robust entry of infectious HIV-1 cores into macrophages.* Retrovirology, 2014. **11**: p. 25.

225. Yanagi, Y., M. Takeda, and S. Ohno, *Measles virus: cellular receptors, tropism and pathogenesis.* J Gen Virol, 2006. **87**(Pt 10): p. 2767-79.

226. Clark, K., et al., *Use of the pharmacological inhibitor BX795 to study the regulation and physiological roles of TBK1 and IkappaB kinase epsilon: a distinct upstream kinase*

mediates Ser-172 phosphorylation and activation. J Biol Chem, 2009. **284**(21): p. 14136-46.

227. Cheng, K., X. Wang, and H. Yin, *Small-molecule inhibitors of the TLR3/dsRNA complex.* J Am Chem Soc, 2011. **133**(11): p. 3764-7.

228. Alexopoulou, L., et al., *Recognition of double-stranded RNA and activation of NF-kappaB by Toll-like receptor 3.* Nature, 2001. **413**(6857): p. 732-8.

229. Rodrigues, V., et al., *Myeloid Cell Interaction with HIV: A Complex Relationship.* Front Immunol, 2017. **8**: p. 1698.

230. Colamonici, O.R. and P. Domanski, *Identification of a novel subunit of the type I interferon receptor localized to human chromosome 21.* J Biol Chem, 1993. **268**(15): p. 10895-9.

231. Flint, J.S.R., V. R.; Rall, G. F., *Principles of Virology: Bundle*. 4th ed. Vol. I & II. 2015: ASM Press.

232. Boxx, G.M. and G. Cheng, *The Roles of Type I Interferon in Bacterial Infection.* Cell Host Microbe, 2016. **19**(6): p. 760-9.

233. Mulcahy, L.R., V.M. Isabella, and K. Lewis, *Pseudomonas aeruginosa biofilms in disease.* Microb Ecol, 2014. **68**(1): p. 1-12.

234. Deng, Q., et al., *Pseudomonas aeruginosa Triggers Macrophage Autophagy To Escape Intracellular Killing by Activation of the NLRP3 Inflammasome.* Infect Immun, 2016. **84**(1): p. 56-66.

235. Parker, D., et al., *Induction of type I interferon signaling by Pseudomonas aeruginosa is diminished in cystic fibrosis epithelial cells.* Am J Respir Cell Mol Biol, 2012. **46**(1): p. 6-13.

236. Huffnagle, G.B. and M.F. Lipscomb, *Pulmonary cryptococcosis.* Am J Pathol, 1992. **141**(6): p. 1517-20.

237. Mempel, T.R., S.E. Henrickson, and U.H. Von Andrian, *T-cell priming by dendritic cells in lymph nodes occurs in three distinct phases.* Nature, 2004. **427**(6970): p. 154-9.

238. Alanio, A., et al., *Cryptococcus neoformans host adaptation: toward biological evidence of dormancy.* MBio, 2015. **6**(2).

239. Garcia-Hermoso, D., G. Janbon, and F. Dromer, *Epidemiological evidence for dormant Cryptococcus neoformans infection.* J Clin Microbiol, 1999. **37**(10): p. 3204-9.

240. Barnden, M.J., et al., *Defective TCR expression in transgenic mice constructed using cDNA-based alpha- and beta-chain genes under the control of heterologous regulatory elements.* Immunol Cell Biol, 1998. **76**(1): p. 34-40.

241. Lyons, A.B. and C.R. Parish, *Determination of lymphocyte division by flow cytometry.* J Immunol Methods, 1994. **171**(1): p. 131-7.

242. Sallusto, F., et al., *Rapid and coordinated switch in chemokine receptor expression during dendritic cell maturation.* Eur J Immunol, 1998. **28**(9): p. 2760-9.

243. Ohshima, Y., et al., *Expression and function of OX40 ligand on human dendritic cells.* J Immunol, 1997. **159**(8): p. 3838-48.

244. Quezada, S.A., et al., *CD40/CD154 interactions at the interface of tolerance and immunity.* Annu Rev Immunol, 2004. **22**: p. 307-28.

245. Zhang, Y., et al., *Regulation of T cell activation and tolerance by PDL2.* Proc Natl Acad Sci U S A, 2006. **103**(31): p. 11695-700.

246. Helft, J., et al., *GM-CSF Mouse Bone Marrow Cultures Comprise a Heterogeneous Population of CD11c(+)MHCII(+) Macrophages and Dendritic Cells.* Immunity, 2015. **42**(6): p. 1197-211.

247. Yauch, L.E., J.S. Lam, and S.M. Levitz, *Direct inhibition of T-cell responses by the Cryptococcus capsular polysaccharide glucuronoxylomannan.* PLoS Pathog, 2006. **2**(11): p. e120.

248. Grijpstra, J., et al., *The Cryptococcus neoformans cap10 and cap59 mutant strains, affected in glucuronoxylomannan synthesis, differentially activate human dendritic cells.* FEMS Immunol Med Microbiol, 2009. **57**(2): p. 142-50.

249. Bose, I., et al., *A yeast under cover: the capsule of Cryptococcus neoformans.* Eukaryot Cell, 2003. **2**(4): p. 655-63.

250. Fries, B.C., et al., *Phenotypic switching of Cryptococcus neoformans can produce variants that elicit increased intracranial pressure in a rat model of cryptococcal meningoencephalitis.* Infect Immun, 2005. **73**(3): p. 1779-87.

251. Meuer, S.C., et al., *Triggering of the T3-Ti antigen-receptor complex results in clonal T-cell proliferation through an interleukin 2-dependent autocrine pathway.* Proc Natl Acad Sci U S A, 1984. **81**(5): p. 1509-13.

252. Holan, V., S. Nakamura, and J. Minowada, *Inhibitory versus stimulatory effects of natural human interferon-alpha on proliferation of lymphocyte subpopulations.* Immunology, 1992. **75**(1): p. 176-81.

253. Erickson, S., et al., *Interferon-alpha inhibits proliferation in human T lymphocytes by abrogation of interleukin 2-induced changes in cell cycle-regulatory proteins.* Cell Growth Differ, 1999. **10**(8): p. 575-82.

254. Zella, D., et al., *IFN-alpha 2b reduces IL-2 production and IL-2 receptor function in primary CD4+ T cells.* J Immunol, 2000. **164**(5): p. 2296-302.

255. Parronchi, P., et al., *Effects of interferon-alpha on cytokine profile, T cell receptor repertoire and peptide reactivity of human allergen-specific T cells.* Eur J Immunol, 1996. **26**(3): p. 697-703.

256. Cella, M., et al., *Plasmacytoid dendritic cells activated by influenza virus and CD40L drive a potent TH1 polarization.* Nat Immunol, 2000. **1**(4): p. 305-10.

257. Tough, D.F., P. Borrow, and J. Sprent, *Induction of bystander T cell proliferation by viruses and type I interferon in vivo.* Science, 1996. **272**(5270): p. 1947-50.

258. Le Bon, A., et al., *Direct stimulation of T cells by type I IFN enhances the CD8+ T cell response during cross-priming.* J Immunol, 2006. **176**(8): p. 4682-9.

259. Drew, B.A., M.E. Burow, and B.S. Beckman, *MEK5/ERK5 pathway: the first fifteen years.* Biochim Biophys Acta, 2012. **1825**(1): p. 37-48.

260. Regan, C.P., et al., *Erk5 null mice display multiple extraembryonic vascular and embryonic cardiovascular defects.* Proc Natl Acad Sci U S A, 2002. **99**(14): p. 9248-53.

261. Heo, K.S., et al., *ERK5 activation in macrophages promotes efferocytosis and inhibits atherosclerosis.* Circulation, 2014. **130**(2): p. 180-91.

262. Giurisato, E., et al., *Myeloid ERK5 deficiency suppresses tumor growth by blocking protumor macrophage polarization via STAT3 inhibition.* Proc Natl Acad Sci U S A, 2018. **115**(12): p. E2801-E2810.

263. Isaacs, A., J. Lindenmann, and R.C. Valentine, *Virus interference. II. Some properties of interferon.* Proc R Soc Lond B Biol Sci, 1957. **147**(927): p. 268-73.

264. Gratz, N., et al., *Type I interferon production induced by Streptococcus pyogenes-derived nucleic acids is required for host protection.* PLoS Pathog, 2011. **7**(5): p. e1001345.

265. Collins, H.L. and G.J. Bancroft, *Encapsulation of Cryptococcus neoformans impairs antigen-specific T-cell responses.* Infect Immun, 1991. **59**(11): p. 3883-8.

266. Vecchiarelli, A., et al., *The polysaccharide capsule of Cryptococcus neoformans interferes with human dendritic cell maturation and activation.* J Leukoc Biol, 2003. **74**(3): p. 370-8.

Appendix

This appendix contains the research articles I have contributed to during my PhD. All previously published work presented in the Thesis was explicitly disclosed and appropriately referenced.

Seoane, P.I., Schneider R. and May, R. C. From peaches to patients: the many faces of Cryptococci, Microbiology Today 2016 (1) pp: 22-25

Gilbert, A.S., Seoane, P.I., Sephton-Clark, P., Bojarczuk, A., Hotham, R., Giurisato, E., Sarhan, A.R., Hillen, A., Vande Velde, G., Gray, N.S., Alessi, D.R., Cunningham, D.L., Tournier, C., Johnston, S.A., May, R.C. Vomocytosis of live pathogens from macrophages is regulated by the atypical MAP kinase ERK5. Sci. Adv. 3, e1700898 (2017)

Lim, J., Coates, C.J., Seoane, P.I., Garelnabi, M., Taylor-Smith, L.M., Monteith, P., Macleod, C.L., Escaron, C.J., Brown, G.D., Hall, R.A., May, R.C. Characterizing the Mechanisms of Nonopsonic Uptake of Cryptococci by Macrophages, JI, 2018, 200:3539-3546.

Seoane, P.I., Taylor-Smith, L.M., Stirling, D., Bell, L.C.K., Noursadeghi, M., Bailey, D., May, R.C. Viral infection enhances vomocytosis of intracellular fungi via Type I interferons BioRxiv 2019 doi: https://doi.org/10.1101/512293

Coloured transmission electron micrograph of *Cryptococcus neoformans*, the cause of cryptococcosis, showing a single, circular encapsulated yeast. CNRI/Science Photo Library

From peaches to patients: the many faces of cryptococci

Paula I. Seoane, Rafael Schneider and Robin C. May

Human diseases caused by fungal pathogens have long been neglected as a medical problem, but the dramatic increase in immunocompromised individuals over the last 50 years, resulting both from the HIV/AIDS pandemic and more widespread use of immunosuppressive therapies, has led to an annual toll of over 2 million deaths due to fungal infections. Additionally, over 300 million people are chronically infected by fungi, leading to problems ranging from skin irritation to blindness.

Cryptococcus species

Amongst the life-threatening fungal pathogens, *Cryptococcus neoformans* and its close relative *Cryptococcus gattii* account for almost 1 million infections per year and around 650,000 deaths. Cryptococcal infections were recognised as a major threat only in the 1980s with the emergence of AIDS, but, in fact, the organism had been first isolated in 1894 by an Italian researcher, Sanfelice, from fermented peach juice and, in the same year, from a patient with a chronic granuloma.

Both pathogenic *Cryptococcus* species are found in a diverse range of niches in the environment, particularly in decaying vegetation of several tree species. *C. neoformans* is also found in bird faeces, which partly explains the high incidence of this species in urban locations.

Cryptococcosis

Cryptococcosis results from inhalation of fungal cells or spores from the environment, causing subsequent lung infection. The first step to disease development is the arrival of fungal cells deep in the alveoli of the lung. Consequently, desiccated yeast cells or spores are considered the most important infectious propagule due to their small size (~3 µm) in comparison to active yeast cells (4–10 µm), since only small cells can penetrate so far into the lung. In most individuals this initial pulmonary infection is rapidly contained, but in people lacking an appropriate immune response, the infection can spread to the blood and central nervous system, causing meningoencephalitis, which is rapidly fatal without treatment.

The ability of these environmental fungi to cause human infections is underpinned by a number of classical virulence factors, most notably the production of a polysaccharide capsule (Fig. 1) which protects *Cryptococcus* from phagocytosis, and the production of melanin pigment, which protects the fungal cell from oxidative damage. Perhaps most remarkable, however, is the ability that cryptococci have to evade immune activation.

Fig. 1. ***Cryptococcus gattii* cell stained with India ink, showing capsule (red), fungal cell wall (blue) and the budding yeast (yellow). Bar, 5 µm.** Paula Seoane, Rafael Schneider and Robin C. May

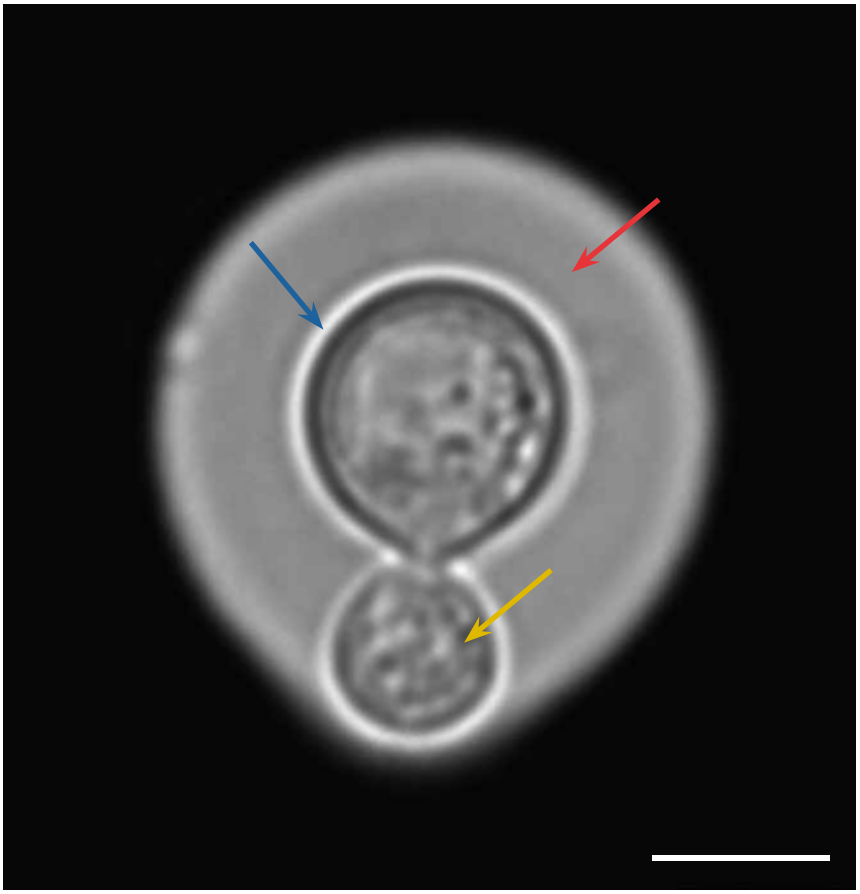

How does *Cryptococcus* evade the immune system?

Normally, exposure to fungal cells triggers a potent inflammatory response. However, *Cryptococcus* yeast cells are remarkably immunologically inert. Not only do they fail to elicit pro-inflammatory cytokines from dendritic cells (as opposed to other fungi such as *Candida albicans*), they actively promote the production of anti-inflammatory cytokines such as IL-10 or IL-4. This cytokine profile enables *Cryptococcus* to repolarise the immune response, reducing the so-called Th1 response (a potent inflammatory and antimicrobial response, which is particularly effective in eradicating intracellular pathogens) and instead shifting towards a Th2 profile, an inflammatory state that is targeted towards large pathogens such as parasitic worms and is ineffective at removing single-celled pathogens such as cryptococci. In parallel, a

proportion of the infecting yeast cells expand dramatically in size to form giant or 'titan' cells. These cells are thought to arise from replication without concomitant mitosis, since they are polyploid and uninucleate, and block phagocytosis both of themselves and, interestingly, of normally-sized neighbouring cryptococci via a mechanism that is not yet characterised.

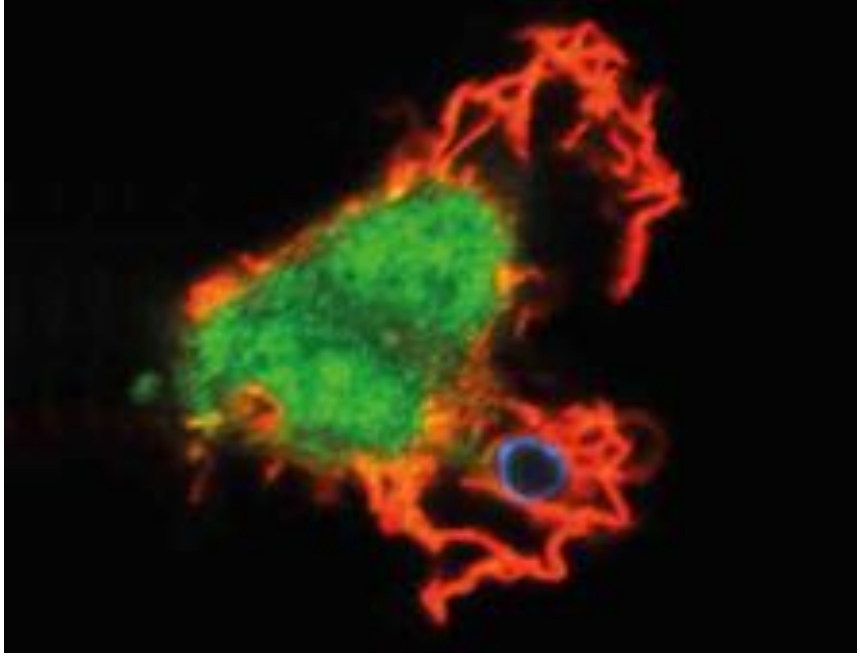

Fig. 2. ***Cryptococcus neoformans*** **cell (blue) being engulfed by a human macrophage (red and green).** Paula Seoane, Rafael Schneider and Robin C. May

Cryptococcus and phagocytes

If these strategies all fail and the invading fungus is engulfed by host phagocytes, cryptococci are able to engage an extra line of defence and persist as facultative intracellular pathogens (Fig. 2). Once inside the host cell, *Cryptococcus* cells have developed numerous mechanisms to both reduce the antimicrobial properties of the phagosome and to neutralise the low pH and reactive oxygen species that are abundant in this organelle.

Once established within the phagocyte, cryptococci are able to replicate rapidly but can also escape the macrophage via an intriguing non-lytic exocytosis, also known as vomocytosis (Fig. 3). Following vomocytosis, both the expelled cryptococci and the macrophage are undamaged. Thus this escape mechanism ensures minimal proinflammatory signaling, and is therefore thought to pose an advantage over lytic escape.

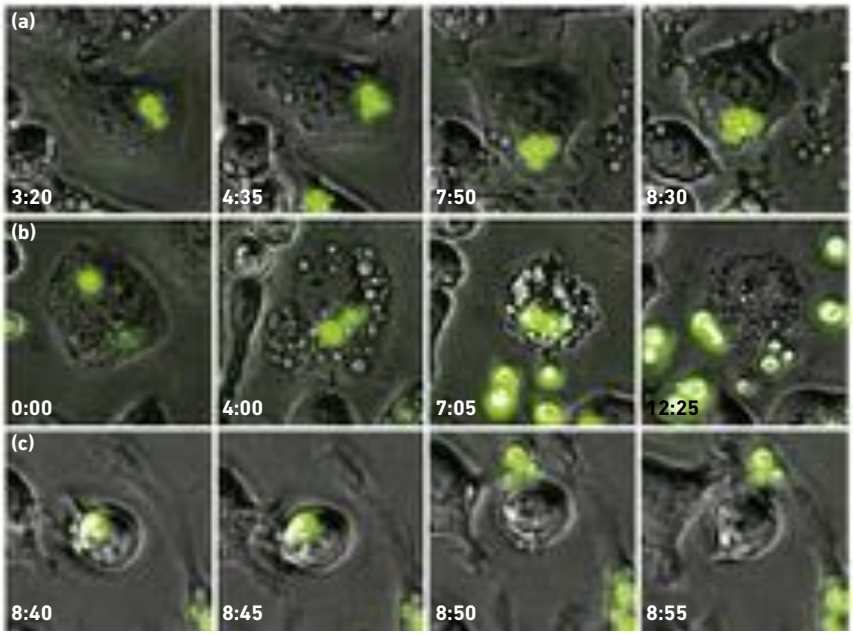

Fig. 3. **Time-lapse images of J774 macrophages infected with GFP-tagged** ***Cryptococcus neoformans*** **exemplifying intracellular replication (a), lytic escape (b) and vomocytosis (c). The time post-infection is shown in each panel.** Paula Seoane, Rafael Schneider and Robin C. May

How does *Cryptococcus* reach the brain tissue?

The most dangerous consequence of cryptococcal infection is meningoencephalitis, resulting from dissemination of the fungus to the central nervous system. To infect this immune privileged site, cryptococci must exit the lungs, enter peripheral blood circulation and bypass the blood–brain barrier (BBB). It now appears that cryptococci accomplish this feat in three ways (Fig. 4). Firstly, yeast cells can make their way through tight junctions of the endothelial cells using proteases such as Mpr1, in a process called paracytosis. Secondly, yeast cells can infiltrate the BBB by transcytosis, a process that is mediated by the interaction between hyaluronic acid in the cryptococcal surface and CD44 present in the luminal endothelium, resulting in direct uptake of the fungus by endothelial cells and migration through the cell's cytoplasm to reach the brain tissue opposite. Finally, a third possibility involves cryptococci crossing the BBB whilst concealed within phagocytes, a so-called 'Trojan Horse' route. Evidence supporting this

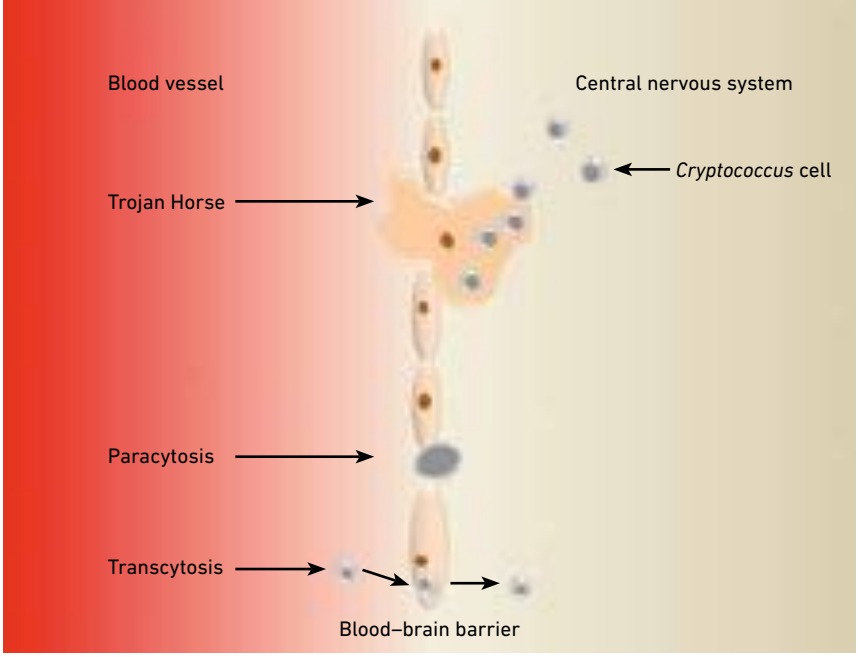

Fig. 4. **Cryptococci can infect the central nervous system by three routes: Trojan Horse, paracytosis or transcytosis.** Paula Seoane, Rafael Schneider and Robin C. May

It now appears that the high pathogenicity of this lineage results from a novel "division of labour" virulence mechanism in which cryptococcal cells collaborate to drive extremely rapid intracellular proliferation and thus overwhelm the host.

mechanism comes from studies in mice where depletion of alveolar macrophages significantly reduced cryptococci burden in the brain tissue and direct infection with *Cryptococcus* results in lower dissemination to the brain than adoptive transfer of infected monocytes.

Cryptococcus: one genus, several pathogens

One of the most remarkable findings of recent years has been the use of comparative genomic/phenotypic studies to reveal subtle differences in the biology of different cryptococcal lineages. Typically, infections with *Cryptococcus gattii,* although much rarer than *Cryptococcus neoformans* infections, cause more aggressive disease symptoms and respond more slowly to antifungal drugs. However, within each species certain lineages appear to be more pathogenic than others. For instance, the VNB lineage of *Cryptococcus neoformans* is associated with poorer patient outcomes than other strains. Most dramatic, however, is the involvement of the VGIIa lineage of *Cryptococcus gattii* in a large cryptococcosis outbreak that started in 1999 on Vancouver Island, Canada. During the following decade, 236 human cases with 19 deaths were reported, almost none of which were in people with classical immune-compromising conditions. Now known as the Pacific Northwest Outbreak, this disease cluster now represents the most serious outbreak of invasive fungal disease in the healthy population to date. It now appears that the high pathogenicity of this lineage results from a novel 'division of labour' virulence mechanism in which cryptococcal cells collaborate to drive extremely rapid intracellular proliferation and thus overwhelm the host, even in the presence of a fully functional immune response.

Summary

Since its recognition as a major threat to human health in the 1980s, research on *Cryptococcus* has highlighted the extraordinary range of virulence factors used by this organism to drive disease. In particular, its ability to modulate host immunity and to enter the central nervous system by hiding inside macrophages has revealed unique aspects of host–pathogen biology. Intensive ongoing genetic, cell, biological and clinical investigations offer the prospect of us soon learning much more about this enigmatic human pathogen.

Acknowledgements

The authors would like to thank Dr Ewa Bielska for providing the image for Figure 1 and Dr Jenson Lim for Figure 2. The authors are supported by funding from the Darwin Trust of Edinburgh (P.S.), the Science Without Borders Program – CNPq (R.S.) and the European Research Council (R.C.M.).

Paula I. Seoane and Robin C. May
Institute of Microbiology and Infection & School of Biosciences, University of Birmingham, Edgbaston, Birmingham B15 2TT, UK

Rafael Schneider
Centro de Biotecnologia, Universidade Federal do Rio Grande do Sul, Porto Alegre, RS 91501-970, Brazil

Further reading

Casadevall A., Steenbergen J. N., Nosanchuk J. D. (2003). 'Ready made' virulence and 'dual use' virulence factors in pathogenic environmental fungi – the *Cryptococcus neoformans* paradigm. *Curr Opin Microbiol* **6**, 332–337.

Johnston S. A. & May R. C. (2013). *Cryptococcus* interactions with macrophages: evasion and manipulation of the phagosome by a fungal pathogen. *Cell Microbiol* **15**, 403–411.

Kwon-Chung & others (2014). *Cryptococcus neoformans* and *Cryptococcus gattii*, the etiologic agents of cryptococcosis. *Cold Spring Harb Perspect Med* **4**, a019760.

IMMUNOLOGY

Vomocytosis of live pathogens from macrophages is regulated by the atypical MAP kinase ERK5

Andrew S. Gilbert,[1] Paula I. Seoane,[1] Poppy Sephton-Clark,[1] Aleksandra Bojarczuk,[2,3] Richard Hotham,[2,3] Emanuele Giurisato,[4,5] Adil R. Sarhan,[1,6] Amy Hillen,[7] Greetje Vande Velde,[7] Nathanael S. Gray,[8,9] Dario R. Alessi,[6] Debbie L. Cunningham,[1] Cathy Tournier,[4] Simon A. Johnston,[2,3] Robin C. May[1]*

Vomocytosis, or nonlytic extrusion, is a poorly understood process through which macrophages release live pathogens that they have failed to kill back into the extracellular environment. Vomocytosis is conserved across vertebrates and occurs with a diverse range of pathogens, but to date, the host signaling events that underpin expulsion remain entirely unknown. We use a targeted inhibitor screen to identify the MAP kinase ERK5 as a critical suppressor of vomocytosis. Pharmacological inhibition or genetic manipulation of ERK5 activity significantly raises vomocytosis rates in human macrophages, whereas stimulation of the ERK5 signaling pathway inhibits vomocytosis. Lastly, using a zebrafish model of cryptococcal disease, we show that reducing ERK5 activity in vivo stimulates vomocytosis and results in reduced dissemination of infection. ERK5 therefore represents the first host signaling regulator of vomocytosis to be identified and a potential target for the future development of vomocytosis-modulating therapies.

INTRODUCTION

Phagocytes are an essential component of the innate immune system, which function to identify, engulf, and destroy foreign particles. Although the vast majority of microbes are readily killed by phagocytes upon internalization, a number of important human pathogens have evolved mechanisms to survive or replicate within this hostile host environment. Phagocytes infected with these organisms have one of two fates: either they successfully recognize and destroy the intracellular pathogen or the pathogen lyses and kills the host cell. More than 10 years ago, we and others discovered a third potential outcome, whereby host macrophages expel the live pathogen residing within it in a process known as vomocytosis or nonlytic extrusion (*1*, *2*). Vomocytosis has subsequently been observed with a diverse range of pathogens (*3*) and in phagocytic cells from mammals (*4*), birds (*5*), fish (*6*), and amoebae (*7*), suggesting that it is an evolutionarily conserved phenomenon. However, despite this marked conservation, the host molecules that regulate vomocytosis have remained enigmatic.

RESULTS

To begin addressing the underlying molecular pathways that regulate vomocytosis, we screened a library of inhibitors that target kinases known to be expressed in macrophages (table S1) (*8*). This initial screen identified one compound [LRRK2-IN-1 (*9*)] that showed a small but significant increase in vomocytosis rates without enhancing cell death. LRRK2-IN-1 inhibits the leucine-rich repeat kinase LRRK2 but has additionally been demonstrated to act against other kinases, including the bromodomain protein BRD4 (*10*) and the extracellular receptor kinase 5 (ERK5) (*11*). Testing an independent second series of inhibitors revealed a potent and reproducible enhancement of vomocytosis with the ERK5 inhibitors XMD17-109 (*12*) or AX15836, but not with a specific inhibitor of BRD4 [JQ1 (*13*)] or with an alternative inhibitor of LRRK2 [HG1010201 (*14*)] (Fig. 1A and table S1). Notably, direct exposure of cryptococci to ERK5 inhibitors in vitro did not alter fungal morphology or growth rate (fig. S1), indicating that the impact of ERK5 inhibition on vomocytosis acts at the level of the host macrophage and not of the pathogen itself. In addition, exposing cells to LRRK2-IN-1 and XMD17-109 together did not enhance vomocytosis levels beyond that of XMD17-109 alone, suggesting that it is the off-target inhibition of ERK5 by LRRK2-IN-1 that accounts for its effect on vomocytosis.

To confirm this role for ERK5 in enhancing vomocytosis, we first exposed human macrophages, differentiated from peripheral blood monocytes, to XMD17-109. It has previously been shown that primary human macrophages show higher basal rates of vomocytosis than phagocytic cell lines (*2*), but nevertheless, as with J774 cells (which are originally derived from mouse), human macrophages showed a significant increase in vomocytosis when ERK5 activity was inhibited (Fig. 1B). Second, we tested the role of ERK5 in vomocytosis directly by depleting ERK5 levels in macrophages using transient small interfering RNA (siRNA)–based knockdown in J774 cells (Fig. 1C) or tamoxifen-inducible *ERK5* gene loss in murine bone marrow–derived macrophages (Fig. 1D). In both cases, we were unable to achieve full loss of the ERK5 protein (fig. S2), but this partial reduction in ERK5 level nevertheless resulted in a reproducible enhancement of vomocytosis. Thus, either pharmacological inhibition or genetic removal of ERK5 enhances vomocytosis in vitro.

Vomocytosis has been reported to occur with a wide range of live phagocytic targets but has never been observed with inert particles or dead pathogens. In line with this observation, pharmacological inhibition of ERK5 similarly enhanced vomocytosis of a second fungal

[1]Institute of Microbiology and Infection, School of Biosciences, University of Birmingham, Edgbaston, Birmingham B15 2TT, UK. [2]Department of Infection, Immunity and Cardiovascular Disease, Medical School, University of Sheffield, Sheffield, UK. [3]Bateson Centre, University of Sheffield, Sheffield, UK. [4]Division of Molecular and Clinical Cancer, School of Medical Sciences, Faculty of Biology, Medicine and Health, University of Manchester, Manchester M13 9PT, UK. [5]Department of Molecular and Developmental Medicine, University of Siena, 53100 Siena, Italy. [6]Medical Research Council Protein Phosphorylation and Ubiquitylation Unit, College of Life Sciences, University of Dundee, Dow Street, Dundee DD1 5EH, Scotland. [7]Biomedical MRI/MoSAIC, Department of Imaging and Pathology, KU Leuven–University of Leuven, Leuven, Belgium. [8]Department of Cancer Biology, Dana-Farber Cancer Institute, Boston, MA 02115, USA. [9]Department of Biological Chemistry and Molecular Pharmacology, Harvard Medical School, 250 Longwood Avenue, SGM 628, Boston, MA 02115, USA.
*Corresponding author. Email: r.c.may@bham.ac.uk

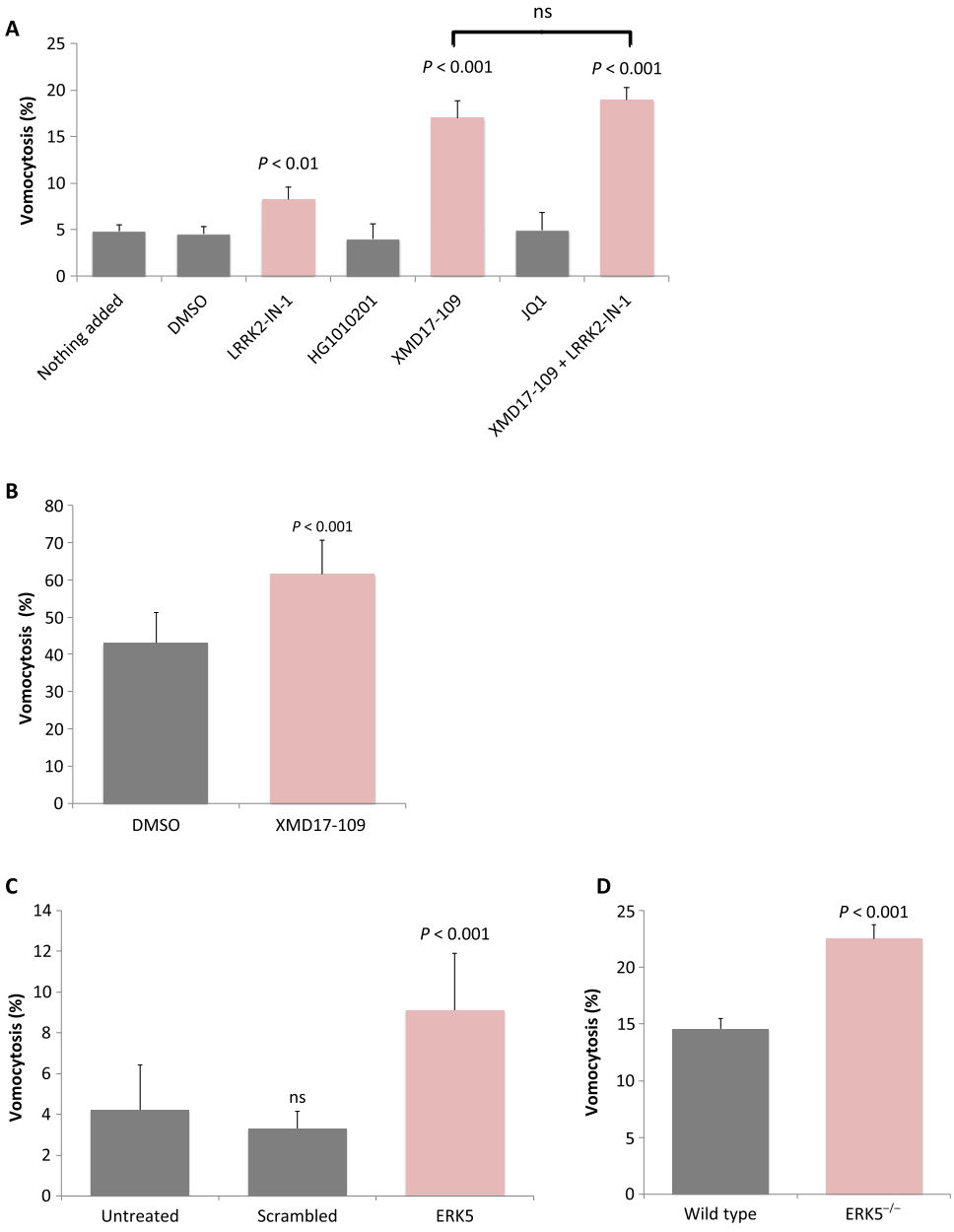

Fig. 1. Pharmacological or genetic inhibition of ERK5 enhances vomocytosis in vitro and ex vivo. (**A**) Vomocytosis is enhanced in J774.A1 cells by the LRRK2 inhibitor LRRK2-IN-1 (1 μM) but not by a second LRRK2 inhibitor, HG1010201 (1 μM). Vomocytosis is more strongly enhanced by specific inhibition of ERK5 (an off-target of LRRK2-IN-1) by XMD17-109 (1 μM) but not by inhibition of a second off-target, BRD4, by the inhibitor JQ1 (1 μM). Dual application of LRRK2-IN-1 and XMD17-109 (1 μM of each) showed significant enhancement of vomocytosis that was not significantly different to that of XMD17-109 alone. ns, not significant. (**B**) Application of 1 μM XMD17-109 to human PBMC-derived macrophages also significantly enhances vomocytosis rates in vitro. (**C**) Partial knockdown of ERK5 expression in J774.A1 by siRNA enhances vomocytosis. (**D**) Tamoxifen-inducible reduction of ERK5 expression ex vivo in murine bone marrow–derived macrophages significantly raises vomocytosis rates. Statistical significance was tested by χ^2 using a Bonferroni correction for multiplicity. All data represent pooled, averaged data from three to nine experimental repeats, with error bars showing the SEM. Example movies used for scoring are shown in movies S1 and S2.

pathogen, *Cryptococcus gattii*, but despite extensive imaging we were not able to observe any expulsion events for latex beads or heat-inactivated cryptococci (Fig. 2A). Thus, ERK5 is acting as a suppressor of the canonical vomocytosis pathway, rather than artificially inducing expulsion of all phagocytic cargo.

The canonical ERK5 pathway involves ERK5 activation via the upstream mitogen-activated protein (MAP) kinase MEK5 (*15*). Inhibition of MEK5 with the specific inhibitor BIX02189 (*16*) similarly raised vomocytosis levels in macrophages (Fig. 2B), suggesting that vomocytosis rates are normally suppressed by the MEK5-ERK5 signaling axis. To test this possibility further, we exposed cells to insulin-like growth factor 2 (IGF2), which has previously been shown to activate MEK5-ERK5 signaling up to eightfold (*17*) and to be implicated in phagocyte behavior (*18*). In line with this, IGF2 stimulation reduced cryptococcal

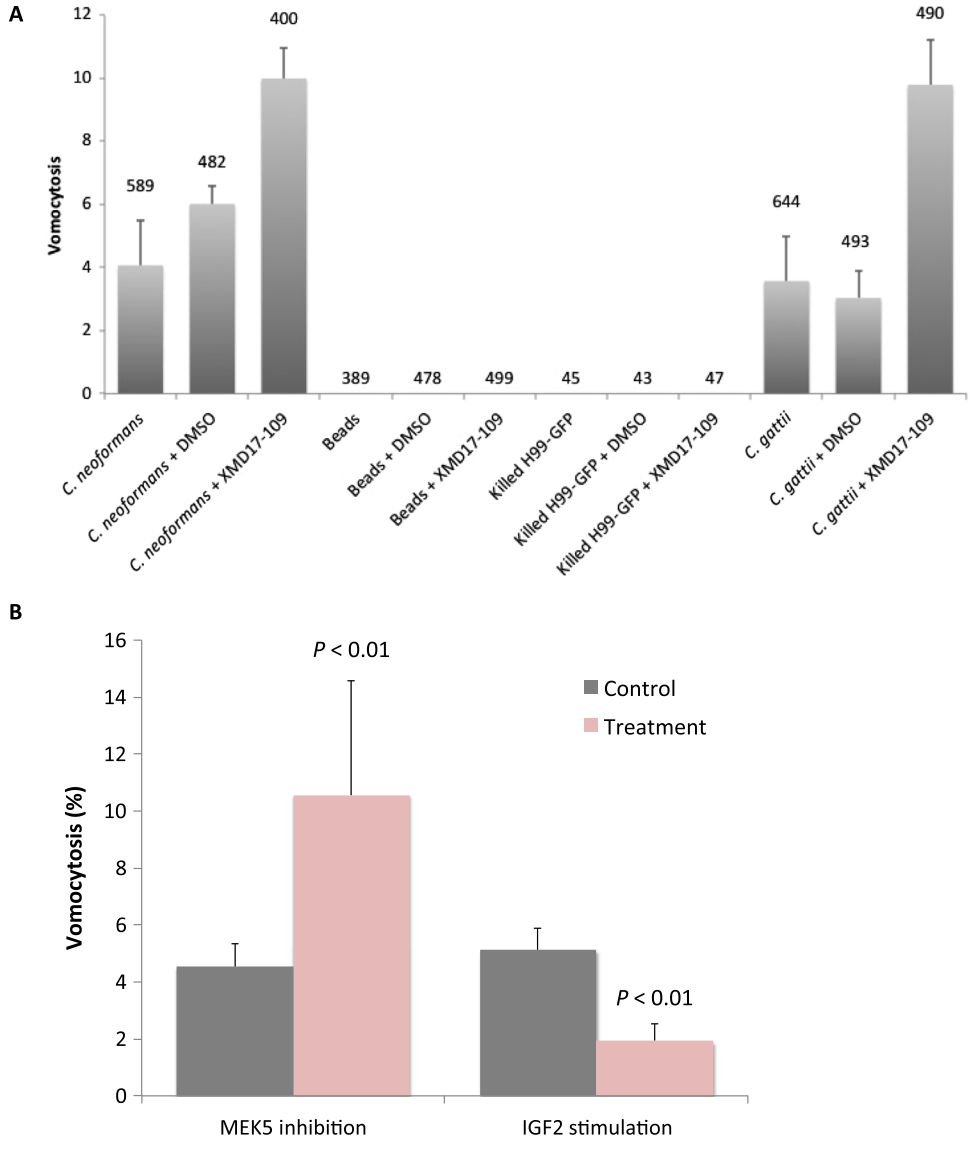

Fig. 2. Modulation of the canonical ERK5 signaling pathway alters vomocytosis rate but does not induce expulsion of inert phagosomal cargo. (**A**) ERK5 inhibition enhances vomocytosis of both *C. neoformans* and *C. gattii* but does not induce vomocytosis of heat-killed cryptococci or inert 3-μm polycarbonate beads. Numbers above each column represent the total number of individual fungal cells or beads scored. (**B**) Inhibition of MEK5 activity (an upstream regulator of ERK5) with 3 μM BIX02189 recapitulates the enhancement of vomocytosis seen with ERK5 inhibition in J774 macrophages, whereas stimulation of the ERK5 pathway via 1 μM IGF2 significantly reduces vomocytosis rates. Statistical significance was tested by χ^2 on raw data from three independent repeats. Error bars represent the SEM.

expulsion rates from macrophages (Fig. 2B). Thus, pharmacological or genetic inhibition of the ERK5 pathway enhances vomocytosis, and indirect stimulation of the pathway via IGF2 suppresses it.

Macrophage behavior is strongly influenced by the local concentration of cytokines, released both by themselves and by other cell types. In particular, different cytokine environments can modulate macrophage activation states (*19*), and we and others have previously shown that altered macrophage polarization states modify vomocytosis rates (*20*). We therefore considered whether ERK5 might regulate vomocytosis by modifying macrophage polarization and the local cytokine environment.

To determine the impact of ERK5 on macrophage polarization, we assessed the expression of surface markers on J774 macrophages exposed to XMD17-109. At rest, macrophages express both the pro-inflammatory marker CD86 and the anti-inflammatory marker MGL but are efficiently polarized to $CD86^{hi}$ (M1-like) cells when exposed to exogenous interferon-γ (IFN-γ) and lipopolysaccharide (LPS) or conversely to MGL^{hi} (M2-like) cells upon exposure to interleukin-4 (IL-4) (Fig. 3A). Cells treated with XMD17-109 showed no change in the expression of CD86 markers (Fig. 3A, i) either at rest or stimulated with IFN-γ and LPS. In contrast, XMD17-109 treatment strongly reduced the expression of MGL both in resting cells and in cells polarized by exposure to IL-4 (Fig. 3A, ii). Thus, ERK5 inhibition in macrophages leads to a modified inflammatory profile that prevents anti-inflammatory polarization without modifying their response to inflammatory stimuli.

To determine the consequence of this modified inflammatory profile, we performed enzyme-linked immunosorbent assay (ELISA) analysis to quantify secreted cytokine levels in supernatants from mouse

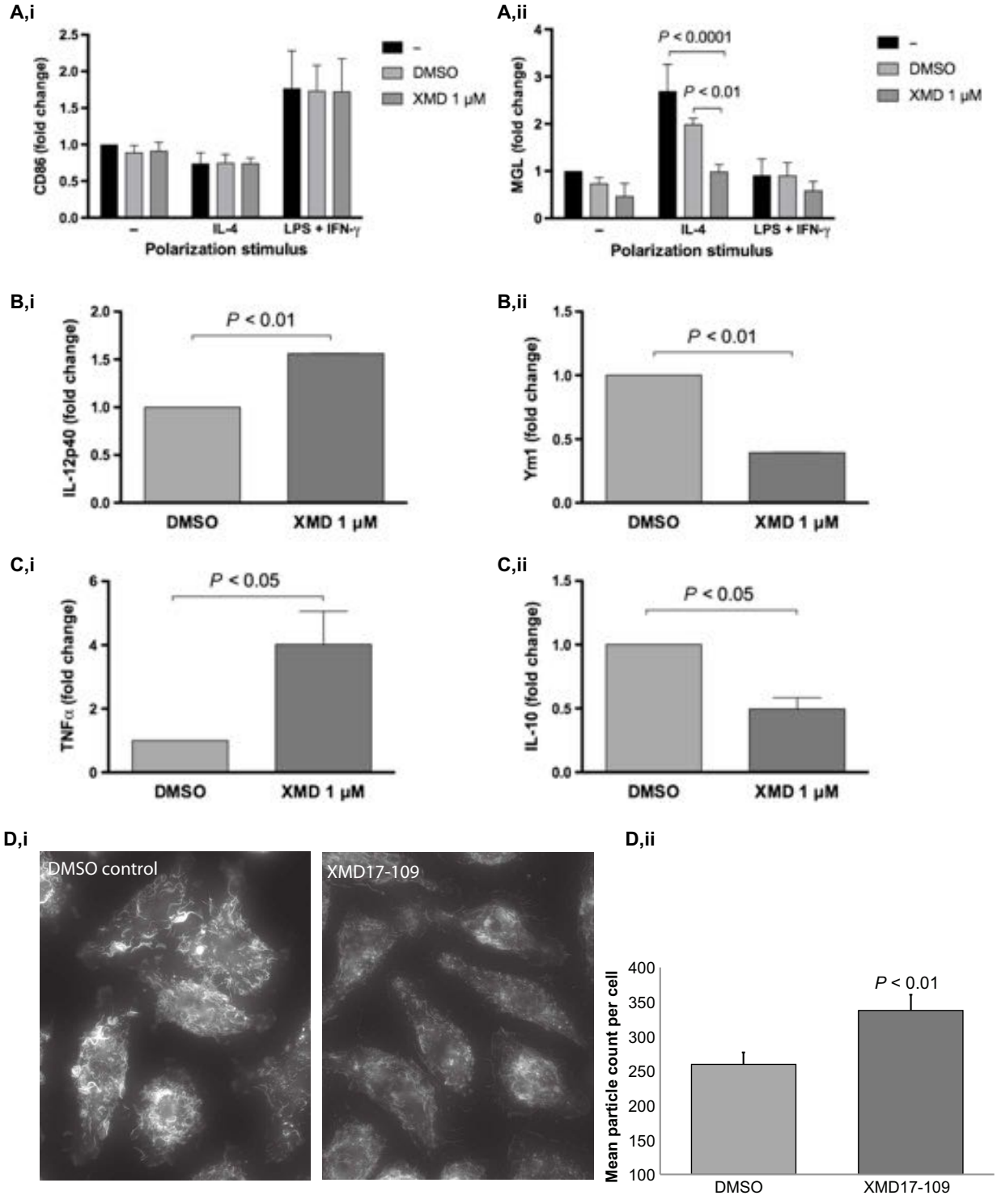

Fig. 3. ERK5 inhibition suppresses M2 macrophage polarization, alters secreted cytokine profiles, and modifies the actin cytoskeleton. (**A**) (i) Pharmacological inhibition of ERK5 with XMD17-109 does not alter expression of the M1 macrophage marker CD86 in J774 macrophages at rest or under M1 (LPS and IFN-γ) or M2 (IL-4) stimulating conditions. (ii) However, IL-4–driven M2 polarization is strongly reduced in the presence of XMD17-109. Significance was tested using two-way analysis of variance (ANOVA) on data from three independent replicates. Error bars show the SEM. (**B**) XMD17-109 inhibition of ERK5 activity in J774 macrophages increases proinflammatory IL-12p40 secretion (i) while reducing the secretion of the M2 marker Ym1 (ii). Significance was tested using a ratio-paired *t* test. (**C**) XMD17-109 inhibition of ERK5 activity in human PBMC-derived macrophages increases proinflammatory TNFα secretion (i) while reducing the secretion of the anti-inflammatory cytokine IL-10 (ii). Significance was tested using a ratio-paired *t* test. (**D**) J774 macrophages treated with XMD17-109 show a reduction in actin ruffles (revealed using Alexa 488–phalloidin; i). (ii) Ruffle disruption by XMD17-109 results in increased numbers of smaller actin-rich fragments, quantified in binary images (n = 33 images from n = 3 replicates, two-tailed *t* test; error bars are SEM). Images were captured using identical illumination, exposure, and postacquisition processing settings.

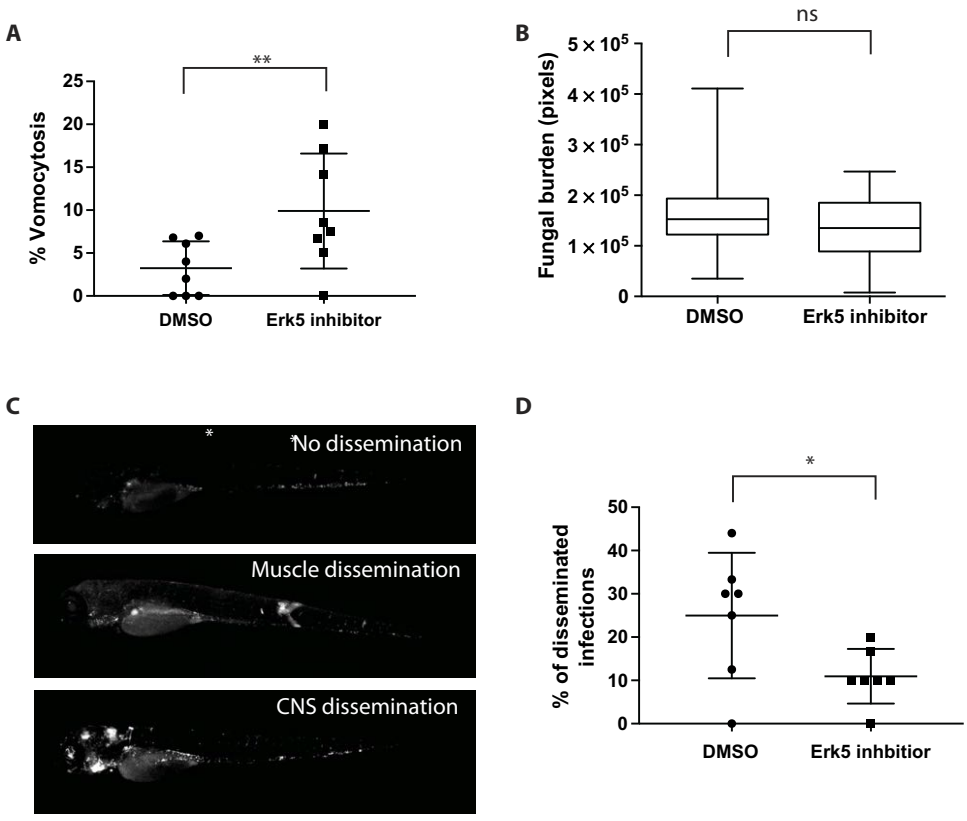

Fig. 4. ERK5 inhibition enhances vomocytosis and reduces dissemination in a zebrafish model of cryptococcosis. (**A**) Infected zebrafish treated with XMD17-109 show a significant ($P = 0.001$, Fisher's exact test) increase in vomocytosis in vivo over 24 hours. Bars represent the median and 5th/95th percentile. (**B**) Overall fungal burden at 3 days after infection is not significantly altered by ERK5 inhibition. Bars represent the median and 5th/95th percentile, with the boxed region representing the interquartile range. (**C**) Individual infections can be individually scored as nondisseminated (restricted to the bloodstream; top), disseminated to muscle/tissue blocks (middle), or disseminated to the central nervous system (bottom). CNS, central nervous system. (**D**) Infected fish treated with XMD17-109 show significantly ($P < 0.05$, Fisher's exact test) reduced dissemination from the site of infection. Bars represent the median and 5th/95th percentile.

macrophages (Fig. 3B) and human monocyte-derived macrophages (Fig. 3C) treated with XMD17-109. In line with the reduction in IL-4 polarization induced by ERK5 inhibition, both cell types showed an increased secretion of proinflammatory cytokines [IL-12p40 or tumor necrosis factor–α (TNFα)] and a reduced secretion of M2-associated proteins (Ym1 or IL-10) upon exposure to XMD17-109.

ERK5 has previously been implicated in cytoskeletal remodeling (*21*, *22*), and previous work has shown that mild inhibition of phagocyte actin dynamics triggers enhanced vomocytosis (*23*). We therefore fixed J774 cells exposed to *C. neoformans* in the presence or absence of XMD17-109 and stained for filamentous actin. ERK5 inhibition did not lead to any gross alteration of the actin cytoskeleton, in line with our observation that XMD17-109 does not alter phagocytosis rates or cell motility (both actin-driven processes). However, we noted a subtle reduction in the number and size of actin-rich ruffles in treated cells, suggestive of a slight destabilization of actin filamentation during ERK5 inhibition (Fig. 3D). Thus, the impact of ERK5 inhibition on vomocytosis likely results from a combination of reduced M2 inflammatory signaling and a diminished ability to constrain cryptococci within filamentous actin "cages."

Vomocytosis was first observed more than a decade ago (*1*, *2*), but an enduring open question in the field has been whether it serves to increase or reduce pathogenesis in infected organisms. Although in vivo vomocytosis has been implied indirectly (*4*), it is only very recently that extended imaging in the zebrafish model has provided direct evidence for its occurrence within a living animal (*6*, *24*).

We exploited this model to explore the impact of modifying vomocytosis rates on cryptococcal disease progression. We infected zebrafish larvae in the presence of XMD17-109 or a dimethyl sulfoxide (DMSO) control and then used extended live-cell imaging of anesthetized fish to quantify vomocytosis in vivo. As with our in vitro studies, ERK5 inhibition led to significantly enhanced vomocytosis rates in vivo (Fig. 4A). However, although the overall fungal burden at day 3 after infection did not differ significantly between control and inhibitor-treated fish, ERK5 inhibition led to a significant decrease in disease dissemination from the initial point of infection (Fig. 4B). In humans, cryptococcal dissemination from the lung (the initial point of entry) to other tissues (in particular, the central nervous system) is thought to depend, at least in part, on "Trojan Horse" transportation within host phagocytes (*25*). Thus, elevating vomocytosis rates presumably reduces dissemination by triggering phagocytes to eject their fungal cargo before they migrate far from the initial site of infection.

DISCUSSION

Together, these findings identify ERK5 as the first cellular signaling component to regulate vomocytosis. There are a number of ERK5 inhibitors under clinical development (*15*), and further work is needed

to understand whether targeting vomocytosis has promising therapeutic value. However, we note that the ERK5 locus is polymorphic in humans and that specific polymorphisms have been linked to lung cancer risk in smokers (*26*) and thus variation in ERK5 activity may contribute to the significant individual variation in vomocytosis rate between healthy donors and, consequently, to the risk of disseminated cryptococcosis.

MATERIALS AND METHODS

All reagents and media were purchased from Sigma-Aldrich, unless specified otherwise.

Cryptococcus strains

Strains used were *C. neoformans* var. *grubii* serotype A wild-type strains H99 or KN99, green fluorescent protein (GFP)–expressing derivatives KN99-GFP or H99-GFP, and *C. gattii* serotype B R265 or its GFP-expressing derivative R265-GFP (*27*). These were grown overnight in yeast peptone dextrose broth (2% glucose, 1% peptone, and 1% yeast extract) at 25°C on an orbital rotator (20 rpm).

J774A.1 cell culture

J774A.1 murine macrophages were cultured at 37°C in 5% CO_2 in complete Dulbecco's modified Eagle medium (DMEM) with 2 mM L-glutamine, streptomycin (100 U/ml) and penicillin (0.1 mg/ml), and 10% fetal bovine serum (FBS) and passaged when confluent by scraping and resuspension in fresh medium.

Human primary macrophage isolation and culture

All work with human tissue was approved by the University of Birmingham Ethics Committee under reference ERN_10-0660. Twenty to forty ml of blood was withdrawn from healthy volunteers by venipuncture and diluted twice in cold phosphate-buffered saline (PBS) before layering on top of 20 ml of Ficoll-Paque. Samples were centrifuged at 400*g* for 30 min at 20°C without braking in a swing bucket rotor. The white disc of peripheral blood mononuclear cells (PBMCs) obtained was washed twice in cold PBS (harvesting cells in between by centrifugation at 300*g* for 10 min), resuspended in PBS, counted, and then plated onto multiwell dishes in RPMI 1640 with 10% FBS and granulocyte-macrophage colony-stimulating factor (50 ng/ml).

Murine bone marrow–derived macrophage isolation and culture

Mice carrying the *erk5F* allele and the CMV-CreER transgenes were identified by polymerase chain reaction (PCR) on genomic DNA, as previously described (*28*). The colony was maintained in a pathogen-free facility at the University of Manchester, and all animal procedures were performed under license in accordance with the UK Home Office Animals (Scientific Procedures) Act 1986 and institutional guidelines. Primary macrophages were obtained from bone marrow cells isolated from femurs of genetically modified mice and cultured in DMEM containing 10% FBS, 1% penicillin/streptomycin, and 20% L929 cell-conditioned medium as a source of CSF-1 (colony-stimulating factor–1). Where indicated, the cells were mock-treated with DMSO or incubated with 4-hydroxytamoxifen (4-HT; 0.1 μM) at day 5 to induce Cre-mediated recombination of the *erk5F* allele.

In vitro infection and imaging

Fungi were opsonized with pooled human AB serum for 1 hour at 37°C and 5% CO_2 before infection. Macrophages were exposed to fungal cells at a multiplicity of infection of 10:1 for 2 hours, with or without the addition of inhibitors or DMSO controls. Extracellular fungi were removed by washing with fresh medium, containing inhibitors or DMSO control, and maintained under these conditions for 18 hours of time-lapse imaging. Time-lapse movies were made using a Ti-E Nikon or Zeiss Axio Observer microscope. Samples were incubated at 37°C and 5% CO_2 in the microscope imaging chamber. Images were taken every 5 min for 18 hours and compiled into single movie files for analysis using NIS Elements or Zeiss Zen software, respectively. Movies were blinded by a third party before manual scoring for vomocytosis and macrophage integrity. Vomocytosis was scored visually using the following preagreed guidelines:

(1) One vomocytosis event is the expulsion of internalized cryptococci from an infected macrophage, regardless of the number of cryptococci expelled if they do so simultaneously.

(2) Vomocytosis events are scored as independent phenomena if they occur in different frames or from different macrophages.

(3) Vomocytosis events are discounted if the host macrophage subsequently undergoes lysis or apoptosis within 30 min.

For fixed cell imaging, cells were plated onto glass coverslips and then infected as above before fixing with 4% paraformaldehyde in PBS (10 min) and then staining with Alexa 488–phalloidin (20 min). Coverslips were mounted onto glass slides using ProLong Antifade and imaged on a Zeiss Axio Observer.

ERK5 siRNA

Accell Mouse MAPK7 (ERK5)–SMARTpool siRNA was purchased from Dharmacon GE Healthcare and used according to the manufacturer's instructions. J774A.1 murine macrophages (5.0×10^3) were seeded into a 96-well plate and incubated at 37°C and 5% CO_2 in a humidified incubator for 24 hours. SMARTpool siRNA, or a scrambled siRNA control, was applied at 1 μM per well, incubated at 37°C and 5% CO_2 in a humidified incubator for 96 hours, and then infected and time-lapse–imaged as described above.

Secreted cytokine quantification

DuoSet ELISA Development kits from R&D Systems were used for all cytokine quantification and used according to the manufacturer's instructions. Secreted murine Ym1 was detected by sandwich ELISA using anti-Ym1 antibody (Abcam). Media supernatants from infected macrophages, treated with XMD17-109 or DMSO for 18 hours, were serially diluted before ELISA analysis and cytokine concentrations derived by reference to a standard curve.

Polarization assays

J774 macrophages were seeded at 0.2×10^6 cells per well in DMEM containing 10% heat-inactivated FBS and then stimulated with IL-4 (20 ng/ml) (ImmunoTools) or LPS (20 ng/ml) (Sigma-Aldrich) + 1000 IU IFN-γ (ImmunoTools), in the presence or absence of 1 μM XMD17-109. After 24 hours, the cells were placed on ice and stained for viability and macrophage activation markers (LIVE/DEAD Aqua Thermo, CD11b-BV605 BD, MGL-PE BioLegend, and CD86-FITC BD). Events were acquired using an Attune flow cytometer, and data were analyzed using FlowJo 8.7.

Statistical analysis

Statistical analysis was performed using a combination of Microsoft Excel, GraphPad Prism, MaxQuant (mass spectrometry tools), and the statistical program R, together with the online software DAVID

(Database for Annotation, Visualization and Integrated Discovery) to detect significant enrichment of gene ontology clusters (*29*).

Zebrafish

Animal work was carried out per guidelines and legislation set out in UK law in the Animals (Scientific Procedures) Act 1986, under Project License PPL 40/3574. Ethical approval was granted by the University of Sheffield Local Ethical Review Panel. We used the Nacre as our wild-type strain. We used the macrophage Tg(mpeg1:mCherryCAAX)sh378 fluorescent transgenic zebrafish line (*6*). Zebrafish strains were maintained according to the standard protocols. Adult fish were maintained on a 14:10-hour light/dark cycle at 28°C in UK Home Office–approved facilities in the Bateson Centre aquaria at the University of Sheffield. Zebrafish were infected as described previously (*6*) with 500 colony forming units of *Cryptococcus* strain KN99-GFP. For time-lapse imaging, zebrafish larvae were mounted in 0.8% low–melting point agarose in E3 containing tricaine (0.168 mg/ml). Images were captured with CFI Plan Apochromat λ [20×; numerical aperture (NA), 0.75 objective lens; 10 *z*-sections 2.5 μm apart], with Perfect Focus system, every 2 min for 12 hours. For co-infection studies, we used H99-GFP (*27*) and H99-dsRed (*30*). For fungal burden and dissemination imaging, zebrafish were imaged in 96-well plates using Nikon Ti-E with a CFI Plan Achromat UW (2×; NA, 0.06 objective lens), using Intensilight fluorescent illumination with ET/sputtered series fluorescent filters 49002 (Chroma). Images were captured with Neo sCMOS (Andor) and NIS Elements (Nikon). Images were exported as tif files, and further analysis was performed in ImageJ (*31*), as described previously (*6*).

SUPPLEMENTARY MATERIALS

Supplementary material for this article is available at http://advances.sciencemag.org/cgi/content/full/3/8/e1700898/DC1

table S1. Screened inhibitors of macrophage-expressed kinases.

fig. S1. Pharmacological inhibition of the MEK5/ERK5 signaling pathway does not alter cryptococcal growth in vitro.

fig. S2. Quantification of ERK5 depletion in macrophages.

movie S1. Example time-lapse movie showing vomocytosis from J774 cells infected with H99-GFP cryptococci and treated with DMSO (control).

movie S2. Example time-lapse movie showing vomocytosis from J774 cells infected with H99-GFP cryptococci and treated with 1 μM XMD17-109.

REFERENCES AND NOTES

1. M. Alvarez, A. Casadevall, Phagosome extrusion and host-cell survival after *Cryptococcus neoformans* phagocytosis by macrophages. *Curr. Biol.* **16**, 2161–2165 (2006).
2. H. Ma, J. E. Croudace, D. A. Lammas, R. C. May, Expulsion of live pathogenic yeast by macrophages. *Curr. Biol.* **16**, 2156–2160 (2006).
3. L. M. Smith, R. C. May, Mechanisms of microbial escape from phagocyte killing. *Biochem. Soc. Trans.* **41**, 475–490 (2013).
4. A. M. Nicola, E. J. Robertson, P. Albuquerque, L. da Silveira Derengowski, A. Casadevall, Nonlytic exocytosis of *Cryptococcus neoformans* from macrophages occurs in vivo and is influenced by phagosomal pH. *MBio* **2**, e00167-11 (2011).
5. S. A. Johnston, K. Voelz, R. C. May, *Cryptococcus neoformans* thermotolerance to avian body temperature is sufficient for extracellular growth but not intracellular survival in macrophages. *Sci. Rep.* **6**, 20977 (2016).
6. A. Bojarczuk, K. A. Miller, R. Hotham, A. Lewis, N. V. Ogryzko, A. A. Kamuyango, H. Frost, R. H. Gibson, E. Stillman, R. C. May, S. A. Renshaw, S. A. Johnston, *Cryptococcus neoformans* intracellular proliferation and capsule size determines early macrophage control of infection. *Sci. Rep.* **6**, 21489 (2016).
7. M. Carnell, T. Zech, S. D. Calaminus, S. Ura, M. Hagedorn, S. A. Johnston, R. C. May, T. Soldati, L. M. Machesky, R. H. Insall, Actin polymerization driven by WASH causes V-ATPase retrieval and vesicle neutralization before exocytosis. *J. Cell Biol.* **193**, 831–839 (2011).
8. J. Bain, L. Plater, M. Elliott, N. Shpiro, C. J. Hastie, H. Mclauchlan, I. Klevernic, J. S. C. Arthur, D. R. Alessi, P. Cohen, The selectivity of protein kinase inhibitors: A further update. *Biochem. J.* **408**, 297–315 (2007).
9. X. Deng, N. Dzamko, A. Prescott, P. Davies, Q. Liu, Q. Yang, J.-D. Lee, M. P. Patricelli, T. K. Nomanbhoy, D. R. Alessi, N. S. Gray, Characterization of a selective inhibitor of the Parkinson's disease kinase LRRK2. *Nat. Chem. Biol.* **7**, 203–205 (2011).
10. B. Seashore-Ludlow, M. G. Rees, J. H. Cheah, M. Cokol, E. V. Price, M. E. Coletti, V. Jones, N. E. Bodycombe, C. K. Soule, J. Gould, B. Alexander, A. Li, P. Montgomery, M. J. Wawer, N. Kuru, J. D. Kotz, C. S.-Y. Hon, B. Munoz, T. Liefeld, V. Dančík, J. A. Bittker, M. Palmer, J. E. Bradner, A. F. Shamji, P. A. Clemons, S. L. Schreiber, Harnessing connectivity in a large-scale small-molecule sensitivity dataset. *Cancer Discov.* **5**, 1210–1223 (2015).
11. N. Weygant, D. Qu, W. L. Berry, R. May, P. Chandrakesan, D. B. Owen, S. M. Sureban, N. Ali, R. Janknecht, C. W. Houchen, Small molecule kinase inhibitor LRRK2-IN-1 demonstrates potent activity against colorectal and pancreatic cancer through inhibition of doublecortin-like kinase 1. *Mol. Cancer* **13**, 103 (2014).
12. J. M. Elkins, J. Wang, X. Deng, M. J. Pattison, J. S. C. Arthur, T. Erazo, N. Gomez, J. M. Lizcano, N. S. Gray, S. Knapp, X-ray crystal structure of ERK5 (MAPK7) in complex with a specific inhibitor. *J. Med. Chem.* **56**, 4413–4421 (2013).
13. P. Ciceri, S. Müller, A. O'Mahony, O. Fedorov, P. Filippakopoulos, J. P. Hunt, E. A. Lasater, G. Pallares, S. Picaud, C. Wells, S. Martin, L. M. Wodicka, N. P. Shah, D. K. Treiber, S. Knapp, Dual kinase-bromodomain inhibitors for rationally designed polypharmacology. *Nat. Chem. Biol.* **10**, 305–312 (2014).
14. H. G. Choi, J. Zhang, X. Deng, J. M. Hatcher, M. P. Patricelli, Z. Zhao, D. R. Alessi, N. S. Gray, Brain penetrant LRRK2 inhibitor. *ACS Med. Chem. Lett.* **3**, 658–662 (2012).
15. B. A. Drew, M. E. Burow, B. S. Beckman, MEK5/ERK5 pathway: The first fifteen years. *Biochim. Biophys. Acta* **1825**, 37–48 (2012).
16. S. Amano, Y.-T. Chang, Y. Fukui, ERK5 activation is essential for osteoclast differentiation. *PLOS ONE* **10**, e0125054 (2015).
17. E. J. Carter, R. A. Cosgrove, I. Gonzalez, J. H. Eisemann, F. A. Lovett, L. J. Cobb, J. M. Pell, MEK5 and ERK5 are mediators of the pro-myogenic actions of IGF-2. *J. Cell Sci.* **122**, 3104–3112 (2009).
18. H.-S. Suh, M. Cosenza-Nashat, N. Choi, M.-L. Zhao, J.-F. Li, J. W. Pollard, R. L. Jirtle, H. Goldstein, S. C. Lee, Insulin-like growth factor 2 receptor is an IFNγ-inducible microglial protein that facilitates intracellular HIV replication: Implications for HIV-induced neurocognitive disorders. *Am. J. Pathol.* **177**, 2446–2458 (2010).
19. P. J. Murray, J. E. Allen, S. K. Biswas, E. A. Fisher, D. W. Gilroy, S. Goerdt, S. Gordon, J. A. Hamilton, L. B. Ivashkiv, T. Lawrence, M. Locati, A. Mantovani, F. O. Martinez, J.-L. Mege, D. M. Mosser, G. Natoli, J. P. Saeij, J. L. Schultze, K. A. Shirey, A. Sica, J. Suttles, I. Udalova, J. A. van Ginderachter, S. N. Vogel, T. A. Wynn, Macrophage activation and polarization: Nomenclature and experimental guidelines. *Immunity* **41**, 14–20 (2014).
20. K. Voelz, D. A. Lammas, R. C. May, Cytokine signaling regulates the outcome of intracellular macrophage parasitism by *Cryptococcus neoformans*. *Infect. Immun.* **77**, 3450–3457 (2009).
21. J. C. Barros, C. J. Marshall, Activation of either ERK1/2 or ERK5 MAP kinase pathways can lead to disruption of the actin cytoskeleton. *J. Cell Sci.* **118**, 1663–1671 (2005).
22. D. Spiering, M. Schmolke, N. Ohnesorge, M. Schmidt, M. Goebeler, J. Wegener, V. Wixler, S. Ludwig, MEK5/ERK5 signaling modulates endothelial cell migration and focal contact turnover. *J. Biol. Chem.* **284**, 24972–24980 (2009).
23. S. A. Johnston, R. C. May, The human fungal pathogen *Cryptococcus neoformans* escapes macrophages by a phagosome emptying mechanism that is inhibited by Arp2/3 complex-mediated actin polymerisation. *PLOS Pathog.* **6**, e1001041 (2010).
24. J. L. Tenor, S. H. Oehlers, J. L. Yang, D. M. Tobin, J. R. Perfect, Live imaging of host-parasite interactions in a zebrafish infection model reveals cryptococcal determinants of virulence and central nervous system invasion. *MBio* **6**, e01425-15 (2015).
25. C. Charlier, K. Nielsen, S. Daou, M. Brigitte, F. Chretien, F. Dromer, Evidence of a role for monocytes in dissemination and brain invasion by *Cryptococcus neoformans*. *Infect. Immun.* **77**, 120–127 (2009).
26. F. Qiu, L. Yang, W. Fang, Y. Li, R. Yang, X. Yang, J. Deng, B. Huang, C. Xie, Y. Zhou, J. Lu, A functional polymorphism in the promoter of *ERK5* gene interacts with tobacco smoking to increase the risk of lung cancer in Chinese populations. *Mutagenesis* **28**, 561–567 (2013).
27. K. Voelz, S. A. Johnston, J. C. Rutherford, R. C. May, Automated analysis of cryptococcal macrophage parasitism using GFP-tagged cryptococci. *PLOS ONE* **5**, e15968 (2010).
28. K. G. Finegan, X. Wang, E.-J. Lee, A. C. Robinson, C. Tournier, Regulation of neuronal survival by the extracellular signal-regulated protein kinase 5. *Cell Death Differ.* **16**, 674–683 (2009).
29. D. W. Huang, B. T. Sherman, Q. Tan, J. Kir, D. Liu, D. Bryant, Y. Guo, R. Stephens, M. W. Baseler, H. C. Lane, R. A. Lempicki, DAVID Bioinformatics Resources: Expanded annotation database and novel algorithms to better extract biology from large gene lists. *Nucleic Acids Res.* **35**, W169–W175 (2007).
30. A. Idnurm, S. S. Giles, J. R. Perfect, J. Heitman, Peroxisome function regulates growth on glucose in the basidiomycete fungus *Cryptococcus neoformans*. *Eukaryot. Cell* **6**, 60–72 (2007).
31. C. A. Schneider, W. S. Rasband, K. W. Eliceiri, NIH Image to ImageJ: 25 years of image analysis. *Nat. Methods* **9**, 671–675 (2012).

Acknowledgments: We thank the Bateson Centre aquaria staff at the University of Sheffield for their assistance with zebrafish husbandry. **Funding:** A.S.G., P.I.S., and R.C.M. are supported by project MitoFun, funded by the European Research Council under the European Union's Seventh Framework Programme (FP/2007-2013)/ERC grant agreement no. 614562 and by a Wolfson Research Merit Award from the Royal Society (to R.C.M.), a Biotechnology and Biological Sciences Research Council Midlands Integrative Biosciences Training Partnership Studentship (to A.S.G.), and a scholarship from the Darwin Trust of Edinburgh (to P.I.S.). S.A.J. and A.B. were supported by Medical Research Council and Department for International Development Career Development Award Fellowship (MR/J009156/1). S.A.J. was additionally supported by a Krebs Institute Fellowship, the Medical Research Foundation (grant R/140419), and the Medical Research Council Center (grant G0700091). R.H. was supported by a Colin Beattie Biomedical Science scholarship. A.R.S. was supported by a scholarship from the Higher Committee for Education Development in Iraq. E.G. was supported by a Marie Curie Research Fellowship, and C.T. is supported by a grant from Worldwide Cancer Research. G.V.V. is supported by a postdoctoral grant from the Flemish Research Foundation. D.R.A. acknowledges funding from the UK Medical Research Council (grant number MC-UU_1201612). **Author contributions:** A.S.G., P.I.S., and R.C.M. devised and led this project. A.S.G., P.I.S., and P.S.-C. conducted most of the in vitro experimental work and analyzed the data. A.B., R.H., and S.A.J. conducted and analyzed the zebrafish experiments. A.R.S., N.S.G., D.R.A., A.H., G.V.V., and D.L.C. provided the reagents, advice, and unpublished data to support this project. A.S.G. conducted the work on ERK5 knockout mouse material in collaboration with E.G. and C.T. All authors read and commented on the manuscript. **Competing interests:** N.S.G. is an author on a patent application related to this work filed by the Dana-Farber Cancer Institute (international application no. PCT/US2010/000050; filed 6 January 2010). N.S.G. is a scientific founder and equity holder in Gatekeeper, Syros, Petra, and C4 Pharmaceuticals. All other authors declare that they have no competing interests. **Data and materials availability:** All data needed to evaluate the conclusions in the paper are present in the paper and/or the Supplementary Materials. Additional data related to this paper may be requested from the authors.

Submitted 23 March 2017
Accepted 24 July 2017
Published 16 August 2017
10.1126/sciadv.1700898

Citation: A. S. Gilbert, P. I. Seoane, P. Sephton-Clark, A. Bojarczuk, R. Hotham, E. Giurisato, A. R. Sarhan, A. Hillen, G. V. Velde, N. S. Gray, D. R. Alessi, D. L. Cunningham, C. Tournier, S. A. Johnston, R. C. May, Vomocytosis of live pathogens from macrophages is regulated by the atypical MAP kinase ERK5. *Sci. Adv.* **3**, e1700898 (2017).

Characterizing the Mechanisms of Nonopsonic Uptake of Cryptococci by Macrophages

Jenson Lim,* Christopher J. Coates,† Paula I. Seoane,‡ Mariam Garelnabi,‡ Leanne M. Taylor-Smith,‡ Pauline Monteith,* Camille L. Macleod,* Claire J. Escaron,§ Gordon D. Brown,¶ Rebecca A. Hall,‡ and Robin C. May‡

The pathogenic fungus *Cryptococcus* enters the human host via inhalation into the lung and is able to reside in a niche environment that is serum- (opsonin) limiting. Little is known about the mechanism by which nonopsonic phagocytosis occurs via phagocytes in such situations. Using a combination of soluble inhibitors of phagocytic receptors and macrophages derived from knockout mice and human volunteers, we show that uptake of nonopsonized *Cryptococcus neoformans* and *C. gattii* via the mannose receptor is dependent on macrophage activation by cytokines. However, although uptake of *C. neoformans* is via both dectin-1 and dectin-2, *C. gattii* uptake occurs largely via dectin-1. Interestingly, dectin inhibitors also blocked phagocytosis of unopsonized Cryptococci in wax moth (*Galleria mellonella*) larvae and partially protected the larvae from infection by both fungi, supporting a key role for host phagocytes in augmenting early disease establishment. Finally, we demonstrated that internalization of nonopsonized Cryptococci is not accompanied by the nuclear translocation of NF-κB or its concomitant production of proinflammatory cytokines such as TNF-α. Thus, nonopsonized Cryptococci are recognized by mammalian phagocytes in a manner that minimizes proinflammatory cytokine production and potentially facilitates fungal pathogenesis. *The Journal of Immunology*, 2018, 200: 3539–3546.

Cryptococcus neoformans and *C. gattii* are encapsulated human fungal pathogens that cause cryptococcosis in immunocompromised and, more rarely, immunocompetent individuals. Often found as free-living cells in soil and avian excreta, Cryptococci are not intrinsic human pathogens. However, Cryptococci become human pathogens because several defense mechanisms possessed by these fungi also act as virulence factors within a human or animal host (1), including the ability, firstly, to survive and replicate within free-living soil amoeba and, secondly, to evade clearance by the host immune system by hiding and persisting within macrophages (2, 3).

As Cryptococci enter hosts via inhalation into the lungs, they are detected and phagocytosed by resident alveolar macrophages (4). Phagocytosis is a multistep process that sequentially involves receptor-mediated particle recognition, actin-driven uptake, phagosome maturation, and particle clearance. It is critical during the early innate immune response to ensure the removal of microorganisms and apoptotic cells as well as subsequent priming of the adaptive immune response through the production and release of cytokines, such as TNF-α (5). Phagocytosis of Cryptococci is typically inefficient unless they are opsonized (coated) by Abs or complement proteins found in serum within the circulatory system. Interestingly, there is a lack of serum opsonins in the alveoli of the lungs, and so the initial uptake of *Cryptococcus* upon colonization is most likely through a nonopsonized route (6).

Nonopsonic phagocytosis requires host cell phagocytic pattern recognition receptors (PRRs) to directly recognize fungal cell wall components (pathogen-associated molecular patterns [PAMPs]) (7) such as β-glucans or mannan polysaccharides, but the nature of this interaction for Cryptococci remains unknown. In this article, we show that nonopsonized *C. neoformans* and *C. gattii* enter macrophages in a spleen tyrosine kinase (Syk)–dependent, mannose receptor–independent manner that involves the receptors Dectin-1 and Dectin-2. This differential uptake of *C. neoformans* and *C. gattii* corresponds to differential exposure of PAMPs found on the fungal cell wall. Phagocytic kinetics of macrophages and insect hemocytes in the absence or presence of cellular receptor inhibitors were similar in response to fungal targets. Finally, we demonstrate that entry of *Cryptococcus* does not affect NF-κB nuclear translocation or subsequent TNF-α release, highlighting the remarkably noninflammatory capabilities of this organism.

*Biological and Environmental Sciences, University of Stirling, Stirling FK9 4LA, United Kingdom; †Department of Biosciences, College of Science, Swansea University, Swansea SA2 8PP, Wales, United Kingdom; ‡Institute of Microbiology and Infection, School of Biosciences, University of Birmingham, Birmingham B15 2TT, United Kingdom; §Protein Reference Unit, South West London Pathology, St. George's University Hospitals NHS Foundation Trust, London SW17 0QT, United Kingdom; and ¶Medical Research Council Centre for Medical Mycology Aberdeen Fungal Group, Institute of Medical Sciences, University of Aberdeen, Aberdeen AB25 2ZD, United Kingdom

ORCIDs: 0000-0001-7417-356X (J.L.); 0000-0002-4471-4369 (C.J.C.); 0000-0001-6323-5470 (P.I.S.); 0000-0001-9948-8242 (M.G.); 0000-0001-6217-6499 (L.M.T.-S.); 0000-0002-1447-9484 (P.M.); 0000-0002-6588-6805 (C.J.E.); 0000-0002-4908-8168 (R.A.H.); 0000-0001-5364-1838 (R.C.M.).

Received for publication May 31, 2017. Accepted for publication March 20, 2018.

This work was supported by the MitoFun project, which supports the May Lab, funded by the European Research Council under European Union's Seventh Framework Programme Grant FP/2007-2013/European Research Council Grant 614562 and by a Wolfson Research Merit Award from the Royal Society (to R.C.M.). G.D.B. is supported by Wellcome Trust Grant 102705, a Wellcome Trust Strategic Award in Medical Mycology and Fungal Immunology (097377), and the Medical Research Council Centre for Medical Mycology at the University of Aberdeen (MR/N006364/1). J.L. is supported by a start-up fund from the University of Stirling.

Address correspondence and reprint requests to Dr. Jenson Lim, University of Stirling, Faculty of Natural Sciences, Stirling FK9 4LA, U.K. E-mail address: jenson.lim@stir.ac.uk

Abbreviations used in this article: BMM, bone marrow macrophage; DC, dendritic cell; KO, knockout; MR KO, mannose receptor KO; p65, 65 kDa subunit; PAMP, pathogen-associated molecular pattern; PRR, pattern recognition receptor; RT, room temperature; Syk, spleen tyrosine kinase; WT, wild type.

Materials and Methods

Reagents

All reagents (e.g., heat-inactivated FBS, DMEM, L-glutamine, powdered yeast-extract peptone dextrose, and PBS) were purchased from Sigma-Aldrich unless stated otherwise. Mouse macrophage–CSF (130-094-129) and human GM-CSF (130-093-862) were purchased from Miltenyi Biotec. Commercially sourced inhibitors tested included the Syk–inhibiting plant metabolite, Piceatannol (527948; Calbiochem); the β-1,3-glucan from brown algae *Laminaria digitata*, Laminarin (L9634; Sigma-Aldrich); and mannan from *Saccharomyces cerevisiae* (M7504; Sigma-Aldrich).

The Abs used in this study were rabbit anti-sheep RBCs, IgG fraction (#55806; MP Biomedicals); rabbit anti-sheep RBCs, IgM fraction (CL9000M; VH Bio/Cedarlane); rabbit anti–65 kDa subunit (p65) NF-κB mAb (clone D14E12, #8242; New England Biolabs/Cell Signaling Technology); rat anti-αM (clone 5c6, MCA2289; Bio-Rad AbD Serotec); and rabbit anti–Phospho-Syk (Tyr525/526 in humans, Tyr519/520 in mice, clone C87C1, #2710; New England Biolabs/Cell Signaling Technology), a kind gift from Y. Senis (University of Birmingham). Rhodamine-Phalloidin and Alexa Fluor–conjugated secondary Abs were purchased from Life Technologies and Calcofluor White from Sigma-Aldrich. Glucan-6-phosphate and mouse anti-cryptococcal capsule Ab (clone 18B7) were kind gifts from D. Williams (East Tennessee State University) and A. Casadevall (Albert Einstein College of Medicine), respectively.

Mice

Mice devoid of specific PRRs (in C57BL/6 background) were reported previously (8, 9) and were housed under pathogen-free conditions in the registered animal facility at the University of Aberdeen. Mice were allocated to experimental groups on the basis of genotype and age-matching. All animal procedures were performed according to the protocols provided by the Animal Welfare and Ethical Review Body of the University of Aberdeen and are regulated by the UK Home Office Animal (Scientific Procedures) Act of 1986 and European Directive 2010/63/EU.

Yeast and bacterial cell growth conditions

C. neoformans strain H99, *C. gattii* strain R265, and *Candida albicans* strain SC5314 were incubated in liquid yeast-extract peptone dextrose medium for 24 h (unless stated otherwise) at 25˚C on a rotator at 20 rpm (or 37˚C, 200 rpm for *C. albicans*). *Escherichia coli* strain DH5α was incubated in Luria-Bertani broth for 16 h at 37˚C in a shaking incubator at 200 rpm. Yeast cells were centrifuged at 3000 × *g* for 2.5 min (or 6000 × *g* for 1 min for *E. coli*), washed three times in PBS, and counted with a hemocytometer prior to use.

Mammalian cell growth conditions

Cells from the murine macrophage–like cell line J774.A1 (American Type Culture Collection number TIB-67) were cultured in DMEM supplemented with 2 mM L-glutamine and 10% heat-inactivated FBS at 37˚C, 5% CO_2 (10). As required, macrophages were scrapped in PBS, counted, and seeded (50,000/well) onto 13 mm acid-washed glass coverslips, and incubated for 24 h at 37˚C, 5% CO_2 prior to experimental use.

Macrophages devoid of specific PRRs were derived from mouse bone marrow. Bone marrows were flushed using a 21-gauge needle from the hind leg bones of either receptor knockout (KO) or litter-matched wild type (WT) mice. Monocytes were differentiated into macrophages with 20 ng/ml M-CSF (Miltenyi Biotec) for 7 d.

Pooled PBMCs were isolated from whole blood from healthy volunteers using density gradient centrifugation with Ficoll-Paque (GE Healthcare). The mononuclear layer was collected and washed with PBS to remove platelets. Monocytes were purified by adherence to plastic in RPMI 1640 media supplemented with 5% heat-inactivated FBS, 2 mM glutamine, 100 mg/ml streptomycin, and 100 U/ml penicillin at 37˚C, 5% CO_2 for 1 h. Nonadherent cells were removed with PBS and adherent cells differentiated into macrophages with 20 ng/ml recombinant human GM-CSF (Miltenyi Biotec) for 7 d. This study was covered by the University of Birmingham's Science, Technology, Engineering, and Mathematics Ethical Review Committee.

Phagocytic challenge

Macrophages were serum starved for 2–16 h with serum-free medium at 37˚C, 5% CO_2. Where needed, inhibitors were added directly and left for a further 30 min. Next, media were removed prior to fresh serum-free medium being added containing either 1 μg/ml 18B7 Ab (against cryptococcal capsule) or unopsonized targets at a multiplicity of infection of either 10:1 or 20:1 for 20–180 min at 37˚C, 5% CO_2. Cells were washed three times with PBS to remove unbound yeast/bacteria cells and fixed in 4% paraformaldehyde for 10 min at room temperature (RT).

Galleria mellonella maintenance

Larvae of the greater wax moth, *Galleria mellonella*, were sourced from Livefoods Direct (U.K.) and stored in wood shavings in the dark at 13˚C. This study was covered by the University of Stirling's Animal Welfare and Ethical Review Body. Healthy larvae weighing between 0.2 and 0.4 g were used in all experiments. Larvae were inoculated with different concentrations of inhibitors via intrahemocele injection 1 h prior to infection with 1 million *C. neoformans* H99 per larva as described previously (11). Controls consisted of larvae that received a 20 μl PBS inoculum. Three to five larvae were used per treatment, with all treatments being performed on at least three independent occasions.

For phagocytosis, larvae were bled and hemolymph treated as previously described (12). Briefly, pooled hemolymph was mixed with 0.5 ml PBS and added onto a 13 mm coverslip in a 24-well plate. Hemocytes were centrifuged onto the coverslips for 10 min at 500 × *g* at RT before washing three times with PBS to remove noninternalized yeasts. Cells were then fixed with 4% paraformaldehyde before permeabilization and immunostained as described below. All determinations were performed on at least three independent occasions.

Immunofluorescence and scoring

Fixed cells on coverslips were permeabilized with 0.1% Triton X-100 for 5 min (if necessary to identify internalized yeasts), washed with PBS, and blocked with 0.5% BSA in PBS for 30 min. Appropriate primary Abs (1:200 dilution) were added to cells, left for 30 min at RT, washed with PBS, and counterstained with the appropriate fluorophore–conjugated secondary Ab, along with Rhodamine-Phalloidin and Calcofluor White. Coverslips were then washed in PBS and distilled water before mounted in ProLong Gold Antifade Reagent (Life Technologies) and analyzed by microscopy.

For counting of phagocytosed yeast/bacteria, fixed but unpermeabilized cells on coverslips were stained with Calcofluor White to highlight the external yeasts. Coverslips were analyzed with a Nikon Eclipse Ti microscope under a 63× oil immersion objective. Between 5 and 10 fields of view of each coverslip were counted for number of macrophages and association of microbial cells. At least 100 macrophages were observed for each coverslip.

The enrichment in phosphorylated Syk at sites of yeast binding and the translocation of p65 into the nucleus during NF-κB activation were studied and scored by the Nikon A1R confocal microscope using 20× to 63× objectives. For the former, a minimum of 25 infected cells per condition were analyzed for a discrete local enrichment in marker signal (Syk) at bound particles. For the latter, between three and five fields of view for each sample/coverslip were counted for the number of macrophages with p65 marker signal located within the nucleus and expressed as a percentage of the total number of macrophages (%NF-κB nuclear translocation).

In vitro cytokine production

J774.A1 and primary human macrophages were cultured in 96-well microtiter plates (Greiner) at 10,000 cells/well in a final volume of 200 μl. Cells were stimulated with either control medium, LPS, or a range of unopsonized pathogenic yeasts. After 6 h of incubation at 37˚C, plates were centrifuged (500 × *g* for 10 min), and the supernatant was collected and stored at −80˚C until cytokine assays were performed. Levels of TNF-α were determined by commercial ELISA kits, used according to the instructions of the manufacturer (R&D Systems).

Statistical analyses

Analysis carried out on the results described in this paper was by a generalized linear model using a Poisson error distribution in R (R Development Core Team). This was tested for significance using a post hoc Tukey honest significant difference (HSD) test.

Results

Uptake of nonopsonized Cryptococci via mannose receptor is activation dependent

As previously observed, the levels of nonopsonic uptake of Cryptococci is very low (e.g., 0.4% of *C. neoformans* serotype

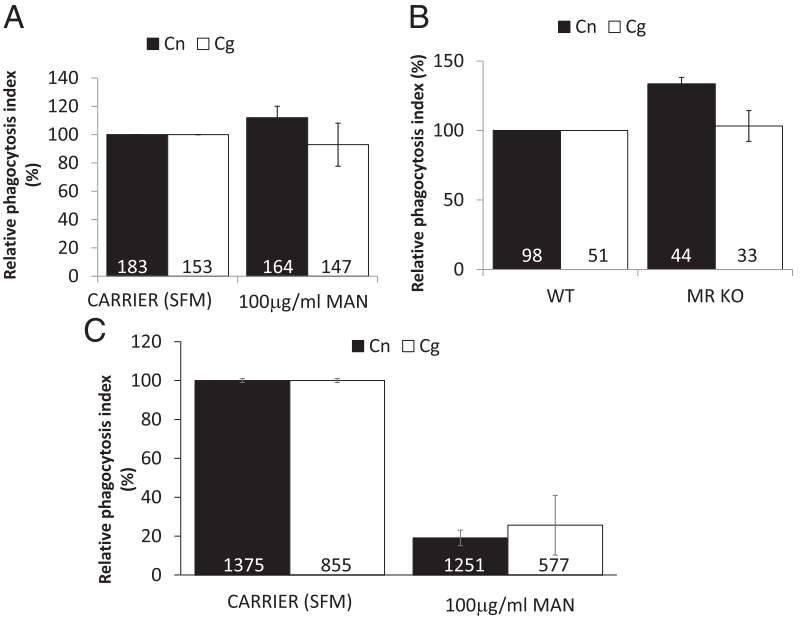

FIGURE 1. Mannose receptor is important but dispensable during uptake of *Cryptococcus* particles. Mouse macrophage cell line J774.A1 (**A**) or differentiated BMMs (**B**) (WT or MR KO) or differentiated primary human macrophages (**C**) were challenged with either *C. neoformans* H99 (Cn, black bars) or *C. gattii* R265 (Cg, white bars) for 60 min, processed for immunofluorescence, and scored for phagocytosis as described in *Materials and Methods*. Where indicated, J774.A1 and primary human macrophages were pretreated with 100 μg/ml mannan (MAN) for 30 min before the addition of *Cryptococcus* particles. Phagocytosis indices were related to the values obtained from the negative controls. Number in bars indicate the total number of phagocytes counted. Results are expressed as the mean ± SD of at least three independent experiments.

D was taken up by unstimulated mouse peritoneal macrophages; or 7–21% of *C. gattii* R265 was taken up by human dendritic cells (DCs); (13, 14)) and our results are in agreement with those findings – 8.89 or 5.83% of primary human macrophages contained one or more *C. neoformans* H99 or *C. gattii* R265, respectively (based on the carrier controls in Figs. 1C, 2B), after 2 h of incubation. The mannose receptor is broadly expressed on macrophages and important for the nonopsonic uptake of fungal pathogens such as *C. albicans* and *Pneumocystis carinii* (15, 16). The uptake of *C. neoformans* H99 or *C. gattii* R265 by J774.A1 macrophages pretreated with soluble mannan (a competitive inhibitor of mannose receptor binding) was unaltered relative to control (untreated) cells (Fig. 1A). Similarly, M-CSF differentiated bone marrow macrophages (BMMs) from mannose receptor KO mice (MR KO) showed no reduction in uptake of either *C. neoformans* or *C. gattii* relative to WT control cells (Fig. 1B). Interestingly, however, GM-CSF–differentiated primary human macrophages showed a strong inhibition of uptake under the same conditions (Fig. 1C), suggesting that the mannose receptor may play a greater role in cryptococcal uptake into human cells than those of mice.

Phagocytosis of unopsonized Cryptococci is Syk-dependent

The other major class of nonopsonic phagocytic receptors for fungi are the dectins (17). Both dectin-1 and dectin-2 require Syk activity for their function, via ITAMs contained within dectin-1 itself or via membrane association with ITAM–containing Fc receptor γ-chain in the case of dectin-2 (18). Inhibiting Syk activity in J774.A1 cells by using piceatannol (19) resulted in a marked reduction in their ability to phagocytose either *C. neoformans* H99 or *C. gattii* R265 (Fig. 2A, $p < 0.05$). The same observation was also seen in GM-CSF–differentiated primary human macrophages from pooled monocytes isolated from human volunteers (Fig. 2B). In line with this, staining with an anti–Phospho-Syk Ab showed intense accumulation of active Syk at phagocytic cups forming around nonopsonized Cryptococci (Fig. 3). This Ab was raised against the tyrosine phosphorylated residues at positions 525 and 526, located in the activation loop of the Syk kinase domain and essential for Syk function (20). Therefore, we propose that the localization of this Ab to the sites of nonopsonic uptake of Cryptococci and the activity of piceatannol in blocking uptake suggests that Syk activity is required for internalization.

Phagocytosis of unopsonized Cryptococci is partially dependent on Dectin-1

To test for a role for the dectin family of receptors during phagocytic uptake of nonopsonized *Cryptococci*, we first exposed J774.A1 macrophages (Fig. 4A) or differentiated primary human macrophages (Fig. 4B) to the dectin-1 inhibitor glucan-6-phosphate before challenging with either unopsonized *C. gattii* R265 or *C. neoformans* H99. This inhibitor

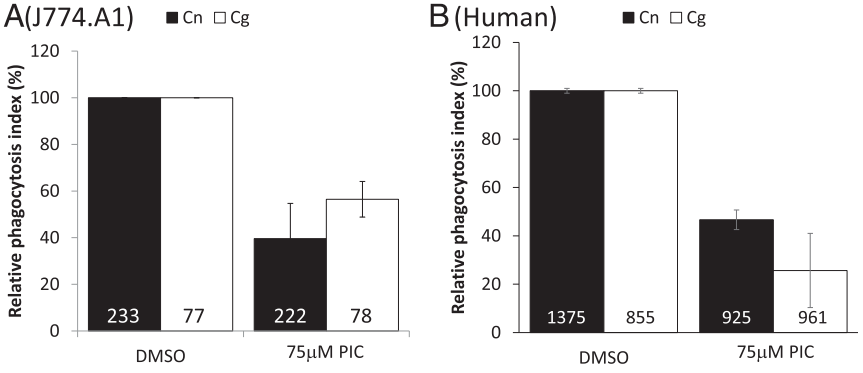

FIGURE 2. Uptake of *Cryptococcus* particles is Syk-dependent. Mouse macrophage cell line J774.A1 (**A**) or differentiated primary human macrophages (**B**) were challenged with unopsonized *C. neoformans* H99 (Cn, black bars) or *C. gattii* R265 (Cg, white bars) for 60 min, processed for immunofluorescence, and scored for phagocytosis as described in *Materials and Methods*. Phagocytosis indices were related to the values obtained from the negative controls. Number in bars indicate the total number of phagocytes counted. Results are expressed as the mean ± SD of at least three independent experiments.

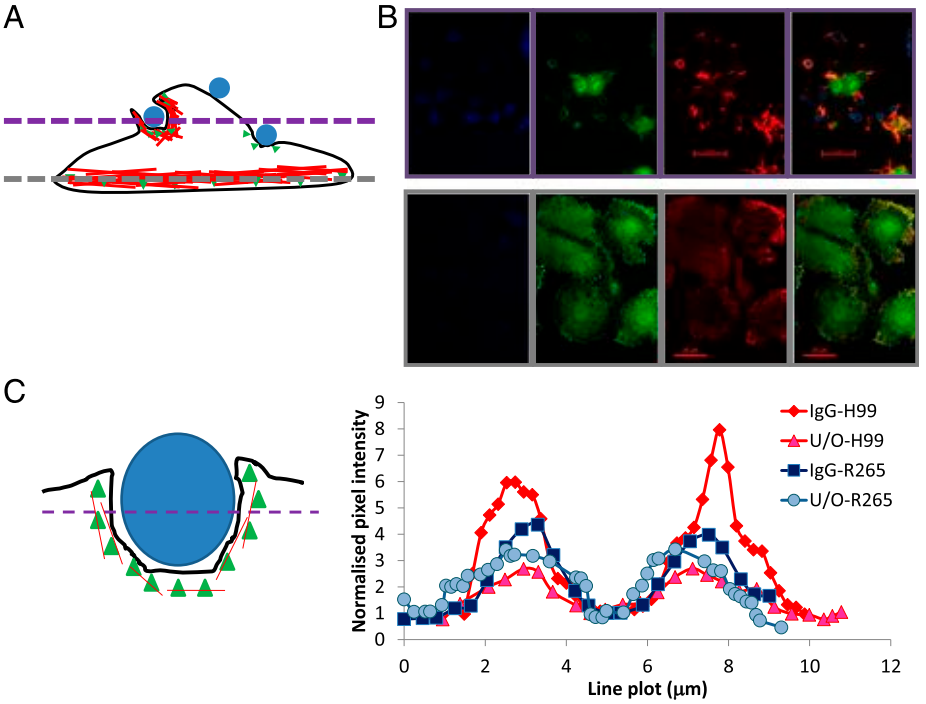

FIGURE 3. Activated Syk is essential for the uptake of *Cryptococcus* particles. Mouse macrophage cell line J774.A1 was challenged with either (IgG-opsonized or unopsonized, U/O) *C. neoformans* H99 or *C. gattii* R265 for 15 min (**B**), processed for immunofluorescence, and analyzed by confocal microscopy of localized phospho-Syk (B and **C**) as described in *Materials and Methods*. (**A**) Schematic diagram J774.A1 macrophage with intracellular actin cytoskeleton (red) and yeast particles (blue). To confirm phospho-Syk localization, the bottom of the cells was observed first [(A), grey dashed line and (B), bottom panels], before moving to the middle of the cells [(A), purple dashed line, (B), top panels]. Pixel intensities for 20 cells per sample were determined [(C), right] and normalized to the intensity at the center of the cell [(C), left]. (A and C) The green triangles denote phospho-Syk. The black line denotes the outline of a cell as imagined from the side (i.e., its *z*-axis). Results are expressed as the mean ± SD of at least three independent experiments. Scale bar, 20 μm.

partially blocked the uptake of both species of *Cryptococcus*, suggesting dectin-1 contributes toward Cryptococci uptake but is not the sole recognition receptor involved in this process (Fig. 4A, 4B). In line with this, M-CSF–differentiated BMMs from dectin-1 and dectin-2 KO mice both showed substantially impaired uptake of *C. neoformans* H99 – surprisingly, this was not the case for *C. gattii* R265 (Fig. 4C). This suggests either the presence of another Syk-dependent nonopsonic receptor or that both dectins are redundant with each other for *C. gattii*, but not *C. neoformans* uptake.

Nonopsonic uptake in the Galleria model

The greater wax moth, *G. mellonella*, is widely used as a model organism in the study of host–pathogen interactions with a variety of human pathogens (21). As with other insects, *G. mellonella* does not possess an adaptive immune system like mammals but possesses a complex innate immune system that includes phagocytic cells, termed hemocytes (22, 23). We therefore tested whether nonopsonic uptake of Cryptococci in *G. mellonella* showed similar receptor dependency as in mammalian cells by pretreating larvae for 1 h with soluble mannan, glucan-6-phosphate,

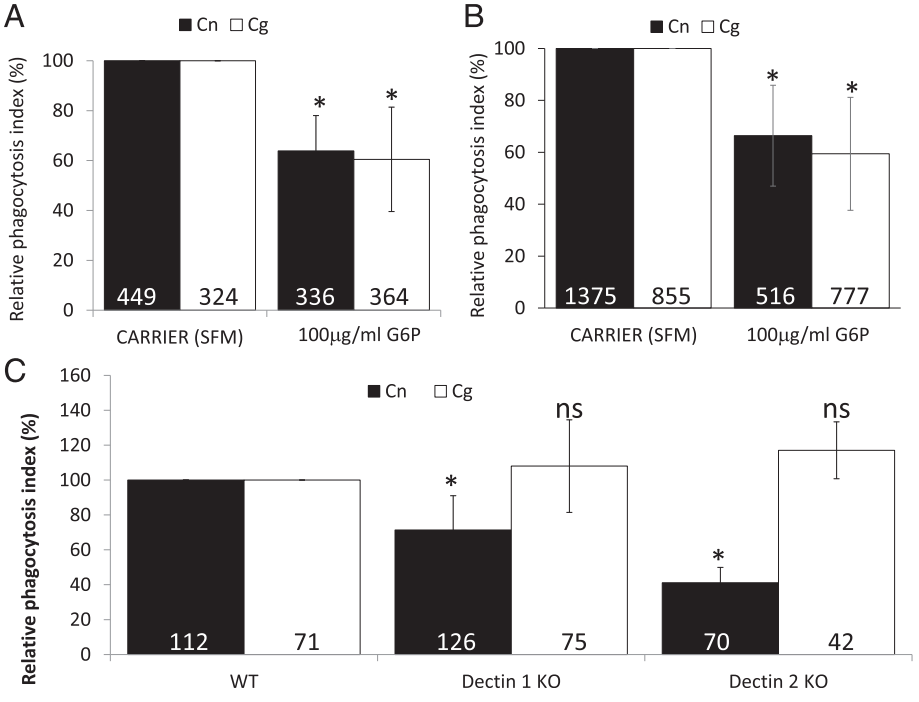

FIGURE 4. Dectins are required for uptake of *Cryptococcus* particles. Mouse macrophage cell line J774.A1 (**A**), differentiated primary human macrophages (**B**), or differentiated BMMs (**C**) (WT, Dectin-1 KO, or Dectin-2 KO) were challenged with either *C. neoformans* H99 (Cn, black bars) or *C. gattii* R265 (Cg, white bars) for 60 min, processed for immunofluorescence, and scored for phagocytosis as described in *Materials and Methods*. Where indicated, J774.A1 were pretreated with 100 μg/ml glucan-6-phosphate (G6P) for 30 min before the addition of *Cryptococcus* particles. Phagocytosis indices were related to the values obtained from the negative controls. Number in bars indicate the total number of phagocytes counted. Results are expressed as the mean ± SD of at least three independent experiments. $^*p < 0.05$. ns, not significant ($p \geq 0.05$).

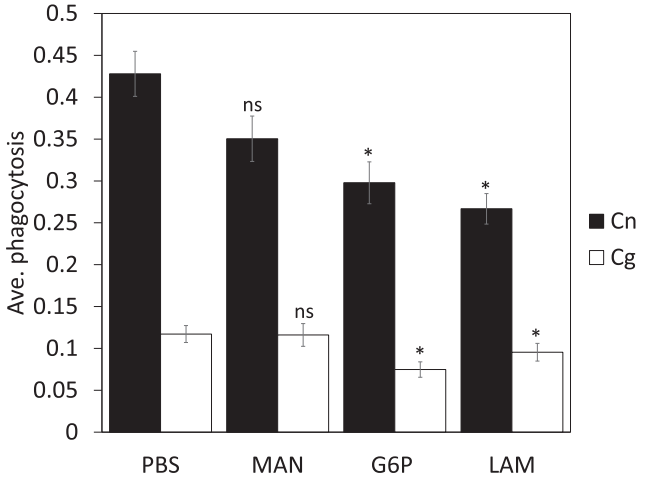

FIGURE 5. Administration of polysaccharides blocks uptake of *Cryptococcus* particles to hemocytes in the *G. mellonella* larvae model. Larvae were inoculated with 60 μg of blocking sugars 1 h prior to infection for 2 h with 10^6 *C. neoformans* H99 (black bars) or *C. gattii* R265 (white bars). Uptake of yeast of hemocytes was determined under light microscopy. Results are expressed as the mean ± SD of at least three independent experiments. *$p < 0.05$ (related to PBS control). ns, not significant ($p \geq 0.05$).

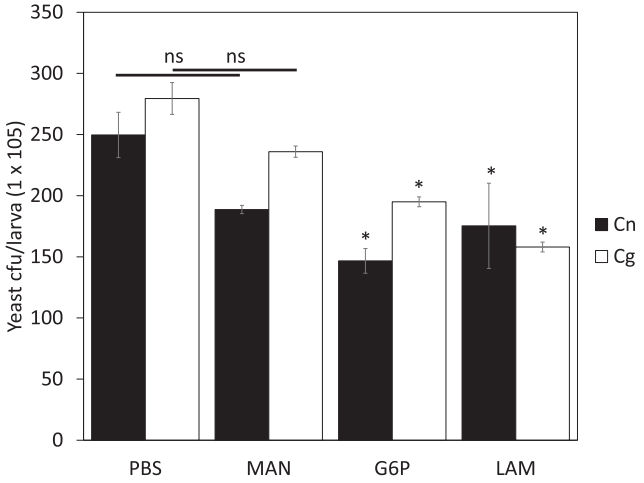

FIGURE 6. Glucan administration protects *G. mellonella* larvae from infection by *C. neoformans* or *C. gattii*. Larvae were inoculated with 60 μg of blocking sugars 24 h prior to infection for a further 24 h with 10^6 *C. neoformans* H99 (black bars) or *C. gattii* R265 (white bars). Fungal load was determined by serially diluting homogenized larvae and plating aliquots onto erythromycin containing agar plates. Yeast cell density were related to the values obtained from the negative (PBS) controls and expressed as cfu × 10^5/larva. Results are expressed as the mean ± SD of at least three independent experiments. *$p < 0.05$ (related to PBS control). ns, not significant ($p \geq 0.05$).

or laminarin. The full genome sequence of *Galleria* is currently available but not fully annotated (24). However, several β-1,3-glucan–binding protein analogs and C-type lectins have been characterized in this species, as well as other Lepidopterans, namely *Manduca sexta* (25, 26), *Bombyx mori* (27), and *Plodia interpunctella* (28). Recognition of fungal PAMPs (e.g., curdlan and mannan) by membrane-bound receptors modulate cellular (hemocyte)-directed immunity in insects (encapsulation, nodulation, and phagocytosis) (29). Although soluble mannan did not significantly reduce association of Cryptococci with *Galleria* hemocytes in data presented in this paper, both glucan-6-phosphate and laminarin led to a marked reduction in uptake (Fig. 5, $p < 0.001$ for both when compared to the PBS controls).

Interestingly, administering glucan-6-phosphate or laminarin for 24 h appeared to partially protect the insect larvae from infection by both unopsonized species of *Cryptococcus* (Fig. 6), suggesting that disease establishment in this model organism requires the fungus to grow intracellularly, something that has previously been proposed for human hosts (30).

Cryptococcal uptake by macrophages does not lead to increased proinflammatory cytokine secretion

Unlike many pathogens, internalization of opsonized Cryptococci into phagocytes is not accompanied by the production of proinflammatory cytokines such as TNF and IL-1α or IL-1β (31, 32). To test whether this is also true of nonopsonic uptake, we measured the secretion of TNF-α and nuclear translocation of p65 (a major regulator of cytokine transcription) from J774.A1 macrophages upon challenge with unopsonized or serum-opsonized *C. neoformans* H99 or *C. gattii* R265. Although LPS-stimulated macrophages showed strong nuclear translocation of p65, neither IgG-opsonized nor unopsonized *C. neoformans* H99 or *C. gattii* R265 stimulated NF-κB activation (Fig. 7A). However, NF-κB activation could be restored in cryptococcal exposed macrophages by the subsequent addition of LPS (Fig. 7B).

Furthermore, to test whether internalization of unopsonized Cryptococci into J774.A1 mouse macrophages or primary human macrophages elicits the production of proinflammatory cytokines such as TNF, we measured the secretion of TNF-α from J774.A1 macrophages or primary human macrophages upon challenge with unopsonized *C. neoformans* H99 or *C. gattii* R265, with *C. albicans* and LPS as controls. With J774.A1 mouse macrophage and primary human macrophages, *C. albicans*- or LPS-stimulated macrophages showed stronger TNF-α production compared to varying doses of *C. neoformans* H99 or *C. gattii* R265 (Fig. 8; $p = 0.04$ for *C. albicans* versus media control, $p > 0.05$ for *C. albicans* versus *C. neoformans*/*C. gattii*). Overall, this suggests that Cryptococci do not actively block inflammatory signaling in host cells and do not induce a strong inflammatory stimulus following nonopsonic uptake.

Discussion

In this study, we examined the phagocytic uptake of unopsonized cryptococcal yeast particles by macrophages. This process relies on the use of phagocytic receptors, which can be categorized either as opsonic or nonopsonic. Opsonic phagocytic receptors include the Fc receptor and complement receptor families, which recognize Ab- or complement-opsonized (coated) particles, respectively. Nonopsonic phagocytic receptors are PRRs, such as the C-type lectin family of receptors, which recognize distinct PAMPs on the fungal surface (33).

Although phagocytosis of *Cryptococcus* within the circulatory system would occur predominantly through an opsonized (coated) uptake route because of the presence of Abs and/or complement proteins found in serum, this is not always the case. For example, the first encounter of the human body with *Cryptococcus* is through the lungs when desiccated yeast cells or spores are breathed in. These cryptococcal particles encounter their initial immunological challenge through resident alveolar macrophages and DCs in a serum-deficient or low-serum environment (34–36). Interestingly, it was reported recently that between 25 and 40% of mouse lung-resident macrophages are able to phagocytose *C. neoformans* particles through a scavenger receptor pathway (37). Therefore, this confirms that initial uptake of *Cryptococcus*

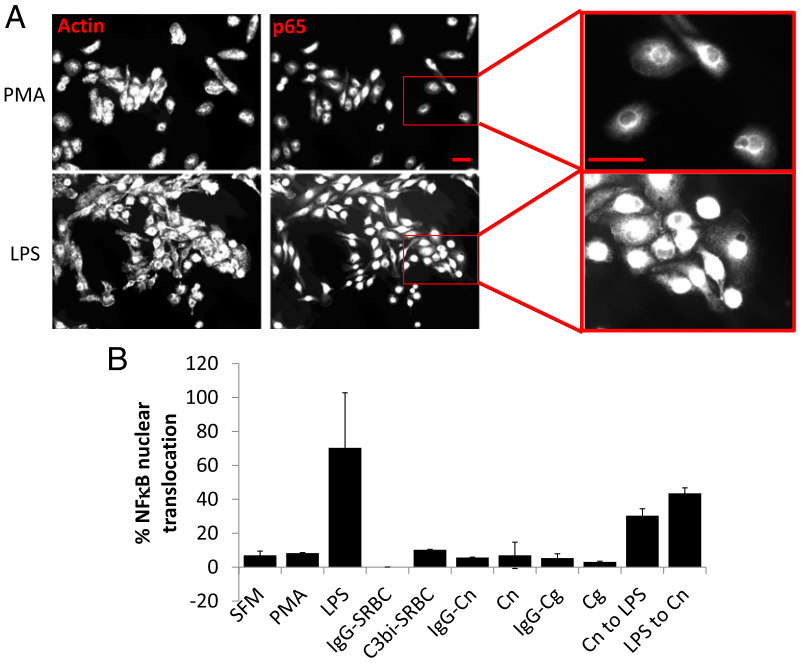

FIGURE 7. Uptake of *Cryptococcus* did not affect NF-κB nuclear translocation. J774.A1 macrophages were challenged with a variety of opsonized or unopsonized pathogenic fungi, SRBCs, or soluble agonists (LPS or PMA), processed for immunofluorescences, analyzed by microscopy (**A**), and scored for p65 nuclear translocation (**B**), as described in *Materials and Methods*. (A) Representative images of PMA- (top) or LPS- (bottom) stimulated J774.A1 macrophages and stained to highlight either actin or p65. Actin was stained using rhodamine-phalloidin; p65 was stained using the anti–65 kDa subunit (p65) NFκB mAb with an anti-rabbit Alexa Fluor–488. Scale bar, 20 μm.

by macrophages is most likely through a nonopsonized route, and there is a need to understand the mechanisms that underpin this process (6). We confirmed that, compared with the bacterium *E. coli* or fungus *C. albicans*, Cryptococci cells are not readily taken up by mammalian macrophages, most likely because of the presence of the capsule, which renders Cryptococci antiphagocytic (38, 39). By using a combination of a soluble mannose inhibitor and MR KO tissue, we demonstrated that mannose receptor was not necessary for the uptake of either species of *Cryptococcus*, in line with recent data from the zebrafish model (40), although this is not the case in primary human macrophages. We note that others have shown MR KO mice to be more susceptible to *C. neoformans* (41) and demonstrated a role for this receptor, along with FcγRII (CD32) in driving cryptococcal uptake into DCs (42). Thus, mannose receptor dependency apparently varies across different cell types and tissue contexts.

Next, we pursued a different set of nonopsonic PRRs, dectin-1 and dectin-2, which are C-type lectin receptors that are highly expressed in macrophages and are key β-glucan receptors (43, 44). Recognition of soluble or surface expressed β-glucans on yeasts is sufficient to initiate and mediate phagocytosis and proinflammatory cytokine responses (45). Both of these receptors require Syk activity (18, 46, 47), and, indeed, our data clearly demonstrate the activation of Syk at phagocytic cups containing unopsonized Cryptococci, as well as a strong dependency on Syk for particle uptake. Interestingly, pharmacological inhibition of dectins inhibited uptake of both *C. neoformans* and *C. gattii* in J774.A1 mouse and human macrophages, but BMMs from dectin-1– and dectin-2–KO mice showed defects only in the uptake of *C. neoformans* and not *C. gattii*, an effect that has been observed before (48). The most parsimonious explanation is therefore that the two dectin receptors are redundant for the uptake of *C. gattii*, but not *C. neoformans*, perhaps reflecting differing surface components between the two species, as reported recently (49). Such surface variation between species, strains, and potentially developmental stages of Cryptococci may explain many of the previous inconsistencies in the literature regarding dectin dependency (or otherwise) (50, 51).

Alongside mouse macrophages, we adopted wax worm larvae (*G. mellonella*) as an alternative model for understanding cryptococcal virulence and host immune responses (52–54) in which cryptococcal phagocytosis has previously been reported (55). Our data demonstrate striking similarities in patterns of uptake between this invertebrate host and murine phagocytes. In addition, we showed that inhibiting phagocytosis in this alternative host reduces disease burden, highlighting the importance of host phagocytes as a niche for cryptococcal replication.

We acknowledge that although there are currently no direct dectin receptor homologs identified in *G. mellonella*, many C-type lectins have been characterized in other insect models, for example; the tobacco hornworm, *Manduca sexta* (immulectin-2 facilitates phagocytosis of bacteria (56)); webworm, *Hyphantria cunea* (lectin (57, 58)); silkworm, *Bombyx mori* (BmLBP and BmMBP (59, 60)); and the cockroach, *Blaberus discoidalis* (a β-glucan–specific lectin (61)). These invertebrate C-type lectins

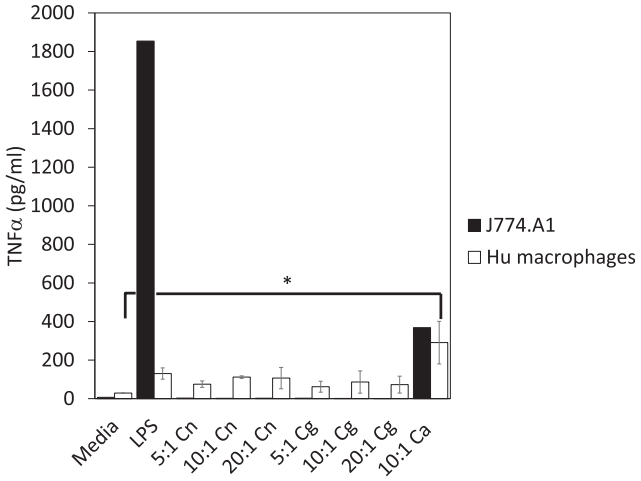

FIGURE 8. Uptake of *Cryptococcus* did not affect proinflammatory cytokine response. J774.A1 macrophages (black bars) or differentiated primary human macrophages (white bars) were challenged with a variety of unopsonized pathogenic fungi (*C. neoformans*, Cn; *C. gattii*. Cg; *Candida albicans*, Ca) or LPS, and subsequent supernatants were analyzed by ELISA, as described in *Materials and Methods*. Results are expressed as the mean ± SD of at least three independent experiments. $*p < 0.05$.

show up to 35% similarity with mammalian C-type lectins and can bind to several PAMPs, including LPS, lipoteichoic acid, and β-glucan and are inducible when the host is exposed to microbial challenge or ligands and the mechanisms for uptake of pathogenic microbes by *G. mellonella* hemocytes are similar to that of human neutrophils (62).

Two key reports have shown that there are at least three scavenger receptors involved in the recognition of different serotypes of *Cryptococcus neoformans*, namely the homologous genes from the nematode *Caenorhabditis elegans*, CED-1 and C03F11.3, as well as the mouse MARCO scavenger receptors (37, 63). Interestingly, knocking out MARCO gene from mice did not abolish uptake of *C. neoformans* by lung-resident mononuclear phagocytes (37), suggesting a role or roles for the extent and distribution of multiple receptors and ligands on the surface of both host cell and yeast.

Finally, we demonstrate that entry of *Cryptococcus* does not affect NF-κB nuclear translocation and its subsequent TNF-α release in the Dectin-1/Syk/NF-κB signaling axis—both in J774. A1 mouse macrophages and in primary human macrophages. Although it is known that Dectin-1 coupling to Syk leads to downstream activation of NF-κB, which coordinates the transcription of innate response genes, including expression of proinflammatory cytokines such as TNF-α (64–66), this appears not to be the case for cryptococcal uptake.

In conclusion, we propose that unopsonized Cryptococci are recognized and engulfed via mannose receptor- or dectin-based recognition in vitro depending on the activation state of the host cells. The absence of an associated proinflammatory cascade allows the yeast to exploit this intracellular niche for rapid disease establishment.

Acknowledgments

We thank Neil Hotchin, Yotis Senis, David Williams, and Arturo Casadevall for sharing reagents and members of the Krachler/Voelz/Hall/May laboratory for helpful scientific discussions as well as Charles Eliot Timothy Paine for assistance with statistical analysis. J.L. thanks the Lim family for help and support during the writing of this manuscript.

Disclosures

The authors have no financial conflicts of interest.

References

1. Idnurm, A., Y. S. Bahn, K. Nielsen, X. Lin, J. A. Fraser, and J. Heitman. 2005. Deciphering the model pathogenic fungus *Cryptococcus neoformans. Nat. Rev. Microbiol.* 3: 753–764.
2. Steenbergen, J. N., H. A. Shuman, and A. Casadevall. 2001. *Cryptococcus neoformans* interactions with amoebae suggest an explanation for its virulence and intracellular pathogenic strategy in macrophages. *Proc. Natl. Acad. Sci. USA* 98: 15245–15250.
3. Feldmesser, M., S. Tucker, and A. Casadevall. 2001. Intracellular parasitism of macrophages by *Cryptococcus neoformans. Trends Microbiol.* 9: 273–278.
4. Fan, W., P. R. Kraus, M. J. Boily, and J. Heitman. 2005. *Cryptococcus neoformans* gene expression during murine macrophage infection. *Eukaryot. Cell* 4: 1420–1433.
5. Flannagan, R. S., V. Jaumouillé, and S. Grinstein. 2012. The cell biology of phagocytosis. *Annu. Rev. Pathol.* 7: 61–98.
6. Walenkamp, A. M., J. Scharringa, F. M. Schramel, F. E. Coenjaerts, and I. M. Hoepelman. 2000. Quantitative analysis of phagocytosis of *Cryptococcus neoformans* by adherent phagocytic cells by fluorescence multi-well plate reader. *J. Microbiol. Methods* 40: 39–45.
7. Johnston, S. A., and R. C. May. 2013. *Cryptococcus* interactions with macrophages: evasion and manipulation of the phagosome by a fungal pathogen. *Cell. Microbiol.* 15: 403–411.
8. Taylor, P. R., S. V. Tsoni, J. A. Willment, K. M. Dennehy, M. Rosas, H. Findon, K. Haynes, C. Steele, M. Botto, S. Gordon, and G. D. Brown. 2007. Dectin-1 is required for beta-glucan recognition and control of fungal infection. *Nat. Immunol.* 8: 31–38.
9. Ifrim, D. C., J. M. Bain, D. M. Reid, M. Oosting, I. Verschueren, N. A. Gow, J. H. van Krieken, G. D. Brown, B. J. Kullberg, L. A. Joosten, et al. 2014. Role of Dectin-2 for host defense against systemic infection with Candida glabrata. *Infect. Immun.* 82: 1064–1073.
10. Caron, E., and A. Hall. 1998. Identification of two distinct mechanisms of phagocytosis controlled by different Rho GTPases. *Science* 282: 1717–1721.
11. Mowlds, P., C. Coates, J. Renwick, and K. Kavanagh. 2010. Dose-dependent cellular and humoral responses in Galleria mellonella larvae following beta-glucan inoculation. *Microbes Infect.* 12: 146–153.
12. Harding, C. R., G. N. Schroeder, J. W. Collins, and G. Frankel. 2013. Use of Galleria mellonella as a model organism to study *Legionella pneumophila* infection. *J. Vis. Exp.* 81: e50964.
13. Kozel, T. R., and E. C. Gotschlich. 1982. The capsule of *cryptococcus neoformans* passively inhibits phagocytosis of the yeast by macrophages. *J. Immunol.* 129: 1675–1680.
14. Huston, S. M., P. Ngamskulrungroj, R. F. Xiang, H. Ogbomo, D. Stack, S. S. Li, M. Timm-McCann, S. K. Kyei, P. Oykhman, K. J. Kwon-Chung, and C. H. Mody. 2016. *Cryptococcus* gattii capsule blocks surface recognition required for dendritic cell maturation independent of internalization and antigen processing. *J. Immunol.* 196: 1259–1271.
15. Porcaro, I., M. Vidal, S. Jouvert, P. D. Stahl, and J. Giaimis. 2003. Mannose receptor contribution to *Candida albicans* phagocytosis by murine E-clone J774 macrophages. *J. Leukoc. Biol.* 74: 206–215.
16. Ezekowitz, R. A., D. J. Williams, H. Koziel, M. Y. Armstrong, A. Warner, F. F. Richards, and R. M. Rose. 1991. Uptake of *Pneumocystis carinii* mediated by the macrophage mannose receptor. *Nature* 351: 155–158.
17. Drummond, R. A., and G. D. Brown. 2011. The role of Dectin-1 in the host defence against fungal infections. *Curr. Opin. Microbiol.* 14: 392–399.
18. Saijo, S., and Y. Iwakura. 2011. Dectin-1 and Dectin-2 in innate immunity against fungi. *Int. Immunol.* 23: 467–472.
19. Oliver, J. M., D. L. Burg, B. S. Wilson, J. L. McLaughlin, and R. L. Geahlen. 1994. Inhibition of mast cell Fc epsilon R1-mediated signaling and effector function by the Syk-selective inhibitor, piceatannol. *J. Biol. Chem.* 269: 29697–29703.
20. Zhang, J., M. L. Billingsley, R. L. Kincaid, and R. P. Siraganian. 2000. Phosphorylation of Syk activation loop tyrosines is essential for Syk function. An in vivo study using a specific anti-Syk activation loop phosphotyrosine antibody. *J. Biol. Chem.* 275: 35442–35447.
21. Desbois, A. P., and S. McMillan. 2015. Paving the way to acceptance of Galleria mellonella as a new model insect. *Virulence* 6: 410–411.
22. Butt, T. M., C. J. Coates, I. M. Dubovskiy, and N. A. Ratcliffe. 2016. Entomopathogenic fungi: new insights into host-pathogen interactions. *Adv. Genet.* 94: 307–364.
23. Mukherjee, K., R. Raju, R. Fischer, and A. Vilcinskas. 2013. Galleria mellonella as a model host to study gut microbe homeostasis and brain infection by the human pathogen listeria monocytogenes. *Adv. Biochem. Eng. Biotechnol.* 135: 27–39.
24. Lange, A., S. Beier, D. H. Huson, R. Parusel, F. Iglauer, and J. S. Frick. 2018. Genome sequence of *Galleria mellonella* (Greater Wax Moth). *Genome Announc.* 6: e01220-17.
25. Yu, X. Q., H. Gan, and M. R. Kanost. 1999. Immulectin, an inducible C-type lectin from an insect, *Manduca sexta*, stimulates activation of plasma prophenol oxidase. *Insect Biochem. Mol. Biol.* 29: 585–597.
26. Ma, C., and M. R. Kanost. 2000. A beta1,3-glucan recognition protein from an insect, *Manduca sexta*, agglutinates microorganisms and activates the phenoloxidase cascade. *J. Biol. Chem.* 275: 7505–7514.
27. Ochiai, M., and M. Ashida. 2000. A pattern-recognition protein for beta-1,3-glucan. The binding domain and the cDNA cloning of beta-1,3-glucan recognition protein from the silkworm, *Bombyx mori. J. Biol. Chem.* 275: 4995–5002.
28. Fabrick, J. A., J. E. Baker, and M. R. Kanost. 2003. cDNA cloning, purification, properties, and function of a beta-1,3-glucan recognition protein from a pyralid moth, Plodia interpunctella. *Insect Biochem. Mol. Biol.* 33: 579–594.
29. Whitten, M. M., I. F. Tew, B. L. Lee, and N. A. Ratcliffe. 2004. A novel role for an insect apolipoprotein (apolipophorin III) in beta-1,3-glucan pattern recognition and cellular encapsulation reactions. *J. Immunol.* 172: 2177–2185.
30. Alvarez, M., T. Burn, Y. Luo, L. A. Pirofski, and A. Casadevall. 2009. The outcome of *Cryptococcus neoformans* intracellular pathogenesis in human monocytes. *BMC Microbiol.* 9: 51.
31. Cross, C. E., and G. J. Bancroft. 1995. Ingestion of acapsular *Cryptococcus neoformans* occurs via mannose and beta-glucan receptors, resulting in cytokine production and increased phagocytosis of the encapsulated form. *Infect. Immun.* 63: 2604–2611.
32. Netea, M. G., R. J. Stuyt, S. H. Kim, J. W. Van der Meer, B. J. Kullberg, and C. A. Dinarello. 2002. The role of endogenous interleukin (IL)-18, IL-12, IL-1beta, and tumor necrosis factor-alpha in the production of interferon-gamma induced by *Candida albicans* in human whole-blood cultures. *J. Infect. Dis.* 185: 963–970.
33. Goodridge, H. S., A. J. Wolf, and D. M. Underhill. 2009. Beta-glucan recognition by the innate immune system. *Immunol. Rev.* 230: 38–50.
34. Lee, S. C., Y. Kress, M. L. Zhao, D. W. Dickson, and A. Casadevall. 1995. *Cryptococcus neoformans* survive and replicate in human microglia. *Lab. Invest.* 73: 871–879.
35. Feldmesser, M., Y. Kress, P. Novikoff, and A. Casadevall. 2000. *Cryptococcus neoformans* is a facultative intracellular pathogen in murine pulmonary infection. *Infect. Immun.* 68: 4225–4237.
36. Velagapudi, R., Y. P. Hsueh, S. Geunes-Boyer, J. R. Wright, and J. Heitman. 2009. Spores as infectious propagules of *Cryptococcus neoformans. Infect. Immun.* 77: 4345–4355.
37. Xu, J., A. Flaczyk, L. M. Neal, Z. Fa, A. J. Eastman, A. N. Malachowski, D. Cheng, B. B. Moore, J. L. Curtis, J. J. Osterholzer, and M. A. Olszewski.

2017. Scavenger receptor MARCO orchestrates early defenses and contributes to fungal containment during cryptococcal infection. *J. Immunol.* 198: 3548–3557.
38. Levitz, S. M., and D. J. DiBenedetto. 1989. Paradoxical role of capsule in murine bronchoalveolar macrophage-mediated killing of *Cryptococcus neoformans. J. Immunol.* 142: 659–665.
39. Del Poeta, M. 2004. Role of phagocytosis in the virulence of *Cryptococcus neoformans. Eukaryot. Cell* 3: 1067–1075.
40. Bojarczuk, A., K. A. Miller, R. Hotham, A. Lewis, N. V. Ogryzko, A. A. Kamuyango, H. Frost, R. H. Gibson, E. Stillman, R. C. May, et al. 2016. *Cryptococcus neoformans* intracellular proliferation and capsule size determines early macrophage control of infection. *Sci. Rep.* 6: 21489.
41. Dan, J. M., R. M. Kelly, C. K. Lee, and S. M. Levitz. 2008. Role of the mannose receptor in a murine model of *Cryptococcus neoformans* infection. *Infect. Immun.* 76: 2362–2367.
42. Syme, R. M., J. C. Spurrell, E. K. Amankwah, F. H. Green, and C. H. Mody. 2002. Primary dendritic cells phagocytose *Cryptococcus neoformans* via mannose receptors and Fcgamma receptor II for presentation to T lymphocytes. *Infect. Immun.* 70: 5972–5981.
43. Brown, G. D., P. R. Taylor, D. M. Reid, J. A. Willment, D. L. Williams, L. Martinez-Pomares, S. Y. Wong, and S. Gordon. 2002. Dectin-1 is a major beta-glucan receptor on macrophages. *J. Exp. Med.* 196: 407–412.
44. Kerscher, B., J. A. Willment, and G. D. Brown. 2013. The Dectin-2 family of C-type lectin-like receptors: an update. *Int. Immunol.* 25: 271–277.
45. Brown, G. D. 2006. Dectin-1: a signalling non-TLR pattern-recognition receptor. *Nat. Rev. Immunol.* 6: 33–43.
46. Rogers, N. C., E. C. Slack, A. D. Edwards, M. A. Nolte, O. Schulz, E. Schweighoffer, D. L. Williams, S. Gordon, V. L. Tybulewicz, G. D. Brown, and C. Reis e Sousa. 2005. Syk-dependent cytokine induction by Dectin-1 reveals a novel pattern recognition pathway for C type lectins. *Immunity* 22: 507–517.
47. Underhill, D. M., E. Rossnagle, C. A. Lowell, and R. M. Simmons. 2005. Dectin-1 activates Syk tyrosine kinase in a dynamic subset of macrophages for reactive oxygen production. *Blood* 106: 2543–2550.
48. Nakamura, K., T. Kinjo, S. Saijo, A. Miyazato, Y. Adachi, N. Ohno, J. Fujita, M. Kaku, Y. Iwakura, and K. Kawakami. 2007. Dectin-1 is not required for the host defense to *Cryptococcus neoformans. Microbiol. Immunol.* 51: 1115–1119.
49. Benaducci, T., J. C. Sardi, N. M. Lourencetti, L. Scorzoni, F. P. Gullo, S. A. Rossi, J. B. Derissi, M. C. de Azevedo Prata, A. M. Fusco-Almeida, and M. J. Mendes-Giannini. 2016. Virulence of *Cryptococcus* sp. biofilms in vitro and in vivo using Galleria mellonella as an alternative model. *Front. Microbiol.* 7: 290.
50. Giles, S. S., T. R. Dagenais, M. R. Botts, N. P. Keller, and C. M. Hull. 2009. Elucidating the pathogenesis of spores from the human fungal pathogen *Cryptococcus neoformans. Infect. Immun.* 77: 3491–3500.
51. Walsh, N. M., M. Wuthrich, H. Wang, B. Klein, and C. M. Hull. 2017. Characterization of C-type lectins reveals an unexpectedly limited interaction between *Cryptococcus neoformans* spores and Dectin-1. *PLoS One* 12: e0173866.
52. Firacative, C., S. Duan, and W. Meyer. 2014. Galleria mellonella model identifies highly virulent strains among all major molecular types of *Cryptococcus* gattii. *PLoS One* 9: e105076.
53. Eisenman, H. C., R. Duong, H. Chan, R. Tsue, and E. E. McClelland. 2014. Reduced virulence of melanized *Cryptococcus neoformans* in Galleria mellonella. *Virulence* 5: 611–618.
54. Mylonakis, E., R. Moreno, J. B. El Khoury, A. Idnurm, J. Heitman, S. B. Calderwood, F. M. Ausubel, and A. Diener. 2005. Galleria mellonella as a model system to study *Cryptococcus neoformans* pathogenesis. *Infect. Immun.* 73: 3842–3850.
55. García-Rodas, R., A. Casadevall, J. L. Rodríguez-Tudela, M. Cuenca-Estrella, and O. Zaragoza. 2011. *Cryptococcus neoformans* capsular enlargement and cellular gigantism during Galleria mellonella infection. *PLoS One* 6: e24485.
56. Yu, X. Q., and M. R. Kanost. 2004. Immulectin-2, a pattern recognition receptor that stimulates hemocyte encapsulation and melanization in the tobacco hornworm, *Manduca sexta. Dev. Comp. Immunol.* 28: 891–900.
57. Shin, S. W., D. S. Park, S. C. Kim, and H. Y. Park. 2000. Two carbohydrate recognition domains of Hyphantria cunea lectin bind to bacterial lipopolysaccharides through O-specific chain. *FEBS Lett.* 467: 70–74.
58. Shin, S. W., S. S. Park, D. S. Park, M. G. Kim, S. C. Kim, P. T. Brey, and H. Y. Park. 1998. Isolation and characterization of immune-related genes from the fall webworm, Hyphantria cunea, using PCR-based differential display and subtractive cloning. *Insect Biochem. Mol. Biol.* 28: 827–837.
59. Koizumi, N., M. Imamura, T. Kadotani, K. Yaoi, H. Iwahana, and R. Sato. 1999. The lipopolysaccharide-binding protein participating in hemocyte nodule formation in the silkworm *Bombyx mori* is a novel member of the C-type lectin superfamily with two different tandem carbohydrate-recognition domains. *FEBS Lett.* 443: 139–143.
60. Watanabe, A., S. Miyazawa, M. Kitami, H. Tabunoki, K. Ueda, and R. Sato. 2006. Characterization of a novel C-type lectin, *Bombyx mori* multibinding protein, from the B. mori hemolymph: mechanism of wide-range microorganism recognition and role in immunity. *J. Immunol.* 177: 4594–4604.
61. Chen, C., A. F. Rowley, R. P. Newton, and N. A. Ratcliffe. 1999. Identification, purification and properties of a beta-1,3-glucan-specific lectin from the serum of the cockroach, Blaberus discoidalis which is implicated in immune defence reactions. *Comp. Biochem. Physiol. B Biochem. Mol. Biol.* 122: 309–319.
62. Browne, N., M. Heelan, and K. Kavanagh. 2013. An analysis of the structural and functional similarities of insect hemocytes and mammalian phagocytes. *Virulence* 4: 597–603.
63. Means, T. K., E. Mylonakis, E. Tampakakis, R. A. Colvin, E. Seung, L. Puckett, M. F. Tai, C. R. Stewart, R. Pukkila-Worley, S. E. Hickman, et al. 2009. Evolutionarily conserved recognition and innate immunity to fungal pathogens by the scavenger receptors SCARF1 and CD36. *J. Exp. Med.* 206: 637–653.
64. Gross, O., A. Gewies, K. Finger, M. Schäfer, T. Sparwasser, C. Peschel, I. Förster, and J. Ruland. 2006. Card9 controls a non-TLR signalling pathway for innate anti-fungal immunity. *Nature* 442: 651–656.
65. Goodridge, H. S., R. M. Simmons, and D. M. Underhill. 2007. Dectin-1 stimulation by *Candida albicans* yeast or zymosan triggers NFAT activation in macrophages and dendritic cells. *J. Immunol.* 178: 3107–3115.
66. LeibundGut-Landmann, S., O. Gross, M. J. Robinson, F. Osorio, E. C. Slack, S. V. Tsoni, E. Schweighoffer, V. Tybulewicz, G. D. Brown, J. Ruland, and C. Reis e Sousa. 2007. Syk- and CARD9-dependent coupling of innate immunity to the induction of T helper cells that produce interleukin 17. *Nat. Immunol.* 8: 630–638.

Viral infection enhances vomocytosis of intracellular fungi via Type I interferons

*Paula I Seoane[1], Leanne M. Taylor-Smith[1], David Stirling[2], Lucy C. K. Bell[2], Mahdad Noursadeghi[2], Dalan Bailey[3], Robin C. May[1]**

[1]Institute of Microbiology & Infection and School of Biosciences, University of Birmingham, Edgbaston, Birmingham, B15 2TT, UK

[2]Division of Infection and Immunity, University College London, Gower Street, London WC1E 6BT, UK

[3]The Pirbright Institute, Ash Rd, Surrey, GU24 0NF, UK

**Correspondence to: r.c.may@bham.ac.uk*

Abstract

Cryptococcus neoformans is an opportunistic human pathogen, which causes serious disease in immunocompromised hosts. Infection with this pathogen is particularly relevant in HIV^+ patients, where it leads to around 200,000 deaths *per annum*. A key feature of cryptococcal pathogenesis is the ability of the fungus to survive and replicate within the phagosome of macrophages, as well as its ability to escape via a novel non-lytic mechanism known as vomocytosis. We have been exploring whether viral infection affects the interaction between *C. neoformans* and macrophages. Here we show that viral infection enhances cryptococcal vomocytosis without altering phagocytosis or intracellular proliferation of the fungus. This effect occurs with distinct, unrelated human viral pathogens and is recapitulated when macrophages are stimulated with the anti-viral cytokine interferon alpha (IFNα). Importantly, the effect is abrogated when type-I interferon signalling is blocked, thus underscoring the

26 importance of type-I interferons in this phenomenon. Our results highlight the importance of
27 incorporating specific context cues while studying host-pathogen interactions. By doing so, we
28 found that acute viral infection may trigger the release of latent cryptococci from intracellular
29 compartments, with significant consequences for disease progression.

30

31 **Non-Technical Author Summary**

32 Infectious diseases are typically studied in the laboratory in isolation, but in real life people
33 often encounter multiple infections simultaneously. Here we investigate how the innate
34 immune response to the fatal fungus *Cryptococcus neoformans* is influenced by viral
35 coinfection. Whilst virally-infected macrophages retain a normal capacity to engulf and kill
36 Cryptococci, they demonstrate a dramatically enhanced propensity to expel them via the
37 process known as non-lytic expulsion or vomocytosis. Activation of vomocytosis is
38 independent of the type of virus encountered, since both HIV and measles (two entirely
39 unrelated viral pathogens) trigger the same effect. Instead it is driven by interferon-α, a generic
40 'antiviral' response, which signals back to the infected macrophage, triggering expulsion of the
41 fungus. We propose that this hitherto unobserved phenomenon represents a 'reprioritisation'
42 pathway for innate immune cells, by which they can alter the frequency with which they expel
43 one pathogen (*Cryptococcus*) depending on the level of threat from a secondary viral infection.

44

Introduction

Since their discovery in 1957 by Isaacs and Lindenmann (1), the antiviral effects of type I interferons have been well documented (2-4). More recently, their roles in non-viral infections have been investigated (5, 6). Different bacterial stimuli have been shown to elicit type I interferon production, and in turn these so called "antiviral cytokines" play a role in the outcome of bacterial infections (7-9). This stems in part from the complex and sometimes contradictory effects that type I interferons have on host cells, for instance in enhancing inflammatory responses in some infectious settings (6) to preventing hyperinflammation in others (10, 11), and even affecting the priming of immune responses at lymph nodes (12).

To date, little is known about the interplay between type I interferons and fungal infections, despite the fact that many life-threatening fungal infections occur in the context of chronic viral infection. This is particularly true of *Cryptococcus neoformans,* a globally distributed opportunistic pathogen that is responsible for nearly 200,000 deaths per year in human immunodeficiency virus (HIV) infected people, where it causes cryptococcal meningitis (13). Extensive work over many years has demonstrated that a key feature of cryptococcal pathogenesis is the ability of the fungus to survive, proliferate within, and then escape from, host macrophages (14-17). Macrophages are among the first immune cells to encounter the fungus within the human host (18) , and thus are very important in the fight against this pathogen. These cells are able to phagocytose and contain the threat, as happens in immunocompetent hosts, but can also by hijacked by Cryptococcal cells and used as a "Trojan horse" to disseminate to distal sites within the body, particularly to the central nervous system (19). Engulfed Cryptococcal cells can escape from host macrophages through lytic or non-lytic mechanisms, the latter being known as vomocytosis or non-lytic extrusion (20, 21). Most

70 studies to date have focused on the interaction of Cryptococcus with healthy host cells, and
71 consequently how this intracellular lifestyle may be impacted by viral coinfection remains
72 unknown.
73
74 Here we show that viral infections enhance vomocytosis of Cryptococci from infected
75 macrophages, without affecting phagocytosis or intracellular proliferation rate of the fungus.
76 This effect is lost when signalling through the type I interferon receptor is blocked, and can be
77 recapitulated by addition of exogenous IFNα. Thus, antiviral responses by the host have a
78 hitherto unexpected impact on the release of intracellular pathogens by vomocytosis.

Materials and Methods

All reagents were purchased from SIGMA unless otherwise stated.

Cryptococcus Strains

Cryptococcal strains were grown in Yeast Peptone Dextrose (YPD) broth (2% glucose, 1% peptone and 1% yeast extract) at 25°C on a rotator (20 rpm). Yeast from overnight cultures were centrifuged at 6500 rpm for 2 minutes and resuspended in PBS at the required concentration. All experiments were carried out using *C. neoformans var. grubii* serotype A strain Kn99α. Wildtype, GFP- (22) or mCherry-expressing (23) derivatives of Kn99α were used, as stated for each figure.

Virus strains

HIV-1 virus stocks were generated by transfection of human embryonic kidney 293T cells (European Collection of Authenticated Cell Cultures) as previously described (24, 25). The R9HIVΔ*env* virus was derived from clade B HIV-1 strain (NL43) with 500bp deletion in *env*, pseudotyped with vesiculostomatitis virus G envelope. SIV3mac single round virus like particles (VLPs) containing vpx (SIV3vpx) were generated by transfection into 293T cells with pSIV3+ and pMDG plasmids (26, 27). At 48, 72h and 96h viral containing supernatant was harvested, centrifuged at 800 x g for 10 min and filtered through 0.45 um filter then centrifuged on a 20% sucrose cushion at 20,000 x g for 2h at 4°C. Purified virus was then re-suspended in RPMI media and frozen at -80°C. To quantify single round HIV infection, a vial was thawed for each harvest and serial dilutions used to infect CCR5/CD4 and CXCR4/CD4 transfected NP-2 cells. At 72h post infection wells were fixed in ice cold acetone-methanol and infected cells were identified by staining for p24 protein using a 1:1 mixture of the anti-p24 monoclonal antibodies EVA365 and EVA366 (NIBSC, Center for AIDS Reagents, UK). Infected cells

were detected by light microscopy to provide a virus titre (focus-forming U/mL). The SIV3vpx particles were quantified after thawing using a reverse transcriptase (RT) assay colorimetric kit (Roche) following the manufacturer's instructions to provide a RT ng/mL titre.

Recombinant MeV strain IC323 expressing green fluorescent protein (MeV-GFP) was generated as previously reported by Hashimoto *et al*. (28) MeV-GFP represents a virulent field isolate from Japan (Ichinose-B (IC-B) strain) and was isolated from a patient with acute measles in 1984 (29). For the generation of virus stocks, Vero (ATCC CCL-81) cells overexpressing human SLAMF1 receptor (vero-hSLAM cells) were grown in T75 tissue culture flasks to approximately 80% confluency in DMEM supplemented with 0.4 mg/mL G418. Flasks were infected with MeV-GFP at an MOI of 0.01:1 in 5 mL media for 1 hour at 37°C. After 1h a further 10 mL of DMEM supplemented with 10% FBS was added and infection allowed to continue for 48 h. At harvest the flasks were frozen to -80°C. After thawing, the collected supernatants were centrifuged at 2500 rpm for 10 min at 4°C to pellet cell debris. Aliquoted virus in supernatant was then frozen to -80°C. MeV-GFP viruses were then titred using the TCID-50 method. Vero-hSLAM cells were seeded into flat-bottomed 96 well plates and infected with serial dilutions of thawed MeV-GFP in triplicate. After 72 h, wells were scored for positive or negative infection under UV illumination on a Nikon TE-2000 microscope.

Ethics Statement

All work with human tissue was approved by the University of Birmingham Ethics Committee under reference ERN_10-0660. Samples were collected specifically for this work and were not stored beyond the duration of the experiments described herein. All donors provided written consent prior to donation.

129

130 **Human macrophage isolation and culture**

131 20-40 mL of blood were drawn from healthy donors by venepuncture. 6 mL of whole blood
132 were carefully layered on top of a double layer of Percoll (densities of 1.079 and 1.098 g/mL).
133 Samples were centrifuged in a swing bucket rotor at 150g for 8 minutes, followed by 10
134 minutes at 1200g, with acceleration and break set to zero. The resulting white disc of peripheral
135 blood mononuclear cells (PBMC) was transferred to a clean vial and incubated with red blood
136 cell lysis buffer at a ratio of 1:3 for 3 minutes, with gentle mixing throughout to prevent clot
137 formation. Cells were then washed with ice cold PBS twice, with centrifugation at 400g for 6
138 minutes in between each wash, and counted with a haemocytometer. $1x10^6$ PBMC were seeded
139 onto 48-well plates in RPMI-1640 media containing 1% penicillin/streptomycin, 5% heat-
140 inactivated AB human serum and 20 ng/mL M-CSF (Invitrogen). Cells were washed with PBS
141 and resuspended in fresh media on days 3 and 6 of differentiation. Macrophages were ready to
142 use on day 7. A yield of $1x10^5$ macrophages per well was estimated.

143

144 ***Cryptococcus* infection**

145 Fungi were opsonised with 10% human AB serum or 18B7 antibody (a kind gift from Arturo
146 Casadevall) for 1 hour and then added to macrophages at a multiplicity of infection of 10:1.
147 Infection was carried out in serum free-media, at 37°C with 5% CO_2. After 2 hours, cells were
148 washed 3 times with PBS to remove any extracellular fungi and fresh serum free-media was
149 added.

150

151 **Drug treatments**

152 Exogenous compounds were added to macrophages at two stages; when infecting with
153 *Cryptococcus* and again when replenishing with fresh media after removing extracellular fungi.

Compounds tested include interferon alpha (IFNα) at concentrations ranging from 5 to 100 pg/mL (Bio-Techne), polyinosinic-polycytidilic acid (polyIC) at 3 and 30 ng/mL (Invivogen), type-I interferon receptor inhibitor (IFNARinh) at 2.5 μg/mL (pbl assay science).

Co-infection assay

Human monocyte-derived macrophages were infected with either attenuated human immunodeficiency virus (HIV) or MeV-GFP as follows:

For attenuated HIV co-infections, 24h before cryptococcal infection, human monocyte-derived macrophages were infected either with R9HIVΔ*env* at a MOI of 10:1, SIV3*vpx* at 3 ng/mL or both in serum free RPMI. At 24 h post infection duplicate wells were fixed in ice cold acetone-methanol and infected cells were identified by staining for p24 protein as described above. Experimental wells were infected with antibody opsonised-*Cryptococcus* Kn99α-GFP for 2 hours, washed to remove extracellular fungal cells, and replenished with fresh serum free-media.

Alternatively, macrophages were infected with MeV-GFP at an MOI of 5:1 in serum free-media and kept at 37°C with 5% CO_2. After 24 hours, cells were washed with PBS and fresh media, supplemented with 5% heat-inactivated human AB serum, was added. After 3 days, cells were co-infected with serum opsonised-*Cryptococcus* Kn99α-mCherry for 2 hours, washed to remove extracellular fungal cells, and replenished with fresh serum free-media.

Live imaging

Infected samples were kept at 37°C with 5% CO_2 in the imaging chamber of a Ti-E Nikon Epifluorescence microscope. Images were taken every 5 minutes over an 18-hour period and compiled into a single movie file using NIS Elements software. Movies were blinded by a third

party before manual scoring for phagocytosis of *Cryptococcus*, virus infection rates, vomocytosis events, intracellular proliferation rates and macrophage integrity.

Growth curve assay

A 10-fold diluted cryptococcal overnight culture was inoculated into YPD broth in a 48-well plate (final dilution in well: 1000-fold), in the presence or absence of type-I interferons. The plate was sealed with a breathable membrane and incubated at 37°C within a fully automated plate reader (FLUOStar, BMG Omega). Optical density readings at 600 nm were taken every 30 minutes over a 24 hour-period, with orbital shaking in between readings.

Data analysis

Statistical analysis was performed using GraphPad Prism 6. Categorical data of phagocytosis or vomocytosis occurrence in the different conditions was assessed using Chi^2 test and Fisher's exact test. If data was normally distributed as assessed by Shapiro-Wilk test, then it was compared using Student's t test. Figures show percentage of *cryptococcus*-infected macrophages experiencing at least one vomocytosis event within each experiment. For intracellular proliferation rates, data was analysed using Mann-Whitney test. Growth curves were fitted to sigmoidal curves and the parameters were compared using Kruskal-Wallis test. All data shown corresponds to at least three independent experiments.

Raw data (collated manual counts for multiple timelapse movies) are provided as supplemental material for each figure. Original timelapse movies, upon which manual scoring was performed, are freely available upon request from the authors.

201 # Results

202

203 Given the relevance of cryptococcosis to HIV$^+$ patients (13), we set out to test whether HIV
204 infection had an effect on vomocytosis of *C. neoformans*. Human monocyte-derived
205 macrophages were infected with HIV-1 capable of a single-round of infection and subsequently
206 with *C. neoformans* and then used for time-lapse imaging over 18 hours. Subsequent scoring
207 showed that virally infected cells had a significantly higher occurrence of cryptococcal
208 vomocytosis (Figure 1A), whilst fungal uptake and intracellular proliferation were unaltered
209 (Figure 1C, 1E).

210

211 The experimental HIV system we used here includes co-transduction with SIV3*vpx* VLPs in
212 order to counteract the antiviral effect of SAMHD1 and ensure maximal HIV infection of the
213 macrophages (26, 30) (Figure S1A). Interestingly, we noted that the addition of SIV3*vpx* or
214 R9HIVΔ*env* alone also increased vomocytosis (Figure S1B). Since neither condition results
215 in widespread viral infection of host cells, this suggested that the enhancement of vomocytosis
216 occurs at the level of viral detection, rather than being a consequence of active HIV infection.

217

218 To explore this further, we tested whether vomocytosis was altered in macrophages infected
219 with an unrelated macrophage-tropic virus (31); measles (MeV, Figure 1B). The measles strain
220 used represents a virulent field isolate from Japan. Once again, infection with the virus resulted
221 in significantly enhanced vomocytosis of *Cryptococcus*. Neither HIV nor measles infection
222 affected uptake of *Cryptococcus* nor the intracellular proliferation rate (IPR) of the fungus
223 (Figure 1C-F), suggesting that the viral effect acts specifically at the level of vomocytosis,
224 rather than fungal pathogenicity *per se*, and that it is independent of the type of virus.

225

To test whether active viral infection was required for enhanced vomocytosis, we mimicked the effect of viral exposure by stimulating macrophages with polyinosinic-polycytidilic acid (polyIC). PolyIC is a double-stranded RNA synthetic analogue, which is known to trigger antiviral responses by binding to TLR3 (32). Human monocyte-derived macrophages were stimulated with polyIC and infected with *C. neoformans* simultaneously. Infected cells were imaged over 18 hours and scored for vomocytosis (Figure 2A). As with HIV or MeV infection, polyIC stimulation enhanced vomocytosis of *Cryptococcus*. Thus, it is likely that the antiviral reaction of the host macrophage, rather than an aspect of viral pathogenesis, is the trigger for enhanced vomocytosis from infected host cells.

The hallmark of the cellular anti-viral response is the induction of type-I interferons. Among these, the best studied are IFNα and IFNβ. During HIV infection specifically, the induction of IFNα is the most relevant (33). We therefore tested whether the impact of viral infection on vomocytosis could be recapitulated by exposure to interferon-α (IFNα). Stimulation of human monocyte-derived macrophages with 10 pg/mL IFNα (a level that closely matches that seen in HIV-infected patients (33)) resulted in significantly enhanced vomocytosis of *Cryptococcus* (Figure 2B) without altering cryptococcal growth, uptake or IPR (Figure S2). Interestingly, we noticed that higher doses of IFNα suppressed this effect, suggesting that the impact of interferons on vomocytosis can be rapidly saturated.

To confirm that type-I interferons were behind the increase in vomocytosis observed, we performed the viral infection experiments in the presence of a type-I interferon receptor (IFNAR) inhibitor (Figure 3). The addition of IFNAR inhibitor blocked the enhancement of vomocytosis otherwise elicited by viral infection in both HIV- and Measles-infection settings, confirming that type-I interferon signalling is necessary for this effect. Interestingly, this effect

was particularly prominent on virally infected cells rather than neighbouring cells which were not infected (Non-MeV; Figure 3B), suggesting that the impact of IFNα signalling on vomocytosis is highly localised and specific to the autocrine responses occurring within infected cells, rather than endocrine responses mediated through cytokines.

Discussion

In this study we set out to explore the consequences, if any, of viral infection on Cryptococcal infection, focusing on the non-lytic escape mechanism known as vomocytosis. Infection with either HIV or measles virus led to an enhancement in vomocytosis of *C. neoformans*, without affecting uptake or intracellular proliferation of the fungus (Figure 1), an effect that could be recapitulated by stimulation with IFNα and abrogated when signalling from type-I interferon receptor was blocked (Figures 2 and 3). Thus, viral coinfection stimulates expulsion of intracellular fungi via Type I interferon signalling.

The effect was seen using two distinct viral pathogens which differ, among other parameters, in the magnitude of anti-viral response they elicit in human macrophages. Relative to other viral infections, HIV is very good at avoiding the induction of type-I interferons (24, 25). Nonetheless, the low levels of type-I interferons induced by HIV, potentially enhanced by the co-infection with *Cryptococcus*, are sufficient to have a significant effect on vomocytosis. Infection with measles virus has been reported to induce limited production of type-I interferons in macaque models, albeit with potent induction of interferon-stimulated genes (34, 35). To date, there is no direct correlation between measles infection and cryptococcosis. However, given that both pathogens have a distinct respiratory phase it is possible that they interact within this shared niche, potentially through low doses of antiviral signalling.

Why might antiviral signalling induce vomocytosis? One possibility is that vomocytosis serves to "reset" phagocytes that have been unable to kill their prey, thus allowing them to serve a useful purpose in phagocytosing other pathogens rather than remaining "unavailable". In that context, a potent inflammatory signal such as IFNα may serve to accelerate this process during

280 localised infection, returning macrophages to functionality faster than would otherwise occur.
281 The consequences of vomocytosis on disease progression, however, are likely to be highly
282 context dependent; in some settings, this may enable a more robust immune response, but in
283 others it may serve to inadvertently disseminate the fungus to distal sites.
284
285 This is supported by previous reports showing variable outcomes of interferon signalling on
286 cryptococcal infection in mice. Sato *et al.* (36) showed that IFNARKO mice have lower fungal
287 burden than WT mice and consequently argue that type-I interferon signalling is detrimental
288 for the host during cryptococcal infection. Supporting this notion but using the sister species
289 *C. gatti*, Oliveira *et al* (37) show that infection with influenza virus worsens the prognosis of
290 subsequent fungal infection. On the other hand, Sionov *et al* (38) showed that stimulation with
291 IFNα or with the double-stranded RNA analogue pICLC protected the host from infection by
292 either *C. neoformans* or *C. gatti* infection. This effect was time-dependent, with the protective
293 effect of pICLC treatment only occurring if administered during the first 72 hpi before the
294 fungus reaches the brain. A tempting model, therefore, is that stimulating vomocytosis via
295 antiviral signalling early in infection (when the fungus remains in the lung) helps prevent
296 dissemination, whilst triggering vomocytosis later on may actually enhance fungal spread and
297 accelerate disease progression.
298
299 Taken together, our findings therefore suggest that the antiviral response, and IFNα in
300 particular, induce the expulsion of intracellular cryptococci and that this effect could be
301 advantageous or detrimental to the host, depending on the localization of the infected
302 phagocyte and timing of the event.
303

304 ## Acknowledgments

305 PIS, LMTS and RCM are supported by funding from the European Research Council under
306 the European Union's Seventh Framework Programme (FP/2007-2013)/ERC Grant
307 Agreement No. 614562. RCM holds a Wolfson Royal Society Research Merit Award and PIS
308 is supported by a Darwin Trust scholarship. MN is supported by a Wellcome Trust Investigator
309 Award (207511/Z/17/Z) and the NIHR Biomedical Research Centre at University College
310 London Hospitals.

311

References

1. Isaacs A, Lindenmann J. Virus interference. I. The interferon. Proc R Soc Lond B Biol Sci. 1957;147(927):258-67.

2. Haller O, Arnheiter H, Gresser I, Lindenmann J. Virus-specific interferon action. Protection of newborn Mx carriers against lethal infection with influenza virus. J Exp Med. 1981;154(1):199-203.

3. Muller U, Steinhoff U, Reis LF, Hemmi S, Pavlovic J, Zinkernagel RM, et al. Functional role of type I and type II interferons in antiviral defense. Science. 1994;264(5167):1918-21.

4. Yan N, Chen ZJ. Intrinsic antiviral immunity. Nat Immunol. 2012;13(3):214-22.

5. MacMicking JD. Interferon-inducible effector mechanisms in cell-autonomous immunity. Nat Rev Immunol. 2012;12(5):367-82.

6. Mancuso G, Midiri A, Biondo C, Beninati C, Zummo S, Galbo R, et al. Type I IFN signaling is crucial for host resistance against different species of pathogenic bacteria. J Immunol. 2007;178(5):3126-33.

7. Bergstrom B, Aune MH, Awuh JA, Kojen JF, Blix KJ, Ryan L, et al. TLR8 Senses Staphylococcus aureus RNA in Human Primary Monocytes and Macrophages and Induces IFN-beta Production via a TAK1-IKKbeta-IRF5 Signaling Pathway. J Immunol. 2015;195(3):1100-11.

8. Kagan JC, Su T, Horng T, Chow A, Akira S, Medzhitov R. TRAM couples endocytosis of Toll-like receptor 4 to the induction of interferon-beta. Nat Immunol. 2008;9(4):361-8.

9. Mancuso G, Gambuzza M, Midiri A, Biondo C, Papasergi S, Akira S, et al. Bacterial recognition by TLR7 in the lysosomes of conventional dendritic cells. Nat Immunol. 2009;10(6):587-94.

337 10. Castiglia V, Piersigilli A, Ebner F, Janos M, Goldmann O, Dambock U, et al. Type I
338 Interferon Signaling Prevents IL-1beta-Driven Lethal Systemic Hyperinflammation during
339 Invasive Bacterial Infection of Soft Tissue. Cell Host Microbe. 2016;19(3):375-87.
340 11. Gratz N, Hartweger H, Matt U, Kratochvill F, Janos M, Sigel S, et al. Type I interferon
341 production induced by Streptococcus pyogenes-derived nucleic acids is required for host
342 protection. PLoS Pathog. 2011;7(5):e1001345.
343 12. Webb LM, Lundie RJ, Borger JG, Brown SL, Connor LM, Cartwright AN, et al. Type
344 I interferon is required for T helper (Th) 2 induction by dendritic cells. EMBO J.
345 2017;36(16):2404-18.
346 13. Rajasingham R, Smith RM, Park BJ, Jarvis JN, Govender NP, Chiller TM, et al. Global
347 burden of disease of HIV-associated cryptococcal meningitis: an updated analysis. Lancet
348 Infect Dis. 2017;17(8):873-81.
349 14. Alvarez M, Casadevall A. Cell-to-cell spread and massive vacuole formation after
350 Cryptococcus neoformans infection of murine macrophages. BMC Immunol. 2007;8:16.
351 15. Feldmesser M, Kress Y, Novikoff P, Casadevall A. Cryptococcus neoformans is a
352 facultative intracellular pathogen in murine pulmonary infection. Infect Immun.
353 2000;68(7):4225-37.
354 16. Tucker SC, Casadevall A. Replication of Cryptococcus neoformans in macrophages is
355 accompanied by phagosomal permeabilization and accumulation of vesicles containing
356 polysaccharide in the cytoplasm. Proc Natl Acad Sci U S A. 2002;99(5):3165-70.
357 17. Voelz K, May RC. Cryptococcal interactions with the host immune system. Eukaryot
358 Cell. 2010;9(6):835-46.
359 18. Osterholzer JJ, Milam JE, Chen GH, Toews GB, Huffnagle GB, Olszewski MA. Role
360 of dendritic cells and alveolar macrophages in regulating early host defense against pulmonary
361 infection with Cryptococcus neoformans. Infect Immun. 2009;77(9):3749-58.

19. Sorrell TC, Juillard PG, Djordjevic JT, Kaufman-Francis K, Dietmann A, Milonig A, et al. Cryptococcal transmigration across a model brain blood-barrier: evidence of the Trojan horse mechanism and differences between Cryptococcus neoformans var. grubii strain H99 and Cryptococcus gattii strain R265. Microbes Infect. 2016;18(1):57-67.

20. Alvarez M, Casadevall A. Phagosome extrusion and host-cell survival after Cryptococcus neoformans phagocytosis by macrophages. Curr Biol. 2006;16(21):2161-5.

21. Ma H, Croudace JE, Lammas DA, May RC. Expulsion of live pathogenic yeast by macrophages. Curr Biol. 2006;16(21):2156-60.

22. Garelnabi M, Taylor-Smith LM, Bielska E, Hall RA, Stones D, May RC. Quantifying donor-to-donor variation in macrophage responses to the human fungal pathogen Cryptococcus neoformans. PLoS One. 2018;13(3):e0194615.

23. Upadhya R, Lam WC, Maybruck BT, Donlin MJ, Chang AL, Kayode S, et al. A fluorogenic C. neoformans reporter strain with a robust expression of m-cherry expressed from a safe haven site in the genome. Fungal Genet Biol. 2017;108:13-25.

24. Rasaiyaah J, Tan CP, Fletcher AJ, Price AJ, Blondeau C, Hilditch L, et al. HIV-1 evades innate immune recognition through specific cofactor recruitment. Nature. 2013;503(7476):402-5.

25. Tsang J, Chain BM, Miller RF, Webb BL, Barclay W, Towers GJ, et al. HIV-1 infection of macrophages is dependent on evasion of innate immune cellular activation. AIDS. 2009;23(17):2255-63.

26. Goujon C, Arfi V, Pertel T, Luban J, Lienard J, Rigal D, et al. Characterization of simian immunodeficiency virus SIVSM/human immunodeficiency virus type 2 Vpx function in human myeloid cells. J Virol. 2008;82(24):12335-45.

385 27. Goujon C, Jarrosson-Wuilleme L, Bernaud J, Rigal D, Darlix JL, Cimarelli A. With a
386 little help from a friend: increasing HIV transduction of monocyte-derived dendritic cells with
387 virion-like particles of SIV(MAC). Gene Ther. 2006;13(12):991-4.
388 28. Hashimoto K, Ono N, Tatsuo H, Minagawa H, Takeda M, Takeuchi K, et al. SLAM
389 (CD150)-independent measles virus entry as revealed by recombinant virus expressing green
390 fluorescent protein. J Virol. 2002;76(13):6743-9.
391 29. Takeda M, Takeuchi K, Miyajima N, Kobune F, Ami Y, Nagata N, et al. Recovery of
392 pathogenic measles virus from cloned cDNA. J Virol. 2000;74(14):6643-7.
393 30. Mlcochova P, Watters SA, Towers GJ, Noursadeghi M, Gupta RK. Vpx
394 complementation of 'non-macrophage tropic' R5 viruses reveals robust entry of infectious HIV-
395 1 cores into macrophages. Retrovirology. 2014;11:25.
396 31. Allen IV, McQuaid S, Penalva R, Ludlow M, Duprex WP, Rima BK. Macrophages and
397 Dendritic Cells Are the Predominant Cells Infected in Measles in Humans. mSphere.
398 2018;3(3).
399 32. Alexopoulou L, Holt AC, Medzhitov R, Flavell RA. Recognition of double-stranded
400 RNA and activation of NF-kappaB by Toll-like receptor 3. Nature. 2001;413(6857):732-8.
401 33. Hardy GA, Sieg S, Rodriguez B, Anthony D, Asaad R, Jiang W, et al. Interferon-alpha
402 is the primary plasma type-I IFN in HIV-1 infection and correlates with immune activation and
403 disease markers. PLoS One. 2013;8(2):e56527.
404 34. Shivakoti R, Siwek M, Hauer D, Schultz KL, Griffin DE. Induction of dendritic cell
405 production of type I and type III interferons by wild-type and vaccine strains of measles virus:
406 role of defective interfering RNAs. J Virol. 2013;87(14):7816-27.
407 35. Shivakoti R, Hauer D, Adams RJ, Lin WH, Duprex WP, de Swart RL, et al. Limited in
408 vivo production of type I or type III interferon after infection of macaques with vaccine or
409 wild-type strains of measles virus. J Interferon Cytokine Res. 2015;35(4):292-301.

410 36. Sato K, Yamamoto H, Nomura T, Matsumoto I, Miyasaka T, Zong T, et al.
411 Cryptococcus neoformans Infection in Mice Lacking Type I Interferon Signaling Leads to
412 Increased Fungal Clearance and IL-4-Dependent Mucin Production in the Lungs. PLoS One.
413 2015;10(9):e0138291.
414 37. Oliveira LVN, Costa MC, Magalhaes TFF, Bastos RW, Santos PC, Carneiro HCS, et
415 al. Influenza A Virus as a Predisposing Factor for Cryptococcosis. Front Cell Infect Microbiol.
416 2017;7:419.
417 38. Sionov E, Mayer-Barber KD, Chang YC, Kauffman KD, Eckhaus MA, Salazar AM, et
418 al. Type I IFN Induction via Poly-ICLC Protects Mice against Cryptococcosis. PLoS Pathog.
419 2015;11(8):e1005040.
420
421

Figure Captions

Fig 1. Viral infection enhances vomocytosis of *C. neoformans*

Human monocyte-derived macrophages were infected with HIV (left) or measles virus (right) and subsequently infected with *C. neoformans*. Time-lapse microscopy videos were manually scored for vomocytosis (top), uptake (middle) and intracellular proliferation rate of *C. neoformans* (bottom). **A-B** Graphs show percentage of *cryptococcus*-infected macrophages which have experienced at least one vomocytosis event. **C-D** Percentage of *crytptococus*-infected macrophages. **E-F** Intracellular proliferation rate of *C. neoformans* over 18 hours. In all cases, data corresponds to at least 3 independent experiments. Categorical vomocytosis and phagocytosis data was analysed by Chi^2 test followed by Fisher's exact test. * $p < 0.05$; **** $p < 0.0001$. IPR data was analysed using Mann-Whitney test.

Fig 2. Antiviral response increases vomocytosis

Human monocyte-derived macrophages were stimulated with different doses of polyIC (**A**) or IFNα (**B**), and infected with *C. neoformans*. Graphs show Mean + SD of percentage of *cryptococcus*-infected macrophages which have experienced at least one vomocytosis event. Chi^2 test followed by Fisher's exact test performed on raw vomocytosis counts. Data corresponds to at least three independent experiments.

Fig 3. Type-I interferon signalling is necessary to enhance vomocytosis

Human monocyte-derived macrophages were infected with HIV (**A**) or GFP-expressing measles virus (MeV-GFP, **B**) and subsequently with mCherry-expressing *C. neoformans* (Kn99α-mCherry), in the presence or absence of an IFNAR blocking antibody. GFP negative cells, which did not have an active Measles infection, were termed “Non-MeV”. Graph shows Mean + SD of percentage of *Cryptococcus*-infected macrophages which have experienced at

447 least one vomocytosis event. Fisher's exact test performed on raw vomocytosis counts. Data
448 corresponds to two and three biological repeats, respectively.
449

450 ## Supporting information

451 **Fig S1**

452 **A.** Human monocyte-derived macrophages were infected with VLPs as indicated. After 24
453 hours, viral infection was assessed by p24 staining (blue).
454 **B.** Cells were infected with VLPs as indicated, and subsequently infected with *C. neoformans*.
455 Time-lapse microscopy videos were manually scored for vomocytosis. Graph shows
456 percentage of *cryptococcus*-infected macrophages which have experienced at least one
457 vomocytosis event. Chi^2 test followed by Fisher's exact test performed on raw vomocytosis
458 counts from 5 independent experiments.
459

460 **Fig S2**

461 **A.** Cryptoccocal cells were grown in the presence or absence of IFNα over 24 hours. Growth
462 was assessed by optical densitiy readings at 600 nm.
463 **B-C.** Human monocyte-derived macrophages were infected with *C. neoformans* in the
464 presence of different doses of recombinant IFNα. Time-lapse microscopy videos were
465 manually scored for phagocytosis and intracellular proliferation rate of the fungus (B and C,
466 respectively).
467 Data corresponds to 3 independent experiments.
468

Figure 1

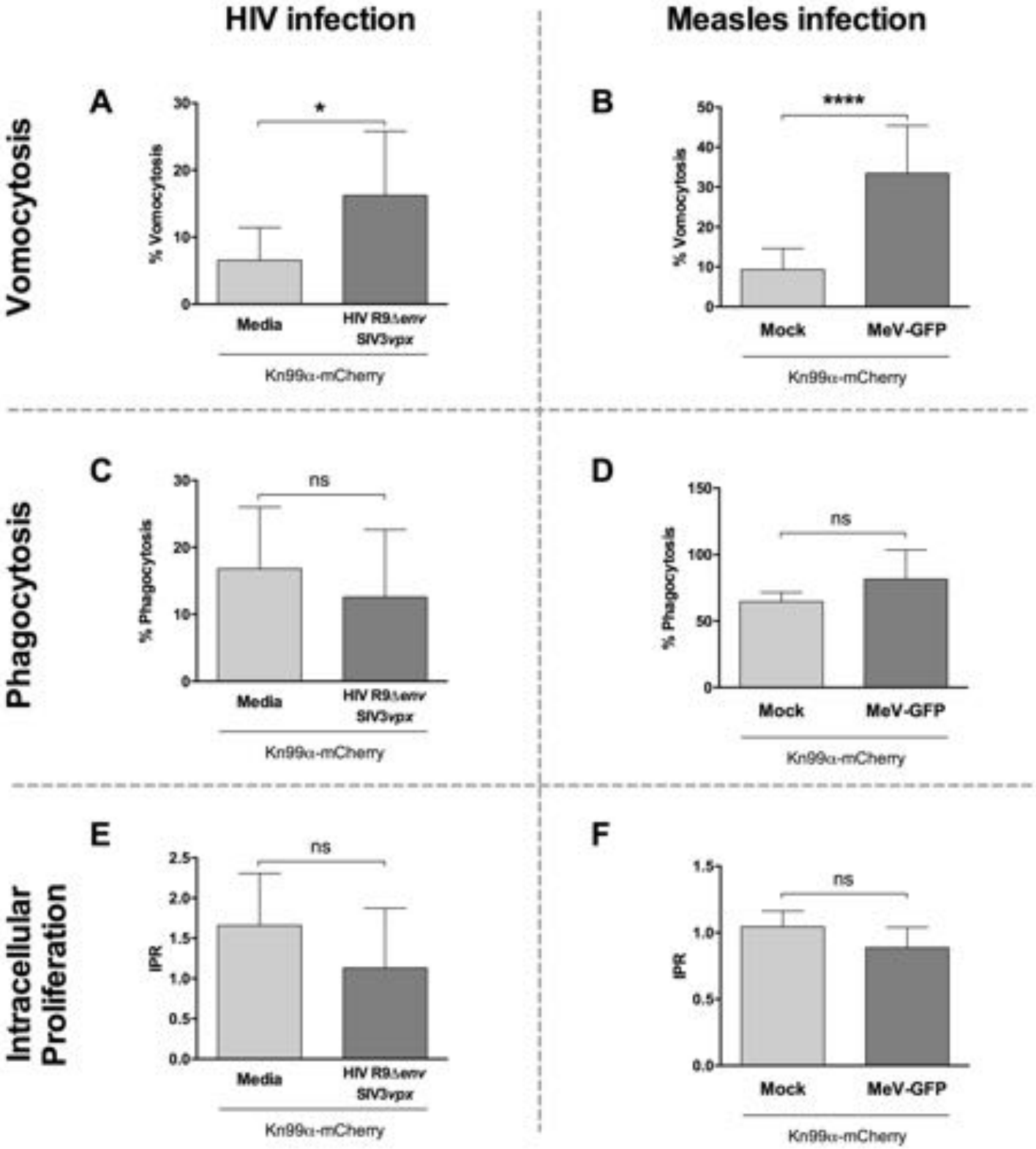

Figure 2

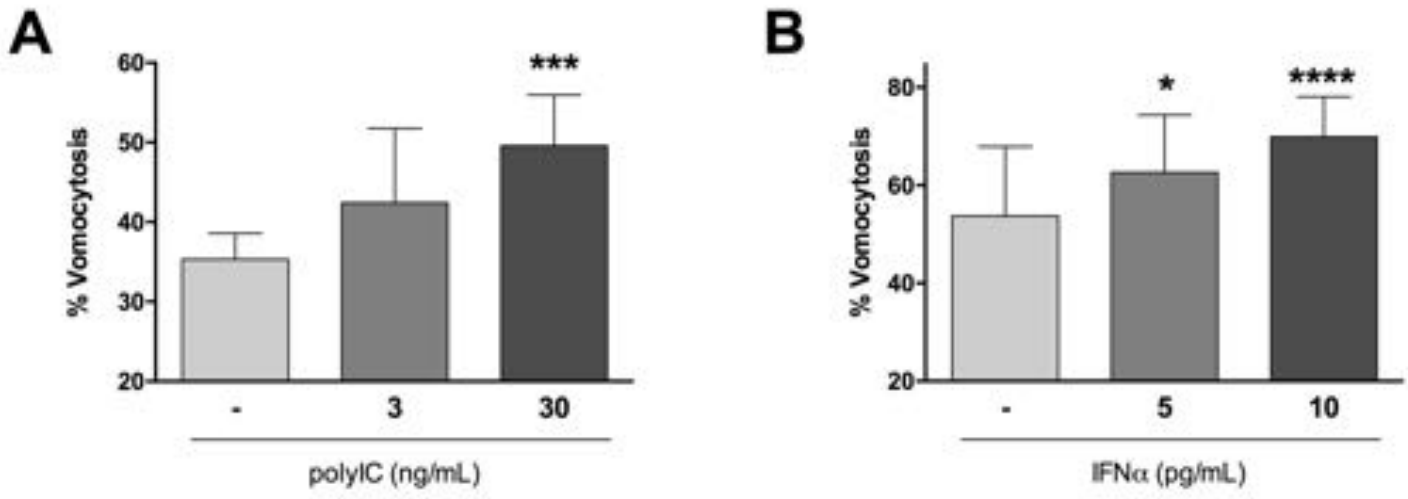

Figure 3